A human alpha-arrestin protein with a potential role in cargo protein trafficking within the endocytic system

David Jonathan Lake, BSc MSc.

Thesis submitted to the University of Nottingham for the degree of Doctor of Philosophy

July 2012

Abstract

β-Arrestins are essential adaptors for G protein-coupled receptor (GPCR) trafficking. Evolutionary ancestors of the β-arrestins – dubbed α-arrestins – are present in yeast/fungi and, similar to β-arrestins, recognise cargo proteins and mediate their intracellular trafficking. Mammalian α-arrestins include five largely uncharacterised arrestin domain-containing (ARRDC1-5) proteins that display a predicted arrestin structure; the current study focuses on human ARRDC2.

Confocal microscopy of exogenous, fluorescent protein-tagged ARRDC2 in U2OS cells in combination with compartment-specific markers indicated that ARRDC2 is dynamically distributed throughout the plasma membrane and endocytic system, predominantly to late endosomes/lysosomes. Anti-ARRDC2 immunostaining in several primary cell lines broadly supported this conclusion. ARRDC2 contains two proline-rich (PPxY) motifs that in other α-arrestins have been reported to mediate interactions with WW domain-containing NEDD4 family E3 ubiquitin ligases. Coimmunoprecipitation indicated that ARRDC2 is able to interact with several NEDD4 E3s via its PPxY motifs, and confocal microscopy suggested that this interaction may influence the subcellular targeting of the ligases. Ubiquitination of ARRDC2 was detected by coimmunoprecipitation, although this modification was independent of ARRDC2 interaction with NEDD4 E3s.

ARRDC2 colocalised with agonist-stimulated, internalised GPCRs (β_2-adrenergic receptor (β_2AR) and δ-opioid receptor (δOR)) and colocalisation analysis indicated that this involved compartmental redistribution of ARRDC2 to receptor-containing early/recycling endosomes, suggesting a specific effect. Interaction of ARRDC2 with δOR was detected using coimmunoprecipitation, and confocal analysis suggested that ARRDC2 may influence δOR and β_2AR intracellular trafficking. ARRDC2 was also found to oligomerise with itself and the β-arrestins. Confocal microscopy showed that ARRDC2 overexpression can induce the redistribution of β-arrestin1 to

ARRDC2-positive vesicles, and a punctate bimolecular fluorescence complementation (BiFC) signal was detected between ARRDC2 and β-arrestin2. From this, it is speculated that α-/β-arrestins may function cooperatively or competitively to mediate discrete GPCR sorting events in the endocytic pathway.

Acknowledgements

I would like to thank my supervisors Dr Nick Holliday and Dr Simon Dawson for their support, advice and encouragement throughout the project. I am also grateful to the members of both labs, especially those in the Institute of Cell Signalling who created a warm and supportive atmosphere to work within. I would like to thank Tim Self for technical support in fluorescence microscopy.

Finally, I would like to thank my family and friends for their invaluable support and encouragement, and my wife, Naomi, for helpful scientific discussions and her unrelenting support and companionship.

List of Contents

List of abbreviations

Abbreviations used throughout the text are listed. Those abbreviations that appear only once are given in the text and are not listed here. Standard three-letter abbreviations for the amino acids are used (further abbreviated to single letters where indicated).

ADP	adenosine 5’-diphosphate
AF	Alexa Fluor
AP2	adaptor protein 2
ARRDC	arrestin-related domain containing protein
ART	arrestin-related trafficking adaptor
ATP	adenosine 5’-triphosphate
β2AR	beta2-adrenoceptor
BRET	bioluminescence resonance energy transfer
BSA	bovine serum albumin
cAMP	cyclic adenosine monophosphate
CCP	clathrin-coated pit
CCV	clathrin-coated vesicle
cDNA	complementary DNA
CXCR	CXC chemokine receptor
DMEM	Dulbecco's modified Eagle's medium
δOR	delta-opioid receptor
DUB	deubiquitinating enzyme
E3	ubiquitin-protein ligase enzyme
ECL	extracellular loop
EEA1	early endosomal antigen 1
eGFP	enhanced GFP
EGFR	epidermal growth factor receptor

Eps15	EGFR pathway substrate 15
ERK	extracellular regulated kinase
ESCRT	endosomal sorting complex required for transport
EST	expressed sequence tag
FRET	fluorescence resonance energy transfer
G protein	guanine nucleotide binding protein
GABA	γ-aminobutyric acid
GDP	guanosine 5'-diphosphate
GFP	green fluorescent protein
GPCR	G protein-coupled receptor
GRK	GPCR kinase
GST	glutathione S-transferase
GTP	guanosine 5'-triphosphate
HA	haemagglutinin
HECT	homologous to E6-associated protein C-terminus
HEK	human embryonic kidney cell line
HRS	hepatocyte growth factor-regulated tyrosine kinase substrate
ICL	intracellular loop
ILV	intralumenal vesicle
JNK	c-Jun N-terminal kinase
kD	kilodalton
LAMP1	lysosome-associated membrane protein 1
MAPK	mitogen-activated protein kinase
Mdm2	murine double minute 2
MEF	mouse embryonic fibroblast
mGluR	metabotropic glutamate receptor
MVB	multivesicular body

NEDD4	neural precursor cell expressed, developmentally-downregulated 4
NMR	nuclear magnetic resonance
PAR	protease-activated receptor
PBS	phosphate-buffered saline
PCR	polymerase chain reaction
PI3K	phosphoinositide 3-kinase
PKA	protein kinase A
PKC	protein kinase C
PPxY	proline-proline-x-tyrosine
R	inactive receptor state
R*	active receptor state
RING	really interesting new gene
RT-PCR	reverse transcriptase PCR
SDS-PAGE	sodium dodecyl sulfate-polyacrylamide gel electrophoresis
SH	src homology domain
SNX	sorting nexin
src	non-receptor src (sarcoma) family tyrosine kinase
ss	signal SNAP
TFN	transferrin
TGN	trans-Golgi network
TM	transmembrane domain
TR	tetracycline repressor
Tsg101	tumour susceptibility gene 101 protein
TXNIP	thioredoxin-interacting protein
U2OS	human osteosarcoma cell line
UV	ultraviolet

Vps	Vacuolar protein sorting
YFP	yellow fluorescent protein

1 Introduction

1.1 Cell signalling and GPCRs

Cells sense their external environment via the ligand-induced modulation of cell surface signalling receptor activity, which initiates multiple overlapping intracellular signalling cascades to produce a wide range of responses. Multicellular organisms depend on this mechanism for cell-cell communication; mediators released into the extracellular milieu give rise to cell responses whose coordinated integration underlies the regulation of many important physiological processes. Adaptation to changes in extracellular signals is essential for organism homeostasis, emphasised by various disease states that arise when cell signalling is in some way deregulated. Fundamental to this regulation in many biological systems are G protein-coupled receptors (GPCRs), which comprise the largest superfamily of cell surface receptors in animals, with around 800 members representing ~2% of the human genome (Vassilatis *et al.*, 2003). GPCRs are sufficiently diverse to enable the selective association with a broad range of endogenous ligands, including photons, ions, small organic compounds, amines, lipids, proteins and nucleotides (Lagerstrom *et al.*, 2008). As such, GPCRs are of huge physiological importance, and it is perhaps not surprising that the pharmaceutical industry is dominated by drugs that modulate GPCR function, accounting for around 30% of the market according to the latest estimate (Overington *et al.*, 2006). However, these drugs act at only a small number (>40) of well-characterised GPCRs. There are ~400 non-olfactory GPCRs that represent potential drug targets, including ~150 whose endogenous ligand is unknown ('orphan' receptors); therefore, there remains a large proportion of GCPRs whose therapeutic potential is unexplored (Lagerstrom *et al.*, 2008).

1.1.1 Classification of GPCRs

GPCRs are integral plasma membrane proteins with a conserved structure consisting of seven transmembrane (TM) α-helices separated by intracellular (ICL) and extracellular loops (ECL), with an extracellular amino(N)-terminal domain and an intracellular carboxy(C)-terminal domain. Based on phylogenetics, GPCRs have been classified into five main families: *Rhodopsin*, *Secretin*, *Glutamate*, *Adhesion* and *Frizzled/Taste2* (Fredriksson *et al.*, 2003).

Rhodopsin-like receptors (also known as class A) form the largest family, with ~670 human members, of which ~390 represent olfactory receptors. Class A receptors bind the widest variety of ligands, from small molecules (e.g. lipids, nucleotides) to larger peptides and proteins. The diversity in ligand preference is a function of the sequence heterogeneity of individual class A GPCRs, with the most variation found within the TM and ECL domains. However, there are several highly conserved amino acid residues within the TM domains that are essential for the structural integrity of the 'helical bundle' and for receptor inactivation-activation. These include the aspartate-arginine-tyrosine (DRY) motif at the cytosolic end of TM3, the asparagine-proline-x-x-tyrosine (NPXXY; X denotes a hydrophobic residue) motif in TM7, and single proline residues within TM5 and TM6 (see section 1.1.2 for more detail).

The *Secretin* receptor family (class B) comprises 15 human members, all of which bind moderately large peptide hormones. In contrast to class A receptors, class B receptors have an extended N-terminal tail (>120 residues) that contains six conserved cysteine residues; these form a network of three disulfide bridges, contributing to an extracellular domain of high structural integrity (Lisenbee *et al.*, 2005). Based on a 3D nuclear magnetic resonance (NMR) structure of the N-terminal domain of the corticotrophin releasing factor receptor 2beta (CRF-R2β; a class B GPCR), it appears that this domain provides a molecular architecture that is critical for class B receptor-peptide ligand interactions (Grace *et al.*, 2004).

The *Glutamate* or class C family includes receptors for metabotropic neurotransmitters (glutamate, gamma-aminobutyric acid [GABA]), taste compounds, amino acids and Ca^{2+}, and has 22 members in humans. Most class C receptors have a very large N-terminal tail that forms a two-lobe structure separated by a cleft, within which the endogenous ligands bind (Kniazeff *et al.*, 2011). Agonist binding leads to rearrangement of the lobes to enclose the agonist, hence the two-lobe structure being known as the Venus flytrap (VFT) domain. Another feature of class C receptors is their constitutive homo- or hetero-dimerisation, which is required for their function (see section 1.1.4).

The *Adhesion* receptor family is the second largest in humans, with 33 members (Yona *et al.*, 2008). Although ancestrally related to *Secretin*/class B receptors (Fredriksson *et al.*, 2003), the *Adhesion* family is distinct, not only in the TM domains, but notably in the presence of a large multidomain N-terminus. Multiple common structural domains within this region are implicated in cell-cell and cell-matrix contacts, hence the nomenclature adopted for these receptors. Unlike other GPCRs, it was thought that *Adhesion* receptors may not couple to intracellular signalling pathways, although there are now several reports suggesting they may retain this ability (Bohnekamp *et al.*, 2011; Iguchi *et al.*, 2008), possibly following cleavage of the extended N-domain (Volynski *et al.*, 2004).

The final GPCR family is a phylogenetic amalgamation of the so-called *Frizzled* and *Taste2* subgroups (Fredriksson *et al.*, 2003). The *Frizzled* subgroup comprises 10 frizzled receptors (FZD1-10) and the smoothened receptor (SMO) in humans. Ligands for the FZDs are secreted lipoglycoproteins of the Wingless/Integration-1 (Wnt) family, whereas SMO mediates sonic hedgehog (SHH) signalling in complex with patched (Klaus *et al.*, 2008; Murone *et al.*, 1999). Both pathways are crucial to development, and are frequently deregulated in cancer. A conserved feature of *Frizzled* receptors is the N-terminal cysteine-rich domain (CRD), which in the FZDs is assumed to be the site for Wnt binding (Dann *et al.*, 2001), although additional receptor regions may be involved (Chen *et al.*,

2004b). The *Taste2* receptors (T2Rs) respond to a diverse array of bitter taste compounds (Chandrashekar *et al.*, 2000). T2Rs lack many conserved motifs (e.g. in class A GPCRs), and consequently are probably divergent in terms of structure and activation mechanisms (Singh *et al.*, 2011).

The proceeding sections will focus largely on class A GPCRs, since these are the most widely studied and have provided the classical models for GPCR structure and function, and are the receptor type that it utilised in the current study.

1.1.2 Molecular mechanisms of ligand binding and receptor activation

The orthosteric binding site (that recognised by the endogenous agonist) for classical small-molecule ligands (e.g. neurotransmitters) is a pocket formed within the upper third of the receptor TM helical bundle (Gether, 2000). For example, adrenaline binding to the prototypic GPCR, the beta2-adrenoceptor (β_2AR), involves residues in the upper sections of TM3 and TM5. In particular, the adrenaline charged amine group forms an ionic bond with Asp113 in TM3 (Strader *et al.*, 1988), and hydroxyls of the adrenaline phenol ring form hydrogen bonds with Ser204 and Ser207 in TM5 (Strader *et al.*, 1989). These contacts are conserved for many GPCRs that bind chemically similar amines (e.g. acetylcholine, dopamine, histamine), and the general mode of ligand binding within a helical bundle pocket is shared by other class A GPCRs that bind small ligands. However, many ligands, especially larger peptides, bind to epitopes formed by the N-domain and ECLs. This is true for ligands binding to class B and C GPCRs as mentioned in section 1.1.1 above, but is also seen for class A receptors, such as in the interaction of substance P with its cognate GPCR, the neurokinin 1 receptor (NK1) (Gether, 2000). Thus, there is great diversity in the modes of ligand binding, even within class A GPCRs. Despite these different modes, multiple class A GPCRs couple to the same preferred intracellular effector, namely, a particular class of guanine nucleotide binding (G)

protein; therefore, mechanistically distinct agonist binding must induce functionally homogeneous active receptor conformations.

This is enabled by intramolecular interactions between conserved motifs within class A GPCRs that constrain the receptor in a 'closed' inactive state, and are disrupted or altered in the active conformation. These include the NPXXY motif at the base of TM7, which participates in a hydrogen bond network with residues in TM1/TM2, and the TM3 DRY motif that was originally thought to form an 'ionic lock' with an aspartate in TM6 (Gether, 2000). Mutation of these motifs was found to induce constitutively active receptor conformations, and these and other biophysical studies led to a global 'toggle switch' model for receptor activation (Schwartz *et al.*, 2006). Activation was proposed to involve breakage of the TM links mentioned above, causing a see-saw movement of TM domains (especially TM6) involving closure on the extracellular side around the agonist, and opening on the intracellular side, thereby providing a cleft for effector binding.

Recent X-ray crystallographic structures have further illuminated the model of receptor activation (Choe *et al.*, 2011; Granier *et al.*, 2012; Lebon *et al.*, 2011b; Park *et al.*, 2008; Rasmussen *et al.*, 2011; Warne *et al.*, 2011; Xu *et al.*, 2011). Except for rhodopsin (Choe *et al.*, 2011), the presence of the DRY ionic lock – and its disruption upon agonist binding – has not been conclusively demonstrated in these studies. The solution of crystal structures for GPCRs except rhodopsin has proved challenging, necessitating the adoption of strategies such as the mutagenic thermostabilisation of specific receptor conformations (Lebon *et al.*, 2011a). Such modifications may be the source of disagreement between the resulting structures and earlier biophysical models. Overall, however, crystal structures support the predicted view of a helical bundle and the toggle switch model for activation. In particular, they demonstrate the likely widespread mechanism of subtle rearrangements in the ligand binding pocket upon agonist interaction (i.e. enclosing the agonist) that are accompanied by large-scale outward movements at the TM cytoplasmic ends (Lebon

et al., 2011b; Rasmussen *et al.*, 2011; Warne *et al.*, 2011; Xu *et al.*, 2011).

1.1.3 Coupling receptor activation to intracellular signalling

The paradigm for transduction of GPCR signalling involves an active conformation – with an open cytoplasmic cleft as described above – that enables interaction with a heterotrimeric G protein. This promotes release of guanosine 5'-diphosphate (GDP) from the G_α subunit; G_α then binds guanosine 5'-triphosphate (GTP), whose intracellular concentration exceeds GDP, resulting in the dissociation of G_α-GTP and $G_{\beta\gamma}$ which couple to their respective downstream effector proteins (Milligan *et al.*, 2006). The concept of a three-way stabilised complex (agonist-GPCR-G protein) has long been central to the simplest model for GPCR activation/signalling, the ternary complex model (De Lean *et al.*, 1980). In this model, the receptor is in equilibrium between inactive (R) and active (R*) states. Agonists bind with higher affinity to R*, thus favouring the active, G protein-coupled conformation. The model was subsequently extended to allow for the spontaneous formation of R* in the absence of agonist (i.e. constitutive activity), and has since been expanded with the identification of multiple possible distinct R* states with or without ligand present (Kenakin, 2004; Samama *et al.*, 1993).

The GPCR-G protein binding interface was probed in detail some years ago (Bourne, 1997). The G_α subunit was found to directly interact with GPCRs, and approaches such as alanine-scanning mutagenesis defined the G_α C-terminal α-helix as the main region responsible (Onrust *et al.*, 1997). Several GPCR regions contribute to a G protein binding surface, with the most important being ICL2, ICL3 and portions of the C-terminal tail. The first crystal structure of a GPCR (the β_2AR) in complex with its entire cognate G protein has recently been published (Rasmussen *et al.*, 2011). The principal interactions discussed above are supported by this report, in

particular the insertion of the G_α C-terminal helix into a cleft formed by outward movement of β_2AR TM6 (section 1.1.2 above).

It is not yet fully clear how G protein subtype selectivity of GPCRs is determined. There are sixteen G_α isoforms, which are divided into distinct subtypes (G_s, G_q, G_i and $G_{12/13}$) based on structural and functional similarities (Hurowitz *et al.*, 2000); individual GPCRs are generally considered to preferentially interact with a particular G_α subtype. The different subtypes couple to discrete signalling pathways via their interaction with different effector proteins (Table 1.1). $G_{\beta\gamma}$ subunits, of which there are five G_β and eleven G_γ isoforms (Hurowitz *et al.*, 2000), were originally considered merely as inhibitors that prevented G_α activation in the absence of receptor stimulation. However, it is now clear that $G_{\beta\gamma}$ subunits also mediate signalling, for example in the regulation of some adenylyl cyclase isoforms (Diel *et al.*, 2006; Steiner *et al.*, 2006) and phospholipase Cβ (Bonacci *et al.*, 2005; Poon *et al.*, 2009), and the activation of mitogen-activated protein kinase (MAPK) (Shi *et al.*, 2003) and c-Jun N-terminal kinase (JNK) (Coso *et al.*, 1996).

Table 1.1 Summary of the signalling profiles of G_α subtypes

G_α subtype	Effector coupling	Outcome
G_s	Stimulates adenylyl cyclase	Increased cAMP
G_i	Inhibits adenylyl cyclase	Decreased cAMP
G_q	Activation of PLCβ	Cleavage of PIP2 to generate IP3 and DAG
$G_{12/13}$	Activation of RhoGEFs	Activation of small monomeric GTPase RhoA

RhoGEFs activated by $G_{12/13}$ include p115-RhoGEF, PDZ-RhoGEF, leukaemia-associated RhoGEF and lymphoid blast crisis-RhoGEF. PLCβ, phospholipase Cβ; PIP2, phosphatidylinositol bisphosphate; IP3, inositol trisphosphate; DAG, diacylglycerol; RhoGEF, RhoGTPase guanine nucleotide exchange factor.

1.1.4 Evolving concepts: allosterism, biased agonism and oligomerisation

Traditionally, GPCR-targeted drug discovery strategies have focussed on the binding site for endogenous agonists, denoted the orthosteric site. However, there is great diversity in the nature of potential ligand binding sites (section 1.1.2), and it has recently

become evident that molecules may bind to distinct regions (designated as allosteric sites) from the orthosteric site (Keov *et al.*, 2010). Such molecules are known as allosteric modulators, since their binding induces receptor conformational changes that may enhance or reduce the affinity or efficacy of an agonist at the orthosteric site. Thus, the allosteric site may represent a tractable pharmacological opportunity for the development of drugs with greater subtype selectivity.

Another recent phenomenon in GPCR research is that of biased agonism, also known as ligand-directed signalling or functional selectivity (Gesty-Palmer *et al.*, 2011; Reiter *et al.*, 2012). As noted in section 1.1.3, GPCRs are now accepted to be capable of adopting multiple distinct R* states. Biased ligands are those that selectively stabilise only a subset of R* states, and thus preferentially activate only certain signalling pathways. This may involve selective receptor interaction with and signalling through specific G_α subtypes, as has been observed for the prostaglandin EP4 receptor, which may signal through $G_{\alpha s}$ or $G_{\alpha i}$, depending on the ligand used (Leduc *et al.*, 2009). Alternatively, in several cases ligands have been found to bias signalling through another group of intracellular GPCR effectors, the arrestins (for detailed description of arrestins, see section 1.2). The molecular mechanisms involved in such bias are just beginning to be elucidated. For example, using site-specific NMR labelling within the β_2AR, Liu and colleagues have identified two distinct active receptor conformations involving movements of TM6 or TM7; ligands functionally biased toward G protein-specific signalling caused a shift in TM6, whereas arrestin-biased ligands primarily impacted the TM7 equilibrium state (Liu *et al.*, 2012). Thus, the mechanism and functional relevance of biased signalling are beginning to be established, investigations that may well pave the way for the development of improved pathway-specific therapeutics with fewer side-effects (Gesty-Palmer *et al.*, 2011).

The final relatively new concept that will be touched upon here is that of GPCR oligomerisation. As mentioned in section 1.1.1, *Glutamate*/class C receptors form constitutive dimers (Kniazeff *et al.*,

2011). For example, the functional GABA receptor unit is a heterodimer composed of $GABA_{B1}$ and $GABA_{B2}$ subunits. $GABA_{B1}$ contains a binding site for GABA, but when expressed alone the nascent protein is unable to escape the endoplasmic reticulum due to a C-terminal retention motif; interaction between coexpressed $GABA_{B1}$ and $GABA_{B2}$ is required to mask this motif, enabling delivery to the cell surface (Margeta-Mitrovic *et al.*, 2000). A similar role for heterodimerisation in the anterograde delivery of a nascent class A GPCR, protease-activated receptor 4 (PAR4), to the plasma membrane has also been reported (Cunningham *et al.*, 2012). Recently, fluorescence resonance energy transfer (FRET) has demonstrated that subunits within mGluR dimers undergo conformational changes relative to each other (Yanagawa *et al.*, 2011), and it is suggested that dimer activation may be transduced in a synergistic manner. Whether class A/B GPCRs dimerise, and whether this is required for signal transduction, has been a more contentious issue. Classically, a single GPCR was thought to couple to a single G protein. This model was challenged by the structural observation of multiple GPCR contacts with both G_{α} and $G_{\beta\gamma}$ and the fact that, based on crystallographic structures, the cytoplasmic surface of a single GPCR alone is not large enough to support these contacts (Terrillon *et al.*, 2004b). However, a section of the GPCR research community still holds to the notion of GPCRs as monomers (Chabre *et al.*, 2005). This has historically been based on classical studies of detergent-solubilised GPCR monomers. More recently, experiments using GPCRs (rhodopsin, β_2AR) in reconstituted lipid particles have indicated that a monomeric GPCR unit is sufficient for G protein coupling (Whorton *et al.*, 2007; Whorton *et al.*, 2008). Nevertheless, there is mounting evidence that GPCRs, including class A, are capable of forming dimers and/or higher order oligomers when coexpressed, and that these species are functionally relevant (Milligan, 2007). Such interactions (for example, allosteric interaction between receptor heterodimers) have the potential for introducing another layer of complexity to GPCR signalling; effects

on receptor function, including pharmacology and trafficking, are just beginning to be established.

1.2 Arrestins and GPCR regulation

In addition to promoting G protein-coupled signalling responses, agonist-dependent GPCR activation initiates the subsequent regulatory processes of receptor desensitisation, endocytosis and trafficking/sorting. The two non-visual arrestin isoforms, β-arrestin1 and β-arrestin2, display ubiquitous cell and tissue expression and are involved in all of these events (Gurevich *et al.*, 2008c; Luttrell *et al.*, 2002).

1.2.1 Desensitisation

Desensitisation refers to the weakening of a receptor-induced response to a given concentration of agonist, upon prolonged exposure to that agonist. The decrease in response may be rapid, and may function to prevent hyperactivation. The paradigm for desensitisation of GPCRs involves their phosphorylation by specific kinase enzymes, within seconds of exposure to agonist. The same R* conformation that interacts with G proteins provides a substrate for phosphorylation at serine/threonine residues in the receptor C-tail and/or IL3 by GPCR kinases (GRKs); receptors are also targets for second messenger-dependent kinases (protein kinase A and C; PKA, PKC) (Ferguson, 2001; Lohse *et al.*, 1992). As described in section 1.1.2, transition to the active receptor state is characterised by exposure of various cytoplasmic residues. These include the ten amino acid segment in the proximal IL2 containing the conserved DRY motif (Marion *et al.*, 2006). The agonist-activated presentation of phosphorylated GPCR C-tail residues and the exposure of cytoplasmic GPCR residues synergistically stabilise the high affinity binding of arrestin, whose activation and phosphate 'sensors' interact with each respective GPCR module (Gurevich *et al.*, 2006b). Notably, G proteins and arrestins may share a common interaction

interface on the receptor; for example, they both interact with IL2 as mentioned above. The structure of arrestins (detailed description in section 1.4) includes a central polar core that is responsible for interaction with GRK-phosphorylated GPCR C-tail residues. GPCR-bound arrestin sterically interdicts G protein binding, resulting in cessation of G protein-dependent signalling.

Several exceptions and additions to this paradigm for desensitisation exist. Arrestin binding does not always require receptor phosphorylation (Chen *et al.*, 2004a; Zhang *et al.*, 2005). Also, desensitisation by GRKs may occur in a phosphorylation-independent manner (Ferguson, 2007), perhaps involving direct GRK binding to GPCRs – and blocking of G protein coupling – in a fashion analogous to arrestins. Additionally, a non receptor-mediated mechanism for desensitisation involves the regulators of GPCR signalling (RGS) proteins, comprising a family of 20 proteins in mammals (Xie *et al.*, 2007). RGS proteins specifically and selectively interact with G_{α} subunits of G_q and $G_{i/o}$ proteins, enhancing the intrinsic GTPase activity of G_{α}, thereby leading to GTP hydrolysis and termination of G_{α}-mediated signalling. RGS proteins can also interact specifically with GPCRs themselves, and accumulating data (for example, from knockout studies (Zachariou *et al.*, 2003)) suggests that RGS regulation of GPCR signalling has important physiological consequences. Thus, although the GRK-arrestin pathway remains the dogma for GPCR desensitisation, a multiplicity of mechanisms exist, the extent of which is far from fully understood.

1.2.2 Internalisation

In addition to uncoupling GPCRs from their cognate G protein, β-arrestins also act as adaptors, coupling the receptor to members of the endocytic machinery that leads to internalisation of the receptor from the plasma membrane to intracellular compartments. Internalisation can occur within minutes of agonist stimulation, and contributes further to GPCR desensitisation since the acidic

endosomal environment promotes ligand dissociation (Ferguson, 2001; Ferguson *et al.*, 1998; Krupnick *et al.*, 1998). The best defined route for GPCR internalisation is the clathrin-mediated endocytic pathway. Clathrin, along with associated proteins such as the adaptor protein 2 (AP2) complex, forms clathrin-coated pits at the plasma membrane. The triskelion structure of clathrin enables the formation of a lattice, along with accessory proteins. This induces membrane curvature, leading to invagination, budding and eventual dynamin-dependent scission to produce an intracellular endocytic vesicle (Ungewickell *et al.*, 2007). β-Arrestins directly interact with the β2-adaptin subunit of AP2 and with clathrin, thereby targeting the associated GPCR cargo to clathrin-coated pits (Goodman *et al.*, 1996b; Laporte *et al.*, 2000).

However, again this is a rule to which there are exceptions. For instance, although protease-activated receptor 1 (PAR1) is desensitised by β-arrestin, its internalisation is β-arrestin-independent (Paing *et al.*, 2002), and is instead mediated by interactions with AP2 and another endocytic adaptor, called epsin-1 (Chen *et al.*, 2011). Moreover, internalisation of cargo receptors is not always via clathrin-dependent endocytosis; clathrin-independent pathways are increasingly recognised (Sandvig *et al.*, 2011). Clathrin-independent routes have been proposed for several GPCRs, including the constitutively internalising mGluR5 and mGluR7 (Fourgeaud *et al.*, 2003; Lavezzari *et al.*, 2007). The M3 muscarinic receptor and β_2AR also undergo a degree of constitutive internalisation; this is clathrin-independent, and may be mechanistically separate from the clathrin-dependent pathway that these receptors enter upon agonist stimulation (Scarselli *et al.*, 2009). The molecular mechanisms behind these alternative pathways are not known; additional unidentified factors/adaptors may well be involved.

1.2.3 Overview of cargo sorting: a conserved role for ubiquitin

Following their biosynthesis, proteins are subject to quality control and complex intracellular sorting at multiple different stages. These processes are essential in determining the subcellular localisation and abundance of proteins, including integral membrane protein cargoes. Ubiquitination is a widely used post-translational modification that influences these decisions, from the quality control and release of nascent proteins in the secretory pathway, to the context-dependent endocytosis of plasma membrane cargo, to the intracellular trafficking of endocytosed cargoes (MacGurn *et al.*, 2012).

Ubiquitin is a highly conserved short polypeptide of 76 amino acids that exists either in a free form within cells, or covalently conjugated to another protein. Attachment of ubiquitin to target proteins, or ubiquitination, involves the formation of a reversible isopeptide bond between the ubiquitin C-terminal glycine residue and an ε-amino group of a lysine residue within the substrate. Proteins may be ubiquitinated by the addition of a single moiety at a single lysine residue (monoubiquitination), or single moieties at multiple residues (multiubiquitination). Additionally, since ubiquitin itself contains seven lysine residues (K^{6}, K^{11}, K^{27}, K^{29}, K^{33}, K^{48}, K^{63}), ubiquitin chains can be formed, linked through any of these residues (polyubiquitination). The type of ubiquitination has different functional consequences for the substrate protein. K^{48}-linked polyubiquitination is well known to target soluble, cytosolic proteins for degradation by the 26S proteasome (Pickart, 1997). In contrast, monoubiquitination or K^{63}-linked chains are the major forms employed in the regulation of endocytosis and membrane protein trafficking (Acconcia *et al.*, 2009).

The process of protein ubiquitination involves the sequential transfer of ubiquitin between an ubiquitin-activating enzyme (E1), an ubiquitin-conjugating enzyme (E2) and an ubiquitin-protein ligase (E3). E3 ligases mediate the final transfer of ubiquitin to the substrate protein, and it is primarily the E3s that determine

substrate specificity and the type of ubiquitination employed (Rotin *et al.*, 2009). The E3s are divided into two main families: really interesting new gene (RING) finger (616 members in humans) and homologous to E6-associated protein C-terminus (HECT) domain (28 members in humans) E3s. HECT E3s contain a catalytic HECT domain of ~350 amino acids in their C-terminus, plus various N-terminal functional domains that prompt their division into three subfamilies: HECT and RCC1 domain (HERC; 6 members), neural precursor cell expressed, developmentally-downregulated 4 (NEDD4; 9 members) and other HECTs (13 members) (Rotin *et al.*, 2009). The current study will focus on the NEDD4 family, since these have been linked to arrestin protein binding and GPCR trafficking (see section 4.1). Here, it is sufficient to note that, in several cases, NEDD4 E3s have been found to ubiquitinate activated plasma membrane cargo proteins (e.g. receptors), thereby signposting them for endocytosis and/or incorporation into the ESCRT sorting pathway (see below). Similar to protein phosphorylation, ubiquitination is a dynamic, reversible process; E3-mediated ubiquitination can be antagonised by the activity of deubiquitinating enzymes (DUBs), comprising over 100 members in humans.

The non-proteasomal functions of ubiquitination in endocytosis and membrane trafficking regularly involve the ubiquitin conjugate providing a platform for interaction between the target protein and another protein, often called an adaptor. These interactions are enabled by the presence of various ubiquitin-binding domains (UBDs) within adaptor proteins, including ubiquitin-interacting motifs (UIMs), Src homology 3 (SH3) and Vps27, Hrs and STAM (VHS) domains. For example, in clathrin-mediated endocytosis, ubiquitinated cargoes (exemplified by the epidermal growth factor receptor, EGFR) interact with accessory proteins such as epsin and EGFR pathway substrate 15 (Eps15) (Bertelsen *et al.*, 2011). Epsin and Eps15 are recruited early in the initiation of clathrin-coated pit formation, and both proteins contain multiple ubiquitin-interacting motifs (UIMs), allowing them to congregate ubiquitinated cargo into the newly forming pits. Additionally, epsin/Eps15 contribute to the initial

deformation of the plasma membrane (Horvath *et al.*, 2007), leading to invagination that is further stabilised by the clathrin lattice.

In the context of cargo sorting (after internalisation into endosomes), ubiquitination is commonly recognised by the endosomal sorting complexes required for transport (ESCRT) machinery, leading to commitment to the lysosomal pathway of degradation. The ESCRT machinery is comprised of four multimeric complexes, ESCRT-0, -I, -II and -III, as well as several accessory proteins (Raiborg *et al.*, 2009). These highly conserved complexes interact with each other, and are localised to early endosomal membranes. Here they facilitate the sorting of cargo through three main activities: first, ubiquitinated cargoes are captured through direct interaction with UIMs present in ESCRT-0, -I and -II complexes; second, assembly of ESCRT components, notably ESCRT-III, causes involution of the endosomal membrane, producing invaginations that contain ubiquitinated cargo (Saksena *et al.*, 2009); third, enzymatic activity of ESCRT-III components (Vps4 AAA-ATPase) catalyses the final membrane scission step (Wollert *et al.*, 2009), forming cargo-containing intralumenal vesicles (ILVs) within a multivesicular body (MVB). MVBs are then committed to maturation into late endosomes and fusion with lysosomes, where the sorted cargo is eventually degraded by acid hydrolases. Deubiquitination also plays an important role in the fine-tuning of these processes. Two DUBs, ubiquitin-specific protease 8 (Usp8) and associated molecule with the SH3 domain of STAM (AMSH) interact with various ESCRT components. In so doing, Usp8 and AMSH are able to deubiquitinate cargo proteins and ESCRTs (Wright *et al.*, 2011), which can negatively regulate lysosomal trafficking and degradation, but may also positively drive cargo MVB incorporation and degradation (Berlin *et al.*, 2010; Sierra *et al.*, 2010).

1.2.4 GPCR sorting

Once internalised, GPCR-containing coated vesicles are uncoated, and subsequently fuse with early endosomes. From these compartments, GPCRs are either recycled back to the plasma membrane (resensitisation) or trafficked to the lysosome for degradation (downregulation) (Hanyaloglu *et al.*, 2008). These decisions – along with the rate of synthesis/delivery of nascent receptors to the plasma membrane – are essential in determining the strength and duration of signalling. Moreover, based on *in vivo* studies performed so far, tight regulation of GPCR endocytosis and sorting is likely to be of high physiological importance (Kim *et al.*, 2008; Odley *et al.*, 2004; Thompson *et al.*, 2010). Factors influencing these decisions include GPCR phosphorylation and ubiquitination profiles. Most GPCRs can be classified into one of two groups. 'Group A' GPCRs, exemplified by the β_2AR, are transiently phosphorylated and ubiquitinated. This produces a transient interaction with β-arrestins, preferentially the β-arrestin2 isoform. β-Arrestin is thus transiently ubiquitinated, and dissociates from the GPCR soon after internalisation; the receptor is rapidly recycled back to the cell surface (Shenoy *et al.*, 2003). Other GPCRs such as the angiotensin II type IA and delta-opioid receptors ($AT_{IA}R$, δOR; 'group B' receptors) display more prolonged phosphorylation and ubiquitination profiles. In particular, a cluster of serine residues in the receptor C-tail are phosphorylated. This leads to more stable association and co-internalisation with β-arrestin and prolonged β-arrestin ubiquitination (Oakley *et al.*, 2001; Shenoy *et al.*, 2003). Thus, group B GPCRs typically exhibit slower resensitisation profiles due to sequestration in endosomes and may be more readily trafficked to the lysosome for degradation (Oakley *et al.*, 1999).

In addition to β-arrestins, there are many other GPCR-interacting proteins that act as adaptors for GPCR endocytic and intracellular sorting (Magalhaes *et al.*, 2012). These include PDZ proteins (**p**ost synaptic density protein 95 [PSD95], **D**rosophila disc large tumour suppressor [Dlg1], **z**onula occludens-1 protein [zo-1]), which contain multiple globular PDZ domains that bind to specific

sequences called PDZ binding motifs in the C-termini of interacting proteins. Many GPCRs contain C-tail PDZ motifs, promoting interactions with various PDZ proteins that differentially impact receptor endocytosis and trafficking. For example, the β_2AR contains a C-tail aspartate-serine-leucine-leucine (DSLL) motif that drives interaction with the PDZ protein NHERF/EBP50 (Na^+/H^+ exchanger regulatory factor /ezrin–radixin–moesin (ERM)-binding phosphoprotein-50). This interaction is required for efficient β_2AR plasma membrane recycling (Cao *et al.*, 1999); indeed, mutagenic incorporation of the DSLL motif into the δOR – a receptor characterised by slow recycling/lysosomal targeting – is sufficient to redirect δOR into a rapid recycling pathway (Gage *et al.*, 2001). Alternatively, association with the PDZ protein PSD-95, whilst not affecting desensitisation, was found to inhibit agonist-induced internalisation of the β_1AR and serotonin 2A receptor (5-HT_{2A}) (Hu *et al.*, 2000; Xia *et al.*, 2003). It is now clear that individual GPCRs may interact with multiple different PDZs, possibly dependent on the cell type and physiological context, and that these interactions have the capacity to modulate many, often opposing, GPCR trafficking events.

GPCR-associated sorting proteins (GASPs) are another family of trafficking adaptors that influence GPCR sorting, in particular following endocytosis. First identified for GASP-1 regulation of the δOR (Whistler *et al.*, 2002), GASPs have been shown to specifically bind to the C-tail of many GPCRs, an interaction that may be required for efficient receptor lysosomal targeting and downregulation (Kargl *et al.*, 2011; Thompson *et al.*, 2011; Tschische *et al.*, 2010). The mechanisms involved are unclear, although it may be that GASPs provide a link between GPCRs and the ESCRT machinery and/or accessory proteins (Marley *et al.*, 2010).

Another recent development is the observed role for sorting nexin-1 (SNX1), a component of the retromer complex involved in endosome-to-*trans*-Golgi retrograde transport, in GPCR trafficking. SNX1 interacts directly with PAR1 (Wang *et al.*, 2002), and small

interfering RNA (siRNA) depletion of SNX1 inhibited PAR1 degradation, implicating SNX1 in the lysosomal sorting of PAR1 (Gullapalli *et al.*, 2006). Interestingly, depletion of other components of the retromer and of the ESCRT-0 complex did not affect PAR1 degradation, suggesting that SNX1 may function independently of these scaffolds. SNX1 regulation of GPCRs is clearly receptor- and/or context-specific, however; in the case of the purinergic P2Y1 receptor, SNX1 is not involved in receptor degradation but instead is required for P2Y1 sorting into a slow recycling pathway (Nisar *et al.*, 2010). Moreover, in these studies several GPCRs were found not to interact with or be regulated by SNX1; hence, the involvement of SNX1 is not likely to be universal to all GPCRs, leaving the door open for additional, as yet unidentified, factors that may be required to link GPCRs to the various appropriate sorting apparatus.

1.3 β-Arrestins: emerging role as multifunctional adaptors

In recent years the role of β-arrestins has been extended beyond their canonical regulation of GPCR desensitisation and endocytosis. It is now known that β-arrestins interact with several catalytically active non-receptor proteins, prompting the recognition of β-arrestins as scaffolds for effector signalling in their own right. Among the β-arrestin interacting partners are protein kinases/phosphatases, ubiquitin ligases, small G proteins and their regulators (Gurevich *et al.*, 2006a; Leftowitz *et al.*, 2005). In many cases interaction with β-arrestin is thought to recruit the signalling effectors to agonist-activated GPCRs, thus opening up a new avenue of previously unrecognised GPCR signalling that is independent of G protein activation. It has also become clear that β-arrestin regulation of cell surface receptors is not limited to GPCRs. β-arrestins have been reported to bind and downregulate several structurally diverse non-GPCR receptors, including the insulin-like growth factor-1 receptor (IGF-1R), transforming growth factor-β

type III receptor (TGFβRIII), peroxisome proliferator-activated receptor-gamma (PPARγ) and Na+/H+ exchangers NHE1 and NHE5 (Chen *et al.*, 2003; Girnita *et al.*, 2005; Lin *et al.*, 1998; Simonin *et al.*, 2010; Szabo *et al.*, 2005). Of these, direct interaction with β-arrestin was only demonstrated for NHE5; it remains possible that the effects seen may be explained by transactivation between, for example, receptor tyrosine kinases (RTKs) and GPCRs, rather than direct regulation. Regardless, these reports expand the scope of β-arrestin influence on cell signalling pathways.

1.3.1 β-Arrestin-dependent signalling

The first indication that β-arrestins might mediate GPCR signalling came from the observed formation of a β-arrestin-dependent β2AR-src tyrosine kinase signalling complex (Luttrell *et al.*, 1999). Since then, β-arrestins have been shown to scaffold multiple signalling complexes. These include other c-Src family kinases (Imamura *et al.*, 2001) and MAPKs (Gong *et al.*, 2008; McDonald *et al.*, 2000), members of the Akt/phosphoinositide 3-kinase (PI3K) pathway (Beaulieu *et al.*, 2005; Povsic *et al.*, 2003), phosphodiesterase 4 (PDE4) (Baillie *et al.*, 2003), diacylglycerol (DAG) kinases (Nelson *et al.*, 2007) and signal transducer and activator of transcription 1 (STAT1) (Mo *et al.*, 2008).

One pathway in which β-arrestin-dependent transduction has been demonstrated for several different GPCRs is the extracellular regulated kinase/MAPK (ERK/MAPK) cascade. Since β-arrestin binding to GPCRs uncouples the receptor and G protein, and promotes internalisation of the GCPR-β-arrestin complex, it would be expected that β-arrestin-dependent signalling be temporally, if not also spatially, segregated from G protein-dependent signalling. Indeed, two discrete phases of ERK1/2 activation have been detected arising from the stimulation of GPCRs such as the angiotensin II type IA receptor ($AT_{IA}R$), lysophosphatidic acid (LPA) receptor and β_2AR (Ahn *et al.*, 2004; Gesty-Palmer *et al.*, 2005; Shenoy *et al.*, 2006). The first rapid, transient phase is dependent

upon G protein activation, not β-arrestins, producing phosphorylated ERK that translocates to the nucleus and initiates the transcription of target genes (Gesty-Palmer *et al.*, 2005). The second, β-arrestin-dependent, phase is slower in onset yet sustained over a longer period, and is insensitive to inhibitors of G proteins (Ahn *et al.*, 2004; Shenoy *et al.*, 2006). Since the internalised GPCR-β-arrestin complex and associated ERK are segregated within endosomes ('signalosome'), this phase produces an endosomal pool of phosphorylated ERK that does not translocate to the nucleus and may therefore have different functional consequences (Ahn *et al.*, 2004; DeFea *et al.*, 2000). The physiological implications of these observations are beginning to be understood. For example, glucagon-like peptide-1 (GLP-1) is a polypeptide hormone that simulates glucose-stimulated insulin secretion in pancreatic β-cells by activating its' cognate GPCR, GLP-1R. β-arrestin1 has been shown to be required for this signalling by mediating the activation of ERK stimulated by GLP-1R (Sonoda *et al.*, 2008)

β-Arrestins interact with nearly all GPCRs, and the conclusion from the above studies is that β-arrestins act as a scaffold for multiple factors. However, a given GPCR-β-arrestin pair only couples to a selection of downstream effectors. Thus, specificity must somehow be introduced in order to scaffold some partners and not others. There are a number of theoretical possibilities for how this could be achieved, discussed below, many of which are supported experimentally. Additionally, it is possible that there are other receptor-binding proteins ('α-arrestins', perhaps; see section 1.4), in addition to β-arrestins, which are required to achieve the observed level of signalling complexity.

First, despite the near ubiquitous presence of β-arrestins, GPCRs and signalling effectors are often expressed in a tissue-specific manner, allowing for the possibility of a particular GPCR recruiting a subset of effectors owing to their cell type-specific availability. Furthermore, GPCRs may be segregated into specific microdomains within the plasma membrane, such as lipid rafts and caveolae, thereby restricting their coupling to only those effectors localised

within the same microenvironment (Patel *et al.*, 2008), a concept known as compartmentalised signalling.

Second, the rapidity and longevity of β-arrestin recruitment varies for different GPCRs and different ligands acting at individual GPCRs, depending on factors including receptor phosphorylation and ubiquitination profiles. This produces spatiotemporal variations in the ability of β-arrestins to scaffold downstream partners.

Third, the affinity of the two β-arrestin isoforms for different GPCRs varies; some receptors preferentially bind one isoform over the other (related to GPCR classification into group A or B), other receptors have no preference (Oakley *et al.*, 2000). Similarly, the affinity of downstream effectors for either β-arrestin isoform may be different, as may be the nature of the complexes formed. For example, both β-arrestin1/2 bind JNK3, but only β-arrestin2 holds JNK3 in an orientation that results in enhanced JNK3 activity (Song *et al.*, 2009). Thus, differential affinities and conformations between GPCR-β-arrestin and β-arrestin-effector may produce specificity the signalling pathways elicited. Further to this, the propensity of GPCRs to oligomerise has been discussed (section 1.1.4). The capacity of β-arrestins to self-associate has also been reported (see Chapter 5 for more detail), although the precise role of such interactions is unclear (Defea, 2008; Xu *et al.*, 2008). Nonetheless, conceptually at least, given the specificities in β-arrestin receptor and effector binding affinity, it is conceivable that the ability to form higher order structures could add yet another level of complexity to the system.

Fourth, interaction with different GPCRs, and stimulation of a single GPCR with different agonists, may result in β-arrestin coupling to specific effectors (biased signalling, as noted in section 1.1.4). β-Arrestin binding to GPCRs induces the exposure of β-arrestin C-tail residues responsible for clathrin/AP2 interaction, known as the 'active' conformation (Krupnick *et al.*, 1997a; Laporte *et al.*, 1999), and it is likely that β-arrestin affinity for various other scaffolding partners will also be higher in the active state (Gurevich *et al.*, 2006b). However, the implication is that the β-arrestin active state is not rigid; there may be multiple receptor-bound β-arrestin

conformations (dependent upon the individual GPCR bound and/or which agonist is responsible for stimulation) that can be considered as active, with variable affinities for different effector proteins. Evidence for distinct β-arrestin active conformations has come from a study in which bioluminescence resonance energy transfer (BRET) was used to detect structural rearrangements within the β-arrestin molecule (Shukla *et al.*, 2008). BRET donor (*Renilla* luciferase) and acceptor (yellow fluorescent protein) were fused to β-arrestin2 N- and C-termini, respectively, such that movement of the globular domains with respect to each other was detected as a change in BRET efficiency. Several different GPCRs were assayed and, as expected, agonist stimulation resulted in an altered BRET signal. However, the change in BRET signal was dependent on the agonist used; β-arrestin-pathway specific biased agonists reduced the BRET signal, whereas standard agonists that also mobilise G protein signalling increased BRET signal. Hence, specific agonists can promote the adoption of distinct GPCR conformations that are transmitted to β-arrestin, which in turn adopts distinct conformations with potentially functionally divergent consequences.

1.3.2 β-arrestins determine intracellular receptor trafficking

As mentioned in section 1.2.4, β-arrestins have been found to influence GPCR sorting decisions following receptor internalisation into endosomes. In addition to the differences between β-arrestin binding kinetics (group A versus B GPCRs), β-arrestins can exert these effects by acting as adaptors for E3 ubiquitin ligases and/or DUBs. For example, β_2AR ubiquitination status is modulated by the HECT E3 ligase neural precursor cell expressed developmentally-downregulated 4 (NEDD4) and DUB ubiquitin-specific 33 (USP33), thereby determining the balance between β_2AR lysosomal trafficking versus recycling (Shenoy *et al.*, 2001; Shenoy *et al.*, 2009; Shenoy *et al.*, 2008). β-Arrestin2 coimmunoprecipitates with NEDD4 in an agonist-dependent manner, and siRNA knockdown of β-arrestin2

inhibits NEDD4 binding to activated β_2AR (Shenoy *et al.*, 2008). USP33 binds to non-stimulated β_2AR, and β-Arrestin2 also coimmunoprecipitates with USP33 in an agonist-dependent manner, although with slower kinetics than the NEDD4 interaction (Berthouze *et al.*, 2009). Thus, it is proposed that β-arrestin2 acts as an adaptor for the recruitment of NEDD4 to the activated β_2AR, and may also compete with the receptor for USP33 binding, thereby having an net positive effect on β_2AR ubiquitination and lysosomal degradation (Berthouze *et al.*, 2009).

β-Arrestin is also involved in the trafficking of the chemokine receptor CXCR4. CXCR4 ubiquitination and sorting to the degradative pathway are mediated by the E3 ligase atrophin-interacting protein 4 (AIP4, also known as Itch) (Marchese *et al.*, 2003). In this case AIP4 interacts directly with CXCR4, removing the need for β-arrestin to act as an adaptor for E3 ligase recruitment and receptor ubiquitination (Bhandari *et al.*, 2009). Nonetheless, β-arrestin1 is required for CXCR4 targeting to lysosomes following internalisation, and β-arrestin1 does interact with AIP4, albeit at a later stage on early endosomes (Bhandari *et al.*, 2007). Interestingly, β-arrestin1 interacts directly with a component of the ESCRT machinery, signal-transducing adaptor molecule-1 (STAM-1), thereby recruiting AIP4 to the complex. This enables AIP4 to ubiquitinate another ESCRT component, hepatocyte growth factor-regulated tyrosine kinase substrate (HRS) (Malik *et al.*, 2010), a function that is reciprocally regulated in conjunction with the DUB USP8 (Berlin *et al.*, 2010). Although β-arrestin1 is clearly required for CXCR4 lysosomal targeting, disruption of the β-arrestin1/STAM-1 interaction actually enhances CXCR4 degradation (Malik *et al.*, 2010). Thus, the authors propose that β-arrestin1 has a dual role in the sorting of CXCR4, initially linking CXCR4 to the ESCRT machinery but then also attenuating CXCR4 degradation via an interaction with STAM-1, thereby determining the fine balance of CXCR4 degradation versus recycling.

The role of β-arrestins in recruiting E3 ubiquitin ligases to promote receptor downregulation has also been extended to non-GPCR

receptor cargoes. For example, β-arrestin1 or 2 recruit the E3 ligase murine double minute 2 (Mdm2) for the ubiquitination and downregulation of IGF-1R or the androgen receptor, respectively; similarly, β-arrestin1 modulates NHE1 ubiquitination and degradation via the recruitment of NEDD4 (Girnita *et al.*, 2005; Lakshmikanthan *et al.*, 2009; Simonin *et al.*, 2010).

Overall, studies on β-arrestin roles in receptor signalling and trafficking have established the arrestin fold as an adaptable scaffold for the mediation of a remarkable array of cell biological functions.

1.4 Expansion of the arrestin family

Arrestins are defined by the presence of two conserved protein sequences known as the arrestin N- and C-domains. The crystal structures of β-arrestin1/2 have been solved (Han *et al.*, 2001; Zhan *et al.*, 2011), revealing that the N- and C-domains form globular β-sheets that give rise to a characteristic β-sandwich fold, separated by a flexible polar core 'hinge' region (Gurevich *et al.*, 2006a). Until recently, humans were assumed to have four proteins that display the arrestin fold: two photoreceptor-specific visual arrestins and two β-arrestins. However, phylogenetic analysis has expanded the evolutionary tree of arrestins to include many previously unrecognised eukaryotic homologues of these four (see Figure 1.1). It is now apparent that the known animal visual/β-arrestins (herein collectively referred to as β-arrestins) are part of a subset of the arrestin family that emerged more recently in evolutionary history, and that many ancient arrestin-related proteins exist that form a second proposed subset (Alvarez, 2008). These novel proteins comprise five mammalian "arrestin domain-containing" proteins (ARRDC1-5), vacuolar protein sorting 26 (Vps26) and thioredoxin-interacting protein (TXNIP), and have been collectively termed 'α-arrestins' as distinct from β-arrestins (Alvarez, 2008). Over the past five or six years a broad mode of action has begun to emerge for the α-arrestins, primarily through studies in lower eukaryotes but more recently in humans.

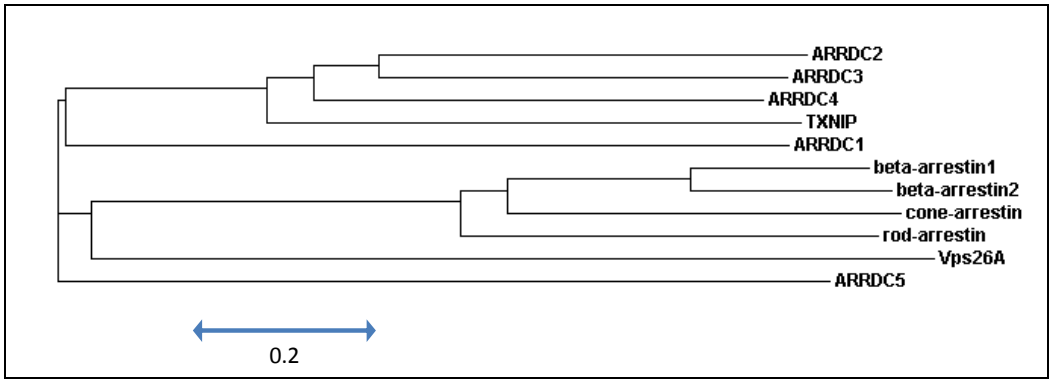

Figure 1.1 Phylogram demonstrating the evolutionary relationship between human arrestin family proteins

A neighbour-joining phylogenetic tree was generated using ClustalW2 (http://www.ebi.ac.uk/Tools/msa/clustalw2/). The scale bar shows the number of substitutions per site (nucleotide position). Note the branching of the β-arrestin subfamily (visual and non-visual β-arrestins) as distinct from the α-arrestins. A more comprehensive phylogenetic tree including orthologous arrestins from other species can be found elsewhere (Alvarez, 2008).

1.4.1 Structural comparison of α- and β-arrestins

Structurally, at least, there is reason to postulate that α-arrestins may perform related roles to β-arrestins. α-Arrestins share a moderate degree of sequence homology with β-arrestins and have the same predicted arrestin N- and C-domain topology (for sequence alignment see Figure 1.2). Furthermore, three-dimensional modelling of the structure of the human arrestin clan proteins indicated that the human α-arrestins likely adopt an overall structure that is very similar to the β-arrestin sandwich fold (Aubry *et al.*, 2009). In addition to the ARRDC proteins, phylogenetic analysis also identified human Vps26, a subunit of the retromer complex, as a more distant arrestin relative (Alvarez, 2008). Interestingly, X-ray crystallography had previously revealed that Vps26 has two arrestin domains that give an overall structure that is remarkably similar to β-arrestin (Collins *et al.*, 2008; Shi *et al.*, 2006). Although it was concluded that there is no protein sequence homology between Vps26 and arrestins (Shi *et al.*, 2006), this was on the basis of comparison with the β-arrestins, not the more

closely related α-arrestins. It has since been proposed that Vps26 is indeed a true homologue of the arrestin clan, and that the α-arrestins map structurally onto known β-arrestin structures with high confidence (Alvarez, 2008), undermining the suggestion that α-/β-arrestin structural similarities are mainly superficial (Collins *et al.*, 2008). The identification of Vps26 as a *bona fide* α-arrestin supports the proposed role of the arrestin fold as a conserved molecular architecture for intracellular protein trafficking, a role which may extend to other α-arrestin members (Aubry *et al.*, 2009).

Despite these similarities, protein sequence alignment indicates that the α-arrestins are clearly distinct from the β-arrestins (for comparison see Table 1.2). Comparison reveals that α-arrestins lack the known C-tail clathrin- and AP2-interacting motifs present in β-arrestins, although interactions between yeast α-arrestins and clathrin/clathrin adaptor proteins have been reported (O'Donnell *et al.*, 2010); hence, it is possible that other as yet unrecognised motifs are capable of performing the same function. α-Arrestins do, however, contain additional 'PPxY' motifs (proline-proline-[any amino acid]-tyrosine sequences, not present in β-arrestins) in their C-terminus that may mediate interaction with WW domain-containing proteins – WW domains are ~40 amino acid modules present in diverse signalling and structural proteins that enable interaction with proline-rich ligands (Macias *et al.*, 2002). β-Arrestins contain a conserved amphipathic α-helix in their N-domain ('helix I') that is sequestered in the inactive state (Han *et al.*, 2001; Hirsch *et al.*, 1999). It was initially proposed that helix I may be released upon receptor engagement to interact with downstream partners or facilitate membrane docking (Han *et al.*, 2001). However, subsequent mutational analysis in this region suggested that helix I is dispensable for receptor internalisation (Dinh *et al.*, 2005) and that, although it may facilitate receptor binding, movement of the helix is not triggered upon binding (Vishnivetskiy *et al.*, 2010). Multiple sequence alignments performed by Alvarez (2008) suggested that the region containing the hydrophobic and basic residues of helix I in β-arrestins is not present in α-arrestins. This

implied that helix I may have evolved later in β-arrestins as a module involved in receptor regulation. However, in contrast, three-dimensional modelling of the human arrestin clan proteins against β-arrestin crystal structures yielded structures of the α-arrestins ARRDC2, ARRDC3 and ARRDC4 that do each contain a characteristic N-domain α-helix (Aubry *et al.*, 2009). Thus, it is unclear whether this motif is present in α-arrestins, a question that may only be conclusively answered through the solution of α-arrestin crystal structures.

```
ARRDC2          -----------MLFDKVKAFSVQLDGATAGVEPVFSGGQAVAGRVLLELSSAARVGALRL 49
ARRDC3          -----------MVLGKVKSLTISFDCLNDSNVPVYSSGDTVSGRVNLEVTGEIRVKSLKI 49
ARRDC4          MGGEAGCAAAVGAEGRVKSLGLVFEDERKG---CYSSGETVAGHVLLEASEPVALRALRL 57
TXNIP           ----------MVMFKKIKSFEVVFN----DPEKVYGSGEKVAGRVIVEVCEVTRVKAVRI 46
beta-arr1       ------------MGDK-GTRVFKKASPNGKLTVYLGKRDFVDHIDLVDPVDGVVLVDPEY 47
beta-arr2       ------------MGEKPGTRVFKKSSPNCKLTVYLGKRDFVDHLDKVDPVDGVVLVDPDY 48
ARRDC1          -------------MGRVQLFEISLSHG----RVVYSPGEPLAGTVRVRLGAPLPFRAIRV 43
ARRDC5          ----MGDREECLSTPQPPMSVVKSIELVLPEDRIYLAGSSIKGQVILTLNSTLVDPIVKV 56
Vps26A          ------MSFLGGFFGPICEIDIVLNDGETRKMAEMKTEDGKVEKHYLFYDGESVSGKVNL 54
Consensus                              .               .       :
Arr domain                                    NNNNNNNNNNNNNNNNNNNNNNNNNNNNN

ARRDC2           ARGRAHVHWTESRS--AGSSTAYTQSYSERVEVVSHRATLLAPDTGETT------TLPP 101
ARRDC3          HARGHAKVRWTESRN--AGSNTAYTQNYTEEVEYFNHKDILIGHERDDDNSEEGFHTIHS 107
ARRDC4          EAQGRATAAWGPSTCPRASASTAALAVFSE-VEYLNVRLSLREPPAGEGII-----LLQP 111
TXNIP           LACGVAKVLWMQGSQ-----------QCKQTSEYLRYEDTLLLEDQPTGENE--MVIMRP 93
beta-arr1       LKERRVYVTLTCAFRYGREDLDVLGLTFRKDLFVANVQSFPPAPEDKKPLTRLQERLIKK 107
beta-arr2       LKDRKVFVTLTCAFRYGREDLDVLGLSFRKDLFIATYQAFPPVPNPPRPPTRLQDRLLRK 108
ARRDC1          TCIGSCGVSNKANDT-----------AWVVEEGYFNSSLSLADKG------------SLP 80
ARRDC5          ELVGRGYVEWSEEAG--ASCDYSRNVICNNKADYVHKTKTFPVEDN-----------WLS 103
Vps26A          AFKQPGKRLEHQGIRIEFVGQIELFNDKSNTHEFVNLVKELALPG-------------EL 101
Consensus
Arr domain      NNNNNNNNNNNNNNNNNNNNNNNNNNNNNNNNNNNNNNNNNNNNNNNNNNNNNNNNNNNN

ARRDC2          GR-HEFLFSFQLPPT--------LVTSFEGKHGSVRYCIKATLHRP-WVPARRARKVFTV 151
ARRDC3          GR-HEYAFSFELPQTP-------LATSFEGRHGSVRYWVKAELHRP-WLLPVKLKKEFTV 158
ARRDC4          GK-HEFPFRFQLPSEP-------LVTSFTGKYGSIQYCVRAVLERP-KVPDQSVKRELQV 162
TXNIP           GNKYEYKFGFELPQGP-------LGTSFKGKYGCVDYWVKAFLDRP-SQPTQETKKNFEV 145
beta-arr1       LGEHAYPFTFEIPPNLPCSVTLQPGPEDTGKACGVDYEVKAFCAEN-LEEKIHKRNSVRL 166
beta-arr2       LGQHAHPFFFTIPQNLPCSVTLQPGPEDTGKACGVDFEIRAFCAKS-LEEKSHKRNSVRL 167
ARRDC1          AGEHSFPFQFLLPATAP--------TSFEGPFGKIVHQVRAAIHTPRFSKDHKCSLVFYI 132
```

```
ARRDC5          AGSHTFDFHFNLPPRLP--------STFTSKFGHVFYFVQASCMGR-EHILAKKRMYLLV 154
Vps26A          TQSRSYDFEFMQVEKP--------YESYIGANVRLRYFLKVTIVRR---LTDLVKEYDLI 150
Consensus             .* *                   .    : . ::.                 :
Arr domain      NNNNNNNNNNNNNNNNNNNNNNNNNNNNNNNNNNNNNNNNNNNNNNNNNNNNNNNNNNN

ARRDC2          IEPVDIN-TPALLAPQAGAREKVARSWYCNRGLVSLSAKIDRKGYTPGEVIPVFAEIDNG 210
ARRDC3          FEHIDIN-TPSLLSPQAGTKEKTLCCWFCTSGPISLSAKIERKGYTPGESIQIFAEIENC 217
ARRDC4          VSHVDVN-TPALLTPVLKTQEKMVGCWFFTSGPVSLSAKIERKGYCNGEAIPIYAEIENC 221
TXNIP           VDLVDVN-TPDLMAPVSAKKEKKVSCMFIPDGRVSVSARIDRKGFCEGDEISIHADFENT 204
beta-arr1       VIRKVQY-APERPGPQPT--AETTRQFLMSDKPLHLEASLDKEIYYHGEPISVNVHVTNN 223
beta-arr2       VIRKVQF-APEKPGPQPS--AETTRHFLMSDRSLHLEASLDKELYYHGEPLNVNVHVTNN 224
ARRDC1          LSPLNLNSIPDIEQPNVASATKKFSYKLVKTGSVVLTASTDLRGYVVGQALQLHADVENQ 192
ARRDC5          QGTSTFHKETPFQNPLFVEAEEKVSYNCCRQGTVCLQIQMERNTFTPGEKVVFTTEINNQ 214
Vps26A          VHQLATY--PDVN--------NSIKMEVGIEDCLHIEFEYNKSKYHLKDVIVGKIYFLLV 200
Consensus                .           :           : :    :   :   : :     .
Arr domain      NNNNNNNN                  CCCCCCCCCCCCCCCCCCCCCCCCCCCCCCCCC

ARRDC2          STRPVLPRAAVVQTQTFMA----RGARKQKRAVVASLAGEPVGPGQRALWQGRALR---- 262
ARRDC3          SSRMVVPKAAIYQTQAFYA----KGKMKEVKQLVANLRGESLSSGKTETWNGKLLK---- 269
ARRDC4          SSRLIVPKAAIFQTQTYLA----SGKTKTIRHMVANVRGNHIASGSTDTWNGKTLK---- 273
TXNIP           CSRIVVPKAAIVARHTYLA----NGQTKVLTQKLSSVRGNHIISGTCASWRGKSLR---- 256
beta-arr1       TNKTVKKIKISVRQYADIC----LFNTAQYKCPVAMEEADDTVAPSSTFCKVYTLTPFLA 279
beta-arr2       STKTVKKIKVSVRQYADIC----LFSTAQYKCPVAQLEQDDQVSPSSTFCKVYTITPLLS 280
ARRDC1          SGKDTSPVVASLLQKVSYK----AKRWIHDVRTIAEVEGAGVKAWRRAQWHEQILVP--- 245
ARRDC5          TSKCIKTVVFALYAHIQYEGFTPSAERRSRLDSSELLRQEANTPVTRFNTTKVVSTFNLP 274
Vps26A          RIKIQHMELQLIKKEITGIG----PSTTTETETIAKYEIMDGAPVKGESIPIRLFLAG-- 254
Consensus         :                                          .
Arr domain      CCCCCCCCCCCCCCCCCCCCCCCCCCCCCCCCCCCCCCCCCCCCCCCCCCCCCCCCCCC

ARRDC2          -IPPVGPSILHCRVLHVDYALKVCVDIPGTSK-LLLELPLVIGTIPLHPFGSRSSSVGSH 320
ARRDC3          -IPPVSPSILDCSIIRVEYSLMVYVDIPGAMD-LFLNLPLVIGTIPLHPFGSRTSSVSSQ 327
ARRDC4          -IPPVTPSILDCCIIRVDYSLAVYIHIPGAKK-LMLELPLVIGTIPYNGFGSRNSSIASQ 331
TXNIP           -VQKIRPSILGCNILRVEYSLLIYVSVPGSKK-VILDLPLVIGSR--SGLSSRTSSMASR 312
beta-arr1       NNREKRGLALDGKLKHEDTNLASSTLLREGAN-REILGIIVSYKVKVKLVVSRGGLLGDL 338
beta-arr2       DNREKRGLALDGKLKHEDTNLASSTIVKEGAN-KEVLGILVSYRVKVKLVVSRGG----- 334
ARRDC1          --ALPQSALPGCSLIHIDYYLQVSLKAPEAT----VTLPVFIGNIAVNHAPVSPRPGLGL 299
ARRDC5          LLLSVSSSTQDGEIMHTRYELVTTVHLPWSLTSLKAKVPIIITSASVDSAICQLS----- 329
Vps26A          --YDPTPTMRDVNKKFSVRYFLNLVLVDEEDRRYFKQQEIILWRKAPEKLRKQRTN---- 308
Consensus                            :                 :.
Arr domain      CCCCCCCCCCCCCCCCCCCCCCCCCCCCCCCCCCCCCCCCCCCCCCCCCCCCCCCCCCC

ARRDC2          ASFLLDWRLGALPERPEAPPEYSE---------VVADTEEAALGQSPFPLPQDPDMSLEG 371
ARRDC3          CSMNMNWLSLSLPERPEAPPSYAE---------VVTE-EQRRNNLAPVSACDDFERALQG 377
ARRDC4          FSMDMSWLTLTLPEQPEAPPNYAD---------VVSE-EEFSRHIPPYPQPPNCEGEVCC 381
```

```
TXNIP          TSSEMSWVDLNIPDTPEAPPCYMD---------VIPE--DHRLESPTTPLLDDMDGSQDS 361
beta-arr1      ASSDVAVELPFTLMHPKPKEEP-------------PHREVPENETPVDTNLIELDTN--- 382
beta-arr2      ---DVSVELPFVLMHPKPHDHIPL---------PRPQSAAPETDVPVDTNLIEFDTNYAT 382
ARRDC1         PPGAPPLVVPSAPPQEEAEAEAAAGGPHFLDPVFLSTKSHSQRQPLLATLSSVPGAPEPC 359
ARRDC5         -------EDGVLPVNPDHQN---------------------------------------- 342
Vps26A         --FHQRFESPESQASAEQPEM---------------------------------------- 327
Consensus                      .
Arr domain     CCCCCCCCCCCCCCCCCC

ARRDC2         PFFAYIQEFRYRPPPLYSEEDPNP-LLGDMRPRCMTC---------------------- 407
ARRDC3         PLFAYIQEFRFLPPPLYSEIDPNPDQSADDRPSCPSR---------------------- 414
ARRDC4         PVFACIQEFRFQPPPLYSEVDPHPSDVEESQPVSFIL---------------------- 418
TXNIP          PIFMYAPEFKFMPPPTYTEVDPCILNNNVQ----------------------------- 391
beta-arr1      DDDIVFEDFARQRLKGMKDDKEEEEDGTGSPQLNNR----------------------- 418
beta-arr2      DDDIVFEDFARLRLKGMKDDDYDD-------QLC------------------------- 409
ARRDC1         PQDGSPASHPLHPPLCISTGATVPYFAEGSGGPVPTTSTLILPPEYSSWGYPYEAPPSYE 419
ARRDC5         ------------------------------------------------------------
Vps26A         ------------------------------------------------------------
Consensus
Arr domain

ARRDC2         --------------
ARRDC3         --------------
ARRDC4         --------------
TXNIP          --------------
beta-arr1      --------------
beta-arr2      --------------
ARRDC1         QSCGGVEPSLTPES 433
ARRDC5         --------------
Vps26A         --------------
Consensus
Arr domain
```

Figure 1.2 Multiple sequence alignment of human arrestin family proteins

ClustalW2 (http://www.ebi.ac.uk/Tools/msa/clustalw2/) was used to generate alignments. PPxY motifs are highlighted in red. The five residues constituting the β-arrestin polar core "phosphate sensor" (Gurevich *et al.*, 2006b) are in orange (Asp^{29}, Arg^{169}, Asp^{290}, Asp^{297}, Arg^{293} in β-arrestin1), as are conserved residues (with the same charge) in α-arrestins (note that all five residues are not conserved in α-arrestins). The two essential residues for β-arrestin binding to β2-adaptin (Phe^{391}, Arg^{395} in β-arrestin1) and the motif for clathrin binding (LIELD in β-arrestin1; residues 376-380)

are underlined. Of these, only the Phe residue is conserved in α-arrestins; it is also underlined. The ARRDC1 residues (Phe^{88}, Gly^{180}, Asn^{191}) recently reported to be required for its membrane targeting (Nabhan *et al.*, 2012) are in green, as are conserved residues. The TXNIP cysteine residue (Cys^{247}) required to form a disulfide bond with thioredoxin (Patwari *et al.*, 2006) is in light blue. Consensus is shown as: *, fully conserved residue; :, stongly similar residues; ., partially conserved residues. The β-arrestin2 PFAM predicted arrestin N- and C-domains are denoted below ("*Arr domain*").

Table 1.2 Comparison of α- and β-arrestins

Similarities	Differences
Primary sequence homology	α-Arrestins lack the endocytic C-tail clathrin- and AP2-interacting motifs present in β-arrestins
Predicted 3D structure (curved β-sandwich) – solved for Vps26 and β-arrestins	α-Arrestins contain WW domain-interacting C-terminal PY motifs not found in β-arrestins
Mediate endocytosis of several cell surface receptors/transporters – e.g. α-arrestins: Hatakeyama *et al.,* (2010); Lin *et al.*, (2008); Nikko and Pelham, (2009); Nikko *et al.*, (2008)	Sequence required for β-arrestin recognition of phosphorylated GPCR C-tail (i.e. phosphate sensor) may not be present in α-arrestins
Determinate intracellular cargo protein trafficking fate	
Mediate ubiquitination of cargo proteins through interaction with E3 ubiquitin ligases	

1.4.2 Lessons from lower eukaryotes

As mentioned above, recent phylogenetic analysis has expanded the tree of known arrestins in eukaryotes, revealing the presence of arrestins in fungi and in all multicellular organisms except plants (Alvarez, 2008). These include members of both the α-arrestin and β-arrestin branches. For example, the fruit fly *Drosophila melanogaster* has two visual arrestins, a non-visual β-arrestin and around fifteen presumed α-arrestins; the nematode worm *Caenorhabditis elegans* has a single β-arrestin and over twenty α-arrestins. To date, it is in lower eukaryotes such as these that the most work has been done to investigate α-arrestin function.

The first α-arrestin to be ascribed a function was PalF, a pH-response regulator protein in the fungus *Aspergillus nidulans* (Herranz *et al.*, 2005; Maccheroni Jr *et al.*, 1997). PalF contains

conserved arrestin N- and C-domains, and was shown to bind directly to the seven-transmembrane domain, putative pH sensor, PalH (Herranz *et al.*, 2005). Mammalian β-arrestin binding to GPCRs directly involves the β-arrestin N-domain, although additional residues in regions including the C-domain contribute to an extensive binding interface and determine receptor binding specificity (Gurevich *et al.*, 1995; Vishnivetskiy *et al.*, 2011; Vishnivetskiy *et al.*, 2004). Similarly, truncated PalF lacking the C-terminal portion produced a moderate interaction with PalH in a yeast two-hybrid assay, but full length PalF was required for full interaction. Moreover, a loss-of-function mutation within the PalF N-domain (Ser86Pro substitution) strongly impaired PalH binding. Ser^{86} is located within the conserved arrestin 'β-strand V', which in mammalian arrestins is essential for GPCR binding (Gurevich *et al.*, 1995). Indeed, mutation of a closely related residue in β-arrestin1 (Val^{53}) similarly impairs the GPCR interaction (Krupnick *et al.*, 1997b). Thus, the structural basis of the arrestin-GPCR interaction may be conserved in α-arrestins.

Interestingly, the PalF-PalH interaction was acutely required for PalH pH-dependent signalling *in vivo*. Furthermore, like the β-arrestins, phosphorylation and ubiquitination of PalF occurred in a manner dependent on signal (pH) and seven-transmembrane protein (PalH). However, there is no apparent role for a G protein in fungal pH signalling, and a potential difference is that PalF had a necessary positive role in the PalH pH-sensitive response, although the ability of β-arrestins to mediate signalling responses is increasingly recognised (section 1.3.1). In a subsequent report, expression of a PalF-ubiquitin fusion protein was found to promote pH signalling activation even in the absence of PalH (Hervas-Aguilar *et al.*, 2010). It seems, then, that PalF does not desensitise PalH; rather, PalF is directly involved in PalH signal transduction in a manner that may depend on endocytosis and coupling to the ESCRT machinery (Herranz *et al.*, 2005; Xu *et al.*, 2004).

Since this first report in fungus, the role of α-arrestins has been further elucidated in studies on various orthologous proteins in the

yeast *Saccharomyces cerevisiae* (Herrador *et al.*, 2009; Lin *et al.*, 2008; Nikko *et al.*, 2009; Nikko *et al.*, 2008). Yeast have eleven candidate α-arrestins, comprising nine so-called arrestin-related trafficking adaptors (ARTs), the yeast orthologue of Vps26 (Pep8), and Spo23 (a protein involved in sporulation) (Aubry *et al.*, 2009). The ARTs have been identified as adaptors for Rsp5, the sole HECT E3 ubiquitin ligase present in yeast. Rsp5 is responsible for the ubiquitination and endocytosis of several plasma membrane transporters and permeases. For example, the manganese transporter, Smf1, is ubiquitinated by Rsp5 in response to its toxic substrate cadmium, leading to Smf1 endocytosis. Smf1 ubiquitination is dependent on ART2 or ART8 (also known as Ecm21 and Csr2, respectively), both of which bind Rsp5 WW domains via their PPxY motifs (Nikko *et al.*, 2008). ART2 was found to bind to Smf1, providing the link between Smf1, Rsp5 and the facilitation of ubiquitination/endocytosis. Indeed, wild-type ART2 was able to rescue Smf1 endocytosis in an arrestin null background, whereas a mutant ART2 lacking its three PPxY motifs was not. The question of whether ART8 also binds Smf1 was not investigated (Nikko *et al.*, 2008). It is notable that the efficient binding of ART2 to Smf1 was dependent upon the constitutive phosphorylation of Smf1. This suggests that yeast ARTs and mammalian β-arrestins may share a dependence on interaction with phosphate modules for their recruitment to cargo proteins. Whether there are also structural parallels between ART-Smf1 binding and that of β-arrestins-GPCRs is unclear since the structure of Smf1 is unknown. Mammalian orthologues of Smf1, the Natural resistance-associated membrane protein (Nramp)/DMT family of divalent-metal transporters (Forbes *et al.*, 2001) are predicted to contain 10-12 transmembrane domains that form a hydrophobic core (Cellier *et al.*, 1995); assuming this domain organisation to be conserved in Smf1, it would appear that ART binding may be structurally distinct to the β-arrestin-GPCR association.

Following on from this study, glutathione S-transferase (GST) pull-down experiments tested the interaction of all the ARTs except

ART4 for interaction with Rsp5; of those tested all but ART9 demonstrated an interaction and, in the case of ART1 and ART2, this was confirmed to require the C-terminus (i.e. likely involvement of ART PPxY motifs) (Lin *et al.*, 2008). Furthermore, similar roles were observed for ART1 and ART2 in the regulation of several specific amino acid transporter cargoes. ART1 (also called Cvs7) is recruited to the plasma membrane in response to changes in nutrient availability and is required for the endocytic downregulation of amino acid transporters Can1 and Mup1 to the vacuole (the yeast equivalent of the lysosome), in a manner dependent on ART1 interaction with Rsp5 (Lin *et al.*, 2008). ART1 or ART2 also mediate stimulus-dependent endocytosis of another amino acid transporter, Lyp1. Since a degree of redundancy in ART roles appeared in these studies, a subsequent report tested the ability of individual ARTs to rescue various functions in an arrestin-null yeast background (Nikko *et al.*, 2009). This again revealed a role for ARTs in specific cargo endocytosis/downregulation: ART5 was required for inositol-induced Itr1 transporter endocytosis/degradation; internalisation of the glucose transporter Hxt6 was mediated by ART4 or ART8 depending on the conditions. A similar role was also elucidated for ART3 (also called Aly2) in the regulation of the aspartate/glutamate transporter, Dip5 (Hatakeyama *et al.*, 2010). As previously observed (Nikko *et al.*, 2009), ART3 also binds the Rsp5 ligase via a PPxY motif-WW domain interaction, and was found to be ubiquitinated by Rsp5 (Hatakeyama *et al.*, 2010). ART3 was shown to interact with phosphorylated Dip5 in an aspartate signal-dependent manner, thereby acting as an adaptor for the recruitment of Rsp5. Rsp5 then ubiquitinates Dip5, promoting its endocytosis and vacuolar degradation.

Although the structures of the ART cargo proteins described above (Can1, Mup1, Lyp1, Itr1, Hxt6 and Dip5) have not been experimentally determined, they are thought to be multipass membrane permeases, typically with 12 TM-spanning domains (based on UniProtKB database predictions). Thus, they may bear

little structural relation to GPCRs, suggesting that ART binding to these transporters may be via an unrelated mechanism.

These studies have led to the development of a model for the mode of action of α-arrestins, in particular in yeast (Figure 1.4), whereby α-arrestins act as adaptors for the recruitment of NEDD4 ubiquitin ligases to plasma membrane cargo, thereby mediating cargo ubiquitination, resulting in internalisation and downregulation. Within this model, it is notable that several α-arrestins have themselves reported to be ubiquitinated by the NEDD4 ligase with which they interact, and that this may represent a dynamic, signal-dependent modulator of α-arrestin function (Becuwe *et al.*, 2012).

In addition to this emerging paradigm, a further mechanism by which ARTs may regulate cargo protein signalling and/or trafficking was identified for ART9 in yeast (also called Rim8; orthologue of the fungal protein PalF, see above) (Herrador *et al.*, 2009). As was observed in fungi (Herranz *et al.*, 2005), ART9 interacts with the putative seven-transmembrane domain pH sensor, Rim21 (PalH in fungi). Interestingly, ART9 was also found to interact directly with Vps23, and coimmunoprecipitated with both Vps23 and Vps28, components of the ESCRT-I complex (Herrador *et al.*, 2009). Furthermore, ART9 overexpression resulted in the redistribution of Vps23 from endosomal structures to the plasma membrane where it colocalised with ART9. From this, the authors proposed a model whereby ART9 recruits the ESCRT machinery to Rim21 at the plasma membrane, allowing Rim21 signalling through ESCRT components, although direct evidence for a Rim21-ESCRT signalling link remains to be uncovered.

Another apparent exception to the paradigm is the α-arrestin-mediated regulation of the intracellular trafficking of the general amino acid permease 1 (Gap1) in yeast (O'Donnell *et al.*, 2010). Both ART3 and ART6 (also called Aly2, Aly1, respectively) were found to interact with Gap1 and, in contrast to the reports described above, increased the levels of Gap1. ART3 and ART6 localised to endosomes, and were required for the efficient recycling of Gap1 from endosomes to the *trans*-Golgi but not Gap1 endocytosis. This

led to the proposal that ART3/6 maintain intracellular and plasma membrane levels of Gap1 via the diversion of the transporter away from a trafficking itinerary that results in vacuolar degradation. As described above, with respect to an alternative specific cargo (Dip5), ART3 acts in agreement with the above paradigm, mediating cargo endocytosis (Hatakeyama *et al.*, 2010). Thus, individual α-arrestins may mediate spatially and mechanistically distinct trafficking events in a cargo-specific manner.

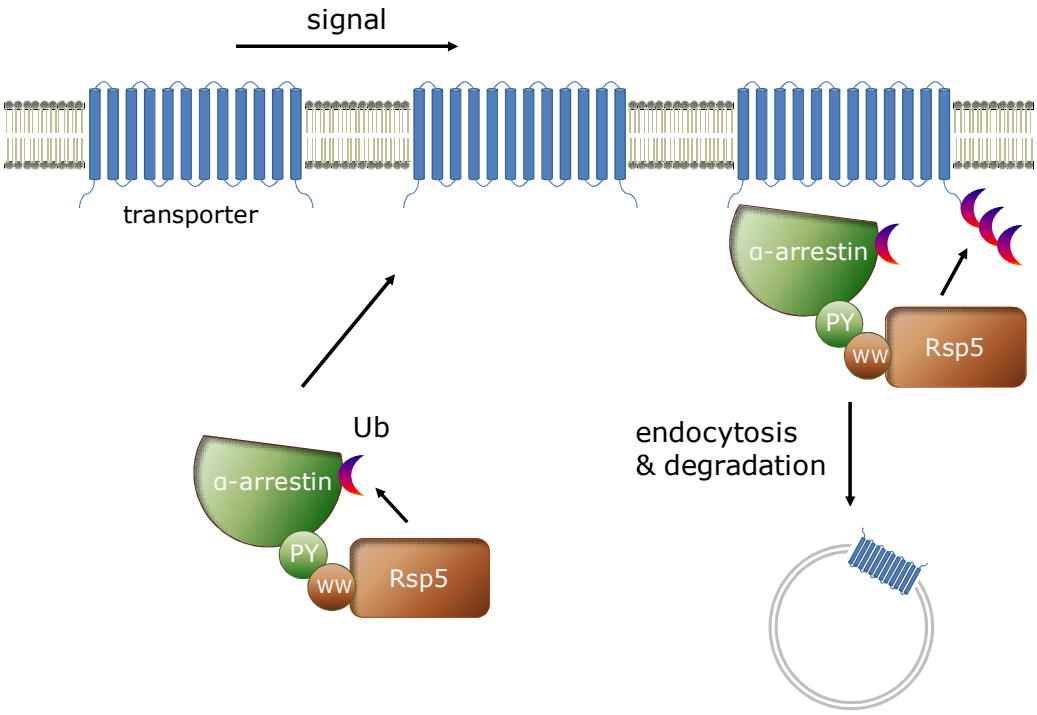

Figure 1.4 α-Arrestins are cargo-specific ubiquitin ligase adaptors

α-Arrestins, in particular in yeast (also called arrestin-related trafficking adaptors, ARTs) act as adaptors for HECT domain E3 ubiquitin ligases of the NEDD4 family, whose sole member in yeast is Rsp5. The PPxY motifs of α-arrestins and WW domains of E3 ligases mediate the interaction, which may result in the ubiquitination of the α-arrestin (Becuwe *et al.*, 2012; Gupta *et al.*, 2007; Hatakeyama *et al.*, 2010; Kee *et al.*, 2006; Lin *et al.*, 2008; Rauch *et al.*, 2011). In response to environmental cues, for example changes in pH or nutrient availability, α-arrestins are recruited to cargoes (e.g. amino acid transporters) at the plasma membrane, a process that may require cargo phosphorylation (Hatakeyama *et al.*, 2010; Lin *et al.*, 2008; Nikko *et al.*, 2008). This results in cargo ubiquitination, which acts as a trigger for endocytosis and subsequent degradation.

1.4.3 α-Arrestins in man

Knowledge pertaining to the human α-arrestins is currently limited, although a few recent reports suggest that the model presented by yeast/fungal α-arrestins may represent a reasonable functional 'template' for their actions in mammalian cells.

1.4.3.1 Primary structure

As mentioned in section 1.4.1, although they share a moderate degree of homology with β-arrestins, the human α-arrestins are clearly a distinct subset within the arrestin clan that appeared earlier in evolutionary history. The α-arrestins themselves share a similar putative domain organisation (see Figure 1.3). They all possess predicted arrestin N- and C-domains, as well as an additional C-terminal 'tail' region that contains two PPxY motifs, except for ARRDC5 and Vps26 which are shorter and do not contain any PPxY motifs. The highest protein sequence identities are between ARRDC2/3/4 at around 50% (see Figures 1.1 and 1.2). At a local level ARRDC2/3/4 display marked similarities too, such as a consensus surrounding the second PPxY motif – P**PPLY**SEXDP(N/H)P (PPxY motif in bold) present in all three – suggesting that the structural integrity of this and possibly other motifs may underlie important conserved functions (in the case of the PPxY motif, presumably interaction with WW domains; see section 1.4.3.3 below). Differences exist, however, such as the lack of PPxY motifs in ARRDC5 and Vps26, and lower overall sequence identity between different members, suggesting that the α-arrestins may have distinct characteristics and roles.

1.4.3.2 Divergent human α-arrestins: TXNIP and Vps26

TXNIP

TXNIP (also called thioredoxin-binding protein-2 (TBP-2) or vitamin D3 up-regulated protein 1 (VDUP1)) is a mammalian α-arrestin that is homologous to the ARRDC proteins; it has predicted arrestin N-

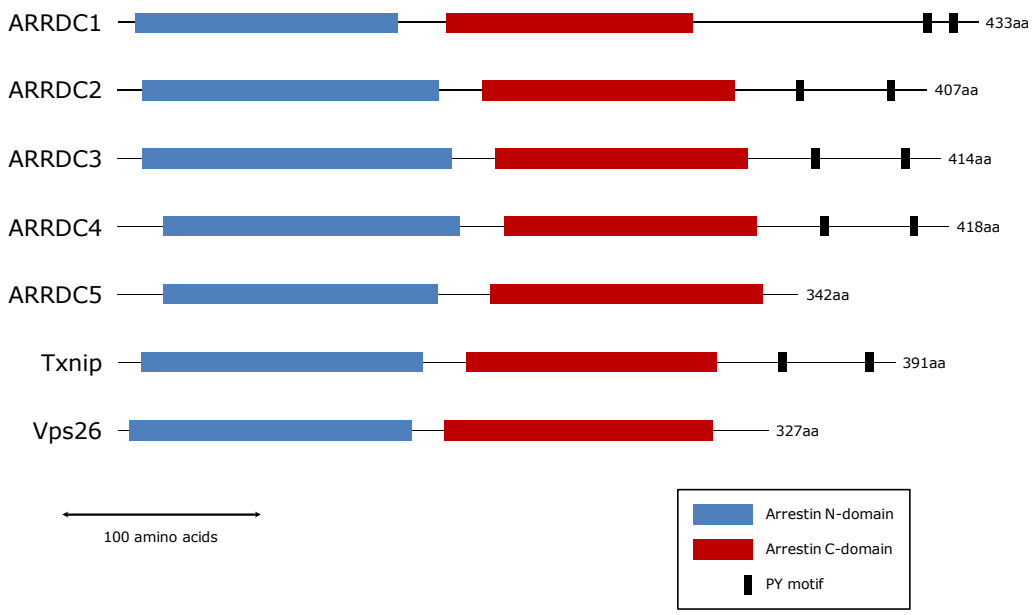

Figure 1.3 Domain organisation of the human α-arrestin proteins

PFAM predicted arrestin N- and C-domains are indicated with blue and red boxes, respectively. For Vps26, X-ray crystal structures indicate that these domains do indeed give an arrestin fold (Collins *et al.*, 2008; Shi *et al.*, 2006). "PY" motifs (black boxes) are conserved PPxY sequences that have been shown to mediate interaction with WW domains.

and C-domains and two PPxY motifs within its C-terminus. Additionally, TXNIP interacts with thioredoxin and inhibits thioredoxin disulphide reducing activity (Junn *et al.*, 2000; Nishiyama *et al.*, 1999). TXNIP interacts with the reduced form of thioredoxin via a disulphide bond involving TXNIP Cys^{247}, a residue that is not conserved in other arrestins (Figure 1.2), and it appears that this interaction is unique to TXNIP; ARRDC2, ARRDC3 and ARRDC4 do not interact with thioredoxin (Oka *et al.*, 2006; Patwari *et al.*, 2006).

Thioredoxin is a small ubiquitous antioxidant protein, and through its interaction with and inhibition of thioredoxin, TXNIP has critical roles in metabolism and controlling the cell redox state (Patwari *et al.*, 2012). TXNIP expression is suppressed by insulin (Parikh *et al.*,

2007), induced by high glucose levels (Schulze *et al.*, 2004; Stoltzman *et al.*, 2008) and upregulated in diabetes (Parikh *et al.*, 2007). The induction of TXNIP expression by glucose forms part of a negative feedback mechanism, whereby TXNIP inhibits insulin-stimulated glucose uptake into fat and muscle (Parikh *et al.*, 2007; Zhou *et al.*, 2010). Thus, TXNIP has been linked to insulin resistance, supported by the finding that TXNIP-null mice are protected against diabetes (Chen *et al.*, 2008). Indeed, elsewhere TXNIP-null mice were found to be hypoglycaemic, hypoinsulinaemic and exhibit enhanced glucose uptake in insulin-responsive tissues (Chutkow *et al.*, 2008).

The mechanisms underlying TXNIP actions in glucose homeostasis remain unclear. A mutant version of TXNIP lacking Cys^{247} retains the ability to inhibit glucose uptake (Patwari *et al.*, 2009). Inhibition of glucose uptake is thus independent of TXNIP interaction with thioredoxin; rather, it is dependent upon the presence of TXNIP arrestin N- and C-domains (Patwari *et al.*, 2009). Interestingly, although ARRDC4 does not bind thioredoxin (Patwari *et al.*, 2006), it too was a potent inhibitor of glucose uptake (ARRDC2 or ARRDC3 had no effect), indicating the potential involvement of conserved arrestin domains in glucose metabolism. The manner in which the arrestin architecture may regulate glucose uptake is not known, although it could be hypothesised that α-arrestins interact with and influence glucose transporter activity (for example, endocytosis/trafficking of the two most abundant glucose transporters, GLUT1/4). A precedent for this has already been described in yeast (section 1.4.2): the α-arrestins ART4 and ART8 are required for endocytosis of the glucose transporter Hxt6 (Nikko *et al.*, 2009). However, GLUT4 or GLUT1 levels were largely unaffected by TXNIP deletion in mice (Andres *et al.*, 2011; Yoshioka *et al.*, 2007); thus, whether the scaffolding of glucose transporters by yeast ARTs is conserved in mammalian α-arrestins is unknown.

Vps26

The retromer is a conserved pentameric complex required for the retrograde sorting of cargo proteins, exemplified by the cation-independent mannose 6-phosphate receptor and Shiga toxin, from late endosomes to the *trans*-Golgi network (TGN) (Attar *et al.*, 2011). The function of the retromer is crucial to several developmental and disease-related events, including the generation of Wnt gradients and sorting of enzymes involved in Alzheimer's disease. Mammalian retromer comprises two subcomplexes: a cargo-recognition heterotrimer consisting of Vps26-Vps29-Vps35; and a membrane-deforming module comprising sorting nexin-bin/amphiphysin/rvs (SNX-BAR) proteins (typically SNX1 and SNX2). As noted in section 1.4.1, the crystal structure of Vps26 – a member of the cargo recognition complex – revealed that it has an arrestin fold (Collins *et al.*, 2008; Shi *et al.*, 2006), and it was later placed in a phylogenetic grouping with the α-arrestins (Alvarez, 2008).

The identification of an α-arrestin as a component of the retromer cargo-recognition complex supports the proposed role of the arrestin fold, found in α- and β-arrestins, as a conserved architecture for intracellular cargo protein trafficking. It could be hypothesised that β-arrestins arose later in evolution as a result of adaptations, such as the polar core and clathrin/AP2-binding motifs (not present in Vps26/α-arrestins; Figure 1.2), that enable their interaction with and regulation of GPCRs, and that α-arrestins do not therefore share these specific capabilities. However, a recent investigation has provided a tentative refutation of this hypothesis (Feinstein *et al.*, 2011). As has been described for several GPCRs (section 1.3.1), signalling by the parathyroid hormone (PTH) receptor (PTHR) – in response to the clinically-used PTH analogue, PTH(1-34) – was found to have a β-arrestin-dependent component; β-arrestin1 overexpression potentiated, rather than inhibited, cAMP accumulation induced by PTH(1-34). This corresponded to the persistence of a PTHR-β-arrestin1 complex on endosomes following PTH(1-34)-induced internalisation, and the authors concluded that the prolonged signalling detected arose from PTHR-β-arrestin1 complexes that remained on endosomes, although the localisation of

the unit responsible for continued signalling was not directly demonstrated. Interestingly, overexpression of various retromer components attenuated PTH(1-34)-induced cAMP accumulation, and conversely siRNA knockdown of the retromer prolonged the response, leading to the proposal that the retromer terminates PTHR signalling on endosomes. A β-arrestin1 mutant that has increased affinity for PTHR was able to rescue the observed attenuation of PTHR cAMP response caused by retromer overexpression, suggesting that β-arrestin1 and retromer may compete for PTHR binding. Agonist-dependent interaction of Vps29 with PTHR was detected by coimmunoprecipitation over a similar time-scale to the observed attenuation effect of the retromer, although whether this represents a direct association was not tested. A candidate for the direct mediator of the retromer-PTHR interaction is Vps26. Given its structural similarity to β-arrestins, Vps26 could conceivably compete with β-arrestin1 for PTHR binding. In future experiments it will be intriguing to determine whether Vps26 does directly bind PTHR, and to elaborate on the possible mechanism of this interaction. Detection of a Vps26-PTHR interaction would support the idea that GPCR binding ability extends to the α-arrestins.

1.4.3.3 Initial identification of ARRDC proteins

As with many proteins, the initial identification of several human ARRDCs was through the observation of physiological or pathophysiological circumstances in which their gene expression is altered. The first of these was *ARRDC4*, whose expression was identified as being significantly lowered in hepatocellular carcinoma (HCC), hence its original designation as *down-regulated in advanced hepatocellular carcinoma* (*DRH1*) (Yamamoto *et al.*, 2001). ARRDC4 was observed within the cytoplasm when expressed exogenously as a green fluorescent protein (GFP) fusion in COS-7 cells, and was frequently downregulated at a late stage of HCC development. Next, rat *ARRDC2* was discovered in a screen for genes responsive to the hallucinogen, lysergic acid diethylamide (LSD) (Nichols *et al.*, 2004).

ARRDC2 (denoted therein as *induced by lysergic acid diethylamide-1*; *ILAD-1*) expression increased significantly (around two-fold) in different brain regions in response to LSD. These increases were partially blocked by co-incubation with antagonists at 5-HT_{2A} receptors (GPCRs involved in neurotransmission), providing the first tentative link between ARRDCs and GPCR function. The mechanism by which 5-HT_{2A} receptors may be involved in regulating *ARRDC2* expression was not investigated.

Also identified was ARRDC3, originally as a homologue of TXNIP. ARRDC3 localised to the plasma membrane, endosomes and lysosomes when expressed exogenously in HeLa, HEK-293, COS-7 or CHO cells. In contrast to TXNIP, ARRDC3 did not bind to thioredoxin, but *ARRDC3* expression was upregulated in HL-60 cells in response to vitamin D3 or activation of peroxisome proliferator-activated receptor-γ (PPARγ) (Oka *et al.*, 2006). Thus, ARRDC3 may have a role in energy metabolism and cell growth inhibition. The *ARRDC3* gene was also reported as downregulated early on in breast cancer (Draheim *et al.*, 2010). Loss of *ARRDC3* expression was correlated with tumour grade, metastatic potential and recurrence; furthermore, overexpression or knockdown of *ARRDC3* expression had potent antagonistic effects on *in vivo* markers of tumourigenicity. In this study, ARRDC3 was coimmunoprecipitated with the cell surface adhesion molecule, β-4 integrin (ITGβ4), a protein strongly associated with the progression of cancer. ARRDC3 preferentially associated with phosphorylated ITGβ4, leading to ITGβ4 internalisation, ubiquitination and proteasome-dependent degradation, hence supporting the purported tumour suppressor activity of ARRDC3.

Collectively, these early studies provided the first indication that human ARRDCs may perform important roles whose dysregulation could lead to various physiological impairments, thus warranting their further investigation.

1.4.3.4 Possible molecular functions of ARRDCs

ARRDC3 mediates β_2AR degradation

The first detailed investigation into the molecular function of a human ARRDC investigated the role of ARRDC3 in the regulation of the prototypic GPCR, β2AR (Nabhan *et al.*, 2010). ARRDC3 was identified in a genome-wide screen for short hairpin RNAs (shRNAs) that inhibited β_2AR degradation. In the screen, a truncated version of the receptor (β_2ARt) was used that lacked the C-terminal recycling sequence, the PDZ-binding motif (DSLL); hence, prolonged agonist stimulation resulted in efficient degradation of β_2ARt. However, in cells expressing *Arrdc3*-specific shRNA, immunostaining and fluorescence-activated cell sorting (FACS) analysis indicated that stimulated β_2ARt levels were higher (>20%) than in cells expressing control shRNAs. Furthermore, siRNA knockdown of ARRDC3 drastically inhibited the agonist-stimulated degradation of β_2ARt, as detected by immunoblotting, and was also suggested to inhibit the degradation of full-length β_2AR, although in this case the effect was expectedly much less pronounced. Hence, ARRDC3 may be required for the degradation of β_2AR.

ARRDC3 was also found to affect β_2AR ubiquitination; siRNA knockdown of ARRDC3 inhibited the agonist-stimulated increase in β_2AR ubiquitination, whereas efficient knockdown of another ARRDC, ARRDC1, had no effect. This suggested that the effect on β_2AR may be specific to ARRDC3, although given that the greater protein sequence similarities exist between ARRDC2/3/4, it may have been more informative to also test for an effect of ARRDC2 or ARRDC4 knockdown. Given the similarities between ARRDC2/3/4, it would also have been informative to know whether the siRNAs used to target ARRDC3 were indeed specific, or also affected ARRDC2 and/or ARRDC4 expression levels.

As for many of the α-arrestins present in lower eukaryotes mentioned in section 1.4.2, ARRDC3 was found to interact with an E3 ubiquitin ligase – the HECT ligase NEDD4 – via its PPxY motifs; ARRDC3 coimmunoprecipitated with NEDD4 in basal conditions in a

manner dependent on the presence of ARRDC3 PPxY motifs. As for the yeast/fungal α-arrestins, the authors proposed that in so doing, ARRDC3 may act as an adaptor for the recruitment of NEDD4 to the activated receptor (in this case, β_2AR), in order to promote receptor ubiquitination and lysosomal degradation. To support this, they showed that ARRDC3 coimmunoprecipitates with β_2AR in an agonist-dependent manner. Importantly, this is the first report of an interaction between any ARRDC and a GPCR; moreover, as for β-arrestins, the apparent interaction was strongly promoted by receptor activation. In addition, a double mutant at the ARRDC3 PPxY motifs that did not coimmunoprecipitate NEDD4 was used to test the role of the ARRDC3-NEDD4 interaction on β_2AR ubiquitination and degradation. It was found that overexpression of the PPxY mutant ARRDC3 drastically inhibited agonist-stimulated β_2AR ubiquitination and degradation, whereas wild-type ARRDC3 had no observable effect. In support of these data, siRNA knockdown of ARRDC3 expression rendered the apparent coimmunoprecipitation between β_2AR and NEDD4 (which, albeit weak, appeared to occur in an agonist-dependent manner) undetectable. It is notable here that, as mentioned in section 1.3.1, the same adaptor role in recruiting NEDD4 to the activated β_2AR had been previously reported for β-arrestin2 (Shenoy *et al.*, 2008). The same result had been reported in this study but for β-arrestin2: siRNA knockdown of β-arrestin2 appeared to abolish the β_2AR-NEDD4 interaction. To address this, Nabhan and co-workers performed the same experiment: siRNA was used to knockdown β-arrestin2 and, in this case, no effect upon the β_2AR-NEDD4 coimmunoprecipitation was observed (Nabhan *et al.*, 2010). Thus, they concluded that ARRDC3, not β-arrestin2, is crucial for NEDD4 recruitment to β_2AR and subsequent receptor ubiquitination and degradation. The reason for the disparity in these results is unclear, although it may stem from the use of different siRNAs and immunoprecipitation conditions. In particular, the β-arrestin2-specific siRNA used by Shenoy and colleagues (2008) appeared to produce a marked reduction in β-arrestin2 expression, as evidenced

by immunoblotting, thus giving an apparent effect on the β_2AR-NEDD4 interaction. In contrast, Nabhan and colleagues (2010) used a different siRNA that was much less efficient at reducing β-arrestin2 expression (indeed it appeared to have more effect on β-arrestin1 levels), making it difficult to detect even a genuine effect. Therefore, it remains unresolved as to whether any one arrestin family member is solely responsible for performing the adaptor role between β_2AR and NEDD4, or whether functional overlap, or indeed cooperativity (see note on arrestin oligomerisation, section 1.3.1), between arrestin members may occur.

ARRDC3: a novel regulator of energy metabolism?

Following on from the study by Nabhan et al. (2010), a subsequent article reported ARRDC3 as a regulator of obesity and energy expenditure via its actions on β-adrenoceptors (Patwari *et al.*, 2011). A precedent for human α-arrestin involvement in metabolism already existed prior to this report in the established ability of TXNIP to modulate glucose metabolism *in vivo* (described in section 1.4.3.2), a role that may also be held by ARRDC4 (Chutkow *et al.*, 2008; Hui *et al.*, 2008; Patwari *et al.*, 2009). ARRDC3 – or indeed ARRDC2 – does not appear to affect glucose transport (Patwari *et al.*, 2009), although a potential link between ARRDC3 and energy metabolism had previously been noted (Oka et al., 2006; section 1.4.3.3). It is worth mentioning that roles in metabolism may be conserved throughout the arrestin family (Patwari *et al.*, 2012), evidenced by the fact that β-arrestin knockout mice are insulin-resistant and that insulin receptor signalling is directly modulated by β-arrestin (Luan *et al.*, 2009; Usui *et al.*, 2004).

Patwari and colleagues (2011) identified a potential metabolic role for ARRDC3 through a genome-wide linkage scan in which an association between single polynucleotide polymorphisms (SNPs) at the *ARRDC3* locus and high body-mass index (BMI) in males was discovered. The authors went on to assess the tissue distribution of *ARRDC3* in human tissues: Northern analysis indicated *ARRDC3* expression in various tissues (including skeletal muscle, kidney, liver,

placenta and lung) but notably not in brain. However, *ARRDC3* was expressed in adipose tissue and, interestingly, this expression positively correlated with BMI in male omental (central) adipose tissue. This implicated ARRDC3 as a potential metabolic regulator in this and maybe other tissues. To test this, the expression of *ARRDC3* was assessed in mice subject to either a fed or fasting regimen. Microarray, real-time PCR and Northern analysis all indicated that *ARRDC3* levels are elevated in the fasting state, most prominently in visceral (epididymal) fat (5.6-fold), but also significantly in brown fat and skeletal muscle. Following this, the authors hypothesised that ARRDC3 deficiency may protect against the development of obesity. Using a mouse strain prone to age-induced obesity, they show that *Arrdc3* null (-/-) males have a significantly lower total body mass than their wild-type counterparts throughout development (15% lower at five weeks of age; 29% lower at twenty weeks). The effect was less pronounced in female mice: no effect was observed at an early stage, but *Arrdc3* null females were resistant to the development of obesity over time, and by twenty weeks total body mass was 29% lower than in wild-type mice. These differences were reflected in the fact that percentage body fat was lower in *Arrdc3* null mice in both males and females.

The mechanism by which *Arrdc3* deficiency may confer resistance to obesity in mice was next investigated. Serum thyroid hormone and catecholamine levels were largely unaffected by the lack of *Arrdc3*, suggesting that ARRDC3 may primarily act downstream of hormone activation at the site of effector tissues in which it is expressed. In agreement with this, several catecholamine-induced genes involved in thermogenesis were found to be upregulated in the brown and white adipose of *Arrdc3* null mice, and mice heterozygous for *Arrdc3* had higher oxygen uptake and heat production. As previously shown (Nabhan *et al.*, 2010), Patwari and colleagues (2010) detected coimmunoprecipitation of ARRDC3 with β_2AR *in vitro*. In this case, immunoprecipitation was performed under unstimulated conditions; whether the interaction is enhanced by β_2AR stimulation was not tested. ARRDC1 and ARRDC4 were also

found to coimmunoprecipitate with β_2AR under these conditions (TXNIP did not; ARRDC2 was not tested). Interestingly, ARRDC3 also coimmunoprecipitated with β_3AR, a GPCR that lacks the phosphorylation sites present in β_1AR and β_2AR that are required for interaction with β-arrestins and desensitisation (Liggett *et al.*, 1993; Nantel *et al.*, 1993). Consistent with the putative role for ARRDC3 in downregulating receptor signalling (Draheim *et al.*, 2010; Nabhan *et al.*, 2010), *Arrdc3* deficiency potentiated the adrenoceptor stimulation of lipolysis, as measured by the increase in glycerol release in response to noradrenaline in *ex vivo* mouse adipose tissue. Levels of cyclic adenosine monophosphate (cAMP), a common second messenger produced in response to β-adrenoceptor signalling, were also elevated in *Arrdc3* null mice adipose compared to controls.

Collectively, these data point to ARRDC3 being a downregulator of β-adrenoceptor signalling whose absence results in increased thermogenesis and therefore may protect against obesity.

ARRDCs as adaptors for PPxY-dependent viral budding

The final stage in the release of retroviruses from infected cells involves fusion with the host cell plasma membrane, budding and scission of a nascent virion particle. Topologically, the membrane deformation and scission of a lipid encased nascent vesicle involved in these events resemble those mediated by the ESCRT machinery in the formation of ILVs of multivesicular bodies MVBs (section 1.2.3), and it has been shown that many viruses co-opt ESCRT components in order to perform these functions (Martin-Serrano *et al.*, 2011). The factors involved are short amino acid sequences called late-budding activity domains (L-domains), present in retroviral group-specific antigen (Gag) proteins (Demirov *et al.*, 2004). At least three categories of L-domains exist in different viruses that bind various components of the ESCRT machinery: these include P(S/T)AP L-domains, which recruit the ESCRT-I subunit tumour susceptibility gene 101 protein (Tsg101), and LYPXL L-domains, which interact with AIP1/ALIX, an ESCRT accessory

protein (reviewed in Demirov and Freed, 2004). The third type of L-domains are PPxY motifs. These are thought to link Gag proteins to the ESCRT machinery via interaction with several NEDD4 family HECT E3 ubiquitin ligases (NEDD4, WWP1, WWP2 and AIP4/Itch). However, direct binding between the E3 ligases and ESCRT components has not been detected: thus, a recent report addressed this by testing whether α-arrestins may act as ligase-ESCRT adaptors in the context of PPxY-dependent viral budding (Rauch *et al.*, 2011).

First, the authors used a yeast two-hybrid system to assay for α-arrestin interactions with the relevant HECT E3 ligases NEDD4, WWP1, WWP2 and AIP4. All α-arrestins tested (ARRDC1, ARRDC2, ARRDC3, ARRDC4 and TXNIP) interacted with each ligase, except for the pairings of ARRDC2-AIP4 and ARRDC4-WWP2. GST experiments using the α-arrestins to pull-down the WW domains of each respective ligase confirmed that all these interactions were direct; in this case even ARRDC2-AIP4 and ARRDC4-WWP2 were shown to interact. The interactions detected were presumed to involve contact between α-arrestin PPxY motifs and ligase WW domains. This was at least supported by the demonstration that an ARRDC1 mutant lacking the C-terminus (containing the two PPxY motifs) was no longer able to produce an interaction with any of the ligases in the yeast two-hybrid assay.

Importantly, out of a panel of all known ESCRT components tested in yeast two-hybrid experiments, ARRDC1, ARRDC2 and ARRDC3 appeared to interact with ALIX, and ARRDC1 also interacted with Tsg101. ARRDC1 is the only human α-arrestin that contains a PSAP motif (in the C-terminus); truncated ARRDC1 lacking the C-terminus failed to interact with Tsg101, implying that the PSAP motif may be responsible for the interaction. All the α-arrestins mentioned above were also found to interact to some degree in yeast two-hybrid experiments with ubiquitin. This suggested that they may be ubiquitinated, or may contain ubiquitin-binding motifs, although this has not been reported elsewhere and was not investigated further by Rauch and Martin-Serrano (2011). In addition, GST pull-down

experiments indicated that ARRDC1 is itself modified by ubiquitin, and that this may be performed by WWP1. In general, this reinforces the idea that the α-arrestins may be involved in the endocytic sorting machinery.

The authors next investigated the potential role of α-arrestins, notably ARRDC1, in viral budding. They presented evidence that ARRDC1 may be recruited to the site of viral assembly: exogenously expressed, fluorescent protein-tagged ARRDC1 in HEK-293 cells redistributed from an intracellular pattern to the plasma membrane upon coexpression with Ebola virus matrix protein VP40. This redistribution required the presence of the PTAPPEY motif in VP40, suggesting that PPxY-dependent viral budding may involve α-arrestin recruitment to the plasma membrane via interaction with a HECT E3 ligase such as WWP1. In support of this, overexpression of ARRDC1, ARRDC2 or ARRDC3 caused a dose-dependent inhibition of the infectious particle production of another PPxY-dependent virus, murine leukaemia virus (MLV). This suggested that multiple α-arrestins may act redundantly as adaptors for PPxY-dependent viral budding; this was further indicated by the fact that targeted siRNA knockdown of individual α-arrestins had no effect on virus budding efficiency.

In addition to establishing a potential role for human α-arrestins in viral budding, the study by Rauch and Martin-Serrano (2011) further developed our knowledge of α-arrestin interactions that point strongly towards their involvement in the endo-lysosomal system. These include their ability to bind to multiple different HECT E3 ligases and be modified by ubiquitin, possibly by those same ligases. Also, interaction with members of the ESCRT machinery, as noted previously for an α-arrestin (ART9) in yeast (Herrador et al., 2009; see section 1.4.2), further suggests that the human α-arrestins may function in the sorting of endocytic cargo proteins, thus adhering to the emerging paradigm in lower eukaryotes.

ARRDC1 mediates microvesicle budding

Cells release a number of membrane-bound particles into the extracellular space, including endosome/MVB-derived vesicles (exosomes), non-endosome/MVB-derived vesicles (microvesicles or microparticles) and apoptic bodies (György *et al.*, 2011). Although far from fully understood, these particles may contain cellular proteins, RNAs and mRNAs that mediate intercellular communication for a variety of biological functions. Recent observations suggest that they share characteristics with virus particles, such as biophysical properties, biogenesis and the ability to transfer biological information between cells (Meckes *et al.*, 2011).

As a corollary to the role described for ARRDC1 in viral budding (Rauch *et al.*, 2011), it has been reported that ARRDC1 mediates the formation and release of a distinct type of extracellular particle, termed ARRDC1-mediated microvesicles (ARMMs) (Nabhan *et al.*, 2012). ARRDC1 was previously found to interact with the ESCRT-I component, Tsg101, likely via its C-terminal PSAP motif (Rauch *et al.*, 2011). Nabhan et al. (2012) corroborate this claim, and report that ARRDC1 targets to the plasma membrane and that the overexpression of ARRDC1 stimulates redistribution of Tsg101 from the cytosol to the plasma membrane in a manner requiring the ARRDC1 PSAP motif. The authors show that ARRDC1 can be packaged into microvesicles in a manner dependent upon the ARRDC1-Tsg101 interaction, revealing a potential link with retroviral budding, in which the retroviral Gag protein recruits Tsg101 via an equivalent motif (PTAP). The apparent plasma membrane targeting of ARRDC1-Tsg101 suggests that ARMMS may bud at this site rather than from an intracellular location (for example, endosomes/MVBs), hence their designation as microvesicles, not exosomes. This is supported by the lack of late endosomal markers present in ARMMS. Nonetheless, ARMMS release is dependent upon the ESCRT machinery (demonstrated for Tsg101 and the Vps4 ATPase) and is enhanced by the NEDD4 family E3 ligase, WWP2, which interacts with and ubiquitinates ARRDC1.

There are notable similarities between ARMMs release and retroviral budding: plasma membrane location, requirement for

ESCRT components – including the P(S/T)AP motif-driven recruitment of Tsg101 – and involvement of NEDD4 family ligases. This led the authors to hypothesise that Gag proteins may have evolved to mimic ARRDC1 in order to hijack what appears to be an intrinsic cellular mechanism for plasma membrane budding.

1.6 Objectives

The emergence of α-arrestins as important novel regulators of protein trafficking and signalling has been described above. Although the majority of these data come from studies in lower eukaryotes, the existence of α-arrestins in man begs the question of whether these proteins perform similar, important roles in the regulation of human cellular functions. The few existing reports detailed above ascribe to the importance of human ARRDCs and their likely mechanistic similarity in function to lower eukaryotic α-arrestins. In particular, the probable structural conservation between arrestin family proteins is noted, and it is hypothesised that this may result in a similar repertoire of interaction partners between α-arrestin orthologues.

The following thesis outlines characterisation of the human α-arrestin, ARRDC2. Initial experiments investigated ARRDC subcellular localisation, which has been poorly addressed thus far in the literature, focussing on ARRDC2. Through the use of a panel of compartment-specific markers in combination with fluorescent protein-tagged ARRDC2 expression in the U2OS cell line, confocal microscopy indicated that ARRDC2 is dynamically targeted to the endocytic system, predominantly the lysosome (Chapter 3). Assessment of endogenous ARRDC2 expression in several primary cell lines was enabled through the development of an anti-ARRDC2 antibody. This supported a plasma membrane and endocytic localisation for ARRDC2.

As mentioned above, ARRDC2 displays sequence similarity to other α-arrestins, retaining sequence motifs such as the C-terminal PPxY motifs that are strongly linked to α-arrestin roles in scaffolding

NEDD4 family ubiquitin ligases. Thus, Chapter 4 describes the detection of interactions between ARRDC2 and the nine human members of the NEDD4 ligase family using coimmunoprecipitation. ARRDC2 interactions with NEDD4 ligases were further delineated through molecular (mutagenesis) and cell biological (coexpression and confocal microscopy) approaches. The ubiquitination status of ARRDC2 was also investigated via coimmunoprecipitation.

In addition to their close homology with α-arrestins from other species, human ARRDCs are ancestrally related to the β-arrestins. Whether the regulation of GPCRs is a newly evolved feature of β-arrestins, or is conserved in α-arrestins, remains unclear, although a few recent reports hint that the latter may be the case (see section 1.4.3). Chapter 5 investigated this by assessing the potential involvement of ARRDC2 in the function of two model GPCRs: β_2AR, a GPCR that rapidly recycles to the plasma membrane following agonist-induced internalisation, and δOR, which in contrast is efficiently delivered to the lysosome for degradation upon agonist stimulation. These studies established to what extent ARRDC2 colocalises and associates with each GPCR, and the potential effect of ARRDC2 upon the trafficking and signalling of the receptors was investigated. Finally, the potential for cooperation or competition between α- and β-arrestins was addressed through testing of the ability of ARRDC2 to oligomerise with itself and β-arrestins.

2 Materials and methods

2.1 Materials and reagents

Tissue culture flasks were from Sarstedt (Numbrecht, Germany). Tissue culture medium and other reagents were from Sigma (Wokingham, UK). Antibiotics used in eukaryotic cell selection/induction were zeocin, G418 and blasticidin (all Invitrogen, Paisley, UK) and tetracycline (Sigma).

2.2 Molecular biology

The approach used here to transfer target complementary DNA (cDNA) sequences of interest into the relevant mammalian expression plasmids (i.e. 'subcloning'), for example into a plasmid containing a desired epitope tag, is summarised in Figure 2.1. Where required, this process included the initial polymerase chain reaction (PCR) amplification of the target cDNA from a pre-existing plasmid, in order to engineer desired restriction endonuclease recognition sequences outside of the coding sequence (Figure 2.1, steps 1-6, left side). Alternatively, pre-existing plasmids containing target cDNAs already flanked by convenient restriction sequences were used for the donation of 'insert' cDNAs without the need for PCR amplification (i.e. entering Figure 2.1 at step 7). The methods involved in each step of this process are detailed here (sections 2.2.1 – 2.2.9).

In addition to the canonical restriction digest-based method above, in some cases the Gateway® method of homologous recombination-based cloning (Invitrogen) was used; this is described in section 2.2.10.

In several instances, PCR was used for the site-directed introduction of mutations into target cDNA sequences. The approach used is described in section 2.2.11.

Lastly, in addition to detailing the general gene cloning and mutagenesis methods used here, the generation of each individual plasmid construct is described in section 2.2.12, including primer sequences/unique conditions, etc.

2.2.1 PCR amplification of target cDNA sequences (step 1)

cDNA sequences of interest were amplified from the relevant host vectors by PCR. PCR reactions included, in a final volume of 50 µl: 5 µl 10X Pwo reaction buffer containing 1.5 mM $MgSO_4$ (Roche, Burgess Hill, UK), dNTPs mix (200 µM of each of dATP, dCTP, dGTP and dTTP; Promega, Madison, WI, USA), 25 ng cDNA template, 600 µM final concentration of each of the oligonucleotide primers and double-distilled H_2O (ddH_2O). Where indicated, 2.5 µl (5%) dimethyl sulphoxide (DMSO, Sigma) was included to reduce primer secondary structure formation.

The reaction mixture was set up in a thin-walled 200 µl PCR tube (Scientific Laboratory Supplies, UK). 'Hot-start' PCR method was used here to avoid nonspecific priming of unwanted templates and/or primer dimer formation that may occur at lower (i.e. less stringent) temperatures. To do this, prior to addition of the DNA polymerase, reaction tubes were placed in a thermocycler block (Mastercycler gradient, Eppendorf, UK) which was set to perform an initial denaturation step at 95ºC for 30 seconds before lowering to the annealing temperature (55-60ºC depending on primers), at which point 0.5 µl (2.5 units) Pwo DNA polymerase (Roche) was added to the reaction mixture. Pwo DNA polymerase was used for its 3' – 5' exonuclease (proofreading) activity that gives it greater accuracy than, for example, Taq DNA polymerase. The thermocycler was then set to continue through 25 cycles of replication as follows: denaturation at 95ºC for 30 seconds, annealing (~55ºC) for 45-60 seconds, and extension at 68-72ºC for ~1 min per kilobase pair (kbp) of template length. This was followed by cooling (hold) at 4ºC.

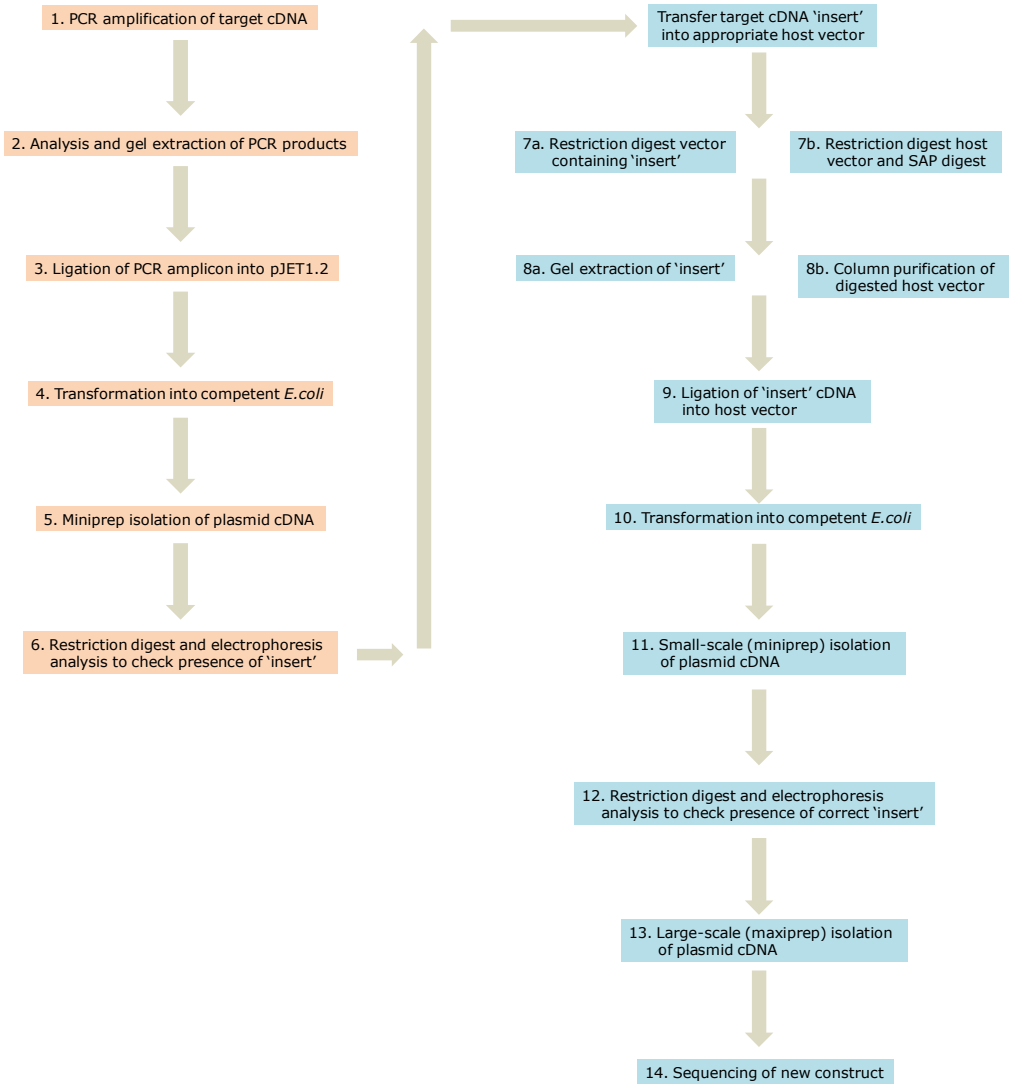

Figure 2.1 Generalised scheme for the subcloning of target cDNA sequences into the preferred mammlian expression plasmids

2.2.2 Analysis and gel extraction of PCR products (step 2)

Following PCR amplification of target cDNA sequences, the entire resulting reaction – 25 µl into each of two lanes – was run on a 1 % (w/v) agarose gel (section 2.2.2.1). Having confirmed the size of the amplified PCR product, the relevant band was excised from the agarose gel and the DNA extracted (section 2.2.2.2).

2.2.2.1 Analysis of DNA samples by agarose gel electrophoresis

DNA samples were analysed in gels consisting of 1 % (w/v) agarose dissolved in tris-borate-ethylenediaminetetraacetic acid (EDTA) buffer (TBE; 89 mM Tris-HCl [pH 7.6], 89 mM Boric acid, 2 mM EDTA) by heating in a microwave oven. Ethidium bromide (Sigma), an intercalating agent, was added to a final concentration of 0.1 µg/ml for the visualisation of DNA under ultraviolet (UV) illumination. The gel was poured into a casting tray with a comb, allowed to set at room temperature, and then inserted into an electrophoresis tank and immersed in TBE buffer. DNA samples, mixed with loading buffer (0.25% w/v bromophenol blue, 0.25% w/v xylene cyanol, 50% v/v glycerol, 1X TBE), were loaded into the appropriate wells alongside a molecular weight marker (BenchTop 1kb DNA ladder, Promega). Gels were run at a constant voltage of 80 V until the dye front had migrated towards the positive electrode an appropriate distance. DNA was visualised by UV illumination on a Syngene GVS-30 Transilluminator. The amount and size of DNA samples could be estimated by reference to the molecular weight marker.

2.2.2.2 Gel extraction of DNA samples

Once DNA samples were confirmed on agarose gels, the desired product bands were carefully excised from the gel, ensuring the minimal possible UV exposure time to prevent damage to the DNA. Excised fragments were transferred to sterile 1.5 ml tubes and the DNA was extracted using the GenElute Gel Extraction Kit (Sigma), using the solutions and columns provided. This kit employs a silica gel-based method of DNA purification by column chromatography. A slice of agarose gel containing the desired plasmid DNA was dissolved in 3 volumes of gel solubilisation solution by heating to 60 ^{o}C for ~10 min. 1 gel volume of isopropanolol was added to this solution prior to column loading. The solubilisation solution contains a chaotropic salt, which removes the water 'shell' surrounding the DNA phosphate backbone; this allows the phosphate residues of the

disordered DNA to adsorb to the silica in the columns. The addition of the alcohol isopropanol also aids dehydration of the DNA phosphates, thereby enhancing binding to the silica. Once this solution was loaded onto a column, the solution was removed by centrifugation leaving the DNA adsorbed onto the silica. The column was then washed with a solution containing solvent (e.g. 50% ethanol), which removed contaminants such as RNA and carbohydrate but did not displace the double-stranded DNA. The plasmid DNA was then eluted in Tris buffer, which rehydrated the DNA leading to disruption of the DNA-silica electrostatic contacts.

2.2.3 Blunt-ended ligation of PCR amplicon into pJET1.2 vector (step 3)

In order to perform restriction digest of newly synthesised PCR amplicons for their insertion into the relevant mammalian expression vectors, the amplicons (blunt-ended, since the DNA polymerase used, Pwo, is a proofreading polymerase) were first subcloned into the pJET1.2/blunt cloning vector (Fermentas; Thermo Fisher Scientific, Massachusetts, USA). This was to aid the DNA digestion, since restriction enzymes inefficiently digest close to the ends of DNA fragments, such as PCR amplicons. The pJET1.2 vector contains the *eco47IR* gene whose product is a restriction endonuclease that is lethal to *E.coli* host cells. Insertion of a PCR amplicon into pJET1.2 disrupts the *eco47IR* gene, thus acting as a mechanism for selection of positive bacterial colonies containing ligated vector after transformation.

Blunt-ended ligation of gel extracted PCR amplicons ('insert') into pJET1.2 ('vector') was performed such that a molar ratio of 1:3 (vector:insert) was achieved for optimal insert incorporation. 50 ng of vector was used in the reaction, and, assuming that the ratio of vector to insert size was 3:1 (e.g. 3 kbp vector; 1 kbp insert) 50 ng of insert was used to achieve a 1:3 molar ratio. Assuming a yield of ~2.5 µg insert (in a total of 50 µl) was obtained from the PCR (this was routinely estimated by reference to the molecular weight

marker on agarose gels), 1 µl of this was required to provide 50 ng. Thus, reactions were prepared in 0.5 ml tubes with a total volume of 20 µl containing: 50 ng pJET1.2/blunt cloning vector DNA, 1 µl insert DNA (derived from 50 µl insert DNA resulting from gel extraction of the PCR product), 10 µl 2X Reaction Buffer (Fermentas) and ddH_2O. The reaction buffer used contains polyethylene glycol (PEG). PEG is a neutral polymer that, by sterically excluding volume, induces a compact structure in DNA, increasing its effective concentration (Louie *et al.*, 1994). Thus, PEG enhances the efficiency of blunt-ended ligations. 1 µl (5 units) T4 DNA ligase (Fermentas) was added and the reaction was allowed to proceed at 22ºC for 30 min by incubation in a bench-top heat block. The products of the ligation were then introduced into competent *E.coli* by transformation (section 2.2.4.2).

2.2.4 Transformation of cDNA into chemically competent *E.coli* (steps 4 and 10)

2.2.4.1 Preparation of chemically competent *E.coli*

Chemically competent XL-1 strain *E.coli* cells were prepared sterile from a previous frozen stock of XL-1 cells streaked onto an agar plate (LB agar, Sigma) containing 10 µg/ml tetracycline, incubated overnight at 37ºC. A single colony from this plate was inoculated into 5 ml LB broth (Sigma) and grown at 37ºC overnight with agitation (250 rpm). Between 1 – 5 ml of the resulting culture was inoculated into 100 ml 2YT medium (Sigma) containing 10 µg/ml tetracycline in a 1 litre flask (the richer 2YT medium was used for faster growth). The culture was incubated at 37ºC with agitation (250 rpm), and growth was regularly monitored by the measurement of optical density at 600 nm (OD_{600}). Once OD_{600} reached between 0.5 – 0.9, the culture was further diluted to 250 ml with 2YT medium, and this culture was grown further until OD_{600} reached 0.6. The culture was rapidly cooled in ice-cold water with gentle shaking, and was then centrifuged for 15 min at 4000 rpm in a pre-cooled centrifuge at 4ºC. The resulting pellet was resuspended

in 50 ml TfB I buffer (30 mM potassium acetate [KAc], 50 mM $MnCl_2$, 64 mM KCl, 10 mM $CaCl_2$, 15% glycerol, pH 5.8) on ice, and this solution was re-centrifuged for 8 min at 4000 rpm, 4ºC. The pellet was resuspended in 10 ml ice-cold TfB II buffer (10 mM 3-(N-morpholino)propanesulphonic acid [MOPS], 1 mM KCl, 75 mM $CaCl_2$, 15% glycerol, pH 7.0), from which 0.5 ml aliquots were transferred into pre-chilled 1.5 ml tubes. The aliquots were snap-frozen in liquid nitrogen and stored at -80ºC.

2.2.4.2 Transformation

An aliquot of competent XL-1 cells was removed from -80ºC storage and thawed on ice. For each transformation reaction, 100 µl of cells was transferred to a pre-chilled sterile 1.5 ml tube. 1.5 µl of 1.4 M β-mercaptoethanol was added, and the cells were incubated with gentle mixing on ice for 10 min. An appropriate volume of DNA (typically 10 ng of plasmid DNA, or 5 µl of a ligation reaction) was added, and the mixture was gently mixed followed by incubation on ice for 30 min. The mix was then subjected to a heat-pulse at 42ºC for 45 seconds, followed by immediately returning the tube(s) to ice for approximately 2 min. 400 µl LB broth was added, and the culture was incubated at 37ºC for 1h with agitation (250 rpm). Between 10 – 200 µl of the transformation culture was streaked onto LB agar plate(s) containing the relevant selection antibiotic, and inverted plates were incubated at 37ºC overnight.

2.2.5 Small-scale (miniprep) isolation of recombinant plasmid cDNA from *E.coli* (steps 5 and 11)

Small yield plasmid preparations were obtained from previously grown XL-1 plate cultures by the inoculation of a single colony into 5 ml LB broth (containing the appropriate antibiotic) followed by incubation of the culture overnight at 37ºC with agitation (250 rpm). cDNA was subsequently isolated from the cells using the GenElute Plasmid Miniprep kit (Sigma), using the columns and reagents

provided and following the manufacturer's instructions, except the final elution step was performed in 100 µl ddH_2O. This kit enables purification of plasmid DNA by a modified alkaline-SDS lysis method (Birnboim *et al.*, 1979) followed by DNA recovery by silica-based spin format column chromatography. Briefly, an overnight culture (typically 2-3 ml of a 5 ml culture) was harvested by centrifugation and the bacterial pellet was resuspended. The bacteria were then lysed in an alkaline solution containing SDS. The strong anionic detergent SDS lyses the cell wall and denatures chromosomal DNA and proteins, as well as releasing plasmid DNA into the supernatant. The alkaline solution disrupts base pairing, but the closed, intertwined structure of plasmid DNA means that the strands do not separate. Cell debris (proteins, lipids, chromosomal DNA) are coated with dodecyl sulphate; a neutralisation solution is next added, which promotes precipitation of this debris by replacement of Na^+ with K^+ ions (Ish-Horowicz *et al.*, 1981). The precipitate is removed by centrifugation, leaving a supernatant lysate containing plasmid DNA that is loaded onto a silica column and purified based on the method described in section 2.2.2.2.

2.2.6 Restriction endonuclease digest analysis (steps 6 and 12)

Purified DNA was typically digested in a total reaction volume of 20 µl containing: ~2 µg DNA, 1 µl (1 unit) each relevant enzyme (FastDigest restriction enzymes, Fermentas), 2 µl 10X FastDigest buffer (supplied with enzyme) and ddH_2O. Mixtures were prepared in sterile 0.5 ml tubes, and the reaction was allowed to proceed for 1 h at 37ºC, followed by incubation at 60ºC for 20 min and then 80ºC for 5 min to denature (inactivate) the enzymes. Typically, uncut, singly digested and doubly digested DNA samples were all analysed by electrophoresis in 1% agarose (w/v) gels (section 2.2.2.1).

2.2.7 Subcloning insert cDNA into new host vectors: preparation (steps 7 and 8)

2.2.7.1 Preparation of insert cDNA (steps 7a and 8a)

In order to prepare an insert for transfer into an alternative plasmid background, it was excised from its' plasmid using the relevant restriction enzymes (section 2.2.6) to produce overhanging ('sticky') ends. The digest reaction was then run on an agarose gel (section 2.2.2.1), and the correct insert-sized band was excised and purified (section 2.2.2.2), with a final elution of purified insert DNA in 50 µl ddH_2O.

2.2.7.2 Preparation of host vector (steps 7b and 8b)

In order to prepare a plasmid into which an insert (from above, 2.2.7.1) was to be transferred (i.e. the 'host' vector), the plasmid was digested with the corresponding restriction enzymes used in section 2.2.7.1 (according to the standard digestion protocol, 2.2.6). The digested (linearised) plasmid was then subjected to treatment with shrimp alkaline phosphatase (SAP), which catalyses 5'-dephosphorylation of DNA ends, thus preventing self re-ligation. 20 µl of the digestion reaction was treated with 2 µl (2 units) SAP (Fermentas) plus 2 µl SAP 10X buffer (provided with the enzyme) and incubated for 60 min at 37^{o}C, followed by inactivation of SAP at 65^{o}C for 20 min. Host DNA was then purified from this reaction using the GenElute PCR Clean-Up kit (Sigma), using the columns and reagents provided and following the manufacturer's instructions, except the final elution step was performed in 40 µl ddH_2O. The method employed in this kit is based on the purification of DNA by high salt binding to silica gel columns that has been described (section 2.2.2.2).

2.2.8 Ligation of overhanging DNA (step 9)

Purified insert cDNA produced in section 2.2.7.1 was transferred into the desired host vector produced in section 2.2.7.2 via DNA ligation.

Ligations were typically performed with an excess of insert DNA; generally the molar ratio of vector:insert included in the ligation was manipulated to approximately 1:3. This was calculated as follows:

For the insert prepared as in section 2.2.7.1, given that the amount of DNA used in the initial digest reaction was 2 µg, and knowing the size of the insert (denoted as 'A') and that of the plasmid from which it had been excised ('B'), and assuming that the yield efficiency of the Gel Extraction kit used is 80%, then the amount of insert DNA recovered in 50 µl eluate will be:

a) 2 µg x (A ÷ B) x 0.8

For the vector prepared as in section 2.2.7.2, given that 2 µg DNA was used in the initial digest reaction, and knowing the size of the vector ('D') and that of the vector minus whatever fragment has been removed in the digest reaction ('C') in order to be replaced by the new desired insert, and assuming 80% yield efficiency of the PCR Clean-Up kit, then the amount of linearised vector recovered in 40 µl eluate will be:

b) 2 µg x (C ÷ D) x 0.8

These calculations enable us to know the concentration of insert and vector DNA. From this knowledge, ligation reactions were prepared in which ~50 ng vector DNA was used. In order to determine the amount of insert DNA to include, the relative size of vector and insert was used to calculate the amount of insert DNA that equates to 3 times the molar amount of vector in 50 ng. That is:

c) Number of moles of vector in 50 ng = Number of moles of insert in 50 ÷ (ratio of sizes of vector:insert in base pairs) ng

Therefore the amount of insert DNA (in ng) calculated in sum (c), multiplied by three to give a 1:3 ratio, was included in the reaction

(the actual amount added in µl was calculated using the concentration determined in sum (a)).

Thus, positive and negative control reactions were set up in 0.5 ml tubes in a total volume of 10 µl containing: 50 ng vector DNA, plus (positive) or minus (negative) three times the molar ratio of insert DNA, 1 µl 10X T4 DNA ligase buffer (Fermentas), 1 µl (5 units) T4 DNA ligase (Fermentas) and ddH_2O. The reaction mixture was incubated at 16^oC for 16 h, and both positive and negative controls were subsequently transformed into competent XL-1 bacteria as in section 2.2.4.2.

2.2.9 Large-scale (maxiprep) isolation of recombinant plasmid cDNA from *E.coli* (step 13)

Large yield plasmid preparations were obtained using previously grown 5 ml XL-1 starter cultures obtained as previously described by the inoculation of a single colony into 5 ml LB broth (as in section 2.2.5). Depending on the growth of the starter culture, between 100 µl – 1 ml (typically ~200 µl) was used to inoculate 120 ml sterile LB broth (containing the appropriate antibiotic) in a 500 ml conical flask. This culture was grown overnight at 37ºC with agitation (250 rpm). DNA was subsequently isolated from the cells using the GenElute HP Plasmid Maxiprep kit (Sigma), using the columns and reagents provided and following the manufacturer's instructions resulting in a 3 ml eluate containing the plasmid DNA (in a 50 ml conical-bottomed tube). Essentially, this is a large-scale version of the method used for small-scale (miniprep) plasmid isolations that has been described (section 2.2.5), in which cells are harvested by centrifugation, subjected to alkaline-SDS lysis and plasmid DNA is recovered using a high salt, silica column-based centrifugation protocol.

The DNA was further concentrated and purified using an ethanol precipitation protocol. 300 µl of 3 M sodium acetate (NaOAc) was added to the 3 ml eluate (i.e. 1:10 volume ratio; final concentration

0.3 M). 2.2 volumes (7.2 ml) ice-cold 100% ethanol was added. Ethanol is less polar than water and acts to remove the water 'shell' surrounding the DNA phosphate groups, thereby exposing their negative charge. NaOAc provides counterions (Na^+) that bind to the phosphate groups, reducing the repulsive charges between DNA molecules such that they precipitate out of solution. The resulting mixture was centrifuged (4000 rpm, 20 min, 4ºC), salt was removed from the DNA pellet by washing in 1 ml ice-cold 70% ethanol, and the solution was further centrifuged (4000 rpm, 5 min, 4ºC). The supernatant was poured off and the DNA pellet further clarified by centrifugation (4000 rpm, 5 min, 4ºC). The DNA pellet was air-dried for 10-15 min and then resuspended in 100-500 µl TE buffer (10 mM Tris-HCl [pH 7.5], 1 mM EDTA), depending on the size of the pellet.

DNA concentration and purity was estimated using a spectrophotometer (BioPhotometer, Eppendorf) and the DNA was sequenced (section 2.2.13). The absorption spectrum of DNA is maximal at 260 nm. Hence, absorption at 260 nm (A_{260}) was used as an estimation of the DNA concentration (for double-stranded DNA, A_{260} = 1 at a concentration of 50 µg/ml). Proteins strongly absorb at higher wavelengths (280 nm), and so the ratio of absorbance at these wavelengths ($A_{260/280}$) has historically been used as an indicator of protein contamination of DNA samples. Here, samples with $A_{260/280}$ between 1.7 – 1.9 were considered pure; less than 1.7 was indicative of protein contamination.

2.2.10 Gateway® cloning

Gateway cloning is based on the bacteriophage lambda (λ) site-specific recombination system, which is required for λ integration into the *E.coli* chromosome. In the technology, recombinant DNA sequences of interest are flanked by λ-based DNA recombination sequences (*att* sites), enabling specific, directional transfer between different vectors *in vitro* (Hartley *et al.*, 2000). Here, transfer of DNA sequences between donating 'entry' vectors and receiving 'destination' vectors was performed. Recombination reactions were

prepared in sterile 0.5 ml tubes, and typically comprised ~38 ng destination vector, ~38 ng entry vector, 1 µl TE buffer and 0.5 µl 5X LR Clonase II enzyme mix, in a total volume of 2.5 µl. The Clonase mix comprises the bacteriophage and *E.coli* enzymes required to catalyse recombination. The reaction was allowed to proceed at room temperature for 2 h. 0.5 µl of the serine protease proteinase K was then added and the reaction was incubated at 37°C for 10 min, in order to inactivate the recombination enzymes and stop the reaction. The reaction mix was diluted with the addition of 7 µl TE buffer, and 1-2 µl of this was typically used in transformations (section 2.2.4.2).

2.2.11 PCR-based site-directed mutagenesis

Desired mutations were introduced into target cDNA sequences using PCR-based site-directed mutagenesis (Figure 2.2). In this method, sense and antisense primers were used that were complementary to the same sequence on opposite strands of the plasmid template. Primers were individually designed such that the desired mutation was central, with ~10-15 flanking bases either side. A minimum of 40% GC content was preferred, and primers were terminated with ≥1 G or C base at each end ('GC clamp') in order to promote efficient annealing. Melting temperatures were calculated according to the following equation:

$$T_M\ (^oC) = 81.5 + 0.41(\%\ GC) - (675/n) - (\%\ mismatch)$$

where n is the length of the primer in bases; % GC is the percentage of bases that are either guanine or cytosine; % mismatch is the percentage of bases that do not match the parental DNA sequence.

The PCR conditions used in section 2.2.1 were maintained except for (i) longer extension times (typically ~1 min per kbp of plasmid length) to allow for extension of an entire plasmid, (ii) fewer reaction cycles (12-18) in order to enhance the mutation efficiency

and avoid non-specific polymerisation in primer-depleted conditions, and (iii) the use of Accuzyme DNA polymerase (Bioline, Taunton, MA, USA), which allows extension of large PCR fragments. 20 µl of the PCR reaction mixture was then treated with 1 µl (10 units) *DpnI* (Promega) for 2 h at 37^{o}C. *DpnI* is a restriction endonuclease that cleaves GATC sequences adenomethylated by the *E.coli* DNA adenine methyltransferase (Dam) enzyme. Thus, inclusion of this step results in the digestion of unwanted parental template DNA. 5 µl of the reaction was then transformed into 100 µl XL-1 competent cells (section 2.2.4.2), the DNA was isolated as normal (sections 2.2.5 and 2.2.9) and sequenced to confirm presence of the mutation (section 2.2.13).

2.2.12 Generation of plasmid constructs used in the current study

The plasmid constructs that were generated during the current study are described here. All other constructs that were used but are not described here were already available within the host laboratories (see list, Table 2.1)

The basics of the plasmid backbones used here are as follows. The pcDNA3.1 vectors comprised a cytomegalovirus (CMV) enhancer-promoter for high level expression, upstream of the multiple cloning site (MCS), which contained various unique endonuclease recognition sites for insertion of transgenes. This was followed by a Bovine Growth Hormone (BGH) polyadenylation (poly(A)) signal and transcription termination site in order to produce mRNA transcripts with a high stability. The vector also contained a Simian Virus 40 (SV40) origin for plasmid replication in cell lines expressing the large T antigen, an ampicillin resistance gene and pUC origin for bacterial selection, and an antibiotic (zeocin or neomycin) resistance gene for selection in mammalian cell lines.

The pcDNA4/TO vector was based on the pcDNA3.1 backbone described above, but additionally contained two copies of the tetracycline operator (TetO2) within the CMV promoter in order to

enable selective binding by the tetracycline repressor and inhibition of transcription (see section 2.3.4.3).

Table 2.1 Plasmid constructs used in the current study

Plasmid	Source
pDEST_ARRDC1-4-eGFP-HA	This study
pDEST_TXNIP-eGFP-HA	This study
p3.1_βarrestin1/2-YFP	Nick Holliday, University of Nottingham, UK
pDEST_ARRDC2(wild-type or ΔΔ)-mCherry	This study
p3.1_EEA1-GFP	Harald Stenmark, Institute of Cancer Research, Oslo University Hospital, Norway
peGFP_RAB5/7/11(wild-type)	Tyson Sharp, Barts Cancer Institute, London, UK
peGFP_RAB5/7/11(constitutively-active mutants)	Simon Dawson, University of Nottingham, UK and This study
pDEST_E3ubiquitinligase-eGFP-HA	Simon Dawson, University of Nottingham, UK and This study
pDEST_ARRDC2(wild-type or ΔΔ)-2FLAG	Simon Dawson, University of Nottingham, UK
p3.1_HA-ubiquitin	This study
p3.1_ARRDC2-vYn/vYc	This study
p3.1_βarrestin1/2-vYn/vYc	Nick Holliday, University of Nottingham, UK
p3.1/p4TO_ARRDC2-GFP	This study
pDEST_ARRDC3-mCherry	Simon Dawson, University of Nottingham, UK
p3.1_ssβ2AR/ssδOR	Nick Holliday, University of Nottingham, UK
pCMV_FLAG-β2AR-GFP	Nick Holliday, University of Nottingham, UK
p3.1_ARRDC2-HA	Simon Dawson, University of Nottingham, UK
p3.1_βarrestin1/2-HA	This study
p3.1_FLAG-βarrestin2	Nick Holliday, University of Nottingham, UK
pCMV_HA-δOR	Nick Holliday, University of Nottingham, UK

The Gateway cloning pDEST vectors were also based on pcDNA3.1, but were previously manipulated to incorporate λ recombination sequences (see section 2.2.10) that flanked the MCS.

2.2.12.1 *ARRDC2* cloning

A previously generated mammalian expression vector carrying the wild-type *ARRDC2* cDNA (NC_000019.9) N-terminally tagged with the haemagglutinin (HA) epitope was used as a template for the PCR amplification (section 2.2.1) of *ARRDC2* (without HA). The oligonucleotide primers used in the PCR reaction (Table 2.2) were designed to introduce endonuclease restriction sites to enable the subcloning of *ARRDC2* into the appropriate vectors. The sense primer was designed to introduce a start codon (ATG) at the beginning of the *ARRDC2* sequence, a Kozak initiation site immediately upstream of this, and an in-frame *EcoRI* restriction site upstream of this. The antisense primer was designed to omit the stop codon (to allow read-through into a C-terminal fusion) and

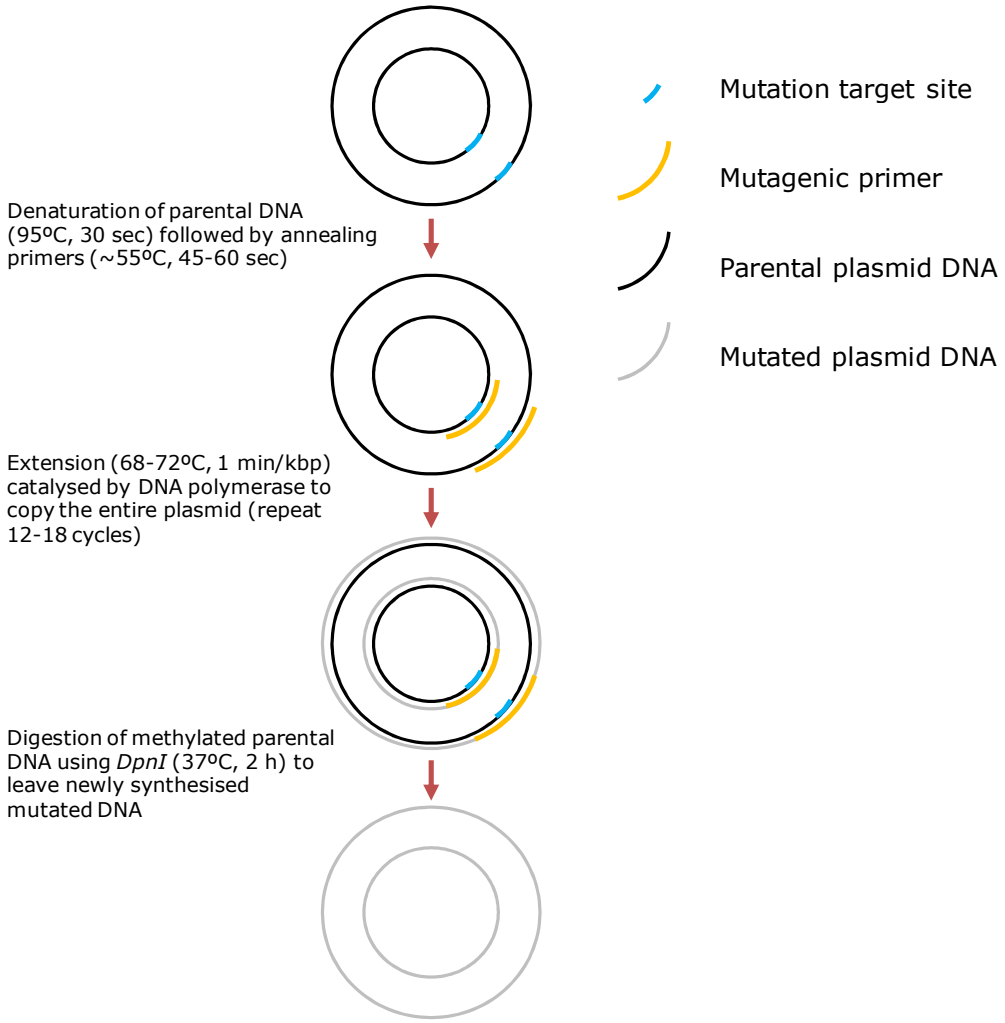

Figure 2.2 Overview of the site-directed mutagenesis method employed to introduce mutations to double-stranded plasmid DNA

introduce an in-frame *NotI* restriction site 3' of the final *ARRDC2* codon. The resultant PCR amplicon comprising *ARRDC2* cDNA flanked by *EcoRI* and *NotI* sites was subsequently analysed and cloned into pJET1.2 according to standard protocols described herein. Standard restriction enzyme methods (Figure 2.1, steps 7-13) were then employed to subclone *ARRDC2* cDNA into pre-existing plasmids containing the relevant epitope or fusion protein cDNAs, in order to create the following expression vectors:

- pcDNA3.1_ARRDC2-GFP
- p4TO_ARRDC2-GFP
- pcDNA3.1_ARRDC2-vYn and pcDNA3.1_ARRDC2-vYc, where vYn and vYc represent amino acid residues 2-173 (β-strands

1–8) or 156–239 (β-strands 8–11) of venus YFP, respectively (Haider *et al.*, 2011; Kilpatrick *et al.*, 2010).

Table 2.2 Primers used to amplify *ARRDC2* for subcloning into various vectors

Parameter	Sense primer	Antisense primer
Sequence	5'-ATAGAATTC**GCCACC**ATGCTATTCGACAAGGTGAAAGC-3'	5'-TAGCGGCCGCTGGCAAGTCATGCAGCGCGGCCTC-3'
T_M	82.2	90.8
% GC content	45	71
Length	38	34

EcoRI (sense) and *NotI* (antisense) sites are underlined; Kozak sequence is in bold; T_M, melting temperature (°C). T_M = 81.5 + 0.41(% GC content) – 675/*N*, where *N* is the primer length.

2.2.12.2 *RAB7Q67L*

The RAB7Q67L mutant was generated by site-directed mutagenesis in the pre-existing plasmid, GFP-RAB7 in pEGFP (Clontech; a gift from Dr Tyson Sharp, School of Biomedical Sciences, University of Nottingham), according to standard protocols (section 2.2.11). The forward and reverse mutagenic primers are denoted in Table 2.3, and confirmation of the altered RAB7 sequence is shown in Figure 2.3.

Table 2.3 Properties of RAB7Q67L mutagenic primers

Parameter	RAB7Q67L primers
Sense sequence	5'-GGGACACAGCAGGAC**T**GGAACGGTTCCAGTCTCTCG-3'
Antisense sequence	5'-CGAGAGACTGGAACCGTTCC**A**GTCCTGCTGTGTCCC-3'
T_M	85.0
% GC content	61
Length	36

Mutant was generated in pDEST_GFP-RAB7. Mutated residue is in bold; T_m, melting temperature.

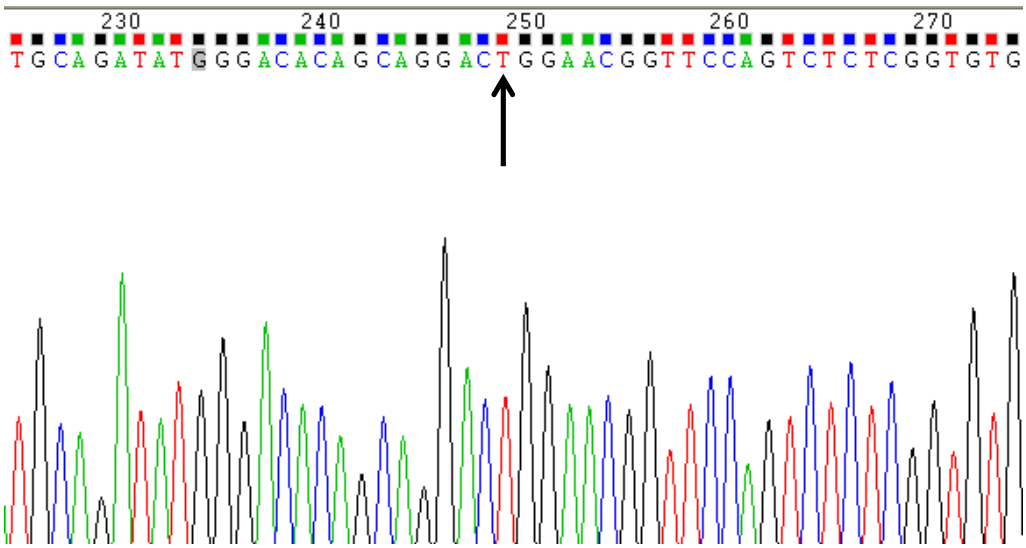

Figure 2.3 Sequencing chromatogram indicating the generation of the RAB7Q67L mutant

Chromatogram generated using Chromas 2. Arrow indicates the altered residue, changing wild-type RAB7 codon 67 CAG (Q) to CTG (L).

2.2.12.3 β-arrestin2-HA

A plasmid expressing β-arrestin2 C-terminally fused with the HA epitope was generated using the pre-existing pcDNA3.1_β-arrestin2-vYc background (Kilpatrick *et al.*, 2010), where vYc is flanked by *NotI* and *XbaI* restriction sites. A HA linker was generated by annealing 5'-phosphorylated primers designed to comprise the HA coding sequence flanked by *NotI* and *XbaI* overhanging sites (Figure 2.4). In a thin-walled 200 µl PCR tube (Scientific Laboratory Supplies) a final concentration of 500 nM of each oligonucleotide primer was mixed with 10 µl 10X T4 DNA ligase buffer (Fermentas), and adjusted to a total volume of 100 µl with ddH_2O. The tube was placed in a thermocycler block (Mastercycler gradient, Eppendorf), and the primers were specifically annealed by heating to 95 ºC followed by cycling down at increments of 10 ºC every 5 min, until they were maintained at 4 ºC until use. The pcDNA3.1_β-arrestin2-vYc plasmid was digested with *NotI*/*XbaI* (section 2.2.7.2) and the HA linker ligated in place of the removed vYc fusion (section 2.2.8).

Figure 2.4 HA linker primers designed for the generation of β-arrestin2-HA

Primers were designed to incorporate the HA epitope coding sequence (underlined) followed by a stop codon (bold) between overhanging *NotI* and *XbaI* sites (indicated). An additional two residues (GG in forward primer) were included in order to maintain the HA read sequence in-frame with β-arrestin2. Primers were 5′-phosphorylated in order to ligate into the appropriate vector.

2.2.13 DNA sequencing analysis

All newly synthesised constructs were analysed by DNA sequencing, carried out by the Biopolymer Synthesis and Analysis Unit (BSAU) in the School of Biomedical Sciences (University of Nottingham), using an automated DNA sequencer.

2.3 Cell culture and transfection

2.3.1 Cell growth and storage conditions

HEK-293TR (Invitrogen) and U2OS (donation from Dr Tyson Sharp) cells were cultured in Dulbecco's modified Eagle's medium (DMEM, Sigma) supplemented with 10% (v/v) foetal bovine serum (FBS; Sigma). Cells were maintained in T75 flasks (Sarstedt) under humidified conditions in 5% CO_2 at 37ºC. Primary cells used (aortic endothelial; pulmonary artery endothelial; aortic smooth muscle; bronchial epithelial; bronchial smooth muscle) were from single donors (Lonza, Slough, UK) and were cultured by Marlene Groenen.

When cells reached 80-90% confluence, they were passaged by trypsinisation. Medium was removed and the cells were washed with sterile Dulbecco's phosphate buffered saline (PBS; Sigma). Trypsinisation was then performed by the addition of 2 ml trypsin. For HEK-293 cells a standard concentration of 0.25% trypsin (w/v) in Versene was used; U2OS cells were observed to be more strongly adherent, so 2X concentration (0.5% w/v) of trypsin was used. Cells were incubated in trypsin solution at 37ºC for approximately 1 min, ensuring that the incubation time did not exceed 2-3 min to avoid trypsin damaging cell surface proteins. Cells were dislodged by gentle tapping of the side of the T75 flask, and trypsin was then deactivated by the addition of ~8 ml medium to the cells. The cell mixture was transferred to a sterile universal tube, and was centrifuged at 1000 rpm for 5 min. The supernatant was removed and the cell pellet resuspended in 5-10 ml medium, and an appropriate volume of the cell suspension was transferred to a new T75 flask containing ~20 ml fresh medium and incubated as above.

In order to freeze stocks of cells for future use, the above passaging protocol was followed until resuspension of the cell pellet. At this point, cells were instead resuspended in an appropriate volume of freezing solution (10% v/v DMSO in FBS), and 1 ml aliquots were transferred to sterile cryovials. Cryovials were placed in a polystyrene container in a -80ºC freezer for at least 24 h for gradual freezing, and were subsequently transferred to a liquid nitrogen container for long-term storage.

2.3.2 Cell counting

Where required, the number of cells in a suspension was estimated by counting using a haemocytometer. A small volume of cell suspension was removed and loaded into the counting chamber of a haemocytometer. The total number of cells in each of two of the counting windows (comprising 25 squares (1 mm^2) with a chamber depth of 0.1 mm; 0.1 µl volume) was counted; the mean of these

two was multiplied by 10^4 to give the approximate number of cells per ml.

2.3.3 Seeding cells and transfection using Lipofectamine reagent

For various experiments, cells were seeded at defined densities (following counting; section 2.3.2 above) onto the appropriate experimental plate and, where required, cells were transfected with the necessary DNA constructs the following day (summarised in Table 2.4).

For the seeding of HEK-293 cells onto glass coverslips, prior treatment of the coverslips was required to facilitate cell adhesion. To do this, sterile coverslips in 6-well plates were treated with 10 µg/ml poly-$_L$-lysine (Sigma) for ~1 h at room temperature. Coverslips were then washed once with PBS followed by cell seeding. In contrast, U2OS cells were observed to be more adherent and so poly-$_L$-lysine treatment was not required.

Transfections were performed the day after cell seeding, at which cells were generally around 70-80% confluent. DNA was introduced to cells via conjugation to Lipofectamine reagent (Invitrogen), according to the manufacturer's instructions, with the amounts of DNA and Lipofectamine scaled as indicated in Table 2.4.

Table 2.4 Cell seeding and transfection conditions

Culture vessel (surface area, cm^2)	Number of cells seeded (per well where appropriate)	Amount of DNA added per well (µg)	Amount of lipofectamine added per well (µl)
T25 flask (25)	~1 x10^6	2	18
6-well plate (10)	1 – 2 x10^5 on coverslips	1	9
	2 – 4 x10^5 on whole well	1	9
MatTek dish (10)	2 x10^5	1	9
24-well plate (2)	5 x10^4 – 1 x10^5	n/a	n/a
96-well plate (0.3)	2 – 4 x10^4	0.05	0.45

2.3.4 Generation and maintenance of stable cell lines

2.3.4.1 Mixed populations

Cells stably expressing a desired plasmid construct were generated by transfection in a T25 flask (according to Table 2.4), followed by passage the following day (at a split ratio of 1:10) into a fresh T25 flask in medium supplemented with the appropriate selection antibiotic, corresponding to the eukaryotic resistance gene expressed by the plasmid in question. The selection concentrations used were: blasticidin 5 μg/ml; zeocin 800 μg/ml; G418 800 μg/ml. Selection of transfectants was then allowed to proceed; over 1 – 2 weeks in selection medium, non-transfected cells died off, leaving antibiotic-resistant colonies expressing the desired plasmid. These were then passaged into T75 flasks for scaling up, analysed appropriately (by Western blotting and/or microscopy), and a subset of cells frozen down for future use. Once selected and passaged into T75 flasks, lower antibiotic concentrations were used to maintain the selection pressure: blasticidin 2.5 μg/ml; zeocin 100 μg/ml; G418 200 μg/ml.

2.3.4.2 Clonal populations

In some cases, the percentage of cells expressing the correct transgene in mixed stable populations was not sufficient for the purposes of experiments performed here. In order to obtain a more homogeneous population of transgene-expressing cells, a dilution cloning protocol was used. This involved the seeding of a previously obtained mixed stable cell population onto 96-well plates (Costar, Corning Life Sciences, Amsterdam, Netherlands) at an approximate density of 1 cell per well (antibiotic concentrations were maintained throughout). Thus, cell colonies obtained from this protocol would be derived from a single parental cell (i.e. clonal). Colony growth was analysed to ensure that each well only contained a single colony (wells in which ≥2 separate colonies were observed were excluded from the protocol). Confluent colonies were scaled-up by passage from 96-well plates onto 24-well plates and then 6-well plates, with a subset of the cells also seeded onto 96-well plates (Greiner

655090, Greiner Bio-One, Stonehouse, UK) for analysis of plasmid expression of fluorescent proteins using an ImageXpress Micro imaging platereader (Molecular Devices, Sunnyvale, CA, USA). Clones demonstrating sufficient percentage expression were further scaled up through passage onto T75 flasks, and clonal populations were then frozen down and maintained as appropriate (as in section 2.3.4.1).

2.3.4.3 Inducible expression of ARRDC2-GFP

For the inducible expression of ARRDC2-GFP in U2OS cells, a dual clonal cell line expressing pcDNA6/TR (Invitrogen) and ARRDC2-GFP cDNA in the pcDNA4/TO vector (p4TO_ARRDC2-GFP) was produced. The pcDNA4/TO vector contains two tetracycline operator sites (TetO2) within a cytomegalovirus (CMV) promoter; in the absence of tetracycline, the tetracycline repressor (TetR; encoded by pcDNA6/TR) binds to the TetO2, repressing expression of the gene of interest. However, upon addition of tetracycline to the cells, tetracycline binds to the TetR, causing it to dissociate from the TetO2, thus allowing transcription.

U2OS cells were first stably transfected (section 2.3.4.1) with pcDNA6/TR, and this line (denoted 'U2OSTR') was subjected to the dilution cloning protocol (section 2.3.4.2). Clonal U2OS lines expressing TetR were identified by transient transfection with p4TO_ARRDC2-GFP, followed by treatment at 24 h with 1 µg/ml tetracycline, and assessment of inducible ARRDC2-GFP expression at 48 h on the ImageXpress Micro platereader.

p4TO_ARRDC2-GFP was then stably transfected onto the U2OSTR line, and the resulting population subjected to another round of dilution cloning.

For experiments utilising ARRDC2-GFP inducible expression, U2OSTR ARRDC2-GFP cells were seeded onto the appropriate culture vessel 48 h prior to the experiment, and normal culture medium was replaced with medium supplemented with or without 1 µg/ml tetracycline at 24 h.

2.4 Immunofluorescence confocal microscopy

The following section describes the use of various protocols for the preparation of cells for analysis by confocal microscopy.

2.4.1 Cell fixing/mounting

The standard protocol used for the fixing of cells expressing gene(s) of interest, and/or stained as appropriate, was as follows. Cells on glass coverslips were transfected as appropriate (section 2.3.3). The next day, the cells were washed once with PBS, followed by fixation in 3% (w/v) paraformaldehyde (PFA) in PBS for 10 min. Cells were then washed twice in PBS for 5 min, followed by mounting inverted onto a microscope slide in PBS:glycerol (1:1). Any air bubbles were removed by carefully pressing down on the coverslip, coverslips were sealed around the edge using clear nail varnish, and slides were stored in the dark at 4^{o}C prior to confocal analysis.

2.4.2 Immunostaining

In some cases, detection of the subcellular localisation of proteins that themselves lacked a fluorescent tag was required (in the current thesis, this included the detection of exogenous ARRDC2-2FLAG, endogenous ARRDC2 and endogenous LAMP1). To do this, an epitope within the protein of interest was detected through the use of a specific primary antibody; the primary antibody was then detected using a fluorescently labelled secondary antibody, thus allowing visualisation of the protein of interest.

All manipulations were performed at room temperature. Cells on glass coverslips were washed and fixed as in section 2.4.1, followed by two 5 min washes (25 mM glycine/PBS, to quench the fixative). Cell membranes were permeabilised in 0.05% (v/v) Triton X-100/PBS for 5 min, followed by two 5 min washes in PBS. In experiments where membrane permeabilisation was omitted as a

control, the Triton X-100 step was replaced by incubation with PBS alone. Saturation of nonspecific sites (blocking) was then performed by incubation in 1% (w/v) bovine serum albumin (BSA, Sigma) in PBS ('blocking solution') for 60 min. Cells were labelled by incubation with the appropriate concentration of primary antibody in blocking solution for 90 min, followed by rigorous washing in blocking solution (3 x 2 min; 1 x 15 min; 1 x 5 min). Primary antibody was detected by incubation with the appropriate fluorophore-conjugated secondary antibody (for example, 1:1000 goat anti-mouse IgG conjugated to Alexa Fluor(AF)-488) in blocking solution for 45 min, followed by rigorous washing (3 x 2 min in blocking solution; 1 x 15 min in PBS; 1 x 5 min in PBS). Cells were then post-fixed in 3 % (w/v) PFA/PBS for 15 min in order to cross-link the antibodies used, followed by two 5 min washes in quenching solution and a final 5 min wash in PBS prior to mounting (section 2.4.1).

The primary and secondary antibodies used in each experiment and their concentrations are denoted in the respective figure legends in the results chapters.

2.4.3 Transferrin labelling

Where transferrin labelling was required, medium on cells on glass coverslips was replaced with medium containing 250 ng/µl AF-633-conjugated transferrin (Sigma) for 15 min at 37^{o}C, followed by cell fixing/mounting as in section 2.4.1. In experiments involving drug treatments (e.g. 1 h treatment with agonist), the transferrin step was included in the final 15 min of the drug treatment protocol; medium plus the appropriate agonist was supplemented with 250 ng/µl AF-633 transferrin followed by fixing/mounting as normal.

2.4.4 LysoTracker labelling

For the labelling of acid compartments (lysosomes) in live cells, cells on 35 mm MatTek dishes (MatTek Corp, Ashland, USA) were

transfected as appropriate. The next day, cell medium was replaced with 0.1% (w/v) BSA in HEPES buffered saline (HBS; 10 mM HEPES, 10 mM glucose, 146 mM NaCl, 5 mM KCl, 1 mM MgSO4, 2 mM sodium pyruvate and 1.3 mM CaCl2, pH 7.45) containing 100 nM LysoTracker™ Red DND-99 (Invitrogen) for 15-30 min at 37ºC. Cells were then imaged live in the same medium using a Zeiss LSM 510 laser scanning microscope (Carl Zeiss, Welwyn, UK).

2.4.5 Confocal imaging

Confocal images were obtained using either Zeiss LSM 510 or 710 laser scanning microscopes (Carl Zeiss) using a 63x Plan-Apochromat NA 1.4 oil objective. Fluorophores were excited with Argon 488 nm (GFP, YFP, AF-488), diode-pumped solid state (DPSS) 561 nm (AF-546), Helium-Neon 594 nm (mCherry) and Helium-Neon 633 nm (AF-633, AF-647, LysoTracker™ Red DND-99) laser lines. Detection was as follows: band pass 505-550 nm for GFP, YFP and AF-488; band pass 566-680 nm for AF-546; band pass 599-696 nm for mCherry; long bandpass of 650 nm for AF-633, AF-647, and LysoTracker™ Red DND-99. However, for experiments in which three channels were excited (using, for example, GFP, AF-546 and mCherry) the filter for detection of AF-546 had to be reduced (typically to between 566-580 nm) to avoid bleed-through from the mCherry channel. The pinhole diameter was set to 1 Airy unit for the longest wavelength. An Airy unit (calculated automatically by within the Zeiss software) corresponds to the theoretical size of the Airy disc – the inner, best-focussed circle of light detected within a diffraction pattern – based on the excitation wavelength and numerical aperture (NA). Thus, setting to 1 Airy unit theoretically gives the best signal:noise ratio. Detector gain and amplifier offset were adjusted to ensure that images were not saturated, and equivalent settings were maintained between the capture of images that were to be compared. In colocalisation experiments, images were regularly checked for bleed-through between channels. Typical experimental procedures involved the collection of at least six

images per condition, with experiments repeated independently at least in duplicate, typically in triplicate.

2.4.6 Quantification of confocal images

2.4.6.1 Colocalisation of fluorescent channels

Zeiss LSM Image Examiner or ZEN 2009 Light Edition were used to quantify the extent of colocalisation of two fluorescent channels from confocal images of cells expressing or labelled with ≥2 spectrally distinct fluorophores. The image analysis software produced plots of two channel intensities against each other, where distinctly colocalised or non-colocalised channels produced characteristic plots (for example see Figure 2.5A,B). Threshold fluorescence intensities, above which level fluorescence was deemed 'specific' (above background), were determined as *mean intensity + 2x standard deviation* for a background region. This was a manually selected region within the cell cytoplasm that represented background, nonspecific staining/labelling. These threshold intensities were set as crosshairs on the plot of channel intensities (Figure 2.5C) in the image analysis software. Thus, the "colocalisation coefficients" determined were defined as:

number of pixels in region 3 (colocalised) ÷ total number of specific pixels for a given channel (see example in Figure 2.5C)

The coefficient thus ranges from 0 (no colocalisation) to 1 (all pixels colocalise).

Where necessary, plasma membrane staining was excluded from this analysis in order to solely determine colocalisation of internalised species. To do this, the above process was followed, except once thresholds were determined an image region of interest (ROI) was drawn manually that enclosed the cytoplasm but excluded the plasma membrane staining (determined using the

plasma membrane staining of the relevant protein fusion present in the experiment, for example, plasma membrane staining of ssβ_2AR). The plot of channel intensities thus only included pixels within this region; setting crosshairs and calculating coefficients for this plot was performed as above.

2.4.6.2 Platereader granularity analysis

Recycling of internalised ssβ_2AR was assessed by high content, quantitative analysis using the ImageXpress Ultra confocal platereader (Molecular Devices Corporation (MDC), CA, USA). Cells stably expressing ssβ_2AR were seeded onto 96-well plates (Greiner 655090, Greiner Bio-one, Stonehouse, UK). 24 h later, cells were 80 – 90 % confluent: ssβ_2AR was labelled by replacing cell medium with 0.1 μM AF-488 conjugated SNAPsurface benzyl guanine (BG) (SNAPsurface BG-AF488, New England Biolabs; NEB, Hitchin, UK) in serum-free DMEM/0.1 % BSA for 10 min. SNAP ligand was removed with two washes in HBS, followed by incubation with vehicle or 10 μM isoprenaline (in serum-free DMEM/0.1 % BSA) for 1 h at 37 ºC. Cells were washed twice with serum-free DMEM/0.1 % BSA, and then incubated in this media with or without 1 μM propanolol for 5 – 60 min at 37 ºC ("wash" step to measure recycling). At room temperature, cells were then washed once in PBS, followed by fixation in 3 % (w/v) PFA/PBS for 10 min. Cells were washed again in PBS, nuclei were stained by incubation with 2 μg/ml Hoechst (H33342) dye in PBS for 10 min, followed by washing twice in PBS. Images were acquired immediately from four central sites per well on the ImageXpress Ultra, using a Plan Fluor 40x NA0.6 extra long working distance objective. Fluorophores were excited with 405 nm (H33342) and 488 nm (BG-AF488) laser lines.

For the quantitative detection of internalised ssβ_2AR (and hence the ability to measure ssβ_2AR recycling as a decrease in internalised receptor present following washout of agonist), a granularity algorithm application module was used (MetaXpress 2.0 software, MDC) (Watson *et al.*, 2012). In the analysis, "vesicles" were

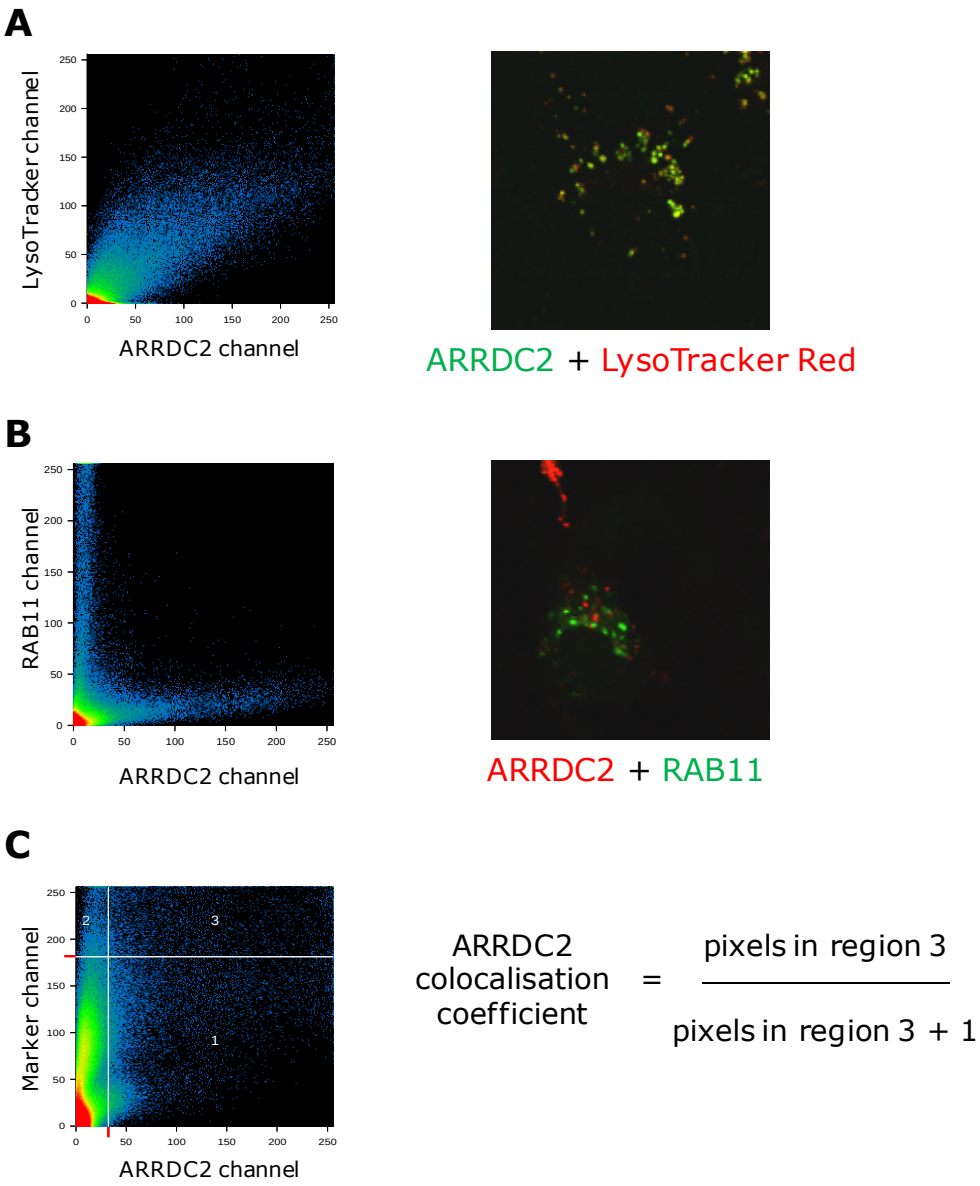

Figure 2.5 Quantification of colocalisation from confocal images

Examples of highly colocalised **(A)** and non-colocalised **(B)** images are shown (right panels). Corresponding channel intensity plots obtained from Zeiss LSM Image examiner are shown (left panels). In **(C)**, the method of quantification is indicated. Crosshairs were set as *mean intensity + 2x standard deviation* for a manually selected background region within the cell, and colocalisation coefficients for a given channel were calculated as indicated in the formula.

specified as compartments between 2 – 15 µm in diameter (488 nm image); nuclei were specified as between 6 – 15 µm (405 nm image). The threshold intensity for classification of vesicles was set with reference to the plate negative and positive controls (vehicle, 10 µM isoprenaline 1 h, respectively). Several parameters

normalised to cell count (determined by number of nuclei stained with H33342) were obtained (vesicle count, area, intensity per cell), for triplicate wells (12 sites per data group). These provided similar results; the data presented herein are vesicle average intensities per cell, normalised (%) to plate negative and positive controls (as above).

2.4.7 Bimolecular fluorescence complementation (BiFC)

In the same way as enzymes such as β-galactosidase, fluorescent proteins can be split into non-active fragments. Fusing the fragments to interacting proteins of interest brings the fragments together, leading to association, refolding and subsequent chromophore maturation (Figure 2.6) (Kerppola, 2008). Thus, BiFC is used as an assay for protein-protein interactions in cells – a fluorescent signal is indicative of an association – and may provide spatial and temporal information regarding interactions. However, it is important to note that BiFC is irreversible, giving the potential for trapping of otherwise transient interactions with potential downstream functional consequences.

BiFC was used to detect interactions between ARRDC2 and β-arrestins in intact cells. Accordingly, cells were transiently cotransfected with ARRDC2 plus β-arrestin, each fused with a respective YFP fragment. The ability of β-arrestins to homo-oligomerise was exploited as a positive control (cotransfection of β-arrestin2-Yn plus β-arrestin2-Yc); singly transfected cells – presumed to be non-fluorescent – were included as negative controls.

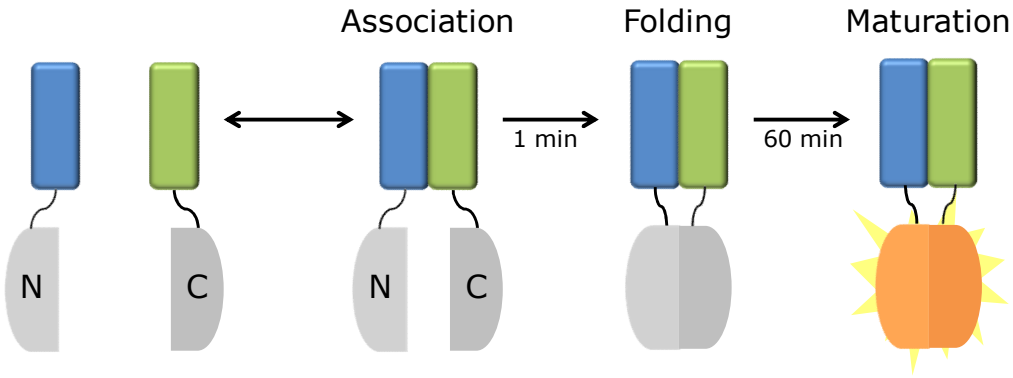

Figure 2.6 Principle of BiFC

A fluorescent protein (for example, enhanced YFP) is split into two non-fluorescent N- and C-terminal fragments (N and C). The fragments are fused to two proteins of interest (shown in blue and green) that are able to interact reversibly (association) until the fluorescent protein fragments refold to form a β-barrel structure ($t_{1/2}$ = 1 minute; folding). The fluorescent protein chromophore then develops over a longer time-scale to generate a fluorescent BiFC complex ($t_{1/2}$ = 60 minutes; maturation). Adapted from (Rose *et al.*, 2010).

2.5 Immunoprecipitation and immunodetection

2.5.1 Preparation of U2OS cell extracts

Cells on 6-well plates were transfected as appropriate. 24-48 h later, cells were washed twice with ice-cold PBS, followed by lysis in ice-cold radioimmunoprecipitation assay (RIPA) buffer (25 mM Tris-HCl [pH 7.6], 150 mM NaCl, 1% (w/v) Nonidet P (NP)-40, 1% (w/v) sodium deoxycholate, 0.1% (w/v) sodium dodecyl sulphate (SDS)) supplemented with a protease inhibitor cocktail containing 4-(2-Aminoethyl)-Benzenesulphonyl Fluoride (AEBSF), Aprotinin, E-64, Bestatin, Leupeptin and Pepstatin (Melford Laboratories, Suffolk, UK). Typically, 2-4 wells were used for each separate transfection/treatment condition, and 200-250 µl lysis buffer was used per well. Cells were incubated in lysis buffer at 4ºC for 5 min, followed by removal of cells using a cell scraper. Complete lysis was ensured by mixing lysates on a rotator at 4ºC for 30 min. They were then briefly sonicated to shear genomic DNA, and clarified by centrifugation at 13,000 rpm at 4ºC for 15 min in order to pellet the

cell debris. Supernatant ('cell lysate') was retained and protein concentration was estimated using a bicinchoninic acid (BCA) protein assay (Smith *et al.*, 1985), using pre-diluted BSA solutions (between 2-20 µg/µl) as standards. Cell lysates were either used immediately (sections 2.5.2, 2.5.3) or stored at -20 ^{o}C for future use.

2.5.2 Immunoprecipitation

In order to specifically isolate HA- or FLAG-tagged proteins (and their interacting partners) from transfected U2OS cells, pull-down experiments (immunoprecipitation) using anti-HA (mouse monoclonal anti-HA-agarose; Sigma) or anti-FLAG (mouse monoclonal anti-FLAG M2 affinity gel; Sigma) agarose beads were performed. Agarose bead suspension (20 µl anti-HA, 15 µl anti-FLAG, per immunoprecipitation) in 1.5 ml tubes was washed in 1 ml ice-cold RIPA buffer, followed by centrifugation at 2000 rpm for 1 min (low centrifugation speed was used to ensure that agarose beads were not crushed by higher pressures) and subsequent removal of the supernatant, taking care not to dislodge the agarose beads. This step was repeated for a total of two washes. Cell lysates, equalised for protein content (see BCA assay above), obtained as in section 2.5.1, were added to the washed agarose beads; typically 500 µl – 1 ml lysate was added per immunoprecipitation. Protein binding to the agarose was allowed to proceed by mixing on a rotator at 4 ^{o}C overnight. The following day, the suspension was centrifuged (2000 rpm, 1 min) and the supernatant carefully discarded as previously. Non-specific binding to the agarose was then removed by washing (5 min at 4 ^{o}C with end-end mixing) in a high salt buffer (RIPA buffer as above except containing 500 mM NaCl) followed by three washes in standard RIPA. Each wash step was separated by centrifugation and careful discarding of supernatants as above. After the final wash step residual traces of RIPA buffer were carefully removed using a narrow-bore pipette tip. Agarose beads and their

associated protein complexes were subsequently processed and analysed as detailed below (section 2.5.3).

2.5.3 Protein separation by denaturing SDS-PAGE and Western blotting

One-dimensional, reducing sodium dodecyl sulphate-polyacrylamide gel electrophoresis (SDS-PAGE) was performed using the Laemmli method (Laemmli, 1970). The Geneflow OmniPAGE (Geneflow, Staffordshire, UK) gel system was used. Protein samples (typically 15-20 μg of cell lysate, or agarose beads from immunoprecipitation; section 2.5.2) were mixed with sample loading buffer to a final concentration: 62.5 mM Tris-HCl (pH 6.8), 5 % (v/v) glycerol, 1 % (w/v) SDS, 0.5 mM EDTA, 100 mM dithiothreitol (DTT), 1 % (v/v) β-mercaptoethanol, 0.0025 % (w/v) bromophenol blue. Samples were incubated at 80 ^{o}C for 10 min before loading onto 10 – 12.5 % polyacrylamide gels (prepared in-house) alongside a molecular weight marker (PageRuler Prestained Protein Ladder, 10 – 170 kD, Fermentas). Immunoprecipitate samples, following incubation at 80 ^{o}C, were additionally centrifuged for 1 min at 2000 rpm in order to pellet the agarose beads; the supernatant was loaded onto gels. Samples were separated by electrophoresis at constant voltage (~150 V) for 1 – 1.5 h in a running buffer (25 mM Tris, 192 mM glycine, 0.01 % [w/v] SDS) until the bromophenol blue dye front just eluted from the bottom of the gel.

The protein gel apparatus was dismantled and the gel was placed alongside a sheet of nitrocellulose membrane of equivalent area (BioTrace NT nitrocellulose membrane; Pall Corporation, Portsmouth, UK) that was pre-soaked in Western transfer buffer (25 mM Tris, 192 mM glycine, 20 % [v/v] methanol). Protein transfer to the membrane was carried out in the blotting tank containing transfer buffer at constant voltage (10 – 20 V) for between 2 – 5 h at room temperature. Membranes were removed and incubated with blocking solution (5 % [w/v] skimmed milk powder in TTBS [Tris-buffered saline containing 0.1 % Tween 20]) at 4 ^{o}C overnight to block non-

specific sites. Subsequent manipulations were performed at room temperature. Membranes were incubated with primary antibody at the appropriate concentration in 1 % (w/v) skimmed milk powder/TTBS ("1 % SMP") for 2 h. Membranes were washed three times with TTBS for 10 min each, followed by incubation with the appropriate secondary antibody in 1 % SMP for 45 – 60 min. The membranes were then washed as above, followed by replacement of the final wash with TBS and imaging using the LI-COR Odyssey imager (LI-COR Biosciences, Nebraska, USA).

Primary antibodies used in immunoblotting were anti-HA (rabbit monoclonal; Sigma), anti-FLAG (rabbit polyclonal anti-ECS [DDDDK]; Bethyl Laboratories, Texas, USA) and anti-GFP (mouse monoclonal JL-8, Clontech, CA, USA). Secondary antibodies for use with the LI-COR system were donkey anti-rabbit or anti-mouse infrared dye (IRDye) 800CW (LI-COR Biosciences).

2.5.4 Development of an anti-ARRDC2 antibody

Prior to the start of the current project, the host laboratory had ordered an anti-ARRDC2 antibody raised in rabbit using a small presumed antigenic peptide corresponding to a region in the ARRDC2 C-terminus (Genosphere, Paris, France). However, no anti-ARRDC2 immunoreactivity was detectable using this antibody in Western blotting experiments (data not shown). Another antibody was produced by the same method (Genosphere), this time using the peptide YSEEDPNPLLGDMRP as antigen. This sequence, corresponding to amino acid residues 388 – 402 of human ARRDC2, was chosen on the basis of several criteria. Estimation of ARRDC2 protein hydrophobicity using two established algorithms (Hopp *et al.*, 1981; Kyte *et al.*, 1982) indicated that the region containing residues 388 – 402 scores relatively low, especially using the Kyte and Doolittle analysis (Figure 2.7A,B). Low hydrophobicity in this region suggested that it may be solvent exposed on the protein surface and therefore may represent a good target for potential antigenic sites. The region has an average score when the

percentage of accessible residues are estimated (Figure 2.7C), further suggesting that it may at least not be buried in the native protein and therefore may be available for antibody interaction. Additionally, the ARRDC2 388 – 402 residue sequence is unique to ARRDC2; although homologous sequences exist in ARRDC3, ARRDC4 and TXNIP (Figure 2.8), the highest sequence identity within this region is 46 %, between ARRDC2 and ARRDC3 sequences. Hence, it was hypothesised that the antibody produced may specifically recognise ARRDC2. Lastly, the antigenic peptide was chosen to include a tyrosine residue (corresponding to ARRDC2 Y^{388}) as this aromatic residue has long been thought to enhance antigen specificity and immunogenicity (Fuchs *et al.*, 1963). Testing of the resultant antibody is described in the first results chapter (section 3.2.3.1).

2.6 ^{3}H-cAMP accumulation

2.6.1 Column Preparation

Dowex columns were prepared using Dowex AG '50' 50W-X4 resin (hydrogen form) mesh 200-400 (BioRad), which was made into slurry with ddH_2O (50:50, volume:volume) and 2.4 ml placed into 'Poly-prep' columns (BioRad). Prior to each experiment, the columns were regenerated with the addition of 10 ml HCl followed by two washes with 10 ml ddH_2O. Alumina columns were prepared by the addition of 0.6 g of Neutral alumina WN-3 (Sigma) to Poly-prep columns. Prior to each experiment, the columns were regenerated with two washes of 10 ml 0.1 M imidazole (Sigma).

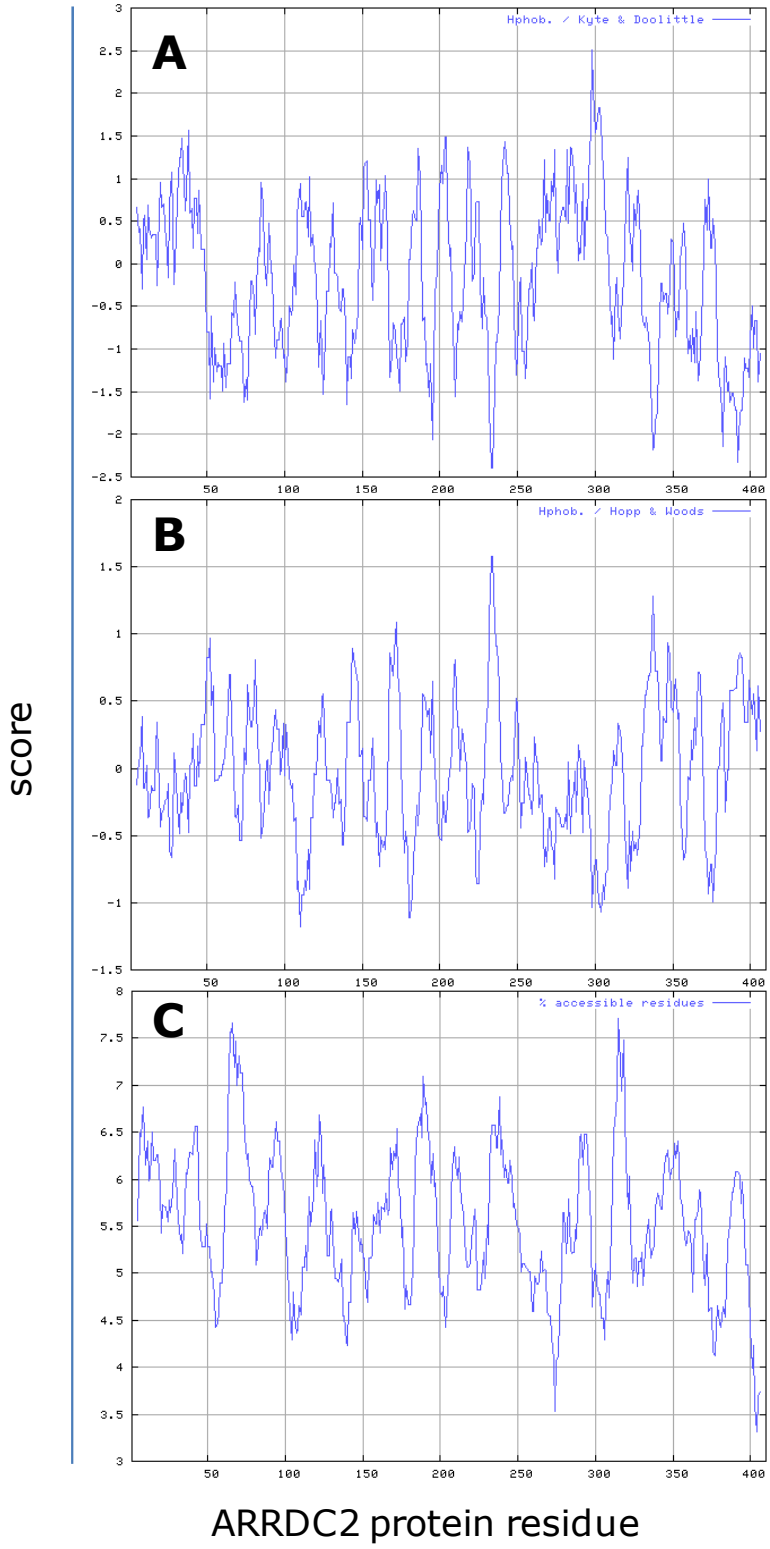

Figure 2.7 ARRDC2 protein sequence analysis

(A) Kyte & Doolittle hydrophobicity plot (window = 9). **(B)** Hopp & Woods hydrophobicity plot (window = 9). **(C)** % accessible residues analysis. All analyses performed using ExPasy ProtScale tool.

```
ARRDC1        YEQSCGGVEPSLTPES---
ARRDC2        ----YSEEDPNPLLGDMRP
ARRDC3        ----YSEIDPNPDQSADDR
ARRDC4        ----YSEVDPHPSDVEESQ
TXNIP         ----YTEVDPCILNNNVQ-
                          :*
```

Figure 2.8 Multiple sequence alignment of the ARRDC2 antigenic peptide with similar α-arrestin sequences

ARRDC2 protein sequence corresponding to amino acid residues 388 – 402 was aligned with similar sequences in ARRDC3, ARRDC4 and TXNIP, as shown using ClustalW2 (http://www.ebi.ac.uk/Tools/msa/clustalw2/). No similar sequences were identified in whole sequence alignments with ARRDC5, Vps26 or β-arrestin1/2. *, fully conserved residue; :, stongly similar residues.

2.6.2 ^{3}H-cAMP accumulation assay

The assay used was Dowex-Alumina chromatography based on a column-based method developed elsewhere (Donaldson *et al.*, 1988). Cells (typically U2OSTR ARRDC2-GFP) were seeded onto 24-well plates (Table 2.4) in normal DMEM plus FBS, followed 24 h later by replacement of the media with media supplemented with or without 1 µg/ml tetracycline, as appropriate. 24 h later, cells were confluent (>90%) and the experiment was performed. Media was removed and the cells were loaded with ^{3}H-adenine by incubating with 500 µl serum-free DMEM containing 1 µl ^{3}H-adenine (550-925 Gigabecquerel [GBq]/mmol) per well at 37 ºC for 2 h. ^{3}H-adenine-containing media was removed and the cells were washed with 1 ml serum-free DMEM. Cells were then incubated in 1ml of 1 mM 3-isobutyl-1-methylxanthine (IBMX; a phosphodiesterase inhibitor) at 37 ºC for 15 min. Agonists, in 10 µl serum-free DMEM, were then added and incubated for a further 5 h at 37 ºC. The reaction was stopped by the addition of 50 µl concentrated HCl per well. 1 µl ^{14}C-cAMP (>8.1 GBq/mmol) was diluted in 5 ml ddH_2O, and 100 µl of this was added to each well as a standard. The samples were frozen down for storage (-20 ºC) and thawed prior to running columns. 100 µl of the ^{14}C-cAMP mix was also added to each of three scintillation vials, which were used as 100% recovery controls.

2.6.3 ^{3}H-cAMP and ^{14}C-cAMP recovery

Samples were thawed, and the entirety of the contents of each well was transferred to the corresponding Dowex column and allowed to drip through. The passage of nucleotides through the columns is delayed as the molecules become adsorbed onto the resin. The columns were then washed with 3 ml ddH_2O, thereby eluting the most negatively charged molecules (e.g. ADP, ATP; two or three phosphate groups, respectively) which are repelled by the negatively charged Dowex. This leaves the less negatively charged AMP and cAMP (one phosphate) still in the Dowex. The Dowex columns were then placed over the Alumina columns, and 6 ml ddH_2O was added to each Dowex column, thus eluting the cAMP (^{3}H-cAMP, ^{14}C-cAMP and unlabelled cAMP) from the Dowex into the alumina columns. The alumina columns were then placed over scintillation vials and 5 ml 0.1 M imidazole was added to each column, eluting the cAMP into the vials. 8 ml scintillation fluid was added to each vial and the 100% recovery vials. All vials were counted on a β-counter capable of dual counting ^{3}H and ^{14}C simultaneously.

2.6.4 Dual detection of β-particle emission

^{14}C and ^{3}H both decay by emitting high-energy electrons ('β-particles') from the nucleus. These are measured by the detection of photons of light which are released when the β-particles collide with molecules in the scintillation fluid. Counting of the photons produced gives counts per minute (cpm) which, in comparison to a control radioactive sample, are corrected to disintegrations per minute (dpm). Dual counting of ^{14}C and ^{3}H relies on the fact that the β-particles emitted from ^{14}C have more energy than those from ^{3}H, enabling the counter to recognise the photons produced by each isotope as a distinct species.

2.6.5 ^{3}H-cAMP accumulation data analysis

The 14C-cAMP dpm from the 100% recovery vials was averaged; this was the expected 14C-cAMP count if the columns were 100% efficient. As an estimate of the efficiency of each column, a 'recovery fraction' was calculated as:

$$\text{Recovery fraction} = \frac{\text{individual column 14C-cAMP count (dpm)}}{\text{mean 100\% recovery vial 14C-cAMP count (dpm)}}$$

3H-cAMP count for each column was then corrected for the column efficiency as follows:

$$\text{Corrected 3H-cAMP} = \frac{\text{individual column 3H-cAMP count (dpm)}}{\text{Recovery fraction}}$$

These corrected dpm counts were then plotted against agonist concentration to give response curves. 24-well plates were organised such that each experimental condition was performed in triplicate or duplicate. Each plate had two basal (no drug) and two maximally stimulated (10 μM isoprenaline) wells, and data were normalised such that for each plate the basal and maximal responses represented 0 and 100% responses, respectively.

2.7 Data analysis

All numerical data were presented as the mean ± S.E.M., and statistical analyses and data presentation were performed using GraphPad Prism v5.01. The statistical significance of three or more data sets compared to a single control data set was determined using one-way ANOVA followed by Tukey post-hoc test for multiple comparison of means. A two-way ANOVA was used to compare data sets with two or more variables. Statistical significance (P) values are stated in the figures and within the text where appropriate; $P < 0.05$ was considered significant.

3 Subcellular localisation of ARRDC2

3.1 Introduction

The human α-arrestins are relatively uncharacterised in terms of their subcellular localisation. Only Vps26 – a retromer component associated with endosomes/TGN (Bonifacino *et al.*, 2008) – and TXNIP – thought to localise to the nucleus (Saxena *et al.*, 2009) – are reasonably documented in terms of their distribution. For the ARRDCs, only a few reports exist to date that have studied their localisation in cultured cells, and in some cases the data presented are contradictory (summarised in Table 3.1). Hence, initial studies investigated ARRDC localisation, focussing on ARRDC2. This information would then be used to develop a hypothesis for a potential role of ARRDC2 within the relevant subcellular system.

Several markers known for their targeting to specific compartments within the endocytic system were used to clarify ARRDC2 localisation. The major stages within the endocytic system following clathrin-mediated endocytosis are described below (see Figure 3.1), highlighting the components that were used as markers in the current investigation.

Table 3.1 Published localisation data for human ARRDCs

ARRDC	Localisation	Cell line(s)	Reference
ARRDC1	Largely PM, no intracellular	HEK-293	Nabhan et al., 2010
	Punctate (vesicular) cytoplasmic	HEK-293	Rauch and Serrano, 2011
	Largely PM, no intracellular	HEK-293T, HeLa, A549	Nabhan et al., 2012
ARRDC2	No data		
ARRDC3	Largely PM, no intracellular	HEK-293	Nabhan et al., 2010
	PM, endosomes and lysosomes	HeLa, COS-7, CHO, HEK-293	Oka et al., 2006
	PM and punctate cytoplasmic	HEK-293	Patwari et al., 2009
ARRDC4	Punctate (vesicular) cytoplasmic	PAE	Vina-Vilasseca et al., 2011
	PM and punctate cytoplasmic	HEK-293	Patwari et al., 2009
ARRDC5	No data		

Clathrin-mediated endocytosis

The best characterised route for endocytosis of materials such as membrane proteins and lipids is the clathrin-mediated pathway

(McMahon *et al.*, 2011). Cargo receptor endocytosis may be constitutive (for example, transferrin receptor; TfR) or ligand-stimulated (exemplified classically by EGFR; many GPCRs are also in this category – see section 1.2.2).

Endocytosis proceeds through five main stages, defined temporally and by the molecular machineries involved. The first stage (initiation) involves the nucleation of plasma membrane subdomains that contain FCH (FES CIP4 homology) domain only (FCHO), Eps15 and intersectin proteins, which selectively bind phosphatidylinositol-4,5-bisphosphate ($PI4,5P_2$), a lipid enriched within the inner leaflet of the plasma membrane. FCHO/Eps15/intersectins generate initial membrane curvature, later to be stabilised by clathrin (Henne *et al.*, 2010). In the second stage (cargo selection), AP2 is recruited via interaction with $PI4,5P_2$ and Eps15/intersectins. AP2 acts as a cargo adaptor, either directly interacting with transmembrane cargo (e.g. TfR) or indirectly via accessory proteins (e.g. β-arrestins as adaptors for GPCR recruitment). Next (coat assembly), clathrin is recruited via interactions with AP2 and accessory proteins. Polymerisation of clathrin triskelia forms a lattice coat, the structure of which further induces membrane curvature leading to an invaginated clathrin-coated pit (CCP). BAR domain-containing proteins (amphiphysin, endophilin, SNX9) have a preference for curved membranes; they bind to the neck of the invaginating CCP, positively inducing further curvature that 'squeezes' the neck. This leads to the next stage (scission): the GTPase dynamin is recruited to the neck and catalyses scission, producing a clathrin-coated vesicle (CCV). Finally, the clathrin coat is disassembled (uncoating) by the ATPase heat shock cognate 70 (HSC70) and its cofactor, auxilin (McMahon *et al.*, 2011).

CCV targeting to early endosomes

Following endocytosis, CCVs undergo heterotypic fusion with early endosomes; early endosomes then undergo homotypic fusion. These

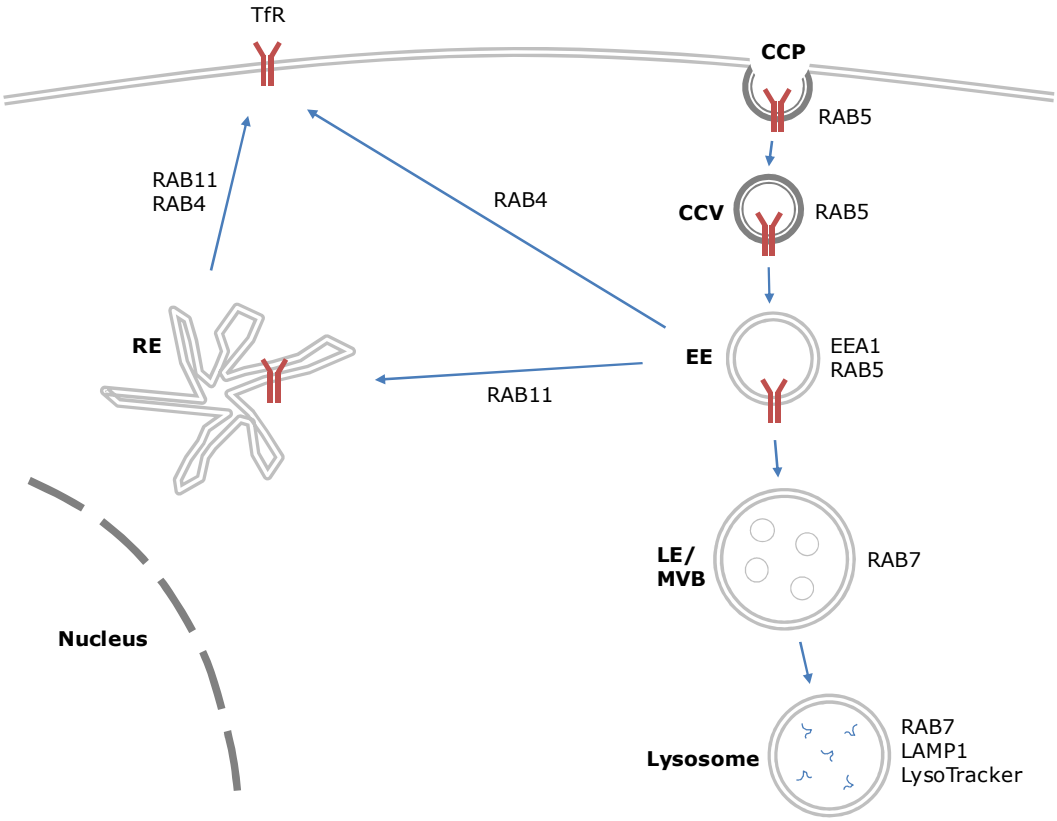

Figure 3.1 Summary of the endocytic system in mammalian cells

Schematic showing the major intracellular compartments following clathrin-mediated cargo endocytosis. Plasma membrane cargo proteins, such as the transferrin receptor (TfR), are internalised through the formation of clathrin-coated pits (CCP) that contain RAB5, which invaginate and bud off to generate clathrin-coated vesicles (CCV). RAB5 is present on CCVs and early endosomes (EE), promoting fusion via the early endosomal 'tether' protein, EEA1. Cargo sorting in EEs determines the itinerary of recycling versus lysosomal trafficking. TfR undergoes recycling to the plasma membrane, either by a direct (rapid) route regulated by RAB4, or indirectly via perinuclear recycling endosomes (RE), involving RAB11 and RAB4 (slow recycling). Cargo in EEs destined for the lysosome is instead sorted into late endosomes/multivesicular bodies (LE/MVB) which contain RAB7; these compartments mature into lysosomes which contain degradative enzymes for the hydrolysis of sorted proteins. Lysosomes also contain RAB7 as well as lysosome-associated membrane protein 1 (LAMP1), and are acidic (pH ~4.5), enabling their visualisation using pH-sensitive dyes such as LysoTracker.

events are mediated by the RAB GTPase, RAB5.

RAB proteins are a family of small GTPases (>60 members in humans) that control multiple aspects of vesicle trafficking including budding, uncoating, fusion and cargo selection (Stenmark, 2009). RABs are specifically associated with distinct intracellular

membranes by the insertion of geranylgeranyl groups covalently attached to RAB cysteine residues. They cycle between an inactive, cytosolic form (guanosine diphosphate (GDP)-bound) and an active, membrane-associated form (guanosine triphosphate (GTP)-bound). Exchange of GTP for GDP is catalysed by guanine nucleotide exchange factors (GEFs), and the GTP-bound form is preferentially bound by various RAB effectors; GTP hydrolysis (accelerated by GTPase-activating proteins; GAPs) provides energy for processes including vesicle budding, uncoating and fusion.

RAB5 localises specifically to the plasma membrane, CCVs and early endosomes. At the plasma membrane, RAB5 can mediate cargo selection; for example, direct RAB5 binding to GPCR C-tails has been observed (Seachrist *et al.*, 2003). CCV-early endosome fusion is mediated by RAB5 in concert with its effector, early endosomal antigen 1 (EEA1). EEA1 localises specifically to early endosomes via a zinc-binding FYVE finger within its C-terminus (Stenmark *et al.*, 1996). FYVE-dependent targeting involves binding to phosphatidylinositol-3-phosphate (PI3P), which is enriched in early endosomes. EEA1 contains two RAB5-binding domains at the N- and C-termini and functions as a dimer (Simonsen *et al.*, 1998); it has thus been proposed that EEA1 tethers RAB5-containing CCVs and early endosomal membranes, thereby facilitating fusion. In the current study, RAB5 and EEA1 were utilised as markers of the early stages of the endocytic system (predominantly CCVs and early endosomes).

The sorting endosome: recycling pathways

Cargo within early endosomes can return directly to the plasma membrane (rapid recycling), be trafficked through an intermediate recycling endosome (also called the perinuclear recycling compartment) before returning to the plasma membrane (slower recycling), or be sorted into the MVB/late endosome pathway for lysosomal degradation. Sorting through these different pathways is complex, but is well characterised in terms of the specific RAB proteins that define each compartment: RAB4 regulates rapid

recycling (van der Sluijs *et al.*, 1992), whereas RAB11 mediates slow recycling through recycling endosomes (Ullrich *et al.*, 1996), as well as retrograde sorting from endosomes to the Golgi. Here, RAB11 was used as a marker of recycling endosomes.

Within this system, endocytosed transferrin was also used as an early/recycling endosomal marker. Transferrin is a plasma glycoprotein that is responsible for the transport of iron within the blood. Transferrin binds up to two Fe^{3+} ions, delivering them into cells via binding and co-internalisation with its receptor (TfR). The mechanism of delivery involves the dissociation of iron from transferrin once within endosomes, since the affinity of iron for transferrin is low at the acidic endosomal pH. However, transferrin affinity for TfR is high at acidic pH; thus, transferrin-TfR remain associated and recycle to the plasma membrane where, due to the low affinity of transferrin for TfR at neutral pH, transferrin is released to scavenge more iron (Dautry-Varsat, 1986). TfR endocytosis and the fusion of subsequent CCVs-endosomes are mediated by RAB5, and TfR can recycle via both RAB4-dependent (rapid) and RAB11-dependent (slow) pathways (Zerial *et al.*, 2001); thus, transferrin/TfR has long been used as a standard marker for endocytic recycling.

These pathways can be perturbed by the expression of mutant versions of RAB proteins. For example, expression of constitutively-active GTP-bound RAB5Q79L promotes homotypic vesicle fusion, resulting in enlarged ring-like structures that contain early endosomal cargo such as transferrin, whose recycling is reduced (Stenmark *et al.*, 1994; Wegener *et al.*, 2010). Constitutively-active RAB11 (RAB11Q70L) similarly stimulates vesicle fusion, but within the slow recycling/retrograde pathways, thereby attenuating the transport of transferrin and markers of early endosome-to-Golgi (*trans*-Golgi network 38; TGN38), but not affecting lysosomal transport (Wilcke *et al.*, 2000). Thus, expression of RAB5Q79L and RAB11Q70L was used here to inhibit transport through early and recycling endosomes, respectively.

Lysosomal trafficking

As described in section 1.2.3, sorting of cargo to the lysosome involves ESCRT-mediated incorporation into MVBs/late endosomes, followed by fusion of late endosomes with lysosomes. RAB7 is specifically targeted to late endosomes/lysosomes, and mediates late endosome maturation and fusion with lysosomes. The segregation of RAB5 to early endosomes and RAB7 to late endosomes is enabled by an elegant 'switch' mechanism. RAB5 recruits the RAB7 GEF, Vps39, leading to RAB7 activation and recruitment; RAB7 recruits a RAB5 GAP up until a critical point, where RAB5 is inactivated and removed (Stenmark, 2009). RAB7 was used as a late endosomal/lysosomal marker here. Similar to the RAB5 and RAB11 mutants described above, constitutively-active RAB7Q67L perturbs late endosomal dynamics, resulting in enlarged MVB structures that contain lysosomal markers such as cathepsin D (Bucci *et al.*, 2000). RAB7Q67L has been used here to enhance visualisation of traffic through late endosomes/MVBs.

Protein degradation within the lysosome is catalysed by lysosomal acid hydrolases, the activity of which is dependent upon an acidic lumenal pH (lysosome pH ~4.5, compared to cytosol pH 7.2). Lysosomal acidity is maintained by vacuolar H^+ ATPases, which pump protons into the lysosome. Lysosome-associated membrane protein 1 (LAMP1) is a ubiquitous integral membrane glycoprotein that is highly enriched in the limiting membrane (outer membrane surrounding MVBs) of late endosomes/lysosomes (Chen *et al.*, 1985). Extensive glycosylation on the lumenal face of LAMP1 may protect the membrane from degradation by lysosomal acid hydrolases (Kundra *et al.*, 1999), and LAMP1 also facilitates lysosome acidification redundantly with LAMP2 (Eskelinen *et al.*, 2003). Hence, LAMP1 has been used here as a lysosomal marker. Additionally, the acidity of lysosomes has been exploited in the design of LysoTracker probes (Invitrogen); these are fluorophores that are linked to a weak base, thereby targeting them to compartments with low pH (lysosomes). Such probes are used in

the live-cell labelling of lysosomes: here LysoTracker Red DND-99 was used.

3.2 Results

3.2.1 Subcellular localisation of exogenously expressed ARRDCs in U2OS cells

Initial experiments aimed to visualise exogenous, fluorescent protein-tagged ARRDCs (especially ARRDC2) in cell lines. HEK-293 cells (immortalised human cell line commonly used in the host laboratory) were first tested for this application. Transient transfection of HEK-293 cells with ARRDC2 constructs (for example, ARRDC2-GFP) resulted in extremely low percentage transfection efficiencies, and those cells that did express the transgene were frequently morphologically abnormal with rounded shape and indistinct structure. To circumvent this problem, stable HEK-293TRex cells were generated that expressed tetracycline-inducible ARRDC2-GFP (in pcDNA4TO plasmid). Cells induced to express ARRDC2-GFP with tetracycline also exhibited altered phenotypes such as multinucleation and high overexpression suggestive of cytotoxicity (Figure 3.2). Dilution cloning of mixed stable HEK-293TRex ARRDC2-GFP cells was performed to obtain a more homogeneous population of pcDNA4TO-ARRDC2-GFP transfected cells; cells were selected for their ARRDC2-GFP expression levels and morphology that appeared normal. This approach produced several stable clonal lines that displayed high percentage (>90%), low level expression of ARRDC2-GFP in a cytoplasmic, punctate pattern. However, expression of the ARRDC2-GFP transgene was rapidly lost over just 2-4 cell passages. Low percentage transfection efficiency and morphological abnormalities were observed for alternatively tagged ARRDC2 constructs (for example ARRDC2-HA, data not shown); hence this was not caused by the GFP tag. Additionally, transient expression of GFP or YFP-tagged alternative proteins such as β-arrestins in HEK-293 cells was high efficiency and

resulted in an expected β-arrestin distribution (not shown), suggesting that the ARRDC2 transgene was the cause of the abnormalities in these cells. Overall these observations suggested that exogenous expression of ARRDC2 in HEK-293 cells may adversely affect cell phenotype, leading to cytotoxicity and loss of transgene expression. Thus, an alternative approach was adopted in order to assess ARRDC2 expression in a system representative of native ARRDC2.

The human cell line, U2OS (osteosarcoma-derived), was tested for its ability to tolerate exogenous ARRDC2. Transient U2OS transfection resulted in much higher percentage expression of ARRDC2 constructs (typically ~40-60%), and cells expressing ARRDC2 (or other ARRDCs, see below) were morphologically indiscernible from non-transfected cells. Therefore, U2OS cells were used in most subsequent experiments. The subcellular localisation of all human ARRDCs was analysed, excluding ARRDC5, which has the least sequence similarity to the rest (ARRDC5 lacks the variable C-terminal region containing PPxY motifs; see Figure 1.4). Plasmids encoding ARRDCs C-terminally tagged with eGFP-HA were transiently expressed in U2OS cells on coverslips, and the cells were fixed and imaged using confocal microscopy. The three ARRDCs with highest homology, ARRDC2/3/4, all shared a highly similar subcellular pattern, although each was expressed separately (although note later experiment in which ARRDC2/3 colocalised when coexpressed, Figure 3.8). Their expression pattern was that of plasma membrane localisation, as well as a large number of discrete intracellular puncta reminiscent of vesicles (Figure 3.3A). In each case, the puncta were distributed throughout the cytoplasm; congregation at a particular area (for example, the perinuclear compartment) was not observed. In some cases – seen sporadically for each of ARRDC2/3/4 – the intracellular puncta were especially large, suggestive of aberrantly oversized vesicles, perhaps due to the overexpression of proteins that have roles in the function and/or formation of the vesicles in question. Thus, ARRDC2/3/4 are

targeted to cytoplasmic vesicular compartments and the plasma membrane in U2OS cells.

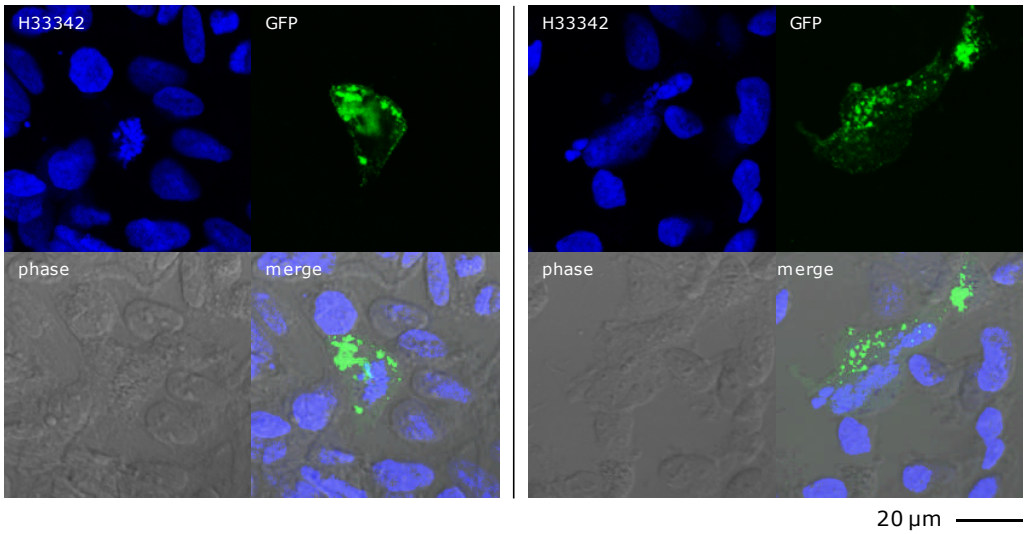

Figure 3.2 Expression of ARRDC2-GFP in HEK-293TRex cells

Confocal microscopic images of stable HEK-293TRex cells expressing tetracycline-induced ARRDC2-GFP. Cells were seeded onto poly-L-lysine-coated coverslips, treated the next day with tetracycline (1 µg/ml) for 24 h and then fixed, nuclei stained (1 µg/ml H33342, 10 min), mounted on slides and imaged.

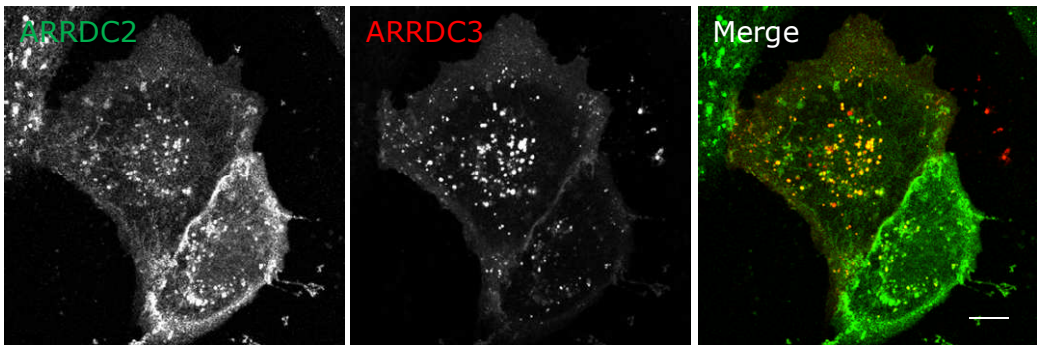

Figure 3.8 Coexpression of ARRDC2 and ARRDC3

Confocal microscopic images of stable U2OSTR ARRDC2-GFP cells expressing tetracycline-induced ARRDC2-GFP, transiently cotransfected with a plasmid expressing ARRDC3-mCherry. In the merged image, ARRDC2 is shown in green, ARRDC3 in red. Image is representative of two independent experiments. Scale bar = 10 µm.

Fusion with large fluorescent proteins such as GFP (~28 kD) and its derivatives (mCherry used here) has the potential to produce artefacts in the observed protein distribution, for example by masking sorting signal(s) within the protein of interest. ARRDC2 alternatively tagged with two copies of a much smaller epitope (FLAG tag: DYKDDDDK) was used to compare to transient ARRDC2-GFP, as well as ARRDC2-mCherry and tetracycline-inducible ARRDC2-GFP. Transiently expressed ARRDC2-mCherry, ARRDC2-2FLAG (immunostained with anti-FLAG antibody) or ARRDC2-GFP, or ARRDC2-GFP expressed upon tetracycline induction in the stable line U2OSTR pcDNA4TO-ARRDC2-GFP, all showed the same overall pattern of localisation to the plasma membrane and cytoplasmic puncta (Figure 3.3B). This suggests that the presence of large GFP-based C-terminal tags does not affect ARRDC2 subcellular targeting.

ARRDC1-eGFP-HA was expressed in a similar pattern to ARRDC2/3/4-eGFP-HA mentioned above, with plasma membrane and cytoplasmic puncta apparent (Figure 3.3A). Additional diffuse ARRDC1 staining was often observed throughout the cytosol, which was not consistently seen for ARRDC2/3/4. Therefore, ARRDC1 is also targeted to vesicular structures in U2OS cells, but may exhibit subtle differences in distribution to ARRDC2/3/4.

As a comparison, TXNIP-eGFP-HA and β-arrestin2-YFP were transiently expressed in U2OS cells. TXNIP has been reported to localise to the nucleus (Saxena *et al.*, 2009). This was observed here: TXNIP-eGFP-HA was strongly expressed within the nucleus, but was also sporadically found in punctate cytoplasmic compartments (Figure 3.3A). The β-arrestins are well known for their diffuse cytosolic distribution (i.e. not membrane-associated) in cells in recombinant systems. This same distribution was seen here for β-arrestin2-YFP in U2OS cells (Figure 3.3A). Thus, TXNIP and β-arrestin2 subcellular targeting in U2OS cells was consistent with previously published observations.

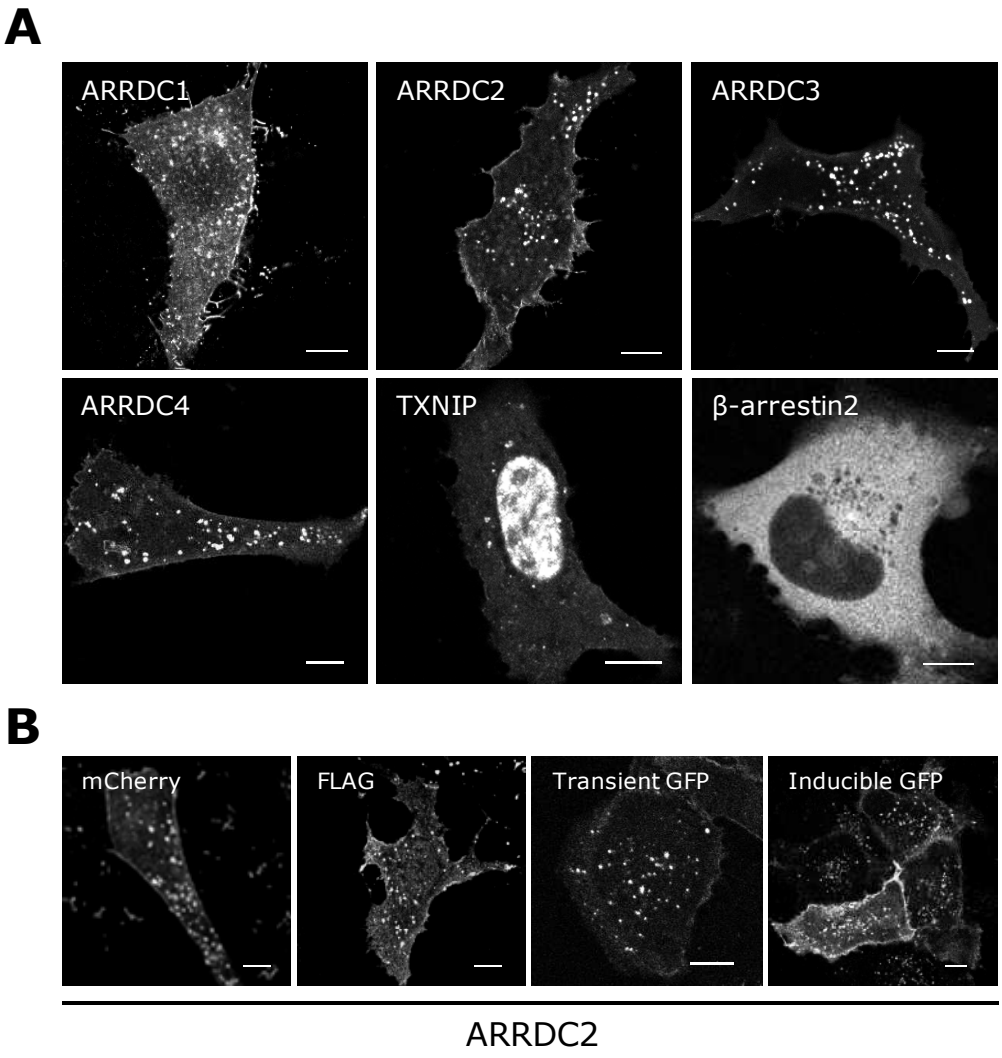

Figure 3.3 Exogenous expression pattern of arrestin clan proteins in U2OS cells

Confocal microscopic images: **(A)** U2OS cells transiently transfected with plasmids expressing ARRDC1/2/3/4 or TXNIP fused with eGFP-HA, or β-arrestin2 C-terminally fused with YFP; **(B)** U2OS cells expressing ARRDC2 fused with the indicated construct. ARRDC2-FLAG was stained using mouse anti-FLAG antibody (1:200 dilution) detected with AF-488-conjugated anti-mouse secondary antibody (1:1000). "Transient GFP" represents transiently expressed ARRDC2-GFP; "Inducible GFP" represents stable U2OSTR ARRDC2-GFP cells expressing tetracycline-induced ARRDC2-GFP. Representative images from at least two independent experiments are shown. Scale bar in all images = 10 μm.

3.2.2 ARRDC2 is dynamically localised to the endo-lysosomal system

3.2.2.1 Colocalisation of ARRDC2 with compartment-specific markers

Several α-arrestins in lower eukaryotes have been implicated in cargo protein sorting in the endo-lysosomal pathway (Herrador *et al.*, 2009; Lin *et al.*, 2008; Nabhan *et al.*, 2010; Nikko *et al.*, 2009; Nikko *et al.*, 2008; Shi *et al.*, 2006), and early reports suggest human ARRDCs may also localise to the endocytic system (see section 1.4.3.3 and Table 3.1). Therefore, it was hypothesised that the ARRDC2-positive intracellular puncta observed in Figure 3.3 may represent a component of this system. To test this, the distribution of transiently expressed, fluorescent protein-tagged ARRDC2 in U2OS cells was analysed in combination with known endocytic markers (detailed in section 3.1). The extent of ARRDC2 colocalisation with each marker was assessed as described (section 2.4.6).

ARRDC2-positive cytoplasmic puncta were largely distinct from transferrin-labelled early/recycling endosomes or EEA1-labelled early endosomes (colocalisation coefficients of 0.111±0.022, 0.137±0.030 for ARRDC2-mCherry colocalisation with AF-633-conjugated transferrin or EEA1-GFP, respectively, Figures 3.4 and 3.6). Furthermore, colocalisation of ARRDC2 with the early endosomal marker, RAB5, or the recycling endosomal marker, RAB11 was rarely observed (0.136±0.034, 0.155±0.045 coefficients for ARRDC2-mCherry colocalisation with GFP-RAB5 or GFP- RAB11, respectively, Figures 3.4 and 3.6). However, sporadic colocalisation of ARRDC2-positive puncta with RAB5 or transferrin (including plasma membrane-localised transferrin) was infrequently observed over several experiments.

In contrast, a much higher proportion of ARRDC2 colocalised with immunostaining for the lysosomal marker, LAMP1 (0.430±0.041 colocalisation coefficient for ARRDC2-mCherry with LAMP1 immunostaining, $P < 0.001$ when compared to ARRDC2

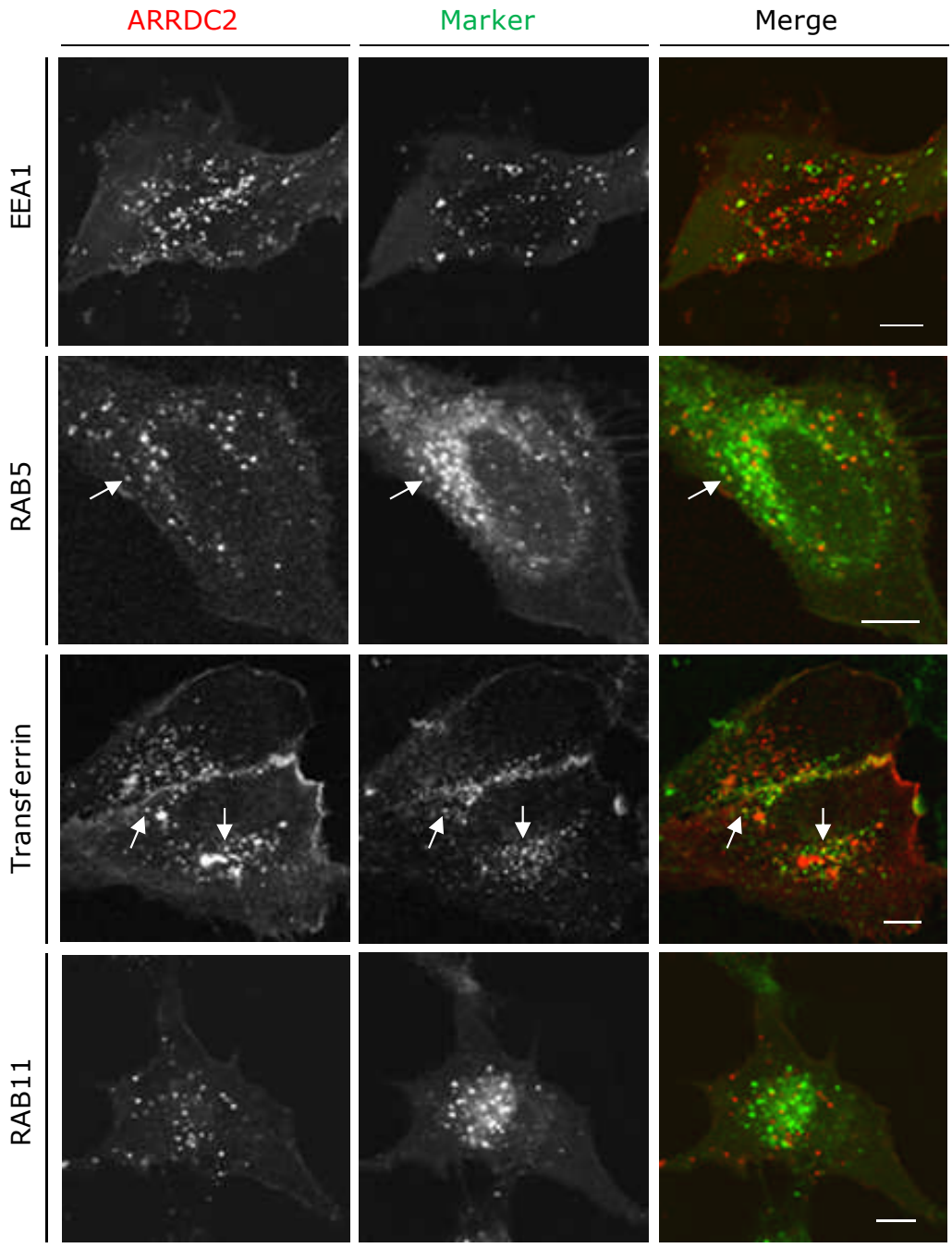

Figure 3.4 ARRDC2 does not colocalise with markers of early/recycling endosomes

Confocal microscopic images of U2OS cells transiently transfected with plasmids expressing ARRDC2-mCherry plus GFP-tagged EEA1, RAB5 or RAB11, or co-stained with 250 ng/µl AF-633-conjugated transferrin for 15 min, as indicated. In merged images, ARRDC2-mCherry is shown in red, marker is shown in green. Infrequent colocalised puncta are highlighted with arrows. Images are representative from at least two independent experiments. Scale bar = 10 µm.

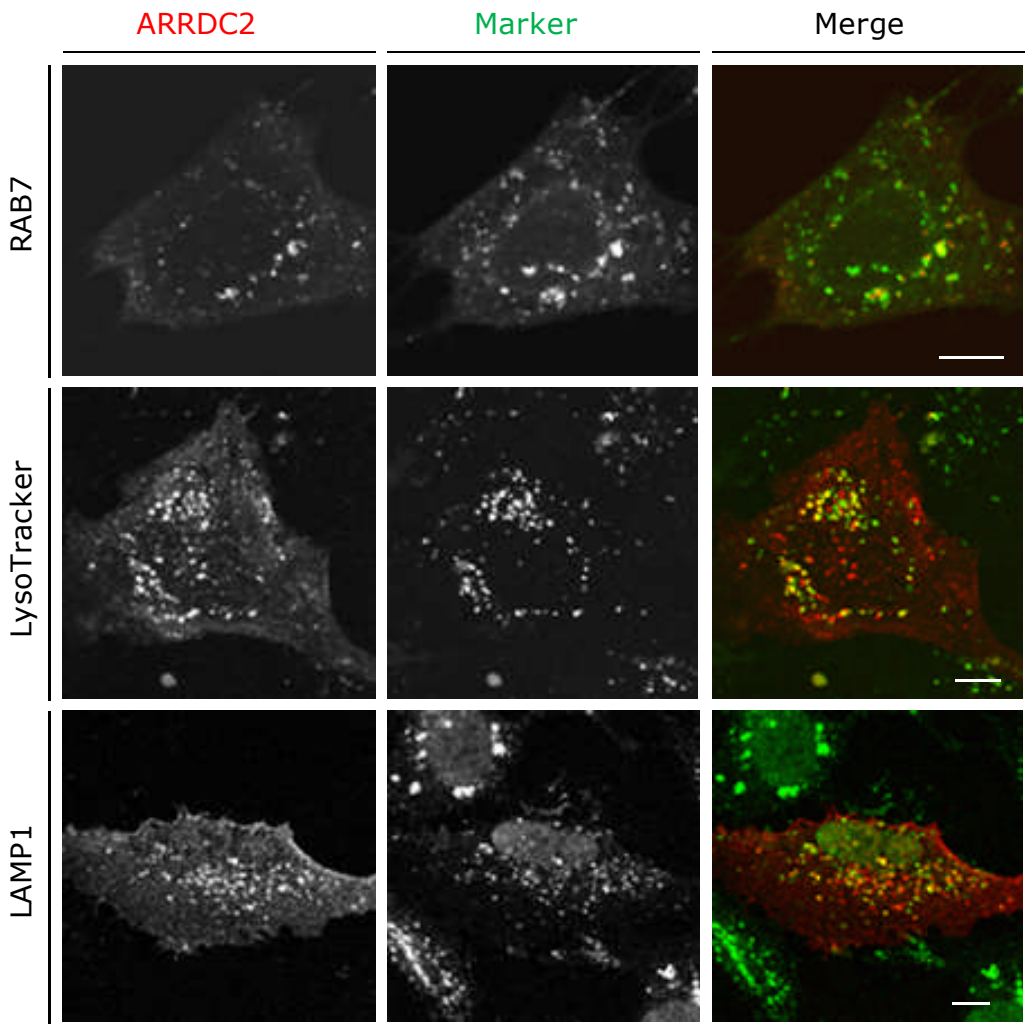

Figure 3.5 ARRDC2 colocalises with markers of late endosomes/lysosomes

Confocal microscopic images of U2OS cells transiently transfected with plasmids expressing ARRDC2-mCherry plus GFP-RAB7, or co-immunostained using rabbit anti-LAMP1 antibody (1:500) detected with AF-633-conjugated anti-rabbit secondary antibody (1:1000); or with ARRDC2-GFP plus co-staining with LysoTracker™ Red DND-99 (100 nM, 15-30 min), as indicated. In merged images, ARRDC2-mCherry or ARRDC2-GFP is shown in red; the indicated marker is in green. Images are representative from at least two independent experiments. Scale bar = 10 µm.

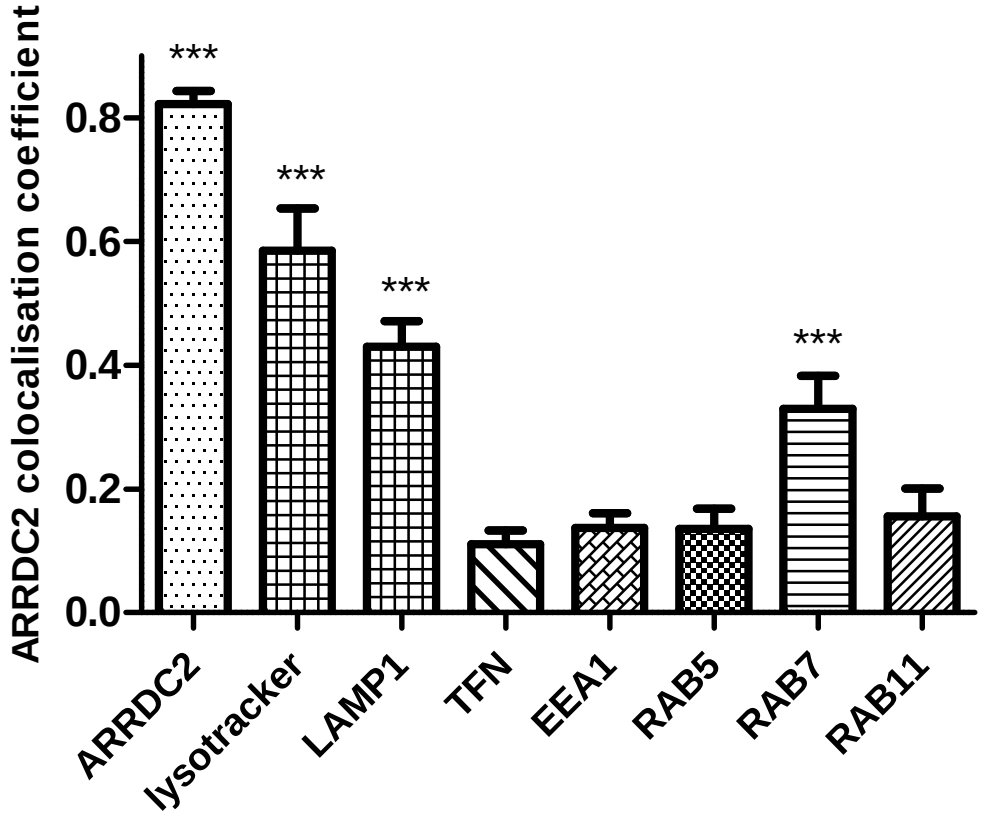

Figure 3.6 Quantification of ARRDC2 colocalisation with compartment-specific markers

Colocalisation analysis of confocal images (example images shown in Figures 3.4 and 3.5) from U2OS cells transiently transfected with ARRDC2 constructs plus the indicated compartment-specific marker. ARRDC2-GFP colocalisation with ARRDC2-mCherry (leftmost bar) is also indicated as a positive control. Colocalisation calculations were performed as described in section 2.4.6.1. Data are mean ± SEM of 5-10 cells analysed for each of ≥ 2 independent experiments. Statistical comparisons are with respect to transferrin (TFN) data. ***P < 0.001, one-way ANOVA plus Tukey test.

colocalisation with transferrin, Figures 3.5 and 3.6). ARRDC2 colocalisation was also higher with acidic compartments (i.e. lysosomes) stained with LysoTracker Red DND-99 (0.586±0.068 colocalisation coefficient for ARRDC2-GFP with LysoTracker™, P < 0.001) and with the late endosomal/lysosomal marker, RAB7 (0.330±0.053 coefficient for GFP-RAB7 colocalisation with ARRDC2-mCherry, P < 0.001, Figures 3.5 and 3.6). As a positive control, ARRDC2 colocalisation with itself was assessed (ARRDC2-GFP colocalisation with ARRDC2-mCherry): a colocalisation coefficient of

0.822±0.021 was measured (Figure 3.6, cell images not shown). Thus, the higher proportion of colocalisation measured with LAMP1, LysoTracker™ and RAB7 (coefficients between 0.330 – 0.586) equates to genuine colocalisation indicative of the presence of ARRDC2 within these compartments. Collectively, these data suggest that ARRDC2 is distinct from early and recycling endosomes in U2OS cells, and may be predominantly targeted to late endosomes/lysosomes, as well as the plasma membrane.

It is worth noting that a reduction in ARRDC2 plasma membrane localisation was often observed upon coexpression with endosomal markers, especially RAB GTPases (Figures 3.4 and 3.5), in comparison to the strong plasma membrane targeting seen in cells overexpressing ARRDC2 alone (Figure 3.3). Thus, overexpression of endosomal proteins may have driven an altered ARRDC2 distribution, although this was controlled for in the use of markers that did not perturb the system (Transferrin, LysoTracker, LAMP1 immunostaining).

3.2.2.2 Effect of constitutively-active RAB mutants on the localisation of ARRDC2

Since ARRDC2 is found both at the plasma membrane and in late endosomes/lysosomes, it was hypothesised that ARRDC2 may traffic through the endocytic system between these compartments.

Expression of constitutively-active RAB7 (GFP-RAB7Q67L) resulted in the accumulation of ARRDC2-mCherry within enlarged GFP-RAB7Q67L-positive vesicles, supporting the proposition that ARRDC2 traffics to the late endosome/lysosome (Figure 3.7, middle row). Interestingly, expression of constitutively-active RAB5 (GFP-RAB5Q79L) also caused accumulation of ARRDC2-mCherry within enlarged GFP-RAB5Q79L-positive vesicles (Figure 3.7, top row). A constitutively-active RAB11 mutant (GFP-RAB11Q70L) had no effect on ARRDC2-mCherry distribution; ARRDC2-mCherry was distinct from GFP-Rab11Q70L-positive vesicles (Figure 3.7, bottom row). Together, these data suggest that ARRDC2 predominantly localises

to late endosomes/lysosomes but may traverse between the plasma membrane, early/late endosomes and lysosomes.

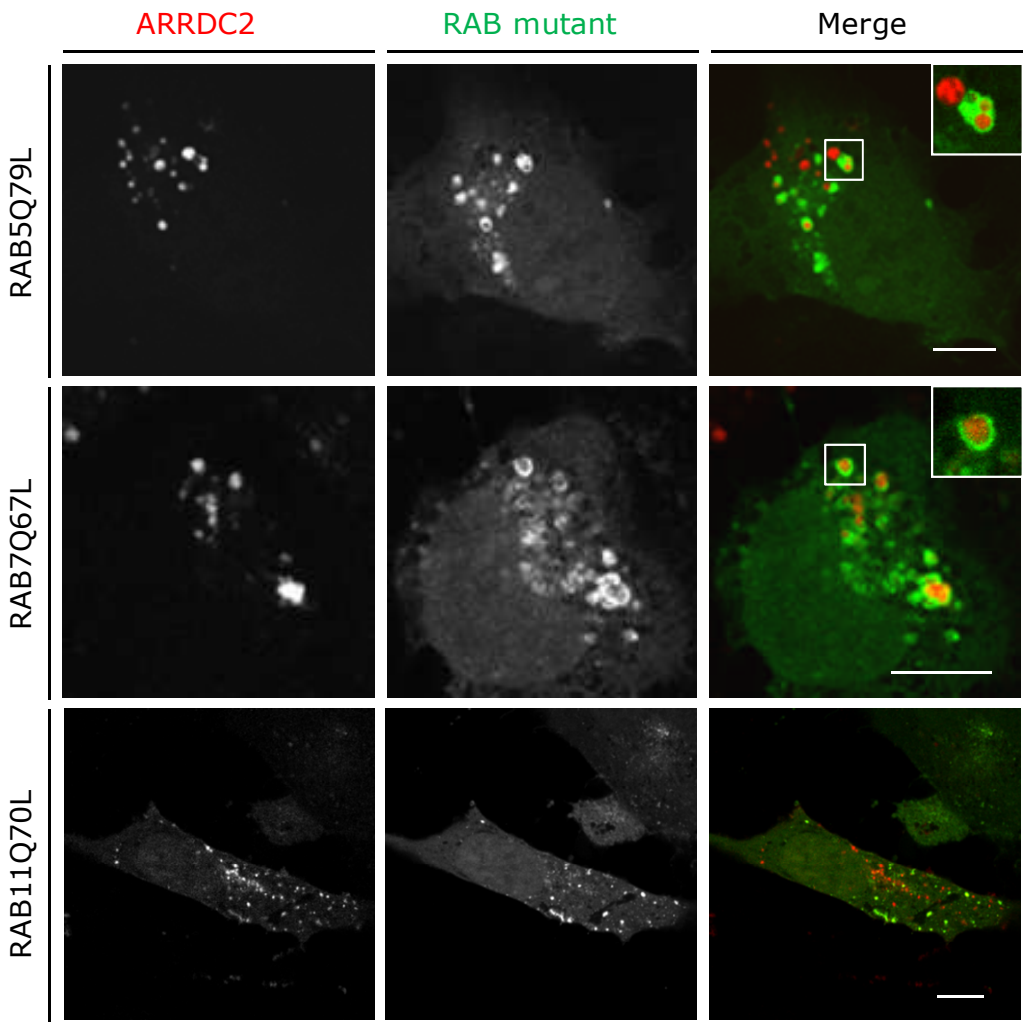

Figure 3.7 ARRDC2 accumulates in enlarged RAB5Q79L- or RAB7Q67L-positive endosomes

Confocal microscopic images of U2OS cells transiently transfected with ARRDC2-mCherry plus GFP fusions of mutant RAB5Q79L, RAB7Q67L or RAB11Q70L, as indicated. In merged images, ARRDC2 is shown in red, RAB mutant is shown in green. Insets show higher magnification image of boxed zone, indicating ARRDC2 accumulation within the relevant RAB mutant endosomes. Images are representative from at least two independent experiments. Scale bar = 10 µm.

3.2.3 Analysis of endogenous ARRDC2 expression in primary and immortalised human cell lines

3.2.3.1 Validation of anti-ARRDC2 antibody

In order to detect endogenous ARRDC2 expression, a polyclonal antibody was raised in rabbit against a selected peptide corresponding to residues 388 – 402 of the ARRDC2 primary sequence (described in section 2.5.4). This antibody was tested for its use in immunostaining and immunoblotting experiments. U2OSTR cells expressing tetracycline-induced ARRDC2-GFP were subjected to immunostaining using the anti-ARRDC2 antibody. Anti-ARRDC2, detected using an AF-633-conjugated anti-rabbit secondary antibody, showed plasma membrane and punctate cytoplasmic staining that was highly colocalised with ARRDC2-GFP (Figure 3.9A, top panel). No immunostaining was observed in a control lacking the anti-ARRDC2 primary antibody (Figure 3.9A, bottom panel), removing the possibility that the staining seen was due to background caused by non-specific secondary antibody labelling. The ARRDCs, in particular ARRDC2/3/4, exhibit a degree of similarity including at the level of primary sequence. However, the peptide region of ARRDC2 chosen to raise the anti-ARRDC2 antibody was distinct from other ARRDC members (Figure 2.8). Nevertheless, the specificity of the anti-ARRDC2 antibody in detecting ARRDC2 alone, and not other ARRDCs, was tested. As shown in Figure 3.9C, no anti-ARRDC2 immunostaining was detected in U2OS cells transiently expressing ARRDC1/3/4-eGFP-HA or the less closely related TXNIP-eGFP-HA or β-arrestin1/2-YFP. In contrast, positive control cells transiently expressing ARRDC2-eGFP-HA showed anti-ARRDC2 immunostaining that mirrored the ARRDC2-eGFP-HA distribution. Thus, the anti-ARRDC2 antibody raised detects exogenous, overexpressed ARRDC2 when used in the immunostaining of intact U2OS cells, and does not exhibit detectable cross-reactivity in this context with other ARRDC members, TXNIP, or β-arrestins.

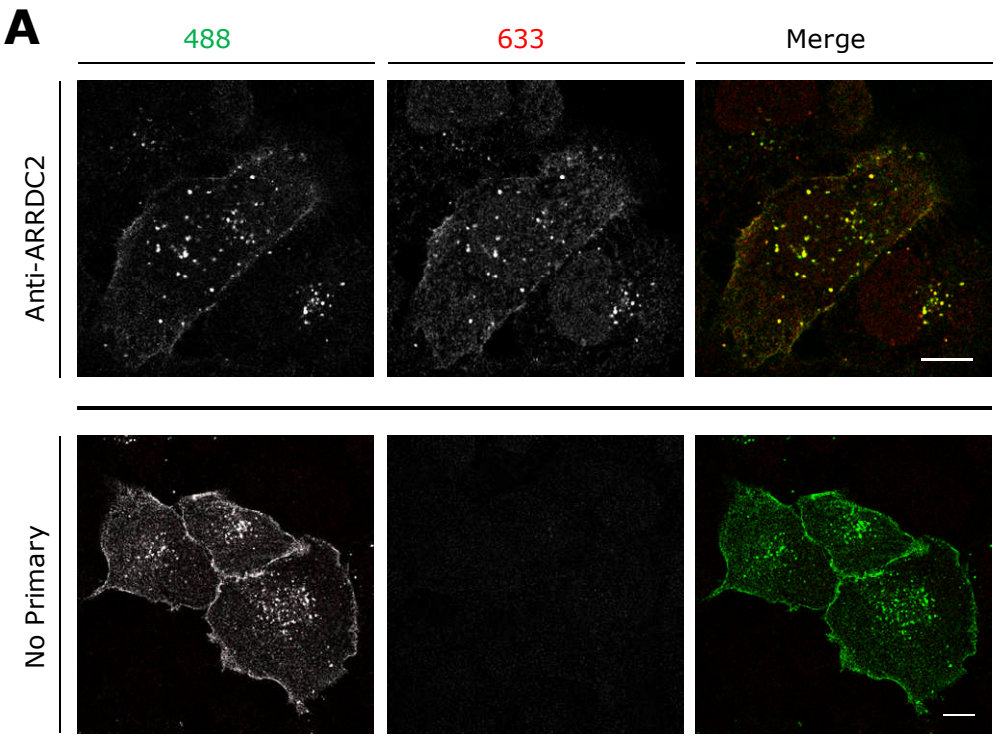
A
488
633
Merge
Anti-ARRDC2
No Primary

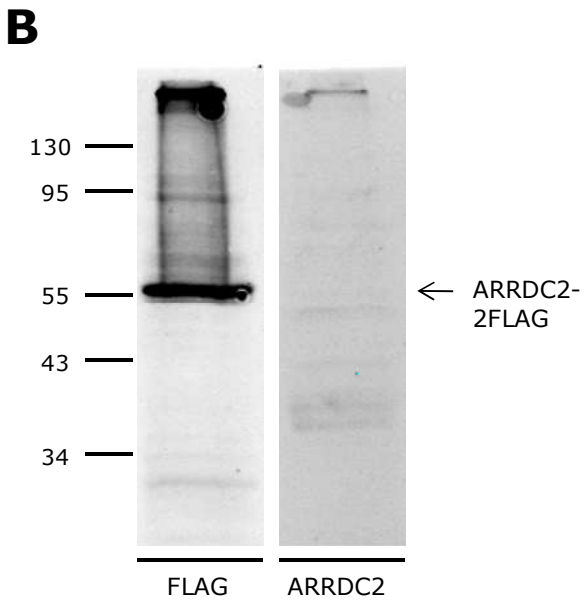
B
130
95
55
43
34
ARRDC2-
2FLAG
FLAG
ARRDC2

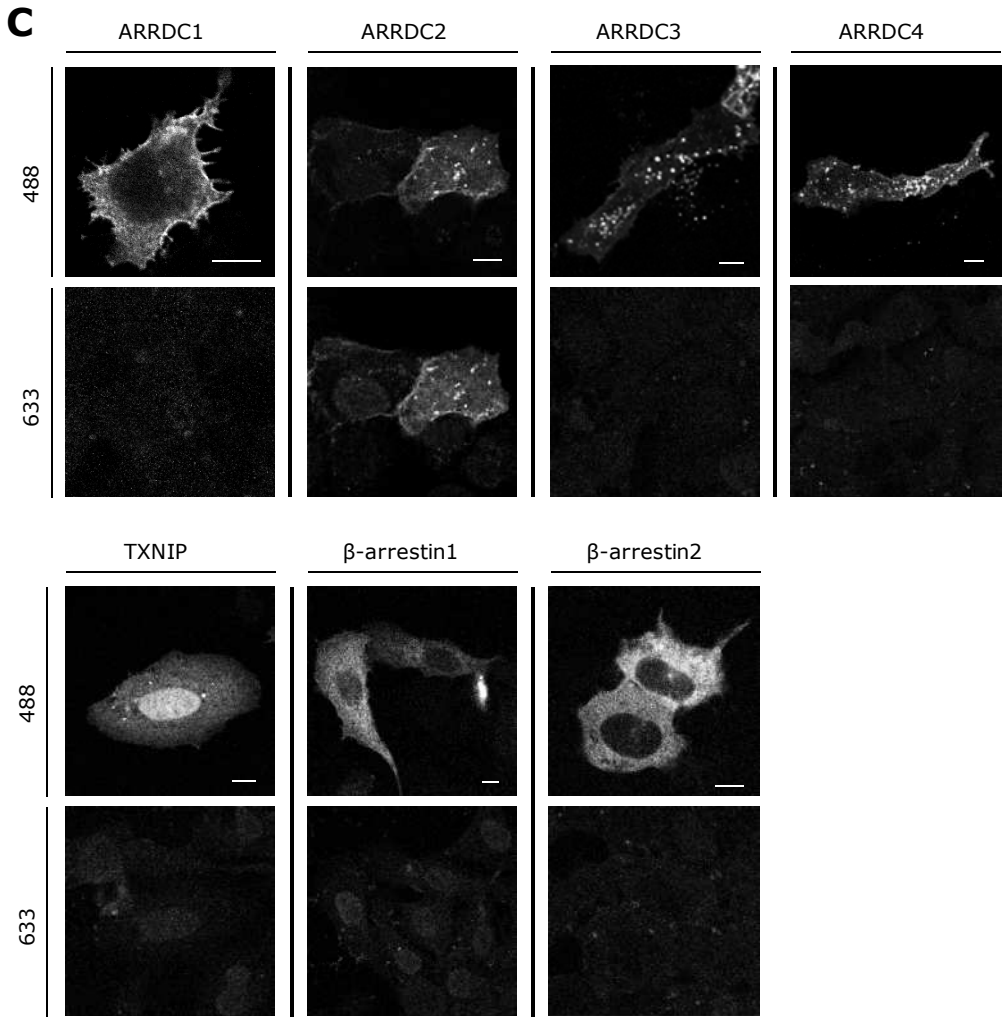

Figure 3.9 Anti-ARRDC2 immunostaining and immunoblotting

(A) Confocal microscopic images of stable U2OSTR ARRDC2-GFP cells expressing tetracycline-induced ARRDC2-GFP (488 channel; green in merged image), stained with rabbit anti-ARRDC2 antibody (1:200 dilution) detected using AF-633-conjugated anti-rabbit secondary antibody (1:1000; 633 channel, red in merged image). Bottom row shows a control in which the same immunostaining protocol was performed in the absence of anti-ARRDC2 primary antibody. **(B)** Lysates from U2OS cells transiently transfected with a plasmid expressing ARRDC2-2FLAG were separated by 12.5% SDS-PAGE and analysed by Western blotting. Left panel shows blotting with anti-FLAG antibody (1:5000); right panel with anti-ARRDC2 (1:1000) detected using IRDye 800CW anti-rabbit secondary antibody (1:10,000). Molecular weight markers are indicated in kD. **(C)** Confocal microscopic images of U2OS cells transiently transfected with ARRDC1/2/3/4 or TXNIP C-terminally fused with eGFP-HA, or β-arrestin1/2 C-terminally fused with YFP (all shown in 488 channel, top row), stained with rabbit anti-ARRDC2 antibody (1:200) detected using AF-633-conjugated anti-rabbit secondary antibody (1:1000; 633 channel, bottom row). Scale bar in all images = 10 μm.

The ability of the antibody to detect ARRDC2 in Western immunoblotting was also tested. Whole cell protein lysates from U2OS cells transiently expressing ARRDC2 C-terminally fused with two copies of the FLAG epitope (ARRDC2-2FLAG) were obtained. Western immunoblotting using an anti-FLAG antibody detected a presumed ARRDC2-2FLAG band at ~55 kilodaltons (kD) (ARRDC2 is predicted to be approximately 44 kD; this difference in size will be commented on in Chapter 4), as well as several higher molecular weight bands (see Chapter 4; Figure 3.9B, left panel). However, immunoblotting the same lysate using the anti-ARRDC2 antibody did not detect any bands corresponding to FLAG-identified ARRDC2, other than potentially at the interface between the stacking and running gels, as suggested by faint immunoreactivity at the top of the gel (Figure 3.9B, right panel). Using different concentrations of anti-ARRDC2 (down to a dilution of 1:500; not shown) did not improve detection of ARRDC2-2FLAG. Hence, although able to detect ARRDC2 in intact cell immunostaining, the anti-ARRDC2 antibody developed is not able to detect ARRDC2 in the context of Western immunoblotting.

3.2.3.2 Analysis of ARRDC2 expression in U2OS and HEK-293 cells

The anti-ARRDC2 antibody was next employed in immunostaining to determine whether ARRDC2 is expressed endogenously in several human cell lines. This was first tested in the immortalised cell lines, U2OS and HEK-293, when overexpressing ARRDC2-GFP (tetracycline-induced expression in U2OSTR; transient expression in HEK-293T). In both U2OS and HEK-293T cells, as mentioned above (see Figure 3.9A), ARRDC2-GFP was detectable using the anti-ARRDC2 antibody (Figure 3.10A). However, in cells not expressing the ARRDC2-GFP transgene (see adjacent cells in both U2OS and HEK-293T images), no anti-ARRDC2 immunostaining was detected. Thus, it appears that neither U2OS nor HEK-293 cells express detectable levels of endogenous ARRDC2 protein.

3.2.3.3 Analysis of ARRDC2 expression in human primary cells

Anti-ARRDC2 immunostaining was next performed in several human primary cell lines (aortic endothelial; pulmonary artery endothelial; aortic smooth muscle; bronchial epithelial; bronchial smooth muscle). ARRDC2 immunoreactivity was apparent in human aortic endothelial cells, pulmonary artery endothelial cells and aortic smooth muscle cells (Figure 3.10B). Given the validation of the anti-ARRDC2 antibody used – especially that it is specific to ARRDC2 and does not cross-react with other arrestin family proteins (section 3.2.3.1) – these results suggest that ARRDC2 is expressed within these cells. Some possible diffuse, weak ARRDC2 immunoreactivity was detectable in bronchial epithelial cells, but no clear signal was detectable in bronchial smooth muscle cells (Figure 3.10B). This suggests that ARRDC2 is not expressed in bronchial smooth muscle cells but may be expressed in bronchial epithelial cells, although this cannot be convincingly concluded from the faint staining seen. These data suggest that ARRDC2 may be expressed in human aortic endothelial cells, pulmonary artery endothelial cells and aortic smooth muscle cells, but that its expression may be cell-type specific.

In aortic endothelial cells, ARRDC2 immunostaining was clearly observed at the plasma membrane, as well as appearing to be present throughout the cytoplasm, most of which was diffuse in pattern although occasionally more discrete puncta were observed (Figure 3.10B). No staining was seen in a control lacking the ARRDC2 primary antibody. This excluded the possibility that the immunostaining observed was due to non-specific secondary antibody labelling. An additional control was performed in which the same immunostaining protocol was followed except for omission of the permeabilisation step (0.05% Triton X-100, see section 2.4.2) normally required to allow antibody entry to the cell interior via permeabilisation of the plasma membrane. Without permeabilisation, little or no immunostaining was observed, indicating that, as

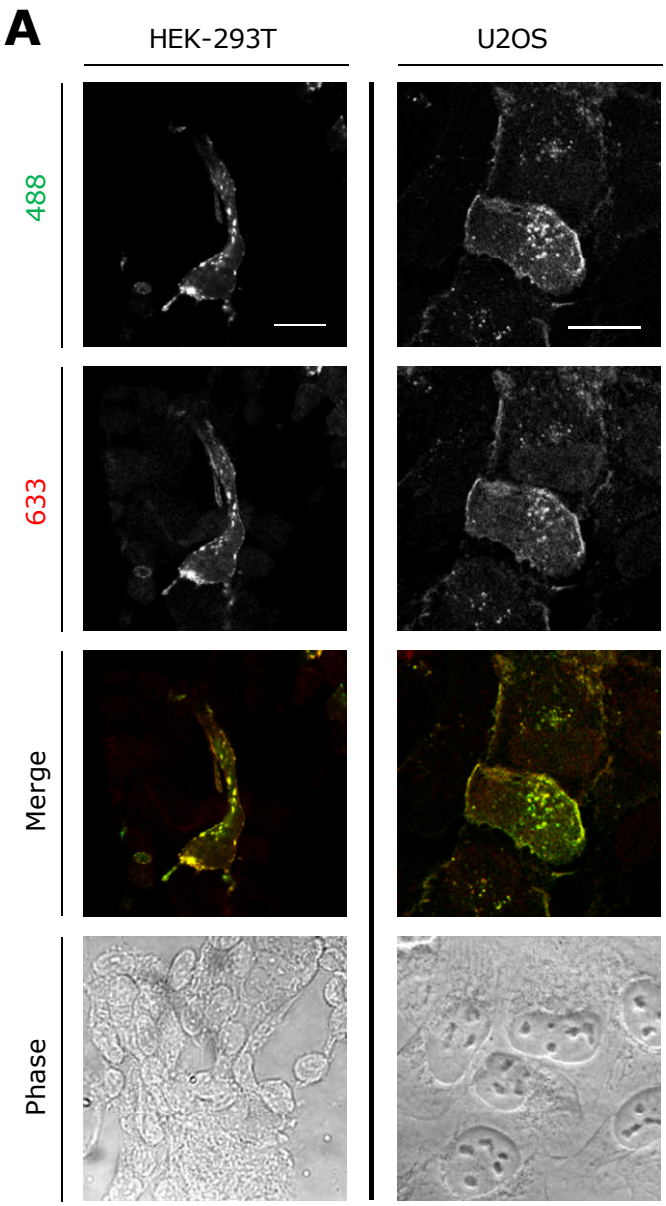
A
HEK-293T
U2OS
488
633
Merge
Phase

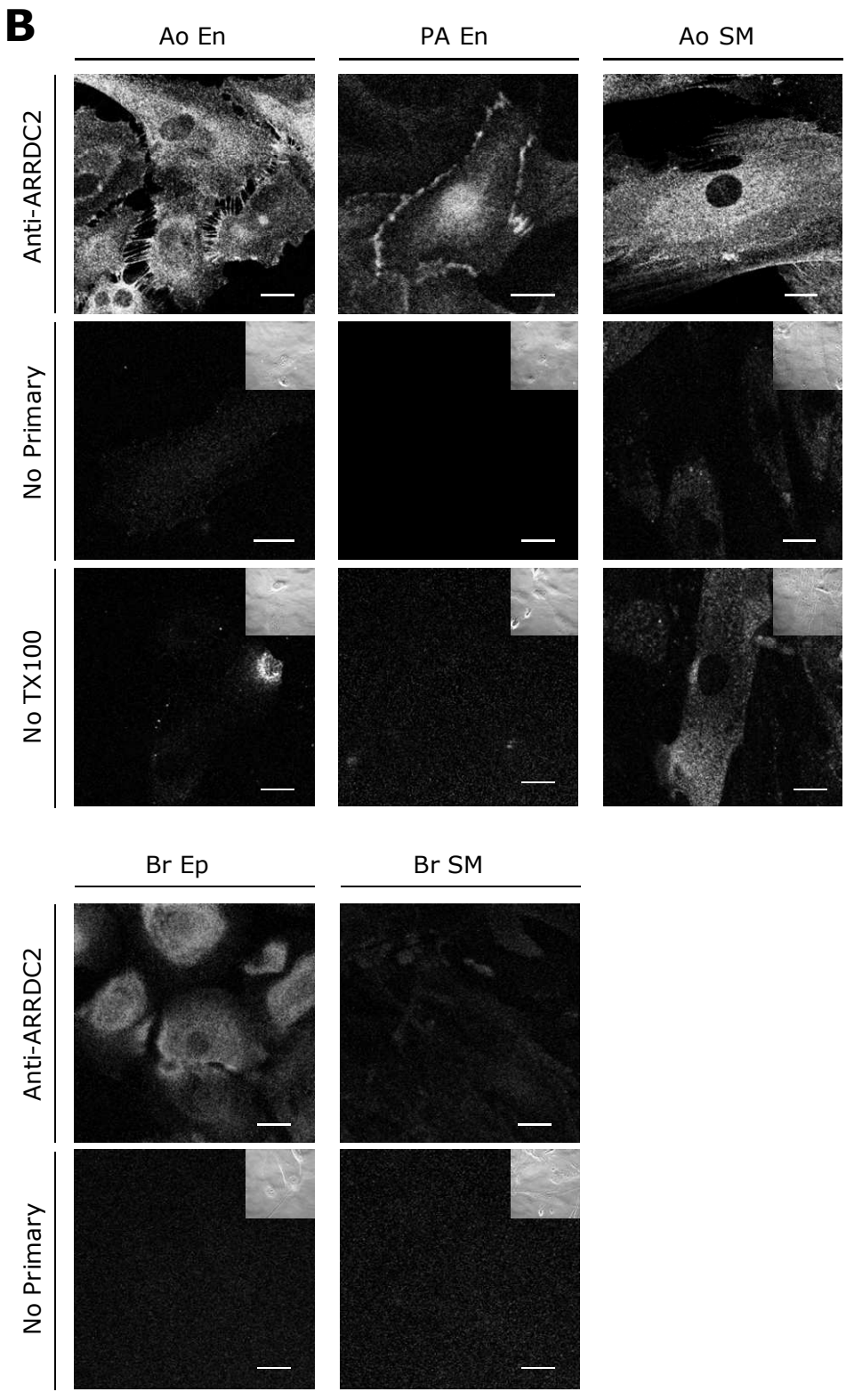

Figure 3.10 Immunofluorescence analysis of endogenous ARRDC2 expression in immortalised and primary human cell lines

(A) Confocal microscopic images: top row (U2OS) shows stable U2OSTR ARRDC2-GFP cells expressing tetracycline-induced ARRDC2-GFP (488 channel; green in merged image), stained with rabbit anti-ARRDC2 antibody (1:200 dilution) detected using AF-633-conjugated anti-rabbit

secondary antibody (1:1000; 633 channel, red in merged image); bottom row (HEK-293T) shows HEK-293T cells transiently transfected with ARRDC2-GFP (488 channel; green in merged image), stained with rabbit anti-ARRDC2 antibody as above. **(B)** Confocal microscopic images of primary human cells (Ao En, Aortic Endothelial; PA En, Pulmonary Artery Endothelial; Ao SM, Aortic Smooth Muscle; Br Ep, Bronchial Epithelial; Br SM, Bronchial Smooth Muscle) stained with rabbit anti-ARRDC2 antibody (1:200) detected using AF-488-conjugated anti-rabbit secondary antibody (1:1000; top row). Controls in which the same immunostaining protocol was performed in the absence of anti-ARRDC2 primary antibody (middle row) or Triton X-100 permeabilisation step (bottom row) are indicated. Corresponding phase images are shown in insets. Scale bars = 20 μm.

expected, detection of the intracellular immunostaining seen required permeabilisation, excluding the possibility of non-specific extracellular plasma membrane labelling. Pulmonary artery endothelial cells also showed ARRDC2 immunostaining at the plasma membrane (Figure 3.10B). There also appeared to be some degree of diffuse staining in the cytoplasm of these cells. Again, when the controls lacking primary antibody or permeabilisation step were performed, no ARRDC2 immunostaining was observed, suggesting that the ARRDC2 immunoreactivity seen was specific. As mentioned, aortic smooth muscle cells also showed a degree of ARRDC2 immunoreactivity (Figure 3.10B). ARRDC2 immunostaining in these cells appeared to be diffusely distributed throughout the cytoplasm and possibly at the plasma membrane, although definitively showing this, even in confocal sections, was difficult due to the flat nature of the cells. Indeed, the diffuse presumed cytoplasmic staining may actually represent plasma membrane, since confocal microscopy may not be able to resolve cytoplasm between two close plasma membrane sheets in these cells. Again, however, no immunostaining was detectable in the primary antibody-deficient control, and very little immunostaining was present when permeabilisation was omitted, suggesting that the anti-ARRDC2 labelling seen was specific.

3.3 Discussion

3.3.1 ARRDCs localise to the endocytic system

Several reports in lower eukaryotes have localised the α-arrestins to the plasma membrane and/or cytoplasmic vesicular compartments, either through direct observation (Guetta *et al.*, 2010; Herrador *et al.*, 2009; Hervas-Aguilar *et al.*, 2010; Lin *et al.*, 2008; O'Donnell *et al.*, 2010) or by inference from their reported roles within the endocytic system (Hatakeyama *et al.*, 2010; Nikko *et al.*, 2009; Nikko *et al.*, 2008). The few studies on human ARRDCs have made broadly the same conclusions, although in some cases reports on a single ARRDC have been contradictory (see Table 3.1). Here, transiently expressed ARRDC1-4 in U2OS cells all distributed in a broadly similar manner: that is, at the plasma membrane and in punctate structures reminiscent of vesicles throughout the cytoplasm. One group has recently reported that ARRDC1 and ARRDC3 localise exclusively to the plasma membrane without any intracellular patterning (Nabhan *et al.*, 2012; Nabhan *et al.*, 2010). However, elsewhere punctate cytoplasmic staining for ARRDC1 (Rauch *et al.*, 2011) and ARRDC3 (Oka *et al.*, 2006; Patwari *et al.*, 2009) has been reported, as was observed here. Overall, the plasma membrane and vesicular pattern seen here for the human ARRDCs is largely in agreement with the limited available literature.

It is notable that the approach used for tagging ARRDC2 – at the C-terminus – enabled visualisation of ARRDC2 without affecting its subcellular targeting. This approach was chosen since ARRDC2 has an extended C-tail that, based on known β-arrestin structures, is predicted to form a flexible structure (Aubry *et al.*, 2009; Han *et al.*, 2001), in contrast to the ARRDC2 (and other ARRDCs) N-terminus that forms the start of the predicted arrestin N-domain, part of the arrestin β-sandwich fold that is hypothesised to be essential for ARRDC2 structure and function. The lack of apparent effect of various C-terminal tags (e.g. 2FLAG, ~2 kD; eGFP, ~28 kD) upon ARRDC2 localisation supports the idea that the ARRDC2 C-terminus may be unessential for subcellular targeting.

3.3.2 ARRDC2 is dynamically localised within the endocytic system, predominantly to late endosomes/lysosomes

Next, the nature of the ARRDC2-positive cytoplasmic puncta noted above was investigated. In U2OS cells, colocalisation studies using exogenous ARRDC2 expressed in combination with compartment-specific markers convincingly indicated that ARRDC2 is largely confined to late endosomes/lysosomes (in addition to the plasma membrane) and is not found within early or recycling endosomes. However, a low degree of colocalisation of ARRDC2 with early endosomal markers (RAB5; transferrin plasma membrane staining, for example) was detected, and the ARRDC2 expression pattern was highly colocalised with that of ARRDC3 (see Figure 3.8), a protein previously reported to localise to transferrin-positive endosomes, as well as lysosomes (Oka *et al.*, 2006). Such reports – of a protein appearing to variably localise to 'distinct' endocytic structures – have contributed to the developing view of an endocytic system that has a degree of plasticity. It is important to emphasise that the supposed specific, restricted targeting of proteins such as the RAB GTPases to particular endocytic domains is more complex than often indicated. For example, as described in section 3.1, the segregation of RAB5 to early endosomes versus RAB7 on late endosomes is the result of a switch mechanism involving competition between RAB5- and RAB7-related factors (McMahon *et al.*, 2011). This likely produces a concentration gradient of each RAB protein; for example, high-to-low concentration of RAB5 in early-to-late endosomes, respectively. Thus, RAB5 is not likely to be completely absent from later endosomal structures, making the observation of sporadic ARRDC2 colocalisation with RAB5 and other early endosomal markers unsurprising.

RAB proteins are essential to the function of their respective endosomes, critically regulating endosomal budding, fusion and maturation, and the flux of cargo through each compartment.

Perhaps unsurprisingly, overexpression of RABs can perturb the trafficking towards these pathways; for example, RAB5 overexpression leads to increased flux of cargo such as the TfR through the endocytic and early endosomal pathways (Bucci *et al.*, 1992). The analysis of ARRDC2 distribution in relation to endogenous RAB GTPases (for example, using anti-RAB immunostaining) would be a preferred method, and would strengthen the case for the ARRDC2 localisation described here being representative of the native system. However, this limitation was controlled for by using alternative markers that do not perturb trafficking (LAMP1, LysoTracker, Transferrin), thereby complementing the RAB GTPase overexpression data.

The fact that ARRDC2 is targeted to the plasma membrane in addition to late endosomes/lysosomes, and sporadically appears within compartments labelled with early endosomal markers, suggested that ARRDC2 may traverse, at least transiently, the earlier stages of the endocytic system. This was further supported by the observed accumulation of ARRDC2 within enlarged endosomes induced by the overexpression of a constitutively active mutant of the early endosomal GTPase, RAB5 (RAB5Q79L). Whether the dynamic movement of ARRDC2 through the endocytic pathway is a feature of its *in situ* function, or merely reflective of the delivery of nascent ARRDC2 to its site of action (i.e. late endosomes/lysosomes) via the plasma membrane/early endosomes, is unclear from these data. In this context it is worth noting that several lysosomal proteins (including RAB7 and LAMP1), when newly synthesised, are thought to be delivered to the lysosome via this same route, and are also found within RAB5Q79L-positive enlarged endosomes (Wegener *et al.*, 2010). Therefore, caution must be taken before concluding that the function of ARRDC2 involves movement between different components of the endocytic pathway, although the concurrent presence of ARRDC2 at the plasma membrane in the absence of targeted perturbations of the endocytic system (seen for exogenous and endogenous [section 3.3.3]

ARRDC2; not seen, for example, for RAB7/LAMP1) further hints that this may be the case.

Possible future experiments that may illuminate upon the question of dynamic ARRDC2 movement (retrograde versus anterograde trafficking) include the use of photoswitchable fluorescent protein variants. Photoswitchable GFP and related fluorescent proteins have been engineered that are protonated in response to a pulse of ultraviolet (UV) irradiation (405 nm), leading to isomerisation and photoconversion of the chromophore, typically from 'green' to 'red' wavelengths (Brejc *et al.*, 1997; Chudakov *et al.*, 2004). UV-induced photoswitching of tagged ARRDC2 at defined regions (for example at the plasma membrane or in co-labelled lysosomes) would enable analysis of its trafficking in and out of these compartments as has been performed, for example, in assessing the movement of proteins to and from defined vesicular clusters (Fang *et al.*, 2010). This approach could also be combined with total internal reflection fluorescence (TIRF) microscopy (Mattheyses *et al.*, 2010) to image dynamic events at or close to the plasma membrane with high resolution.

3.3.3 Detection of endogenous ARRDC2

In order to study endogenous ARRDC2, an antibody was raised against a short peptide sequence unique to ARRDC2 (section 2.5.4). This antibody detected exogenously expressed ARRDC2 in intact cell immunofluorescence staining in U2OS or HEK-293 cells, and did not cross-react with any other human ARRDCs, TXNIP, or β-arrestins in this system. However, the antibody was unable to detect overexpressed ARRDC2 in Western immunoblotting. The reason for this is unknown, although it may be that the antibody binds to an epitope within the ARRDC2 protein whose structural integrity is important to the interaction, and whose integrity may be lost under the denaturing conditions used in SDS-PAGE.

The anti-ARRDC2 antibody was used to investigate endogenous ARRDC2 expression pattern in several immortalised and primary

human cell types. No ARRDC2 immunostaining was detectable in the U2OS and HEK-293 lines, suggesting that ARRDC2 is not expressed in these cell types. However, several primary cell types (aortic endothelial; pulmonary artery endothelial; aortic smooth muscle) showed specific ARRDC2 immunostaining; other primary cells did not (bronchial epithelial; bronchial smooth muscle cells). As far as is known from current literature, there is no data available on the endogenous expression of ARRDC2 in human tissues, although expressed sequence tag (EST) database information suggests that the *ARRDC2* gene is widely (but not ubiquitously) expressed (http://www.ncbi.nlm.nih.gov/unigene). Thus, this is a novel demonstration: that ARRDC2 protein is expressed in human aortic endothelial, pulmonary artery endothelial and aortic smooth muscle cells. It is notable that ARRDC2 expression may be tissue specific; for example, although expression was detected in some smooth muscle cells (aorta) it was not in others (bronchial).

Each primary cell type used here that expressed ARRDC2 showed some degree of plasma membrane immunostaining, in addition to possible diffuse cytoplasmic staining; very little evidence of punctate vesicular localisation was obtained. This appeared to be in contrast to the exogenous expression data presented, where punctate vesicular structures were easily observed (sections 3.3.1 and 3.3.2). It is possible that exogenous overexpression of ARRDC2 may lead to enhanced flux through the endocytic pathway to lysosomes (where most exogenous ARRDC2 was detected). That is, the subcellular targeting seen for ARRDC2 may represent an exaggeration of the native system, as may be the case in any study that uses exogenously overexpressed proteins. However, it is important to note that the apparent flat nature of the primary cells used rendered the resolution of cellular substructures difficult (see next paragraph). Furthermore, endosomes/lysosomes are relatively small structures (typically around 100-200 nm), and the expression level of endogenous proteins (such as ARRDC2) within them is likely to be lower than in the overexpressed system, making their definitive identification above the level of cytoplasmic background difficult.

Hence, it remains likely that the proposed late endosomal/lysosomal localisation of ARRDC2 will represent the native situation. Indeed, subsequent data presented in the current thesis (Chapters 4 and 5) attest to a potential role for ARRDC2 in the endocytic system in support of this claim.

The recent development of an anti-ARRDC2 antibody enabled these studies on endogenous ARRDC2 in primary cells. Further characterisations using this system would be essential to define a physiologically relevant function for ARRDC2. First, it would be desirable to clarify the endogenous expression observed here, for example by using reverse transcriptase PCR (RT-PCR) to detect *Arrdc2* mRNA expression in the relevant primary lines, and by including an additional control in the primary cell immunostaining protocol (co-incubation with the antibody-raising peptide in order to specifically compete out anti-ARRDC2 binding to the presumed endogenous protein). Subsequent experiments would aim to more convincingly determine the localisation of endogenous ARRDC2 using, for example, 3D reconstruction analysis of confocal images (enabling greater resolution in the z direction). This may well reveal that the putative diffuse cytoplasmic staining seen actually represents plasma membrane staining, unable to be resolved due to the closeness of the plasma membrane sheets in the flat cells used. The use of alternative primary cell types whose intracellular compartments are more readily visualised could potentially add credence to the vesicular targeting seen in the exogenous studies. Additionally, an approach to uncovering a physiological role for ARRDC2 in GPCR regulation would be to assess whether ARRDC2 distribution is affected by stimulation of primary cells with various GPCR agonists (at endogenously expressed or transfected GPCRs), which may indicate ARRDC2-GPCR recruitment.

In summary, human ARRDCs are targeted to intracellular vesicular compartments and the plasma membrane. In the case of ARRDC2, the compartments represent components of the endocytic pathway,

predominantly late endosomes/lysosomes. ARRDC3 likely localises to similar endocytic compartments, evidenced by a high degree of ARRDC3-ARRDC2 colocalisation. The appearance of ARRDC2 throughout the endocytic system points to a potential dynamic role therein, and ARRDC2 flux through the system is indicated by the ability of RAB GTPase mutants to block ARRDC2 within early or late endosomes. Immunostaining indicates that ARRDC2 is expressed by some human cell types (aortic endothelial; pulmonary artery endothelial; aortic smooth muscle), but that its distribution may be tissue-specific. Broadly, the distribution seen within these primary cells – especially plasma membrane targeting – supports the proposed endocytic targeting of ARRDC2, suggesting that it may have a physiologically relevant role within this system.

4 ARRDC2 is a ubiquitin ligase adaptor

4.1 Introduction

Ubiquitination is increasingly being recognised as a critical signal that regulates intracellular cargo protein sorting pathways (Acconcia *et al.*, 2009; Hislop *et al.*, 2011; Raiborg *et al.*, 2009). In addition to the direct ubiquitination of cargo proteins for their lysosomal trafficking, ubiquitination of components of the ESCRT sorting machinery regulates their function (Hoeller *et al.*, 2006), as is also evident for ubiquitin ligase adaptors (Macdonald *et al.*, 2011). This may also be true for arrestins: β-arrestins and α-arrestins have also been reported to be regulated by ubiquitination (Shenoy *et al.*, 2007) (Becuwe *et al.*, 2012; Gupta *et al.*, 2007; Hatakeyama *et al.*, 2010; Kee *et al.*, 2006; Lin *et al.*, 2008; Rauch *et al.*, 2011). In the case of α-arrestins ubiquitination may be performed by the NEDD4 family ligase with which they interact.

As described in section 1.2.3, E3 ubiquitin ligases determine the specificity of ubiquitination, and are divided into RING finger and HECT domain families. The RING E3 ligases are scaffolds that bind E2s (ubiquitin-conjugating enzymes), recruiting them to the vicinity of substrates and activating the direct transfer of ubiquitin (Deshaies *et al.*, 2009). In contrast, HECT E3 ligases contain a conserved Cys residue that forms an intermediate thioester bond with ubiquitin before transferring it to the substrate (Rotin *et al.*, 2009). The Cys residue is within the C-terminal region of the HECT domain, a bilobal structure whose N-terminal region contacts the E2 enzyme. The HECT domain is present in the C-terminal portion of all HECT E3 ligases. In addition to this characteristic domain, HECTs have multiple other domains within their N-terminus that delineate them into the HERC, NEDD4 and other HECTs subfamilies. For the NEDD4 family, these include a C2 domain in the extreme N-terminus and two to four WW domains (Figure 4.1A). The C2

domain interacts with phospholipids (possibly in a Ca^{2+}-dependent manner), targeting NEDD4 family ligases to membrane compartments such as the plasma membrane and endosomes (Dunn *et al.*, 2004; Lu *et al.*, 2011). An autoinhibitory role for the C2 domain has also been reported for the NEDD4 ligase SMURF2, whereby an intramolecular interaction between the C2 and HECT domains reduces the HECT catalytic activity (Wiesner *et al.*, 2007). WW domains are protein-protein interaction domains that contain two conserved Trp residues. The WW domains bind to proline-rich sequences (such as PPxY motifs) in substrate proteins or adaptors (Sudol *et al.*, 1995), and provide the major means for recognising substrates or being targeted to them.

Although they share a common HECT domain, NEDD4 ligases have various unique roles. These include the regulation of cell signalling (NEDD4, SMURF1/2, AIP4), protein trafficking (NEDD4, NEDD4L) and viral budding (NEDD4, WWP1). For example, SMURF1 and SMURF2 negatively regulate signalling induced by transforming growth factor β (TGFβ), a key regulator of processes including proliferation, differentiation and apoptosis. TGFβ binding to its receptor activates signal transduction via various intracellular Smad proteins, the termination of which also involves other, inhibitory Smads. Smads contain PPxY motifs, enabling them to bind to SMURF1/2, an association that leads to ubiquitination and degradation of Smads themselves, TGFβ receptor or TGFβ-induced transcription factors (Inoue *et al.*, 2008).

Several NEDD4 family ligase roles in intracellular trafficking and viral budding have been described in Chapter 1. The impact of ubiquitination upon GPCR signalling and trafficking was also touched upon therein. RING finger and HECT domain ligases have been implicated in GPCR ubiquitination and regulation, both of which may be mediated by arrestins. For example, β-arrestin2 recruits the RING E3 ligase, Mdm2, to agonist-stimulated β_2AR, leading to ubiquitination of the receptor and arrestin, and thus to enhanced β_2AR lysosomal degradation (Shenoy *et al.*, 2001). β-Arrestins have also been reported to bind the NEDD4 family members NEDD4 and

AIP4, interactions that may similarly influence the ubiquitination and turnover of GPCRs and other cell-surface cargo (Bhandari *et al.*, 2007; Shenoy *et al.*, 2008; Simonin *et al.*, 2010). β-Arrestins do not contain PPxY motifs, and the mechanisms underlying these interactions are unclear. As has been described in Chapter 1, many α-arrestin-NEDD4 family ligase interactions have been uncovered, the majority of which are thought to be mediated by a canonical PPxY motif-WW domain mechanism.

Therefore, the background to the current chapter is the emerging role for α-arrestins as adaptors for NEDD4 E3 ligases in intracellular trafficking. The observation that ARRDC2 is targeted to the endocytic system (Chapter 3) in which the NEDD4 E3 ligases carry out many of their functions suggested that ARRDC2 may fit into this paradigm, together with the PPxY motifs located in the ARRDC2 C-terminus that may enable an interaction. Hence, the potential ability of ARRDC2 to scaffold NEDD4 E3 ligases was investigated. Whether ARRDC2 itself is subject to ubiquitination was also determined.

4.2 Results

4.2.1 PPxY motif-dependent interaction of ARRDC2 with multiple members of the NEDD4 family of HECT E3 ubiquitin ligases

To test for ARRDC2 interaction with all nine NEDD4 family E3 ligases present in man, ARRDC2-2FLAG and individual ligases C-terminally tagged with eGFP-HA (*ligase*-eGFP-HA) were transiently expressed either alone or in combination in U2OS cells. Protein lysates from these cells were incubated with anti-HA agarose beads in order to immunoprecipitate the *ligase*-eGFP-HA fusions. Western immunoblotting was then performed on whole cell lysates or immunoprecipitates to assess for the presence of coimmunoprecipitated ARRDC2-2FLAG ($n \geq 2$).

ARRDC2-2FLAG was efficiently expressed, as evidenced by an anti-FLAG immunoreactive band at ~55 kD in lysates obtained from

ARRDC2-2FLAG transfections, not present in lysate lacking ARRDC2-2FLAG transfection (Figure 4.1, bottom panel). ARRDC2 is predicted to be ~44 kD which, combined with two copies of the FLAG epitope, would only be expected to total ~46 kD. The disparity between this and the observed size of the ARRDC2-2FLAG band is discussed in section 4.2.3. The eGFP-HA-tagged NEDD4 family ligases were also efficiently expressed in transient transfections (evidenced by microscopy; see, for example, Figure 4.3) and several were detected in immunoprecipitates blotted using an anti-HA antibody (Figure 4.1, middle panel). For example, WWP2 is predicted to be ~99 kD; plus eGFP-HA (~29 kD) would equal ~128 kD, the approximate size that is seen on the blot. However, detection of several of the ligases on immunoblotting was weak or absent, possibly due to poor exposure of the HA epitope or inefficient transfer of the large proteins from gel to nitrocellulose. Nevertheless, coimmunoprecipitation of ARRDC2-2FLAG was observed with multiple NEDD4 family members (Figure 4.1, top panel). The immunoprecipitate derived from cells transfected with ARRDC2-2FLAG alone (without *ligase*-eGFP-HA) showed only a very faint anti-FLAG immunoreactive band at ~55 kD. This is possibly indicative of background nonspecific ARRDC2-2FLAG binding to the anti-HA agarose, despite multiple wash steps (see section 2.5.2). However, a much stronger ARRDC2-2FLAG band was observed for immunoprecipitates obtained from lysates in which NEDL1, AIP4, WWP2 or SMURF1 (tagged with eGFP-HA) were coexpressed with ARRDC2-2FLAG, suggesting that these ligases associate with ARRDC2. In addition to the strong coimmunoprecipitation of ARRDC2 with the above four ligases, ARRDC2-2FLAG bands also appeared to be present in the NEDL2, NEDD4, WWP1 and SMURF2 immunoprecipitates that were stronger than the control ARRDC2-2FLAG immunoprecipitate lacking *ligase*-eGFP-HA. Therefore, specific ARRDC2 interactions with NEDL2, NEDD4, WWP1 and SMURF2 were also detected. Immunoprecipitation with the remaining ligase, NEDD4L, gave a weak ARRDC2-2FLAG band that could not be convincingly distinguished from the background control,

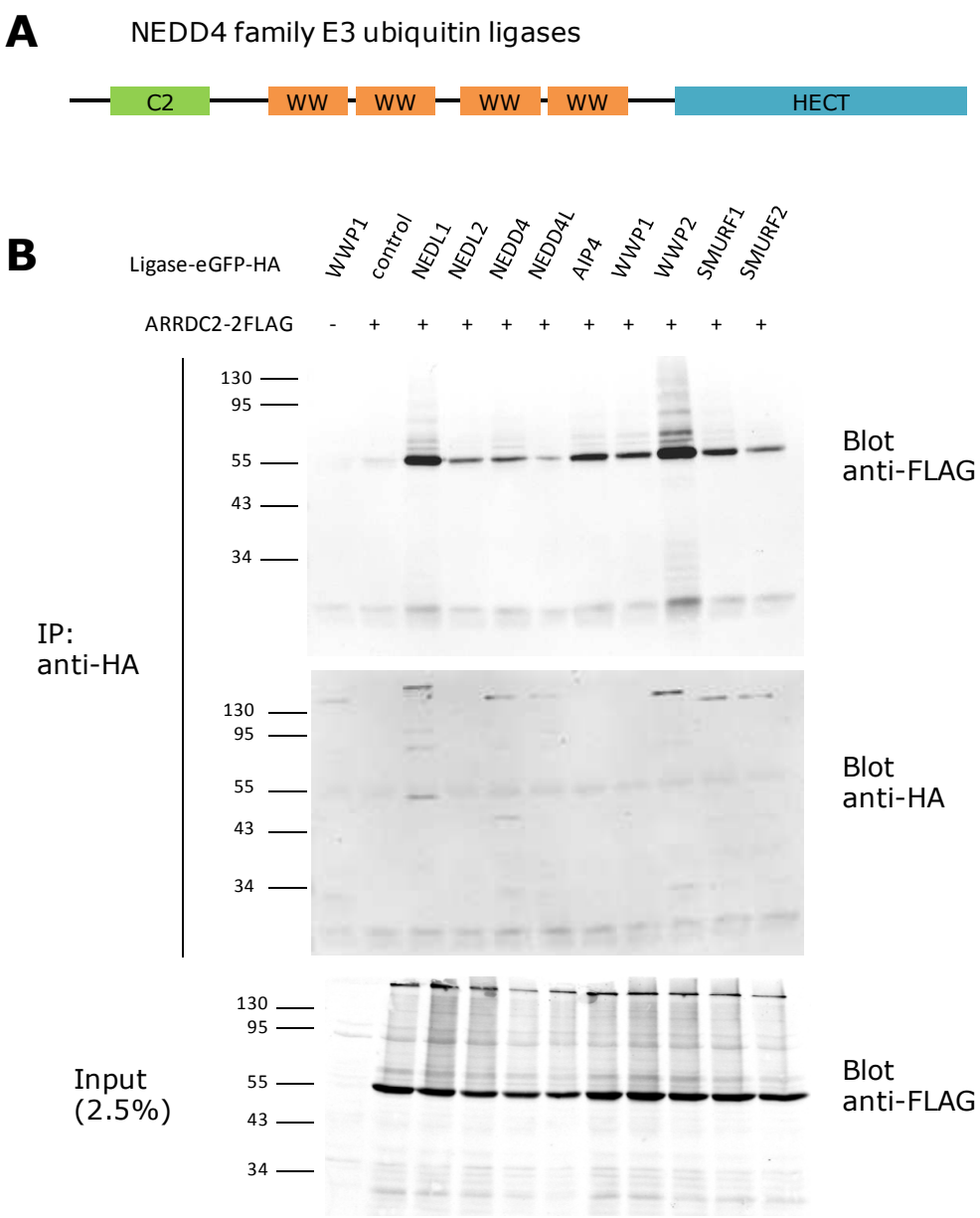

Figure 4.1 Coimmunoprecipitation of ARRDC2 with the NEDD4 family of HECT E3 ubiquitin ligases

(A) Generalised domain organisation of the NEDD4 family of HECT E3 ligases. All members contain an N-terminal C2 domain, a C-terminal HECT domain, and two to four WW domains. **(B)** U2OS cells were transiently cotransfected with plasmids expressing ARRDC2-2FLAG and/or the indicated ligase tagged with eGFP-HA. Cell lysates (2.5% input) and immunoprecipitates (IP) obtained by incubation with anti-HA agarose were separated by 12.5% SDS-PAGE and analysed by Western blotting using anti-HA or anti-FLAG antibodies (both at 1:5000 dilution), as indicated, detected using IRDye 800CW anti-rabbit secondary antibody (1:10,000). Molecular weight markers are shown in kD.

suggesting that ARRDC2 may not interact with NEDD4L. NEDD4L-eGFP-HA appeared to be expressed in this experiment, as evidenced by the presence of a band at over 130 kD (NEDD4L is estimated to be ~105 kD; eGFP-HA ~29 kD). Together, these data suggest that ARRDC2 is able to interact with several members of the NEDD4 family of E3 ligases, with the possible exception of NEDD4L.

The regions of ARRDC2 required for interaction with NEDD4 family ligases were investigated. Interaction with NEDL1 and WWP1 was tested: as seen above, coimmunoprecipitation of wild-type ARRDC2-2FLAG was detected with either NEDL1- or WWP1-eGFP-HA (Figure 4.2B, C, top panels). However, a mutant ARRDC2 in which the Tyr residues of both PPxY motifs were mutated to Ala (denoted 'ARRDC2ΔΔ') failed to coimmunoprecipitate with NEDL1 or WWP1; although faint ARRDC2ΔΔ-2FLAG bands were detectable, they were no stronger than the background level in the absence of NEDL1- or WWP1-eGFP-HA. These results indicated that the PPxY motifs of ARRDC2 are required for its binding to NEDL1 and WWP1. For NEDL1, single PPxY motif mutants of ARRDC2 were also tested for their ability to coimmunoprecipitate following ligase pull-down (Figure 4.2B). Mutation of the first PPxY motif (ARRDC2Y342A) resulted in a similar abrogation of coimmunoprecipitation with NEDL1 as the ARRDC2ΔΔ double PPxY mutant. Mutation of the second PPxY motif (ARRDC2Y388A) also seemed to reduce detected coimmunoprecipitation compared to wild-type ARRDC2, but did not appear to completely remove NEDL1 binding, as evidenced by some residual ARRDC2Y388A-2FLAG present in the immunoprecipitate that was stronger than the background level. This suggested that both ARRDC2 PPxY motifs may contribute to its binding to NEDL1, but that the first PPxY motif (corresponding to Tyr^{342}) may be most important. It is notable that the apparent amount of NEDL1-eGFP-HA present, detected by blotting with anti-HA, varied between conditions and was markedly lower in the ARRDC2ΔΔ transfected sample; thus, comparisons between the level of ARRDC2 pull-down in different samples must be made with caution.

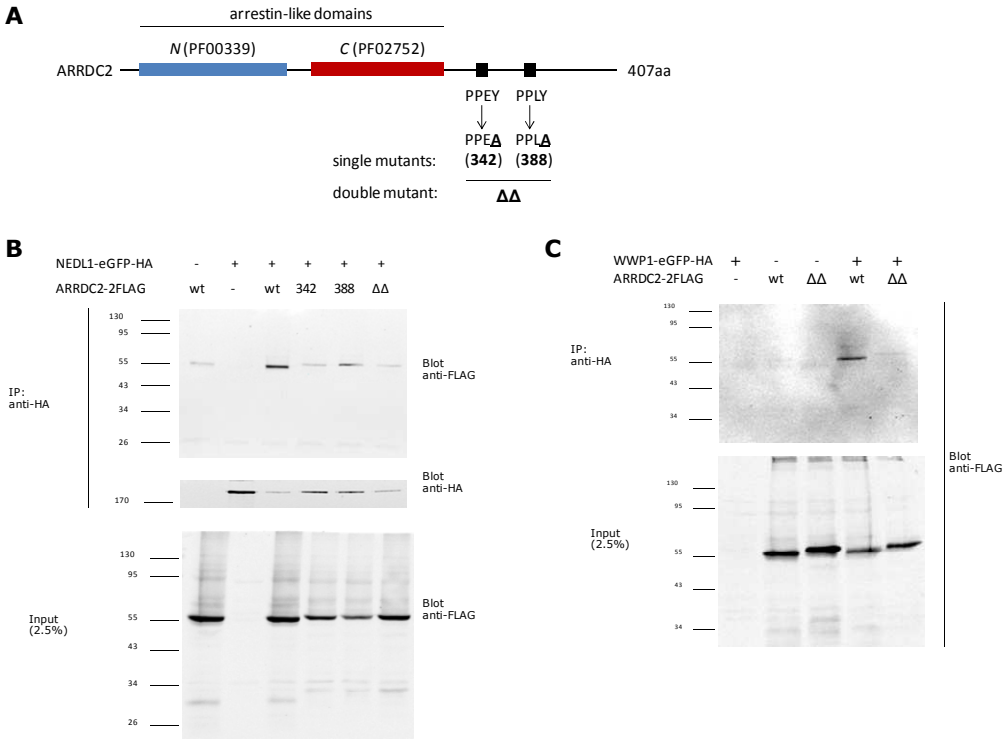

Figure 4.2 ARRDC2 interaction with NEDL1 and WWP1 is dependent on the presence of ARRDC2 PPxY motifs

(A) Domain organisation of ARRDC2: the two PPxY motifs are shown, indicating that constructs used in which Tyr^{342} is mutated to Ala, Tyr^{388} is mutated to Ala, or both residues are mutated to Ala are denoted as "342", "388" or "ΔΔ", respectively. **(B, C)** U2OS cells were transiently cotransfected with plasmids expressing ARRDC2-2FLAG and/or NEDL1-eGFP-HA or WWP1-eGFP-HA, as indicated. Cell lysates (2.5% input) and immunoprecipitates (IP) obtained by incubation with anti-HA agarose were separated by 12.5% SDS-PAGE and analysed by Western blotting using anti-HA or anti-FLAG antibodies (both at 1:5000 dilution), as indicated, detected using IRDye 800CW anti-rabbit secondary antibody (1:10,000). Molecular weight markers are shown in kD.

4.2.2 ARRDC2 overexpression alters the subcellular distribution of several NEDD4 family ligases

Next, the role of ARRDC2 interaction with NEDD4 family ligases in determining ARRDC2 and/or ligase subcellular localisation was investigated by confocal microscopy. First, the distribution of ARRDC2 wild-type (wt) or PPxY motif double mutant (ΔΔ) fused to mCherry was analysed in transiently transfected U2OS cells. The distribution of ARRDC2ΔΔ was indistinguishable from ARRDC2wt; both were found within cytoplasmic vesicular structures and at the

plasma membrane (Figure 4.3A), as previously seen for various ARRDC2wt fusion proteins (section 3.2.1), although the precise identity of the ARRDC2ΔΔ-positive vesicles was not determined.

The distribution of all nine NEDD4 family ligases (fused to eGFP-HA), alone or in combination with ARRDC2wt/ΔΔ-mCherry, was also assessed by transient transfection of U2OS cells and confocal microscopy. WWP1 was diffusely localised throughout the cytosol when expressed alone, with no punctate vesicular structures observed (Figure 4.3A). However, when coexpressed with ARRDC2wt, in addition to diffuse staining, WWP1-positive puncta were frequently observed, and these were highly colocalised (0.563±0.039 coefficient for WWP1-eGFP-HA colocalisation with ARRDC2wt-mCherry, n = 3) with ARRDC2wt puncta (Figure 4.3B, left panel). In contrast, ARRDC2ΔΔ overexpression did not affect WWP1 distribution; WWP1 remained diffusely distributed without any observable puncta upon coexpression with ARRDC2ΔΔ (Figure 4.3B, right panel). No obvious change in ARRDC2wt/ΔΔ distribution was observed when coexpressed with WWP1 in comparison to ARRDC2wt alone. These observations further supported the PPxY-dependent interaction of ARRDC2 with WWP1 (section 4.2.1), and suggested that this interaction may affect the subcellular distribution of WWP1.

A similar effect, albeit less marked, of ARRDC2 overexpression was observed for SMURF1, another ligase found to coimmunoprecipitate with ARRDC2 (Figure 4.1B). SMURF1 was also diffusely distributed when expressed alone in U2OS cells, without any cytoplasmic puncta observed (Figure 4.3A). Coexpression with ARRDC2wt resulted in the sporadic appearance of SMURF1 puncta that colocalised with ARRDC2wt (Figure 4.3D, left panel). The SMURF1-positive puncta were seen less frequently than for WWP1, and their identification was hampered by the high level of diffuse cytosolic SMURF1 staining that remained. Nevertheless, SMURF1-positive puncta did appear to be induced by ARRDC2wt overexpression and again, this was not seen upon coexpression with ARRDC2ΔΔ (Figure 4.3D, right panel). Thus, interaction with

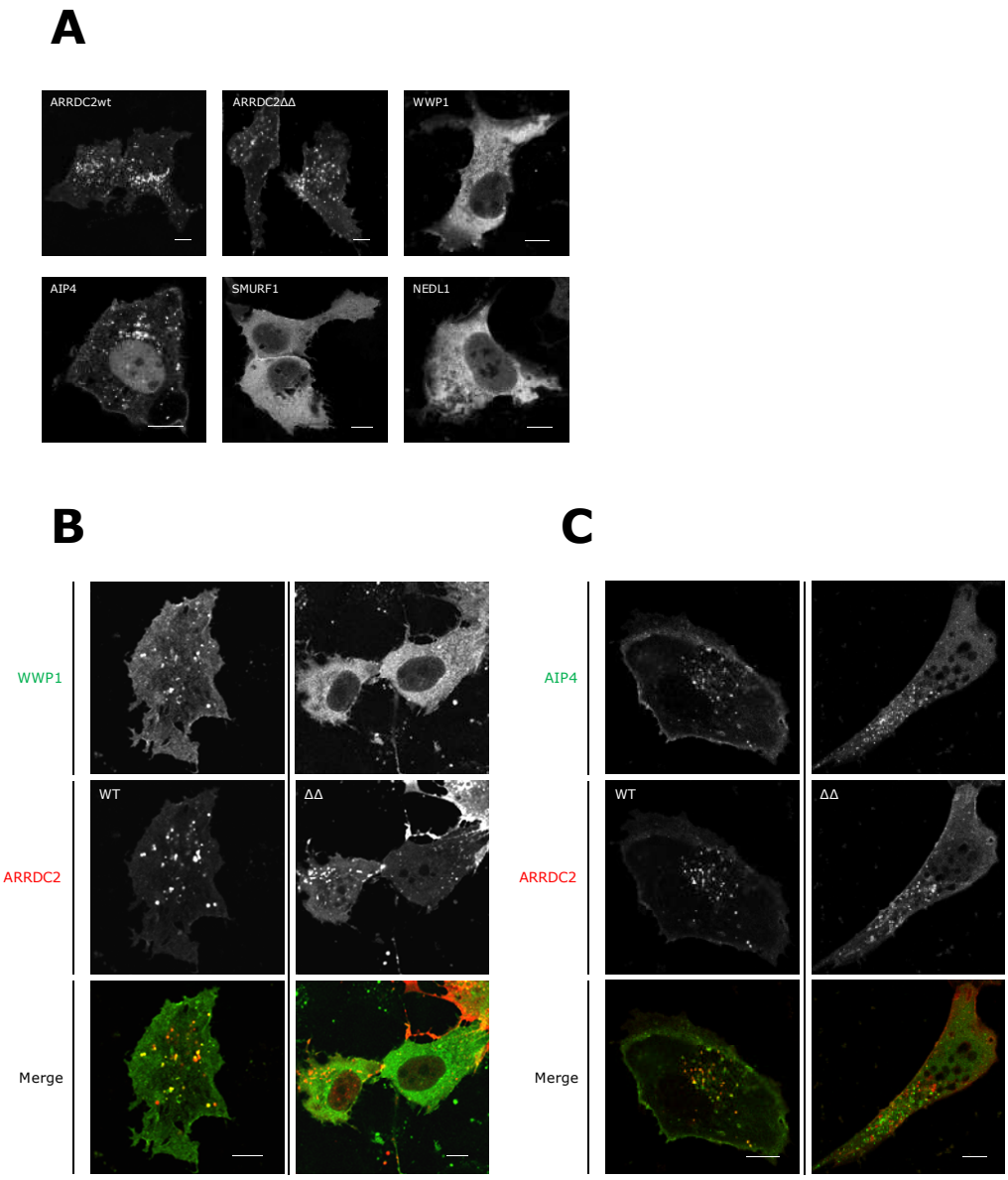
A
ARRDC2wt
ARRDC2ΔΔ
WWP1
AIP4
SMURF1
NEDL1
B
C
WWP1
ARRDC2
Merge
WT
ΔΔ
AIP4
ARRDC2
Merge
WT
ΔΔ

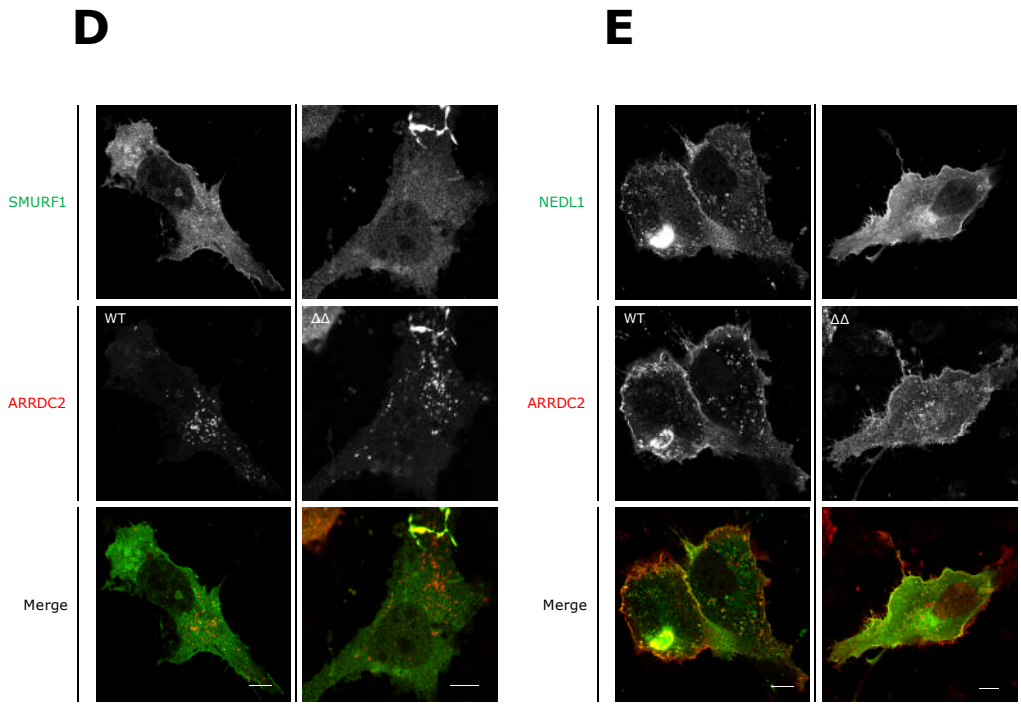

Figure 4.3 ARRDC2 may associate with NEDD4 family ubiquitin ligases in living cells

Confocal microscopic images of U2OS cells: **(A)** transiently transfected with plasmids expressing ARRDC2-mCherry (wild-type, wt; or PPxY mutant, ΔΔ), WWP1-eGFP-HA, AIP4-eGFP-HA, SMURF1-eGFP-HA or NEDL1-eGFP-HA. **(B, C, D, E)** transiently cotransfected with plasmids expressing ARRDC2-mCherry (wild-type, WT; or PPxY mutant, ΔΔ) and WWP1, AIP4, SMURF1 or NEDL1 tagged with eGFP-HA, except for in **E**, where ARRDC2 WT/ ΔΔ shown is the construct tagged with 2x FLAG epitope (ARRDC2-2FLAG), stained using mouse anti-FLAG antibody (1:200) detected with AF-633-conjugated anti-mouse secondary antibody (1:1000). In merged images, ARRDC2 is shown in red; the indicated ligase is in green. Images are representative of at least two independent experiments. Scale bar = 10 µm.

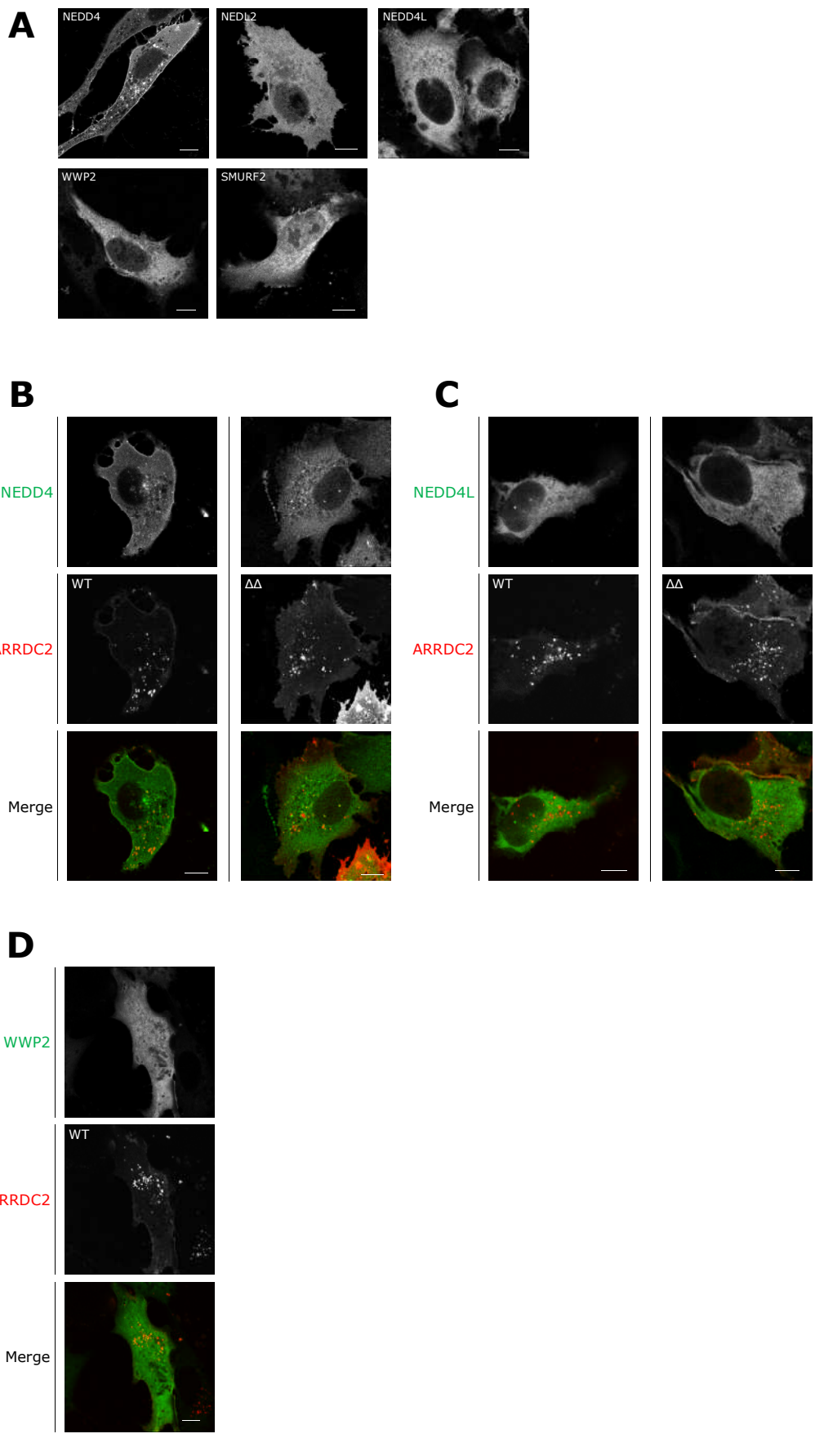
A
NEDD4
NEDL2
NEDD4L
WWP2
SMURF2
B
NEDD4
WT
ΔΔ
ARRDC2
Merge
C
NEDD4L
WT
ΔΔ
ARRDC2
Merge
D
WWP2
WT
ARRDC2
Merge

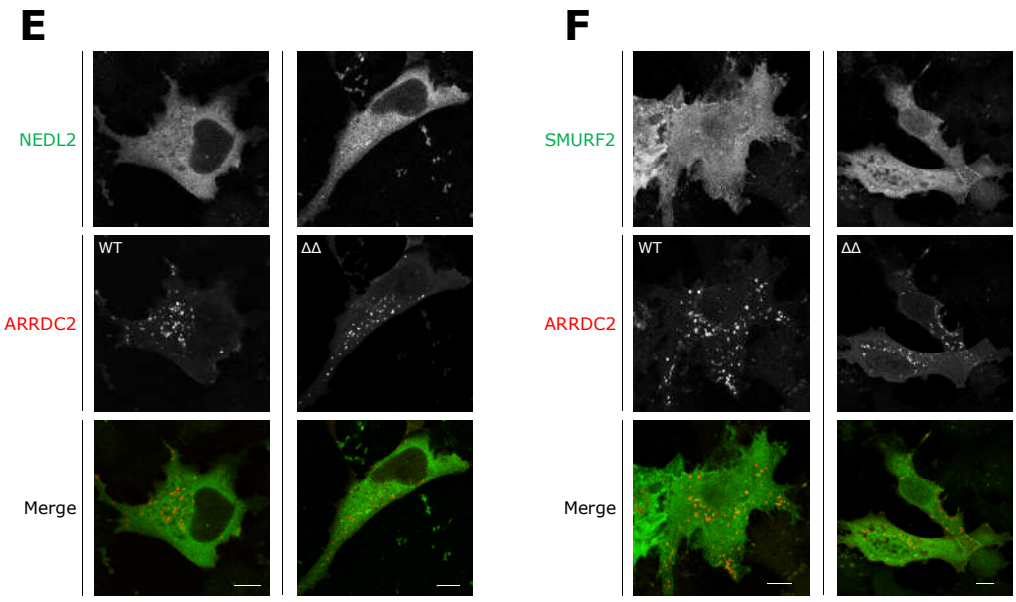

Figure 4.4 ARRDC2 overexpression does not affect NEDD4, NEDD4L, WWP2, NEDL2 or SMURF2 distribution

Confocal microscopic images of U2OS cells: **(A)** transiently transfected with plasmids expressing NEDD4, NEDD4L, WWP2, NEDL2 or SMURF2 N-terminally fused with eGFP-HA. **(B, C, D, E, F)** transiently cotransfected with plasmids expressing ARRDC2-mCherry (wild-type, WT; or PPxY mutant, ΔΔ) and NEDD4, NEDD4L, WWP2, NEDL2 or SMURF2 tagged with eGFP-HA. In merged images, ARRDC2 is shown in red; the indicated ligase is in green. Images are representative of at least two independent experiments. Scale bar = 10 μm.

ARRDC2 may also influence the localisation of SMURF1.

AIP4, another ligase that coimmunoprecipitated strongly with ARRDC2 (Figure 1B), localised to punctate cytoplasmic vesicles and the plasma membrane when expressed alone in U2OS cells (Figure 4.3A). In this case, the coexpression of ARRDC2wt had no obvious effect upon AIP4 distribution; AIP4 remained localised to cytoplasmic puncta and the plasma membrane (Figure 4.3C, left panel). However, ARRDC2wt did colocalise highly with AIP4-positive puncta (0.519±0.012 coefficient for ARRDC2wt-mCherry colocalisation with AIP4-eGFP-HA). Furthermore, although AIP4 remained punctate in distribution upon ARRDC2ΔΔ coexpression, the AIP4 puncta did not appear to colocalise with ARRDC2ΔΔ; AIP4- and ARRDC2ΔΔ-positive vesicles were largely distinct (Figure 4.3C, right panel; 0.146±0.005 ARRDC2ΔΔ-mCherry colocalisation coefficient with AIP4-eGFP-HA, p = 0.009, upaired t test). This differential colocalisation of AIP4 with variants of ARRDC2 (colocalised with ARRDC2wt; not with ARRDC2ΔΔ) suggests that AIP4 distribution may be influenced by ARRDC2.

ARRDC2 overexpression did not affect the distribution of the remaining six NEDD4 family ligases. For example, NEDL1 was localised diffusely throughout the cytosol but was also sporadically present within discrete punctate compartments when expressed alone in U2OS cells (Figure 4.3A). Although the NEDL1 puncta occasionally colocalised with coexpressed ARRDC2wt, there was no discernable effect upon NEDL1 distribution, and colocalisation with ARRDC2ΔΔ was also observed (Figure 4.3E). Of the remaining five NEDD4 family ligases, NEDL2, NEDD4L, WWP2, and SMURF2 were all diffusely distributed when expressed alone, and this distribution was unaffected by overexpression of ARRDC2 (Figure 4.4). When expressed alone, NEDD4 was localised diffusely throughout the cytoplasm, but also appeared in punctate cytoplasmic structures and at the plasma membrane (Figure 4.4A); this distribution was also unaffected by overexpression of ARRDC2 (NEDD4-positive puncta sporadically colocalised with both ARRDC2wt/ΔΔ when coexpressed [Figure 4.4B]). Hence, although ARRDC2 overexpression is capable

of affecting NEDD4 family ligase (WWP1, SMURF1 and AIP4) subcellular distribution, this is not ubiquitous to all NEDD4 family members.

4.2.3 ARRDC2 is modified by ubiquitin independent of ARRDC2-NEDD4 family ligase interaction and lysosomal function

As mentioned in section 4.2.1, on Western immunoblots, transiently expressed ARRDC2-2FLAG appeared as an anti-FLAG immunoreactive band at ~55 kD, around 10 kD higher than would be expected for monomeric, unmodified ARRDC2-2FLAG protein. The reason for this disparity is unclear, although it is possible that ARRDC2 may be modified by ubiquitination. A single ubiquitin moiety adds ~8 kD to the molecular weight of a protein. Hence, the predominant form of ARRDC2 may be monoubiquitinated, which would explain the major band detected at ~55 kD. Further to this, additional more slowly migrating bands were detectable above the molecular weight of ARRDC2-2FLAG at discrete intervals (for example, see Figure 4.5A, bottom panel). These additional bands are suggestive of further ubiquitinated forms of ARRDC2, indicating that ARRDC2 may be multi- and/or polyubiquitinated. Whether ARRDC2 is indeed ubiquitinated was tested by the transient expression of ARRDC2-2FLAG with or without ubiquitin N-terminally tagged with HA (HA-ubiquitin) in U2OS cells. Resulting protein lysates were incubated with anti-HA agarose beads in order to immunoprecipitate HA-ubiquitin; Western immunoblotting was performed on whole cell lysates or immunoprecipitates to assess for the presence of coimmunoprecipitated ARRDC2-2FLAG.

ARRDC2wt coimmunoprecipitated with ubiquitin; although, as in previous coimmunoprecipitation experiments, a low level of background ARRDC2wt-2FLAG binding to the anti-HA agarose was evident by the presence of faint anti-FLAG immunoreactive bands at~55 kD in the HA-ubiquitin-negative immunoprecipitate, a much stronger band was observed for ARRDC2wt-2FLAG when

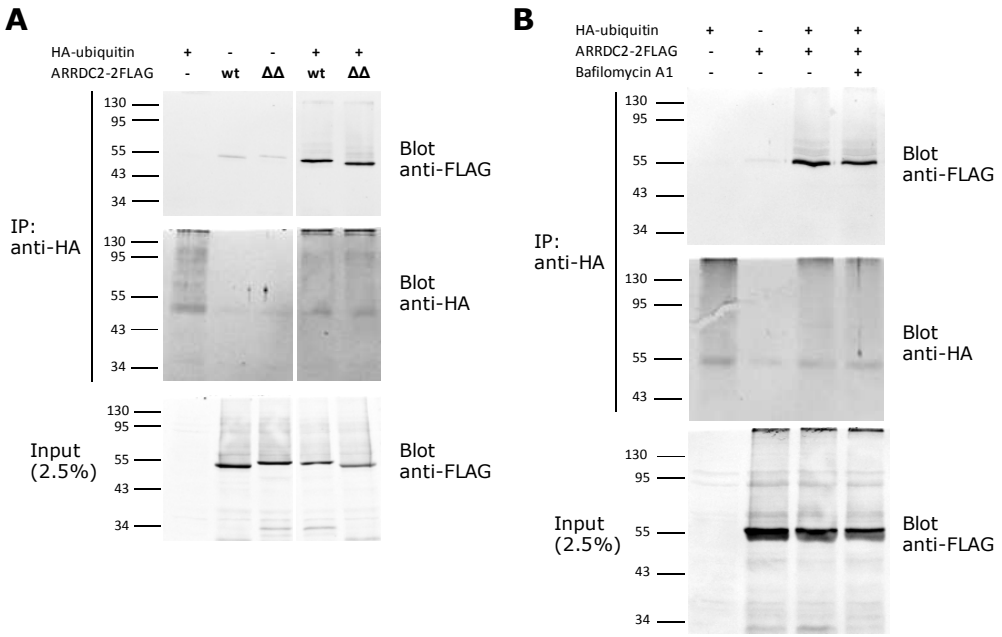

Figure 4.5 ARRDC2 ubiquitination is independent of its PPxY motifs and is unaffected by lysosomal inhibition

(A) U2OS cells were transiently cotransfected with plasmids expressing ARRDC2-2FLAG wild-type (wt) or PPxY mutant (ΔΔ) and/or HA-ubiquitin, as indicated. **(B)** U2OS cells were transiently cotransfected with plasmids expressing ARRDC2-2FLAG wild-type and/or HA-ubiquitin, as indicated. In addition, cells were treated plus/minus 1 µM Bafilomycin A1 (inhibitor of lysosomal function) for 24h prior to cell lysis. In both A/B, cell lysates (5% input) and immunoprecipitates (IP) obtained by incubation with anti-HA agarose were separated by 12.5% SDS-PAGE and analysed by Western blotting using anti-HA or anti-FLAG antibodies (both at 1:5000 dilution), as indicated, detected using IRDye 800CW anti-rabbit secondary antibody (1:10,000). Molecular weight markers are shown in kD.

HA- ubiquitin was coexpressed (Figure 4.5A, top panel). Furthermore, a number of more slowly migrating bands were detected above the ~55 kD band. These observations indicate that ARRDC2 may be modified by ubiquitin, predominantly involving monoubiquitination but also multi- and/or polyubiquitination.

The ability of ARRDC2 to interact with NEDD4 family E3 ligases has been previously shown (section 4.2.1). NEDD4 ligases have been implicated in the ubiquitination of α-arrestins (Becuwe *et al.*, 2012; Gupta *et al.*, 2007; Hatakeyama *et al.*, 2010; Kee *et al.*, 2006; Rauch *et al.*, 2011), and it is notable that overexpression of several NEDD4 ligases (NEDL1 and WWP2 in particular) appeared to result in an increase in the intensity of high molecular weight ARRDC2

bands detected in immunoprecipitates, suggestive of an enhancement of ARRDC2 ubiquitination (Figure 4.1, top panel). Therefore, it was hypothesised that ARRDC2 ubiquitination may be dependent upon ARRDC2-ligase interaction. However, the ARRDC2ΔΔ PPxY motif mutant coimmunoprecipitated with ubiquitin in a comparable manner to ARRDC2wt (Figure 4.5A, top panel). It is worth noting that an alternative interpretation of the coimmunoprecipitation of ARRDC2 and ubiquitin is that ARRDC2 binds to ubiquitin, rather than being modified by the covalent attachment of it, as has been suggested elsewhere (Rauch *et al.*, 2011). This possibility underlines the importance of subsequent alternative approaches to measuring ARRDC2 ubiquitination (see section 4.3).

As mentioned (section 4.1), ubiquitination (especially polyubiquitination) of protein substrates within the endocytic system is frequently used as a signal for their targeting to the lysosome for degradation. Hence, it is possible that the ubiquitination of ARRDC2 detected here serves this purpose for the turnover of the protein. To address this, the expression and ubiquitination of ARRDC2-2FLAG was assessed in cells treated with or without the vacuolar-type ATPase inhibitor, bafilomycin A1, which prevents the acidification and maturation of endosomes, thereby blocking transport from late endosomes to lysosomes (van Weert *et al.*, 1995). ARRDC2 expression and ubiquitination (as detected by coimmunoprecipitation as above) were comparable in cells treated or untreated with bafilomycin A1 (Figure 4.5B); that is, accumulation of ubiquitinated ARRDC2 was not detected upon lysosomal inhibition. It is noted that in these experiments an expected high molecular weight smear of ubiquitinated proteins was only weakly detected and the characteristic low molecular weight band (~10 KDa) of unconjugated ubiquitin was not seen in anti-HA blots, suggesting that ubiquitin may have been poorly expressed.

4.3 Discussion

Coimmunoprecipitation demonstrated that ARRDC2 is able to interact, at least indirectly, with multiple members of the NEDD4 family of HECT E3 ubiquitin ligases. The ARRDC2 C-terminal PPxY motifs must be present in order to detect coimmunoprecipitation with NEDD4 ligases (demonstrated here for NEDL1 and WWP1). This suggests that the ARRDC2-ligase interaction may be direct, involving ARRDC2 PPxY motif contact with ligase WW domains, in agreement with the emerging paradigm for α-arrestin-NEDD4 family ligase interactions. Coimmunoprecipitation also indicated that ARRDC2 is modified by ubiquitin. Mutation of ARRDC2 PPxY motifs did not appear to affect its ubiquitination, suggesting that the modification is independent of ARRDC2 interaction with NEDD4 ligases. Finally, ARRDC2 ubiquitination was detected regardless of lysosomal function, suggesting that the modification may have some function other than targeting ARRDC2 for lysosomal degradation.

4.3.1 ARRDC2 interaction with NEDD4 family ligases

Many α-arrestins have been reported to interact with NEDD4 family ligase members (Andoh *et al.*, 2002; Hatakeyama *et al.*, 2010; Herrador *et al.*, 2009; Lin *et al.*, 2008; Nabhan *et al.*, 2010; Nikko *et al.*, 2008; Rauch *et al.*, 2011). In particular, Rauch and Martin-Serrano (2011) investigated the interaction of several NEDD4 ligases with human ARRDCs, including ARRDC2. Using a yeast two-hybrid screen, they showed that ARRDC2 is capable of binding WWP1, WWP2 and NEDD4, and furthermore showed using GST pull-downs that ARRDC2 can directly interact with WWP1, WWP2, NEDD4 and AIP4. These observations are in agreement with the coimmunoprecipitation data presented here, and collectively argue strongly for the ability of ARRDC2 to directly interact with NEDD4 family ubiquitin ligases.

The interaction of ARRDC2 with NEDD4 ligases was found to be PPxY motif-dependent (shown here for interactions with NEDL1 and WWP1), as has been shown for many other α-arrestin-NEDD4 ligase

interactions (Andoh *et al.*, 2002; Hatakeyama *et al.*, 2010; Herrador *et al.*, 2009; Lin *et al.*, 2008; Nabhan *et al.*, 2010; Rauch *et al.*, 2011). ARRDC2 contains two PPxY motifs in its C-tail. Mutation of both PPxY motifs abolished ARRDC2 interaction with NEDL1 (and WWP1), whereas some residual NEDL1 binding was detectable with single ARRDC2 PPxY mutants. This suggests that both PPxY motifs contribute to the ARRDC2-ligase interaction. This is in agreement with other studies where α-arrestin interaction with ligases is reduced, but not completely abolished, by mutation of single PPxY motifs (Lin *et al.*, 2008; Nabhan *et al.*, 2010). The discovery that ARRDC2 binds several NEDD4 ligases via its PPxY motifs strongly suggests that the interaction is mediated canonically by the ligase WW domains. However, mutation of individual ligase WW domains and analysis of the impact upon ARRDC2 coimmunoprecipitation would be needed to directly demonstrate this.

The relevance of ARRDC2-NEDD4 family ligase interactions to any molecular or physiological mechanisms has not been addressed elsewhere to date. In the case of ARRDC1, interaction with ligases – notably WWP1 – and ubiquitination by those same ligases may provide a link between the ligases and the ESCRT machinery during PPxY-dependent viral budding (Rauch *et al.*, 2011). For ARRDC3, PPxY-dependent interaction with NEDD4 has been suggested to recruit NEDD4 to the agonist-stimulated β_2AR, thereby mediating receptor ubiquitination and downregulation (Nabhan *et al.*, 2010). Thus, ARRDC-NEDD4 family ligase interactions may serve to recruit the ligases to specific subcellular localisations and/or substrate proteins, where their ubiquitination of substrates is required under particular conditions.

Data presented here suggest that this is true for ARRDC2: that is, the interaction of ARRDC2 with NEDD4 family ligases can influence the localisation of the ligases, and thus may determine their site of action. This was shown for WWP1 and SMURF1, both of which exhibited a diffuse cytosolic distribution when expressed alone but, when coexpressed with ARRDC2wt, also became localised to punctate structures that colocalised with ARRDC2wt. Importantly,

WWP1 or SMURF1 redistribution was not induced upon coexpression with ARRDC2ΔΔ. The ARRDC2 PPxY motifs were demonstrated to be required for its interaction with WWP1; although not tested here, based on the amount of literature supporting PPxY motif-WW domain interactions it is expected that this is also the case for the ARRDC2-SMURF1 interaction. Thus, the ARRDC2 PPxY motif-dependent redistribution of WWP1 and SMURF1 to a more punctate pattern is likely to be a result of direct interaction with ARRDC2 and recruitment to vesicular compartments in which ARRDC2 resides.

An effect of ARRDC2 overexpression upon AIP4 distribution was also potentially detected, since AIP4 puncta colocalised with ARRDC2wt but not ARRDC2ΔΔ. This suggests that interaction with ARRDC2 may also determine the precise localisation pattern of AIP4. Hypothetically, it is conceivable that when expressed alone, AIP4 localises to discrete vesicular compartments (for example, endosomes) that are separate from ARRDC2-positive compartments (i.e. lysosomes) such that, upon overexpression of ARRDC2ΔΔ, the two populations are not colocalised; overexpressed ARRDC2wt, however, is able to interact with AIP4 and recruits it to ARRDC2wt-positive lysosomes. This assumes that ARRDC2ΔΔ is targeted to the lysosome in the same way as ARRDC2wt. Although ARRDC2wt and ARRDC2ΔΔ exhibited the same overall pattern of distribution – plasma membrane plus cytoplasmic puncta – additional experiments such as co-staining specific compartments (for example with transferrin or LysoTracker) would be needed to clarify this. Regarding the impact of the ARRDC2-AIP4 interaction, the reverse hypothesis is also possible: namely that AIP4 causes ARRDC2 redistribution. Again, additional experiments using compartment-specific co-staining of AIP4- and ARRDC2-containing puncta would be required to distinguish these two possibilities.

With reference back to the localisation studies on ARRDC2 (Chapter 3), the fact that ARRDC2ΔΔ retains the ability to target to vesicular compartments (although as noted above, the nature of these compartments is unknown) suggests that ARRDC2 is not targeted to membranes by its association with NEDD4 ligases, but

by some other unknown mechanism. In contrast, a recent report showed that deletion of the PPxY motif-containing C-terminus of ARRDC4 abolishes its membrane targeting, resulting in a diffuse cytosolic pattern of distribution (Vina-Vilaseca *et al.*, 2011). However, since a large portion (the last 68 amino acids) of the ARRDC4 C-terminus was deleted, it is unclear whether this effect is due to the lack of NEDD4 ligase binding. It could be that other residues within this region form membrane contacts (directly or indirectly), or that the C-tail is essential for the overall structure of the protein which, when disrupted, is unable to support the same molecular interactions.

It is worth noting that the strategy for assessing ARRDC2 interactions with NEDD4 family ligases involved the use of ligases that were C-terminally tagged with eGFP-HA, both in microscopic localisation studies and immunoprecipitations. This approach was chosen in order to avoid disrupting the N-terminal phospholipid-binding C2 domain, which is known to be required for correct subcellular targeting (Dunn *et al.*, 2004; Lu *et al.*, 2011). However, since the completion of the current project it has become clear that the extreme C-terminus of NEDD4 ligases contains a conserved phenylalanine residue that is critical for substrate ubiquitination (Salvat *et al.*, 2004). Disrupting this activity may not have affected the ligase subcellular targeting, making the conclusions of the localisation experiments reported here unaltered. But for immunoprecipitation experiments altered ligase activity and possibly conformation may have affected the results; it would therefore be ideal to replicate the results using alternative methods (ligases fused to HA alone; immunoprecipitation of endogenous ligases).

4.3.2 ARRDC2 ubiquitination

Coimmunoprecipitation of ARRDC2 with ubiquitin demonstrated that ARRDC2 can be modified by ubiquitin. The presence of sequential higher molecular weight bands on ARRDC2 Western blots upwards of the major ARRDC2 band suggested that this may involve multi-

or polyubiquitination, as has been seen for ARRDC1 (Nabhan *et al.*, 2012). However, the predominant form of ARRDC2 may be monoubiquitinated, since the major ARRDC2 band detected on Western blots was consistently ~10 kD larger than the predicted molecular weight of monomeric, unmodified ARRDC2. A similar observation has been made for the yeast α-arrestin, ART1, which appeared on Western blots as a weak band corresponding to unmodified ART1 plus a stronger band ~8 kD larger in size (Lin *et al.*, 2008). Pull-down of ART1 and anti-ubiquitin immunoblotting confirmed that this major band was an ubiquitinated form of ART1, presumably monoubiquitinated. For ARRDC2 this could be similarly tested by pull-down of ARRDC2 followed by immunoblotting with an antibody targeted against ubiquitin (and analysis of the size of the resultant bands). Such an approach would also provide a more meaningful assessment of the proportion of ARRDC2 that is modified by the attachment of endogenous ubiquitin, information that is not available from the above experiment in which total, overexpressed ubiquitin was immunoprecipitated, and any ARRDC2 bound to it was detected.

Inhibition of lysosomal function by the addition of bafilomycin A1 did not appear to affect the level of ARRDC2 protein or its ubiquitination status, suggesting that the ARRDC2 ubiquitination detected may not represent a signal for lysosomal sorting and degradation. Rather, it is tempting to speculate that the ubiquitination of ARRDC2 may directly influence its function – as is the case for other α-arrestins (Becuwe *et al.*, 2012; Rauch *et al.*, 2011) – within the endo-lysosomal system. Given the influence of NEDD4 family ligases upon sorting processes within this system, that ARRDC2 interacts with several NEDD4 family members (section 4.2.1), and that other α-arrestins are reported to be ubiquitinated by NEDD4 family ligases (Becuwe *et al.*, 2012; Hatakeyama *et al.*, 2010; Rauch *et al.*, 2011), it was hypothesised that the ubiquitination of ARRDC2 may be carried out by NEDD4 family ligases. However, it was shown here that the ARRDC2ΔΔ mutant, which does not interact with NEDD4 family ligases (demonstrated

here for NEDL1 and WWP1), retains its ability to coimmunoprecipitate efficiently with ubiquitin. As mentioned above, the experimental approach used – pull-down of ARRDC2 with overexpressed ubiquitin – may yield positive coimmunoprecipitation results that exaggerate the 'real' situation.

Nonetheless, this result suggests that NEDD4 family ligase interaction is not required for ARRDC2 ubiquitination, implying that other ligases may be responsible. This would not be the first time that a PPxY motif-containing ubiquitin ligase adaptor has been reported to be ubiquitinated independent of a known NEDD4 family ligase interaction (Edwards *et al.*, 2009). However, it is in contrast to several reports on other α-arrestins. ART1, as mentioned above, is monoubiquitinated, and this modification was abolished by mutation of the two ART1 PPxY motifs (Lin *et al.*, 2008). The human α-arrestin ARRDC1 is ubiquitinated: this is enhanced by the overexpression of WWP1, and abolished by the overexpression of a catalytically inactive WWP1 mutant or the deletion of the ARRDC1 PPxY motif-containing C-terminus (Rauch *et al.*, 2011). Thus, the ubiquitination of ARRDC2 by a non-NEDD4 family ligase would represent a new mechanism of α-arrestin regulation. It would be important to perform the reverse ARRDC2-ubiquitin pull-down experiment described above before making this conclusion. Indeed, as noted in section 4.2.3, overexpression of several NEDD4 ligases (NEDL1 and WWP2) appeared to increase the intensity of high molecular weight ARRDC2 bands, suggestive of an enhancement of ARRDC2 ubiquitination. Thus, the combination of more sensitive approaches such as observing the effect of NEDD4 ligase siRNA knockdown or catalytic mutant overexpression on ARRDC2 ubiquitination would be required to convincingly demonstrate that NEDD4 ligases are not responsible.

In summary, the endocytic targeting of ARRDC2 was described in Chapter 3. This has been supported by the discovery that ARRDC2 can interact with several members of the NEDD4 ubiquitin ligase

family, ubiquitous regulators of signalling and trafficking within the endocytic system. Interaction with NEDD4 ligases requires ARRDC2 PPxY motifs, suggesting that the mechanism involved may be similar to that used by several other α-arrestins. Moreover, interaction with ARRDC2 can influence the subcellular targeting of several NEDD4 ligases (notably WWP1, SMURF1), providing a basis for the hypothesis that ARRDC2 may represent an adaptor for specific NEDD4 ligase ubiquitination events. ARRDC2 itself can be ubiquitinated, a modification that may influence ARRDC2 *in situ* function, rather than lysosomal targeting. Biochemical experiments hint that the predominant form of ARRDC2 may be monoubiquitinated, in addition to higher order ubiquitin oligomers. Preliminary data suggest that this modification may not be carried out by NEDD4 ligases, although additional experiments will be needed to clarify the ligase(s) responsible.

5 Putative role for ARRDC2 in GPCR regulation

5.1 Introduction

The GPCRs used in the current study were the *Rhodopsin*/class A receptors, β_2AR and δOR.

β_2AR is perhaps the most widely studied GPCR, and much of the knowledge gleaned from β_2AR studies has shaped the understanding of GPCR signalling and regulatory mechanisms. β_2AR responds to the endogenous catecholamine agonists, adrenaline and noradrenaline (Goldstein, 2001). Adrenaline and, to a lesser extent, noradrenaline, are secreted in response to sympathetic nervous system (SNS) stimulation of the adrenal medulla. Adrenaline/noradrenaline act peripherally to stimulate both α- and β-adrenoceptors, producing physiological effects including enhanced cardiac output and skeletal muscle vasodilation, characteristic of the "fight-or-flight" stress response. They also act upon the lungs to produce airway relaxation, hence the use of adrenoceptor agonists (at the β_2AR) to treat asthma. Noradrenaline also acts centrally as a neurotransmitter to regulate cognitive functions such as arousal, mood and memory (Ramos *et al.*, 2007; Sara, 2009). Such knowledge has led to the use of compounds which alter noradrenaline physiology, for example in the treatment of depression (tricyclic antidepressants inhibit noradrenaline re-uptake, as do amphetamine/cocaine).

The canonical pathway for β_2AR signalling involves agonist-dependent coupling to G_s, which activates adenylyl cyclase leading to increased production of cAMP and the subsequent activation of PKA, which phosphorylates various target proteins. At high agonist concentrations, β_2AR also couples to inhibitory G_i proteins in a manner dependent on receptor phosphorylation by PKA, which induces a switch in coupling from G_s to G_i (Daaka *et al.*, 1997; Liu *et al.*, 2009). As has been described (Chapter 1), β_2AR also undergoes

agonist-dependent phosphorylation by GRKs, leading to β-arrestin association and desensitisation, as well as clathrin-mediated endocytosis. Agonist-stimulated β_2AR is subject to ubiquitination, originally thought to be carried out by the RING E3 ligase, Mdm2, which is recruited by β-arrestin (Shenoy *et al.*, 2001) although NEDD4 appears to be a more likely candidate for the ligase responsible (Nabhan *et al.*, 2010; Shenoy *et al.*, 2008). β_2AR falls into group A (section 1.2.4) of GPCRs that are transiently phosphorylated and ubiquitinated, from which β-arrestin rapidly dissociates. Thus, β_2AR is used here as a model GPCR that is targeted to early/recycling endosomes upon internalisation (Moore *et al.*, 2004; Seachrist *et al.*, 2000), leading to rapid recycling to the plasma membrane (Pippig *et al.*, 1995; Shenoy *et al.*, 2003) and hence inefficient lysosomal sorting and degradation; reductions in β_2AR levels of just ~10 and ~25% are detected upon isoprenaline stimulation (10 μM) for 3 and 24h, respectively (Nabhan *et al.*, 2010; Shenoy *et al.*, 2003).

Opioid receptors are divided into four subtypes based on their pharmacological responsiveness to a variety of opioid ligands: mu-, kappa-, delta- and nociceptin/orphanin-opioid receptors (μ-, κ-, δ- and N-opioid receptors) (Waldhoer *et al.*, 2004). δOR is expressed in the brain and mediates analgesic and antidepressant responses to opiates; specifically, endogenous δOR peptide ligands include various enkephalin derivatives. These can be mimicked by therapeutic agonists (for example, morphine – although note that morphine preferentially activates μOR), the chronic application of which is well known to cause tolerance, presumably through receptor downregulation. δOR is a G_i/G_o-coupled receptor: δOR activation leads to inhibition of adenylyl cyclase and presynaptic Ca^{2+} channels (Law *et al.*, 2000). The mechanism of desensitisation and endocytosis of δOR is highly similar to that of β_2AR, involving ligand-dependent phosphorylation by GRKs, recruitment of β-arrestins and coupling to the clathrin-mediated endocytic machinery (von Zastrow, 2010). Thus, δOR is internalised into homologous early endosomal compartments to β_2AR (Tsao *et al.*, 2000).

However, from here, the fate of δOR is markedly distinct from β_2AR; the δOR undergoes sorting into the lysosomal pathway, leading to efficient proteolysis and downregulation; whereas, as described above, just ~10% of β_2AR is degraded over 3 h agonist stimulation, for δOR this rises to ≥50% (Tsao *et al.*, 2000). Under the GPCR classification system described (section 1.2.4), δOR is a group B GPCR whose phosphorylation and ubiquitination is thought to be more prolonged, leading to more stable β-arrestin association, intracellular retention and lysosomal trafficking. Despite this definition, the mechanism of δOR segregation into the lysosomal pathway remains incompletely understood. Experiments indicate that GPCR-associated sorting proteins (GASPs) are required, although their precise role remains undefined (Whistler *et al.*, 2002). Surprisingly, lysosomal sorting can occur in mutant δOR receptors devoid of ubiquitin-targeted cytoplasmic lysine residues (Tanowitz *et al.*, 2002), yet still requires components of the ESCRT machinery (Hislop *et al.*, 2004), which is normally involved in MVB sorting of ubiquitinated cargoes (section 1.2.3). It appears that δOR ubiquitination – performed by the NEDD4 family ligase AIP4 – plays a regulatory, rather than obligatory role in δOR degradation by enhancing the efficiency of receptor incorporation into ESCRT-mediated ILVs (Henry *et al.*, 2011). Here, δOR is used as a model GPCR that undergoes efficient lysosomal trafficking and degradation.

If ARRDC proteins are involved in GPCR regulation – as supported by aforementioned studies on ARRDC3 – one mechanism by which this might occur is via oligomerisation with β-arrestins. Homo-oligomerisation of visual arrestin is well established, and is thought to perform a regulatory role in limiting the proportion of 'active' monomer available in retinal cells (Kim *et al.*, 2011; Schubert *et al.*, 1999). Homo- and hetero-oligomerisation of β-arrestins has also been reported using methods including coimmunoprecipitation and resonance energy transfer (Storez *et al.*, 2005), and may be supported at physiological concentrations by the presence of the cytosolic lipid, inositol hexakisphosphate (IP_6) (Hanson *et al.*, 2007). The homodimerisation interface of β-arrestin2 was mapped using a

spot peptide array, and it was found that this same surface defines the ERK1/2 signalling platform (Xu *et al.*, 2008). This led to the suggestion that β-arrestin dimers – similar to visual arrestins – may represent inactive 'storage' forms in which signalling interactions are masked, and that disruption of dimerisation upon receptor association is required for their scaffolding functions. However, β-arrestin2 binding to the alternative partner, JNK3, was unaffected by mutations that disrupted dimerisation (Xu *et al.*, 2008), and interaction with Mdm2 has been reported to require β-arrestin2 dimerisation (Boularan *et al.*, 2007), suggesting that β-arrestin dimers may be functionally relevant, perhaps determining the specific subset of downstream effectors with which β-arrestin can interact. Furthermore, the apparent involvement of both β-arrestins in various signalling pathways suggests that heterodimerisation of β-arrestins could play an important role (Defea, 2008). Moreover, the ability of arrestins to act as dimers or higher order oligomers is conceptually plausible. The potential for GPCR oligomerisation has been noted (section 1.1.4), and it has been recognised that the association of arrestin and GPCR dimers might provide the extensive surface required for the scaffolding of the apparent multitude of arrestin effectors (Gurevich *et al.*, 2008a). The ability of arrestin family proteins to hetero-oligomerise would provide yet another level of complexity to this system.

The current chapter investigates a potential role for ARRDC2 in the regulation of GPCRs, focussing on β_2AR and δOR. This was prompted by several lines of evidence, including (i) the similarity of α-arrestins, including ARRDC2, to the canonical GPCR regulatory adaptors, the β-arrestins; (ii) the reported involvement of other α-arrestins, notably ARRDC3, in GPCR regulation (see section 1.4.3) (iii) the fact that ARRDC2 is specifically targeted to the endocytic system, including the plasma membrane (Chapter 3), the environment in which GPCRs function and are regulated by trafficking; (iv) the detection of ARRDC2 ubiquitination and interactions with NEDD4 family ubiquitin ligase members (Chapter 4), both of which represent important determinants of multiple cargo trafficking

processes, including those involving GPCRs. As mentioned, the potential for homo- and hetero-oligomerisation of ARRDC2 with arrestin members was also investigated.

5.2 Results

5.2.1 ARRDC2 regulation of a prototypic recycling receptor: β_2AR

5.2.1.1 ARRDC2 colocalises with internalised β_2AR

As a preliminary indicator for the involvement of ARRDC2 in β_2AR regulation, the colocalisation of coexpressed fluorescent protein fusions of ARRDC2 and β_2AR was assessed in U2OS cells. In these experiments, β_2AR was fused with either C-terminal GFP (β_2AR-GFP) or extracellular N-terminal SNAP tag (plus N-terminal signal sequence; ssβ_2AR). The expression pattern and agonist responsiveness of these fusions in U2OS cells was first validated. β_2AR-GFP or ssβ_2AR were efficiently expressed in transiently transfected cells. In the absence of agonist stimulation expression was largely confined to the plasma membrane, whereas agonist stimulation (isoprenaline, 10 μM, 1 h) resulted in receptor internalisation into cytoplasmic vesicles (Figure 5.1). Hence, the expression pattern and responsiveness of the β_2AR fusions in U2OS cells was in agreement with that widely known for β_2AR (Kallal *et al.*, 1998). Coexpression of ARRDC2 constructs with β_2AR (ARRDC2-mCherry with β_2AR-GFP; ARRDC2-GFP with ssβ_2AR labelled with AF-633-conjugated SNAP ligand) had no obvious effect upon the distribution of either protein in unstimulated conditions (Figure 5.2A,B, top panels); β_2AR-GFP/ssβ_2AR remained largely at the plasma membrane, ARRDC2-mCherry/ARRDC2-GFP retained the punctate intracellular distribution (with some plasma membrane staining) that has already been described (Chapter 3). Agonist stimulation, as seen above, caused β_2AR internalisation into cytoplasmic vesicles; interestingly, ARRDC2 puncta exhibited a high degree of colocalisation with internalised β_2AR (Figure 5.2A,B,

bottom panels; for example, a coefficient of 0.672±0.023 was measured for ARRDC2-mCherry colocalisation with β_2AR-GFP, *n* = 5).

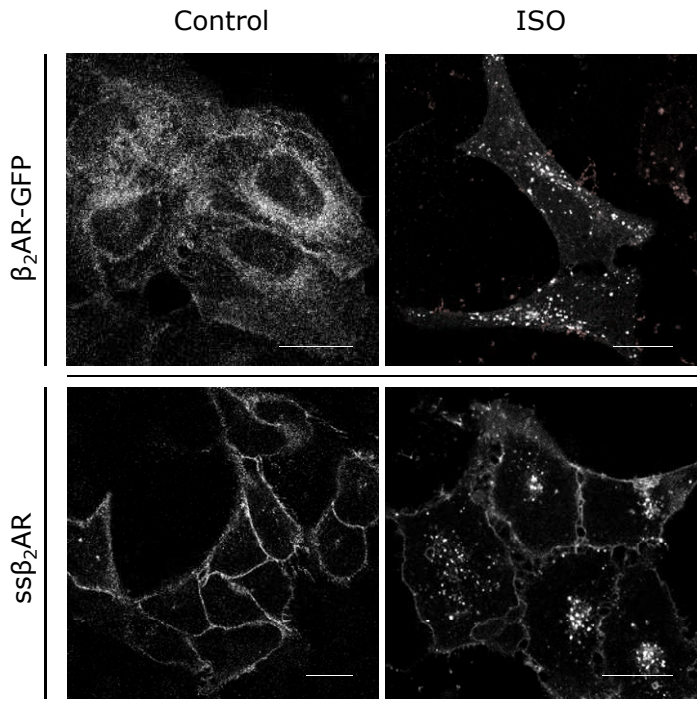

Figure 5.1 Exogenous expression of β_2AR constructs in U2OS cells

Confocal microscopic images of U2OS cells transiently transfected with plasmids expressing β_2AR tagged with GFP (β_2AR-GFP) or SNAP tag (ssβ_2AR), treated with isoprenaline (ISO, 10 µM, 1h) or without (Control), as indicated. ssβ_2AR was visualised by labelling with 0.1 µM SNAPsurface BG-AF546 prior to the experiment. Images are representative of at least three independent experiments. Scale bar = 20 µm.

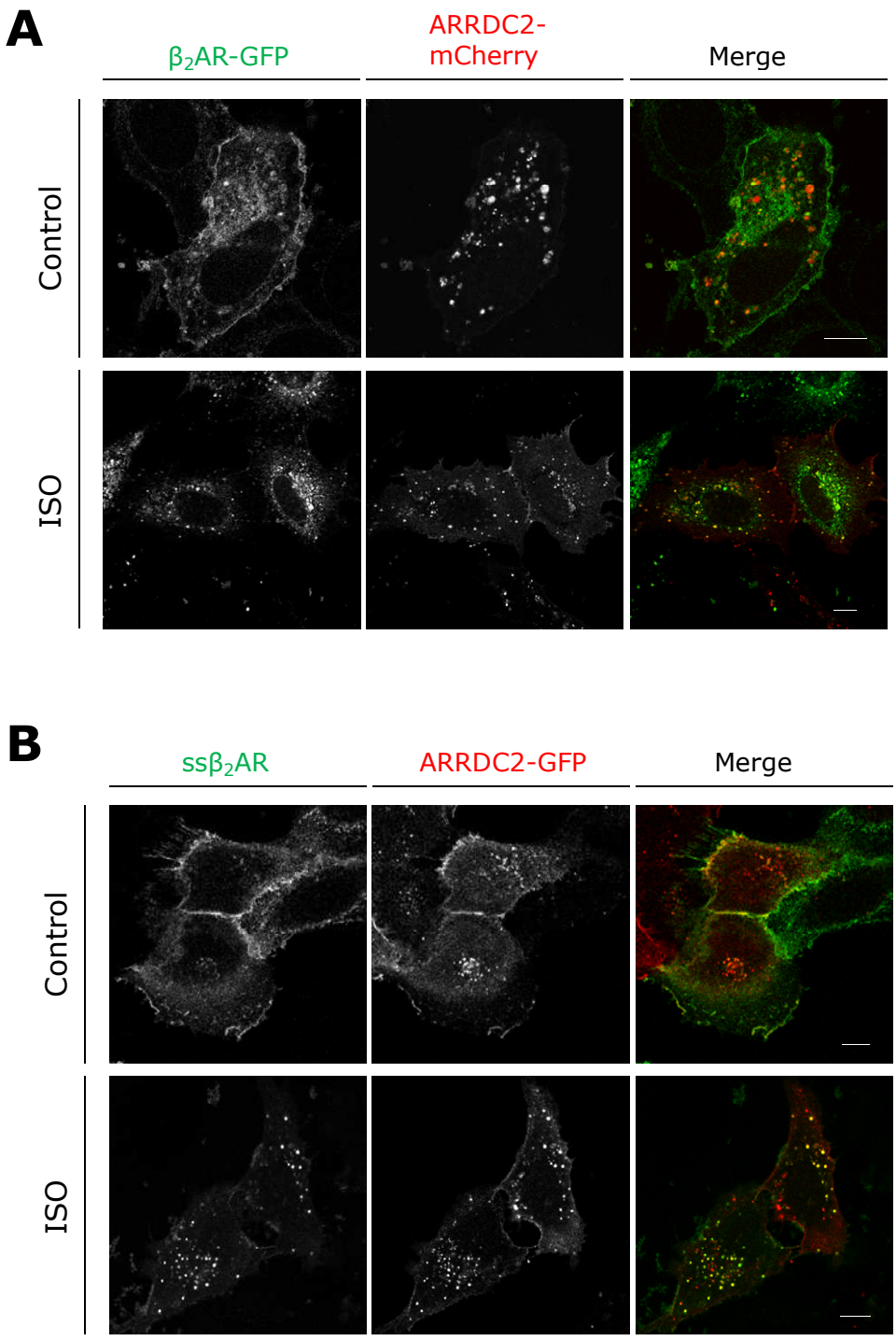

Figure 5.2 ARRDC2 colocalises with agonist-stimulated β_2AR

Confocal microscopic images of U2OS cells transiently transfected with plasmids expressing ARRDC2-mCherry plus β_2AR-GFP **(A)**, or with ARRDC2-GFP plus ssβ_2AR **(B)**. Cells were treated with isoprenaline (ISO, 10 µM, 1h) or without (Control), as indicated. ssβ_2AR was visualised by labelling with 0.1 µM SNAPsurface BG-AF633 prior to the experiment. In merged images, β_2AR is in green, ARRDC2 is in red. Images are representative of at least three independent experiments. Scale bar = 10 µm.

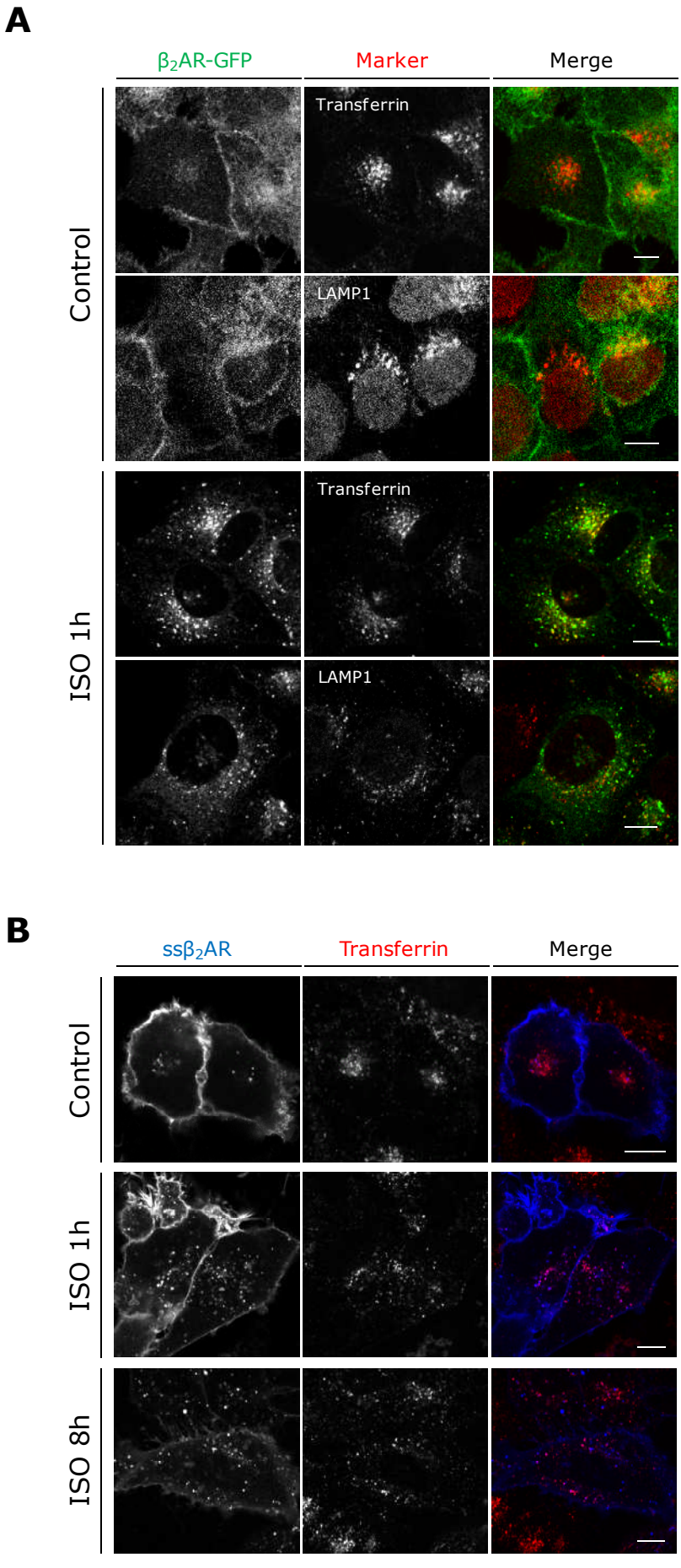
A
β2AR-GFP
Marker
Merge
Control
Transferrin
LAMP1
ISO 1h
Transferrin
LAMP1
B
ssβ2AR
Transferrin
Merge
Control
ISO 1h
ISO 8h

Figure 5.3 Internalised β_2AR is found within transferrin-positive early endosomal/recycling compartments in U2OS cells

Confocal microscopic images of U2OS cells transiently transfected with plasmids expressing β_2AR-GFP **(A)** or ssβ_2AR **(B)** were treated with isoprenaline (ISO, 10 µM, 1h or 8h, as indicated) or without (Control), as indicated. In addition, cells were co-stained with 250 ng/µl AF-633-conjugated Transferrin for the final 15 min of the plus/minus isoprenaline incubation, or co-immunostained post-fixing using rabbit anti-LAMP1 antibody detected with AF-633-conjugated anti-rabbit secondary antibody, as indicated. ssβ_2AR was visualised by labelling with 0.1 µM SNAPsurface BG-AF546 prior to the experiment. In merged images, β_2AR-GFP is in green, ssβ_2AR is in blue and transferrin/LAMP1 (Marker) is in red. Images are representative of at least three independent experiments. Scale bar = 10 µm.

5.2.1.2 ARRDC2/β2AR colocalisation involves compartmental ARRDC2 redistribution

The observation that ARRDC2 colocalises with agonist-stimulated, internalised β_2AR was interesting given that ARRDC2 has been found to reside within late endosomal/lysosomal compartments (Chapter 3) and that, in contrast, β_2AR is widely believed to rapidly recycle to the plasma membrane via early/recycling endosomes (Parent *et al.*, 2009; Shenoy *et al.*, 2003). Indeed, experiments performed here confirmed that in U2OS cells, agonist-stimulated, internalised β_2AR (10 µM isoprenaline, 1 h) was found within transferrin-positive early/recycling endosomes and was distinct from LAMP1-labelled lysosomes (Figure 5.3). Moreover, high-content imaging indicated that the receptor was efficiently recycled (Figure 5.4). Cells stably expressing ssβ_2AR were stimulated for 1 h with 10 µM isoprenaline, followed by two rinse washes and a final wash step of between 5 – 60 min in serum-free DMEM/0.1 % BSA with or without 1 µM propanolol, a β_2AR antagonist. Although there was only an ~11 % reduction in isoprenaline-stimulated ssβ_2AR internalisation over a 30 min wash period without propanolol, inclusion of propanolol – assumed to compete for binding to ssβ_2AR with isoprenaline, which may not be fully removed in the wash steps – resulted in a ~64 % reduction in internalisation over the same time-scale, and an ~89 % reduction over the full 1 h. This result is contrasted with the profile

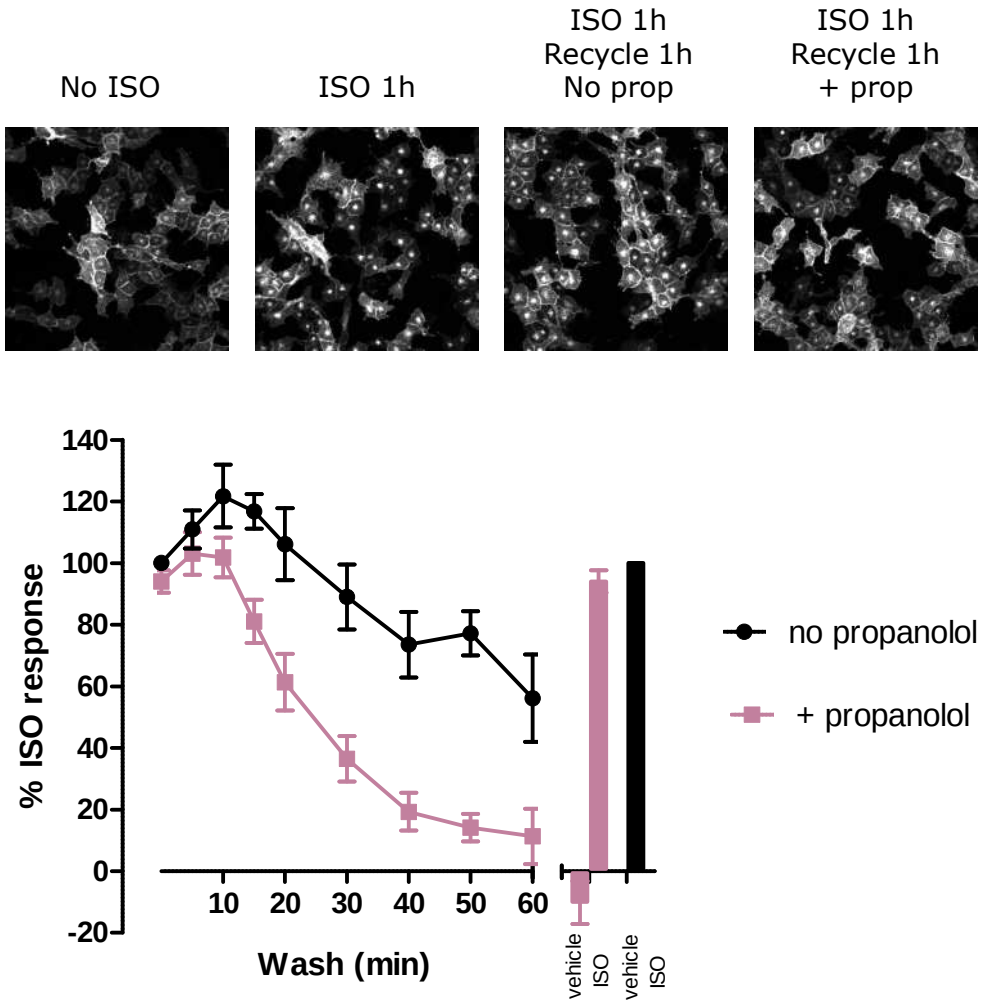

Figure 5.4 Internalised β_2AR recycles rapidly to the cell surface

ssβ_2AR recycling to the plasma membrane following agonist stimulation was quantified by granularity analysis of IX Ultra platereader images (see section 2.4.6.2). U2OS cells stably expressing ssβ_2AR on 96-well plates were labelled with 0.1 µM SNAPsurface BG-AF488, followed by incubation with vehicle or 10 µM isoprenaline (ISO; in serum-free DMEM/0.1 % BSA) for 1 h at 37 ºC. Cells were washed twice with serum-free DMEM/0.1 % BSA, and then incubated in this media with or without 1 µM S-propanolol for 5 – 60 min at 37 ºC ("wash") before fixation. The pooled granularity data plotted are average intensities per cell, normalised to 10 µM ISO control responses without a wash step. Data are the mean ± S.E.M. of 4 experiments performed in triplicate. Representative images are shown above of cells without isoprenaline stimulation ("No ISO"), stimulated for 1 h with no wash ("ISO 1h"), 1 h wash without propanolol ("ISO 1h recycle 1h no prop") or 1 h wash plus propanolol ("ISO 1h recycle 1h + prop"), as indicated.

of GPCR 120 (GPR120), a non-recycling receptor that exhibited less than 25 % recycling over a 30 min period, assessed using the same

method (Watson *et al.*, 2012). Thus, β_2AR is efficiently recycled to the plasma membrane in the U2OS system used.

The nature of these compartments containing internalised β_2AR and ARRDC2 was analysed by additional co-staining for either transferrin-positive early/recycling endosomes or LAMP1-positive lysosomes. In cells coexpressing β_2AR-GFP and ARRDC2-mCherry, ARRDC2-mCherry localised to late endosomes/lysosomes in the absence of agonist (0.543±0.018, ARRDC2-mCherry colocalisation coefficient with LAMP1, and 0.182±0.011 with transferrin, $P < 0.001$; Figure 5.5 top row, 5.7A), in agreement with previous localisation data (Chapter 3). However, in cells stimulated with isoprenaline (10 μM, 1 h), ARRDC2-mCherry colocalised with transferrin (0.426±0.013) but not with LAMP1 (0.189±0.011, $P < 0.001$; Figure 5.5 bottom row, 5.7A, $n = 4$).

This change in ARRDC2 localisation was also observed when the alternative constructs, ssβ_2AR and ARRDC2-GFP, were used. In these experiments, only colocalisation with transferrin-positive early/recycling endosomes was assessed. Nevertheless, ARRDC2-GFP colocalisation with transferrin was similarly low in unstimulated conditions (0.239±0.027; Figure 5.6 top row, 5.7B). Again, stimulation with isoprenaline (10 μM, 1 h) resulted in a significant increase in ARRDC2 localisation to early/recycling endosomes (0.556±0.050 ARRDC2-GFP colocalisation with transferrin, $P < 0.001$; Figure 5.6 middle row, 5.7B). In this experiment, the effect of 8 h isoprenaline incubation was also assessed. After 8 h stimulation, ARRDC2-GFP colocalisation with transferrin returned to near the level without agonist present (0.301±0.049; Figure 5.6 bottom row, 5.7B). Collectively, these data indicate that ARRDC2 colocalisation with agonist-stimulated, internalised β_2AR involves a change in ARRDC2 distribution, from LAMP1-labelled late endosomes/lysosomes to transferrin-labelled early/recycling endosomes.

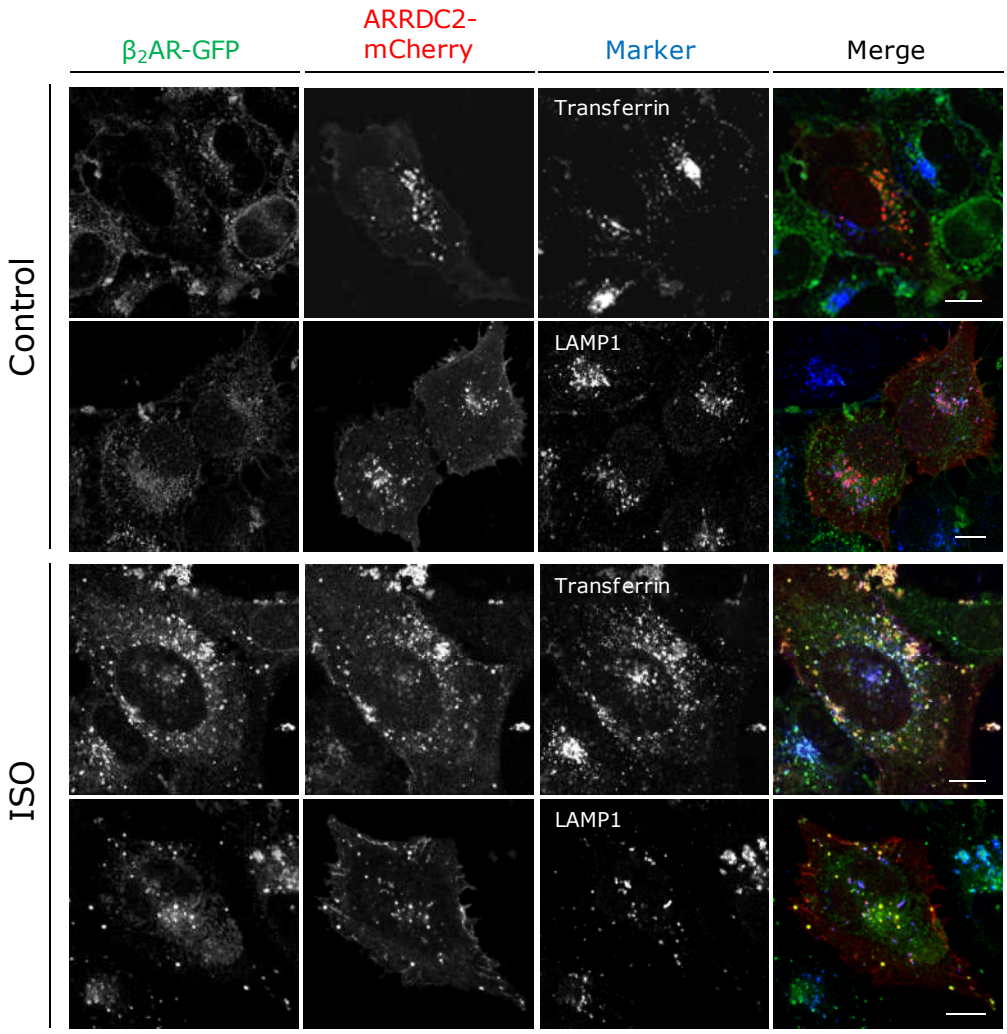

Figure 5.5 ARRDC2 colocalisation with agonist-stimulated β_2AR-GFP involves compartmental redistribution of ARRDC2

Confocal microscopic images of U2OS cells transiently transfected with plasmids expressing β_2AR-GFP plus ARRDC2-mCherry. Cells were treated with isoprenaline (ISO, 10 µM, 1h) or without (Control), as indicated. In addition, cells were co-stained with 250 ng/µl AF-633-conjugated Transferrin for the final 15 min of the plus/minus isoprenaline incubation, or co-immunostained post-fixing using rabbit anti-LAMP1 antibody detected with AF-633-conjugated anti-rabbit secondary antibody, as indicated. Merged images show β_2AR in green, ARRDC2 in red and transferrin/LAMP1 (Marker) in blue. Images are representative of at least three independent experiments. Scale bar = 10 µm.

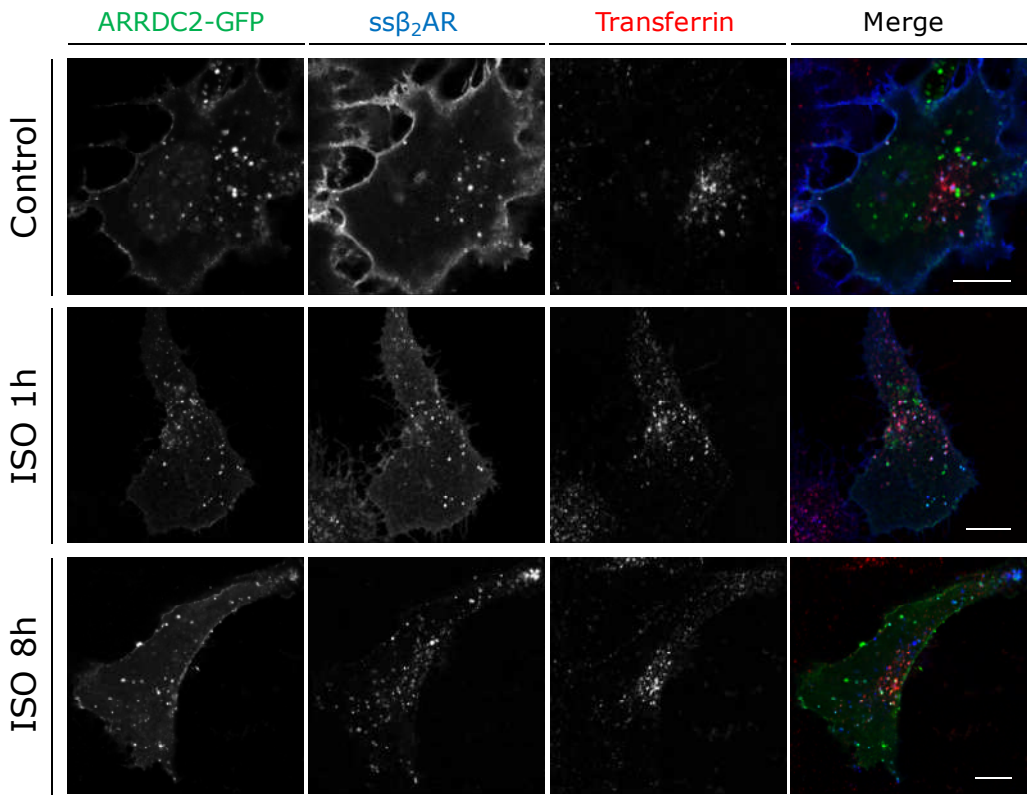

Figure 5.6 ARRDC2 colocalisation with agonist-stimulated ssβ$_2$AR involves compartmental redistribution of ARRDC2

Confocal microscopic images of U2OS cells transiently transfected with plasmids expressing ssβ$_2$AR plus ARRDC2-GFP. Cells were treated with isoprenaline (ISO, 10 µM, 1h or 8h, as indicated) or without (Control), as indicated. In addition, cells were co-stained with 250 ng/µl AF-633-conjugated Transferrin for the final 15 min of the control/ISO incubation. ssβ$_2$AR was visualised by labelling with 0.1 µM SNAPsurface BG-AF546 prior to the experiment. In merged images, ARRDC2 is shown in green, ssβ$_2$AR is in blue and transferrin is in red. Images are representative of at least three independent experiments. Scale bar = 10 µm.

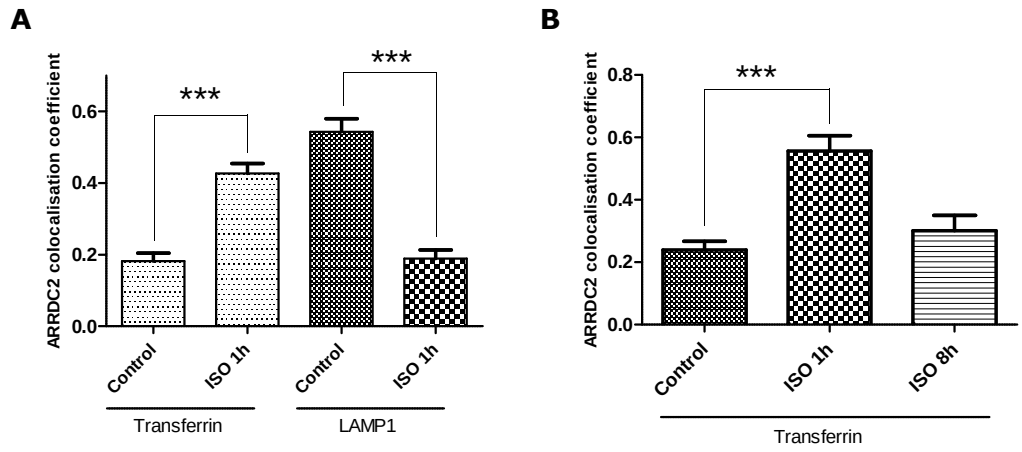

Figure 5.7 Quantification of ARRDC2 compartmental redistribution in response to agonist-stimulated β_2AR internalisation

Colocalisation analysis of confocal images (example images shown in Figures 5.4 and 5.5) from U2OS cells transiently transfected with ARRDC2-mCherry plus β_2AR-GFP **(A)**, or ARRDC2-GFP plus ssβ_2AR **(B)**. Graphs show coefficients for ARRDC2-mCherry colocalisation with AF-633-conjugated Transferrin or anti-LAMP1 antibody labelling (as indicated), in cells treated with isoprenaline (ISO, 10 μM, 1h or 8h, as indicated) or without (Control), as indicated. Colocalisation calculations were performed as described in section 2.4.6.1. Data are mean ± SEM of 6-15 cells analysed for each of ≥ 3 independent experiments. ***P < 0.001, one-way ANOVA plus Tukey post test.

5.2.1.3 Effect of ARRDC2 overexpression upon β_2AR trafficking and signalling

The trafficking profile of β_2AR and its downstream signalling in U2OS cells were compared with or without the exogenous overexpression of ARRDC2-GFP.

The analysis of ARRDC2-GFP colocalisation with transferrin in the presence of ssβ_2AR (treated with or without agonist) has been described above (section 5.2.1.2). In these experiments, colocalisation of internalised ssβ_2AR with transferrin was also assessed (the analysis excluded plasma membrane-localised ssβ_2AR; see section 2.4.6), in singly transfected cells or cells co-transfected with ARRDC2-GFP. In the absence of agonist, ssβ_2AR exhibited a degree of constitutive internalisation (Figure 5.6 top row) which was highly colocalised with transferrin, irrespective of ARRDC2-GFP overexpression (0.737±0.050, 0.759±0.047 ssβ_2AR colocalised with

transferrin in cells with/without ARRDC2-GFP, respectively; Figure 5.6 top row, 5.8). In cells without ARRDC2-GFP, upon 1h isoprenaline stimulation, internalised ssβ_2AR colocalisation with transferrin was moderately lowered, and after 8 h stimulation this decrease was more pronounced (Figure 5.8). This same pattern occurred in cells overexpressing ARRDC2-GFP, such that at each given time-point, no significant difference between cells with or without ARRDC2-GFP was measured. This indicated that overexpression of ARRDC2-GFP had no major effect upon the trafficking of internalised ssβ_2AR. However, the decrease observed in ssβ_2AR colocalisation with transferrin between 0 and 1 h agonist stimulation was less pronounced in cells overexpressing ARRDC2-GFP (the apparent difference was rendered no longer significant; Figure 5.8), hinting that ARRDC2 overexpression may have delayed the exit of ssβ_2AR from transferrin-positive compartments. However, this effect, if any, was extremely subtle and should not be over interpreted given the relatively low sensitivity of measuring receptor trafficking with the colocalisation analysis employed here. It would require further investigation to establish whether this was a genuine effect; that is, whether ARRDC2 has a regulatory role in β_2AR traffic from transferrin-positive early/recycling endosomes, for example using different, potentially more sensitive methods such as knockdown of ARRDC2 expression (see section 5.3.1).

The effect of ARRDC2 overexpression upon the signalling elicited by β_2AR was also investigated. β_2AR couples to the G_s subtype of heterotrimeric G proteins: β_2AR agonist stimulation leads to the dissociation of $G\alpha_s$, which activates adenylyl cyclase resulting in the increased formation of intracellular cAMP and activation of PKA (Kobilka, 1992). U2OS cells express endogenous βARs: stimulation with the broad-spectrum βAR agonist isoprenaline resulted in PKA activation, which was sensitive to the selective β_2AR antagonist, ICI118,551, indicating that U2OS cells express this subtype (Stefan *et al.*, 2007). Hence, a cAMP accumulation assay (see section 2.6) was used to measure the endogenous response to isoprenaline in U2OS cells with or without induced overexpression of ARRDC2-GFP.

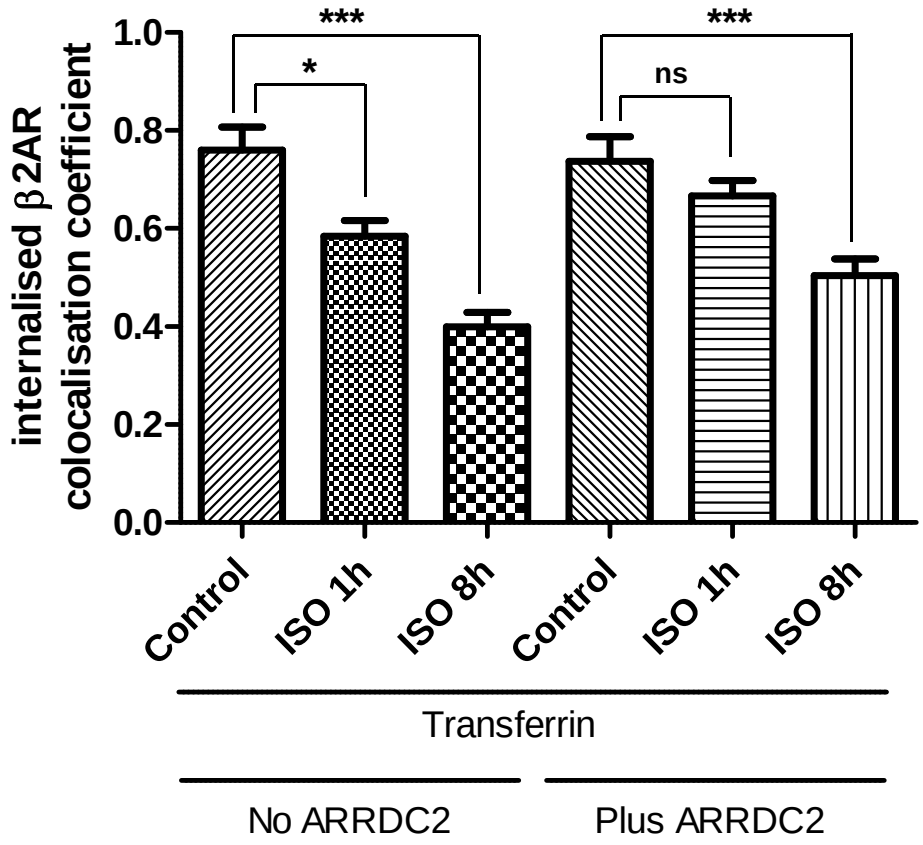

Figure 5.8 Effect of ARRDC2 overexpression upon β_2AR trafficking

Colocalisation analysis of confocal images (representative images shown in Figures 5.3B and 5.5) from U2OS cells transiently transfected with ssβ_2AR alone (No ARRDC2) or in combination with ARRDC2-GFP (Plus ARRDC2). Graph shows coefficients for colocalisation of internalised ssβ_2AR with AF-633-conjugated Transferrin, in cells treated with isoprenaline (ISO, 10 μM, 1h or 8h) or without (Control), as indicated. Colocalisation calculations were performed as described in section 2.4.6.1. Data are mean ± SEM of 6-15 cells analysed for each of ≥ 3 independent experiments. *P < 0.05, ***P < 0.001, ns = not significant; one-way ANOVA plus Tukey post test. No significant differences were measured between "No ARRDC2" versus "Plus ARRDC2" data for each time-point.

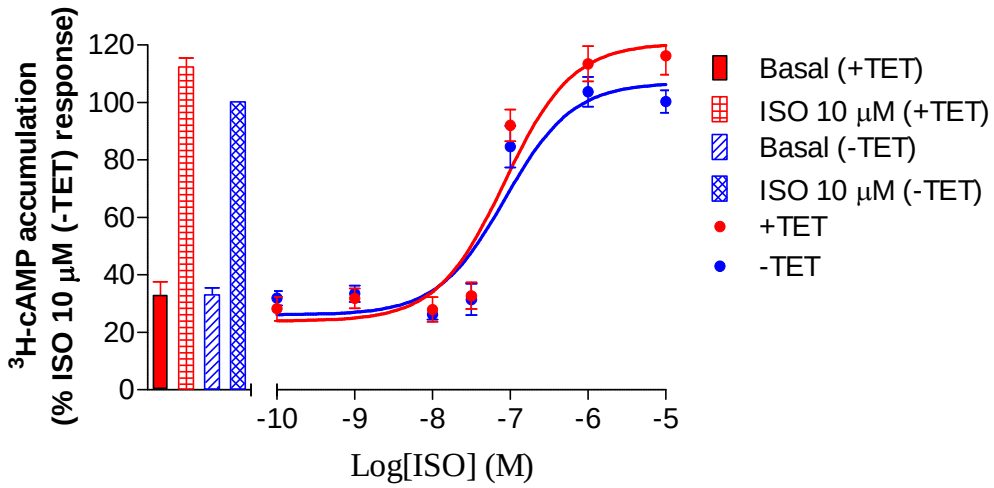

Figure 5.9 Isoprenaline-stimulated [^{3}H]-cAMP accumulation in U2OSTR ARRDC2-GFP cells was unaffected by ARRDC2 overexpression

The columns represent [^{3}H]-cAMP accumulation under basal or maximal stimulation (10 µM isoprenaline for 5 h, ISO) conditions. Data points for each individual experiment were the mean of triplicate determinations; these were expressed as a percentage of the maximal response to ISO in each experiment (without tetracycline), and the means of six independent experiments were pooled to give the data presented here, shown as pooled means ± SEM. No significant effect of tetracycline induction was detected (two-way ANOVA, p = 0.09). –TET, non tetracycline-treated; +TET, overnight tetracycline induction prior to experiment.

In the absence of induced ARRDC2-GFP expression, 5h isoprenaline incubation stimulated cAMP production with a potency (pEC_{50}) of 7.07 ± 0.13 (Figure 5.9). Overexpression of ARRDC2-GFP did not affect isoprenaline-induced cAMP production: the pEC_{50} in the presence of induced ARRDC2-GFP was 7.07 ± 0.12 and, although the maximal response appeared elevated this did not reach statistical significance (Figure 5.9).

5.2.1.4 Detection of associations between β_2AR and arrestins by coimmunoprecipitation

The potential ability of ARRDC2 to interact with β_2AR was investigated using coimmunoprecipitation, using the association of β_2AR with β-arrestin2 as a positive control.

In one approach, coimmunoprecipitation of FLAG-β_2AR-sfGFP (stably expressed) in cells transiently transfected with ARRDC2-HA or β-arrestin2-HA appeared to have been detected (Figure 5.10A). Anti-HA immunoprecipitates blotted with anti-GFP antibody showed bands for IgG heavy and light chain (at ~50 and ~25 kD, respectively) and an unidentified presumed non-specific band at ~100 kD, present in all immunoprecipitates. In addition, a band was detectable at ~75-85 kD, which may represent FLAG-β_2AR-sfGFP (predicted to be ~75 kD). This putative FLAG-β_2AR-sfGFP band was barely detectable in lysates lacking ARRDC2-HA or β-arrestin2-HA cotransfection. In cells transfected with β-arrestin2-HA, the putative FLAG-β_2AR-sfGFP band remained weak in unstimulated conditions, but was markedly stronger when cells were stimulated with isoprenaline for 5 min, whereas stimulation for 1 h resulted in a less pronounced band, suggesting that the band seen may indeed represent FLAG-β_2AR-sfGFP. In cells transfected with ARRDC2-HA, the putative FLAG-β_2AR-sfGFP band was difficult to distinguish from the background level, although it appeared stronger in cells stimulated with isoprenaline for 1 h, suggesting that an interaction with ARRDC2-HA may have been detected.

Experiments in which FLAG-β_2AR or HA-β_2AR were pulled down using the relevant anti-FLAG or anti-HA agarose were also performed. However, immunoblotting for coimmunoprecipitated ARRDC2 or β-arrestin2 fusions did not detect any bands, despite their presence in whole cell lysates (Figure 5.10B,C, top panels). The reverse experiments were also performed, in which ARRDC2 or β-arrestin2 was pulled down and immunoprecipitates were blotted for β_2AR. In general, no β_2AR bands were detected using this approach, possibly hampered by the inability to solubilise β_2AR; β_2AR may have aggregated, resulting in it not entering gels (see Figure 5.10C, middle panel; β_2AR bands seen at the interface between stacking/running gels).

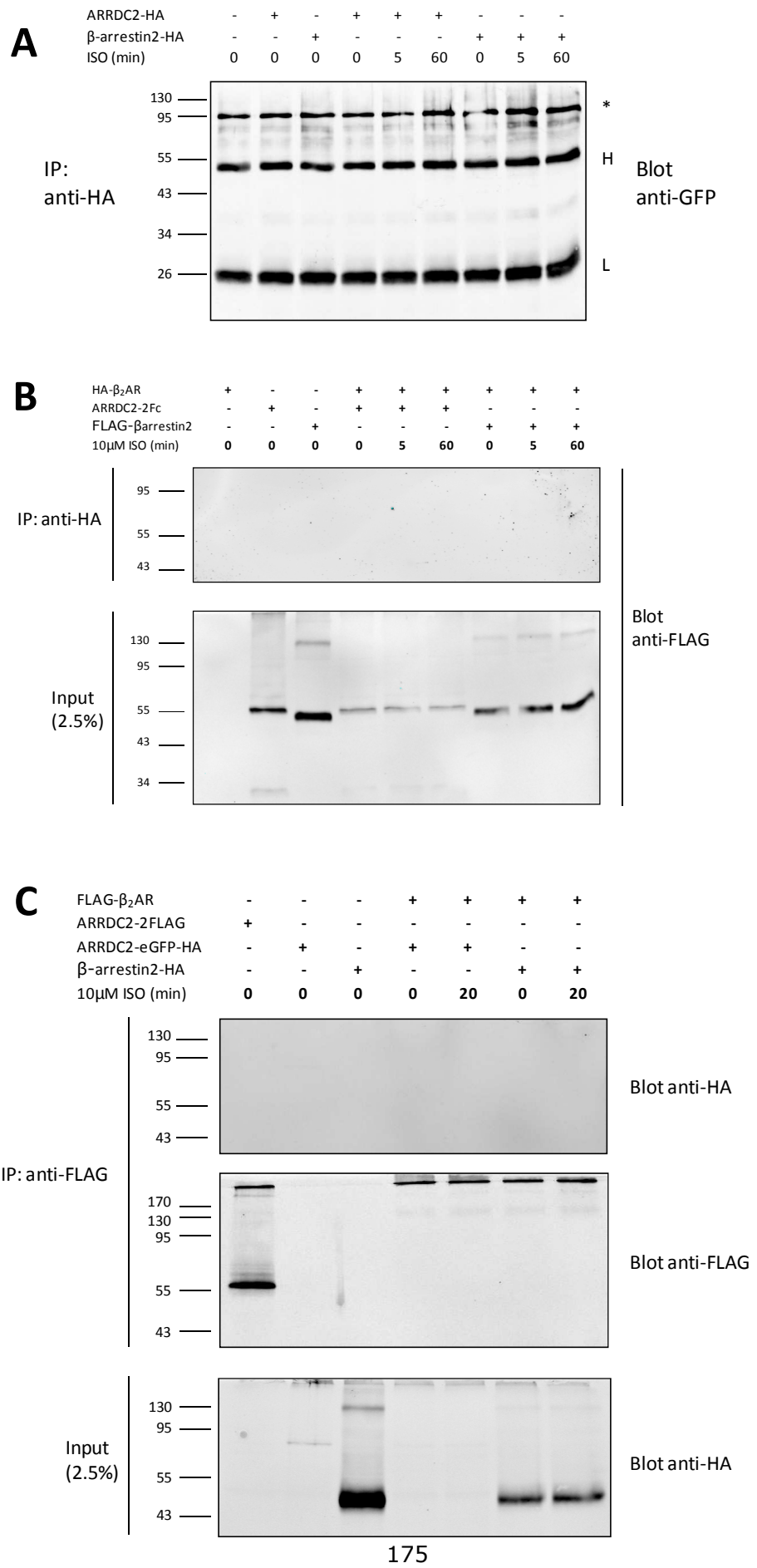
A
ARRDC2-HA - + - + + + - - -
β-arrestin2-HA - - + - - - + + +
ISO (min) 0 0 0 0 5 60 0 5 60
130
95
55
43
34
26
IP: anti-HA
*
H
L
Blot anti-GFP
B
HA-β2AR + - - + + + + + +
ARRDC2-2Fc - + - + + + - - -
FLAG-βarrestin2 - - + - - - + + +
10μM ISO (min) 0 0 0 0 5 60 0 5 60
IP: anti-HA
95
55
43
Input (2.5%)
130
95
55
43
34
Blot anti-FLAG
C
FLAG-β2AR - - - + + + +
ARRDC2-2FLAG + - - - - - -
ARRDC2-eGFP-HA - + - + + - -
β-arrestin2-HA - - + - - + +
10μM ISO (min) 0 0 0 0 20 0 20
IP: anti-FLAG
130
95
55
43
Blot anti-HA
170
130
95
55
43
Blot anti-FLAG
Input (2.5%)
130
95
55
43
Blot anti-HA

Figure 5.10 Attempts to detect interactions between β_2AR and arrestins

U2OS wild-type cells **(B,C)** or cells stably expressing FLAG-β_2AR-sfGFP **(A)** were transiently transfected with plasmids expressing the indicated constructs. Cells were treated 24 h later with/without isoprenaline (ISO, 10 μM) as indicated prior to cell lysis. Cell lysates (2.5% input) and immunoprecipitates (IP) obtained by incubation with anti-HA or anti-FLAG agarose (as indicated) were separated by 12.5% SDS-PAGE and analysed by Western blotting using anti-HA, anti-FLAG or anti-GFP antibodies (all at 1:5000 dilution), as indicated, detected using IRDye 800CW anti-rabbit (HA, FLAG) or anti-mouse (GFP) secondary antibodies (all at 1:10,000). In **(A)**, IgG heavy (H) and light (L) chain are highlighted, as is an unidentified nonspecific band (*). Molecular weight markers are shown in kD.

5.2.2 ARRDC2 regulation of a lysosome-targeted receptor: δOR

5.2.2.1 ARRDC2 colocalises with internalised δOR

The colocalisation of ARRDC2 with δOR was next assessed, using transient transfection of plasmids expressing ARRDC2-GFP and δOR N-terminally fused with SNAP tag (ssδOR). In U2OS cells, ssδOR was largely targeted to the plasma membrane in unstimulated cells, and was internalised into cytoplasmic vesicles upon δOR agonist stimulation (1 μM DADLE, 1 h; Figure 5.11A), as expected from the literature (Trapaidze *et al.*, 1996). Coexpression of ARRDC2-GFP with ssδOR had no obvious effect upon the distribution of either protein in unstimulated conditions (Figure 5.11B top row); ssδOR remained largely at the plasma membrane, whereas ARRDC2-GFP retained the punctate intracellular distribution (with some plasma membrane staining) that has been described (Chapter 3). Agonist stimulation, as seen above, caused ssδOR internalisation into cytoplasmic vesicles. ARRDC2 puncta exhibited a high degree of colocalisation with internalised ssδOR (Figure 5.11B, bottom row).

5.2.2.2 ARRDC2/δOR colocalisation also involves compartmental ARRDC2 redistribution

The nature of the compartments containing internalised δOR and ARRDC2 observed here was analysed by co-staining for transferrin-positive early/recycling endosomes. In cells expressing ARRDC2-GFP alone in the absence of agonist, ARRDC2-GFP targeting was distinct from early/recycling endosomes (0.111±0.022 ARRDC2-GFP colocalised with transferrin; Figure 5.13), in agreement with ARRDC2 localisation to transferrin-negative late endosomes/lysosomes (Chapter 3). However, in cells coexpressing ssδOR and ARRDC2-GFP, ARRDC2-GFP colocalisation with transferrin in the absence of agonist was moderately increased, and was further increased by ssδOR stimulation (0.260±0.032, 0.407±0.025 colocalisation with transferrin without/with 1 μM DADLE, 1 h, respectively, $P < 0.01$, $P < 0.001$; Figure 5.12 and 5.13). Thus, ARRDC2 colocalisation with internalised δOR involves redistribution of ARRDC2 from transferrin-negative to transferrin-positive compartments, as seen for ARRDC2 colocalisation with β_2AR seen above.

5.2.2.3 ARRDC2 influences δOR trafficking

The trafficking profile of δOR in U2OS cells was compared with or without the exogenous overexpression of ARRDC2-GFP. The analysis of ARRDC2-GFP colocalisation with transferrin in the presence of ssδOR (treated with/without agonist) has been described above (section 5.2.2.2). In these experiments, colocalisation of internalised ssδOR with transferrin was also assessed, in singly transfected cells or cells co-transfected with ARRDC2-GFP. In the absence of agonist, ssδOR exhibited a degree of constitutive internalisation (Figure 5.12) which was colocalised to a small degree with transferrin, irrespective of ARRDC2-GFP overexpression (0.310±0.027, 0.340±0.030 ssδOR colocalised with transferrin in cells with/without ARRDC2-GFP, respectively; Figure 5.12 and 5.14). Upon agonist stimulation (1 μM DADLE, 1 h), internalised ssδOR

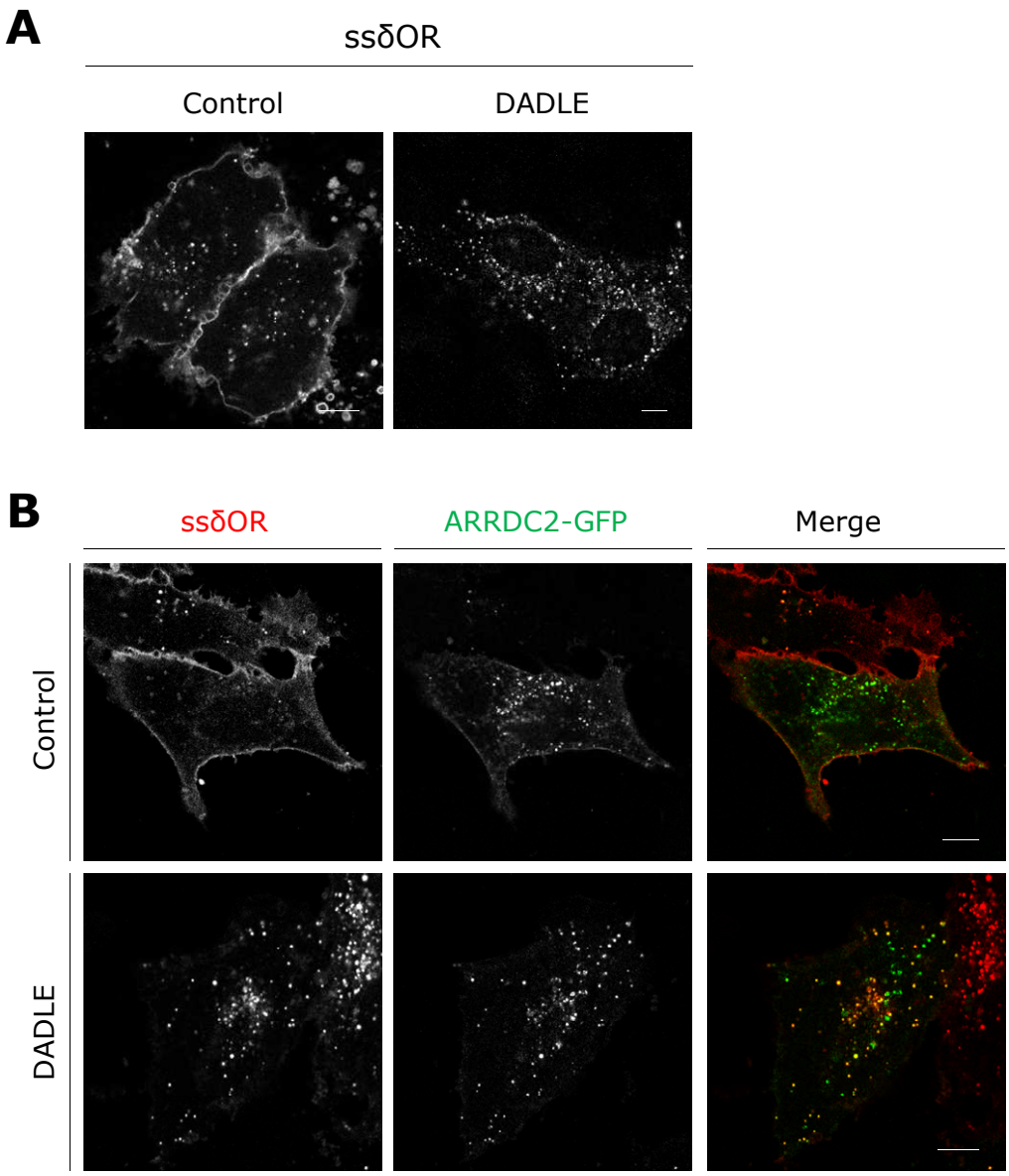

Figure 5.11 ARRDC2 colocalises with agonist-stimulated δOR

Confocal microscopic images of U2OS cells transiently transfected with plasmids expressing ssδOR alone **(A)** or ssδOR plus ARRDC2-GFP **(B)**. Cells were treated with DADLE (1 µM, 1h) or without (Control), as indicated. ssδOR was visualised by labelling with 0.1 µM SNAPsurface BG-AF546 prior to the experiment. In merged images, ssδOR is in red, ARRDC2 is in green. Images are representative of at least three independent experiments. Scale bar = 10 µm.

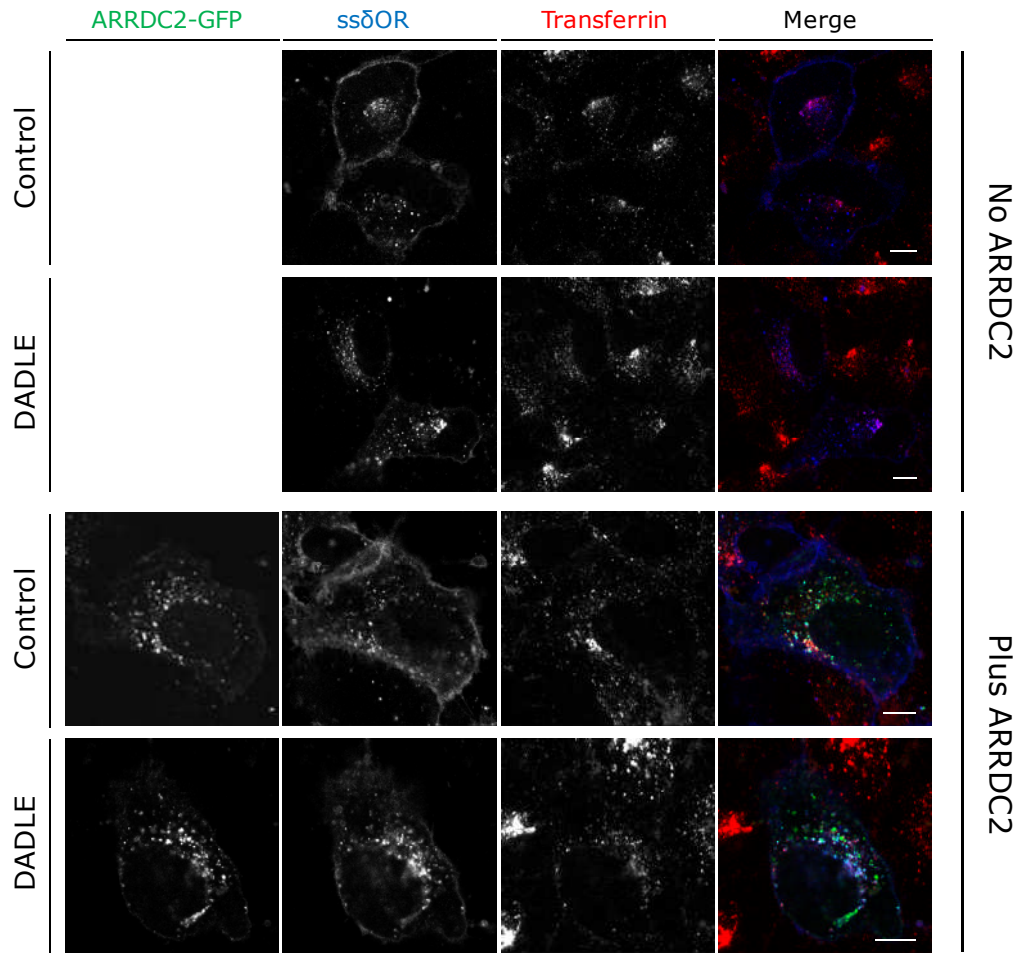

Figure 5.12 ARRDC2 colocalisation with agonist-stimulated δOR involves compartmental redistribution of ARRDC2

Confocal microscopic images of U2OS cells transiently transfected with plasmids expressing ssδOR alone (top two rows) or ssδOR plus ARRDC2-GFP (bottom two rows). Cells were treated with DADLE (1 µM, 1h) or without (Control), as indicated. In addition, cells were co-stained with 250 ng/µl AF-633-conjugated Transferrin for the final 15 min of the plus/minus DADLE incubation. ssδOR was visualised by labelling with 0.1 µM SNAPsurface BG-AF546 prior to the experiment. In merged images, ARRDC2 is in green, ssδOR is in blue, Transferrin is in red. Images are representative of at least three independent experiments. Scale bar = 10 µm.

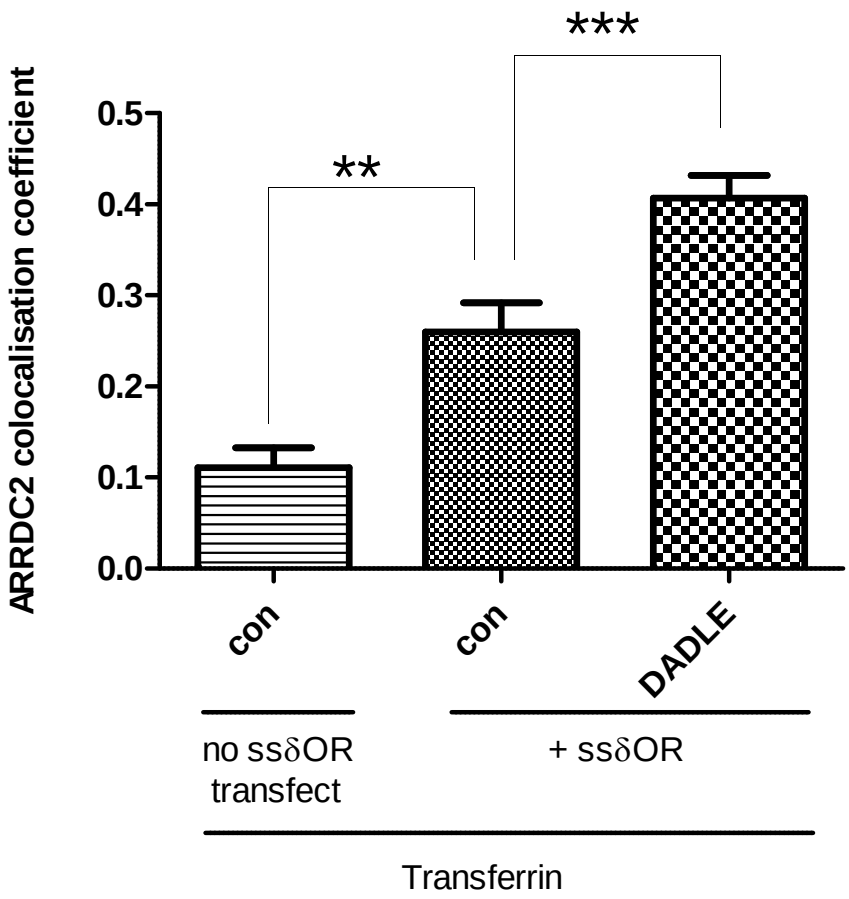

Figure 5.13 Quantification of ARRDC2 compartmental redistribution in response to agonist-stimulated δOR internalisation

Colocalisation analysis of confocal images (example images shown in Figure 5.11) from U2OS cells transiently transfected with ARRDC2-GFP with or without ssδOR, as indicated. Graphs show coefficients for ARRDC2-GFP colocalisation with AF-633-conjugated Transferrin, in cells treated with DADLE (1 μM, 1h) or without (con), as indicated. Colocalisation calculations were performed as described in section 2.4.6.1. Data are mean ± SEM of 6-9 cells analysed for each of 3 independent experiments. $^{**}P < 0.01$, $^{***}P < 0.001$, one-way ANOVA plus Tukey post test.

colocalisation with transferrin was moderately increased; this increase was enhanced by ARRDC2-GFP overexpression (0.461±0.028, 0.618±0.028 ssδOR colocalised with transferrin in cells without/with ARRDC2-GFP, respectively, $P < 0.001$; Figure 5.12 and 5.14). Hence, internalised ssδOR partially localised to transferrin-positive compartments upon 1 h agonist stimulation, and this appeared to be enhanced by ARRDC2-GFP overexpression.

5.2.2.4 ARRDC2 coimmunoprecipitates with δOR

To test for ARRDC2 interaction with δOR, ARRDC2-2FLAG and δOR N-terminally fused with HA (HA-δOR) were transiently expressed either alone or in combination in U2OS cells, followed by anti-HA immunoprecipitation of HA-δOR. Western immunoblotting was then performed on whole cell lysates or immunoprecipitates to assess for the presence of ARRDC2-2FLAG (n = 2).

Expression of HA-δOR in these experiments was unable to be detected by anti-HA immunoblotting of lysates or immunoprecipitates from HA-δOR-transfected cells (not shown).

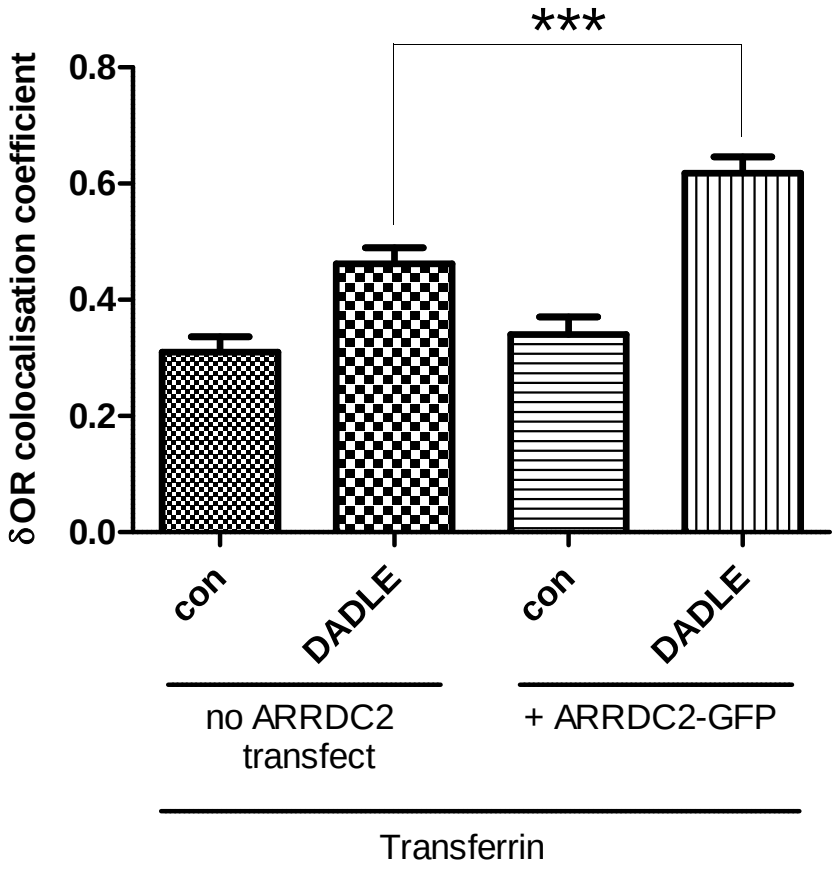

Figure 5.14 ARRDC2 influences δOR trafficking

Colocalisation analysis of confocal images (representative images shown in Figures 5.11) from U2OS cells transiently transfected with ssδOR alone or plus ARRDC2-GFP, as indicated. Graph shows coefficients for colocalisation of internalised ssδOR with AF-633-conjugated Transferrin, in cells treated with DADLE (1 μM, 1h) or without (con), as indicated. Colocalisation calculations were performed as described in section 2.4.6.1. Data are mean ± SEM of 6-11 cells analysed for each of ≥ 3 independent experiments. ***P < 0.001, one-way ANOVA plus Tukey post test.

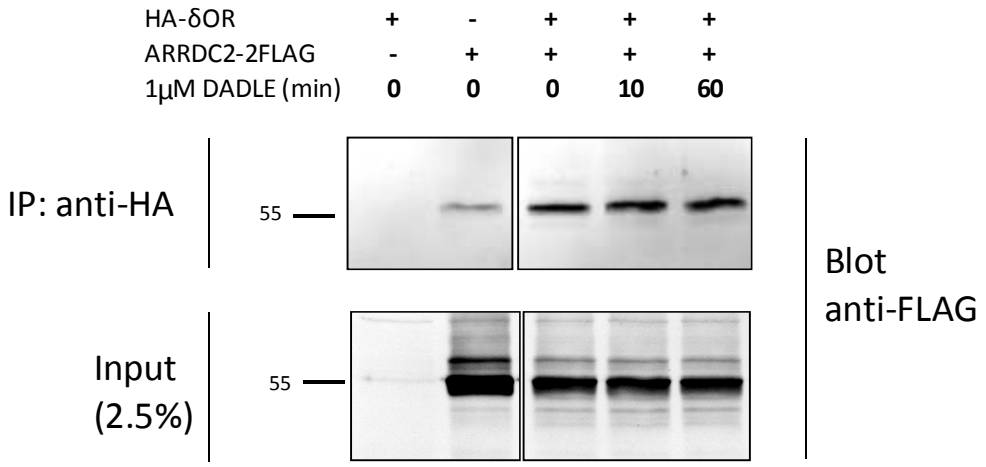

Figure 5.15 Attempts at coimmunoprecipitation of ARRDC2 with δOR

U2OS cells were transiently cotransfected with plasmids expressing HA-δOR and/or ARRDC2-2FLAG. 24 h later cells were treated with/without δOR agonist (DADLE, 1 μM) for the indicated time-points, followed by isolation of cell lysates. Cell lysates (5% input) and immunoprecipitates (IP) obtained by incubation with anti-HA agarose were separated by 12.5% SDS-PAGE and analysed by Western blotting using anti-FLAG antibody (1:5000), detected using IRDye 800CW anti-rabbit secondary antibody (1:10,000). Molecular weight marker is shown on the left in kD.

This may be due to poor exposure of the HA epitope or inefficient transfer of the protein from the gel to nitrocellulose. Nevertheless, coimmunoprecipitation of ARRDC2-2FLAG was observed with HA-δOR (Figure 5.15). The immunoprecipitate derived from cells transfected with ARRDC2-2FLAG alone showed a faint anti-FLAG immunoreactive band at ~55 kD, possibly indicative of background nonspecific ARRDC2-2FLAG binding to the anti-HA agarose, as has been seen previously (see Chapter 4). However, a stronger ARRDC2-2FLAG band was observed for immunoprecipitates obtained from lysates in which HA-δOR was coexpressed with ARRDC2-2FLAG, suggesting that ARRDC2 may interact with δOR. This interaction appeared to be agonist-independent, since δOR stimulation (1 μM DADLE, 10 min or 1 h) had no detectable effect upon the level of ARRDC2-2FLAG coimmunoprecipitation with HA-δOR. This result is preliminary both in the sense that the experiment itself is subject to

some caveats – the relatively high level of background nonspecific binding of ARRDC2-2FLAG to the HA agarose and that no effect of agonist stimulation was detected – and that it is the only approach that was used to support an interaction. Subsequent experiments would look to strengthen the tentative claims made here by providing alternative lines of evidence, for example coimmunoprecipitation in the alternative orientation (pull-down of ARRDC2 and detection of δOR) or biophysical detection using techniques such as BRET or BiFC.

5.2.3 Oligomerisation of arrestin family proteins

5.2.3.1 ARRDC coimmunoprecipitates with itself and with β-arrestins

To assess whether ARRDC2 may form a complex with itself and with β-arrestins, HA- or FLAG-tagged ARRDC2 and/or β-arrestin1/2 were transiently expressed in U2OS cells, followed by anti-HA immunoprecipitation and Western blotting. As has been reported elsewhere (Xu *et al.*, 2008), homo-oligomerisation of β-arrestin2 was observed, as detected by the coimmunoprecipitation of FLAG-β-arrestin2 with β-arrestin2-HA (Figure 5.16A). Interestingly, homo-oligomerisation of ARRDC2 was also detected by coimmunoprecipitation of ARRDC2-2FLAG with ARRDC2-HA (despite weak detection of ARRDC2-HA expression in immunoprecipitates – note that immunoprecipitation was performed using anti-HA agarose; Figure 5.16A,B). Furthermore, the coimmunoprecipitation of ARRDC2-2FLAG with β-arrestin1-HA (despite poor β-arrestin1-HA detection in immunoprecipitates) or β-arrestin2-HA suggested that ARRDC2 may form hetero-oligomers with β-arrestins (Figure 5.16A,B). In the case of ARRDC2-2FLAG coimmunoprecipitation with β-arrestin2-HA, the effect of stimulation of endogenous β_2AR (isoprenaline 10 μM, 10 min) on the interaction was assessed. However, isoprenaline stimulation had no detectable effect on the ARRDC2-β-arrestin2 association (Figure 5.16B).

5.2.3.2 ARRDC2 interacts with β-arrestins in living cells

The relevance of potential ARRDC2-β-arrestin interactions in intact cells was tested by the coexpression of various ARRDC2 and β-arrestin fusion proteins in U2OS cells, followed by confocal imaging.

When expressed alone, β-arrestin1-YFP or β-arrestin2-YFP were diffusely localised throughout the cytoplasm, in addition to a degree of nuclear targeting of β-arrestin1-YFP (Figure 5.17A,B), in agreement with the known targeting of exogenous β-arrestin proteins (Goodman *et al.*, 1996a; Hoeppner *et al.*, 2012). However, upon coexpression of ARRDC2-mCherry, β-arrestin1-YFP became localised to more punctate, vesicular structures that colocalised with ARRDC2-mCherry (the effect was seen to varying degrees; representative images are shown in Figure 5.17B). In contrast, no effect of ARRDC2-mCherry overexpression upon β-arrestin2-YFP distribution was detected (Figure 5.17B). However, the ability of ARRDC2 to interact with β-arrestin2 was also assessed using BiFC (described in section 2.4.7). When expressed alone, β-arrestin2 fused with either N- or C-terminal YFP fragments (vYn-β-arrestin2; β-arrestin2-vYc) did not exhibit any fluorescence when excited at 488 nm (Figure 5.18A). However, coexpression of vYn-β-arrestin2 and β-arrestin2-vYc resulted in the detection of a BiFC signal, with diffuse staining throughout the cytoplasm, indicative of homo-oligomerisation of β-arrestin2 (Figure 5.18B). Similarly, no BiFC signal was detected upon expression of ARRDC2-vYn alone (Figure 5.18A), but BiFC was detected upon coexpression with β-arrestin2-vYc (Figure 5.18C). The ARRDC2-β-arrestin2 BiFC signal was present in a punctate, vesicular pattern throughout the cytoplasm, as well as possibly some plasma membrane staining. Collectively, these data indicate that ARRDC2 can interact with β-arrestins in living cells, and suggest that these interactions may influence β-arrestin subcellular targeting.

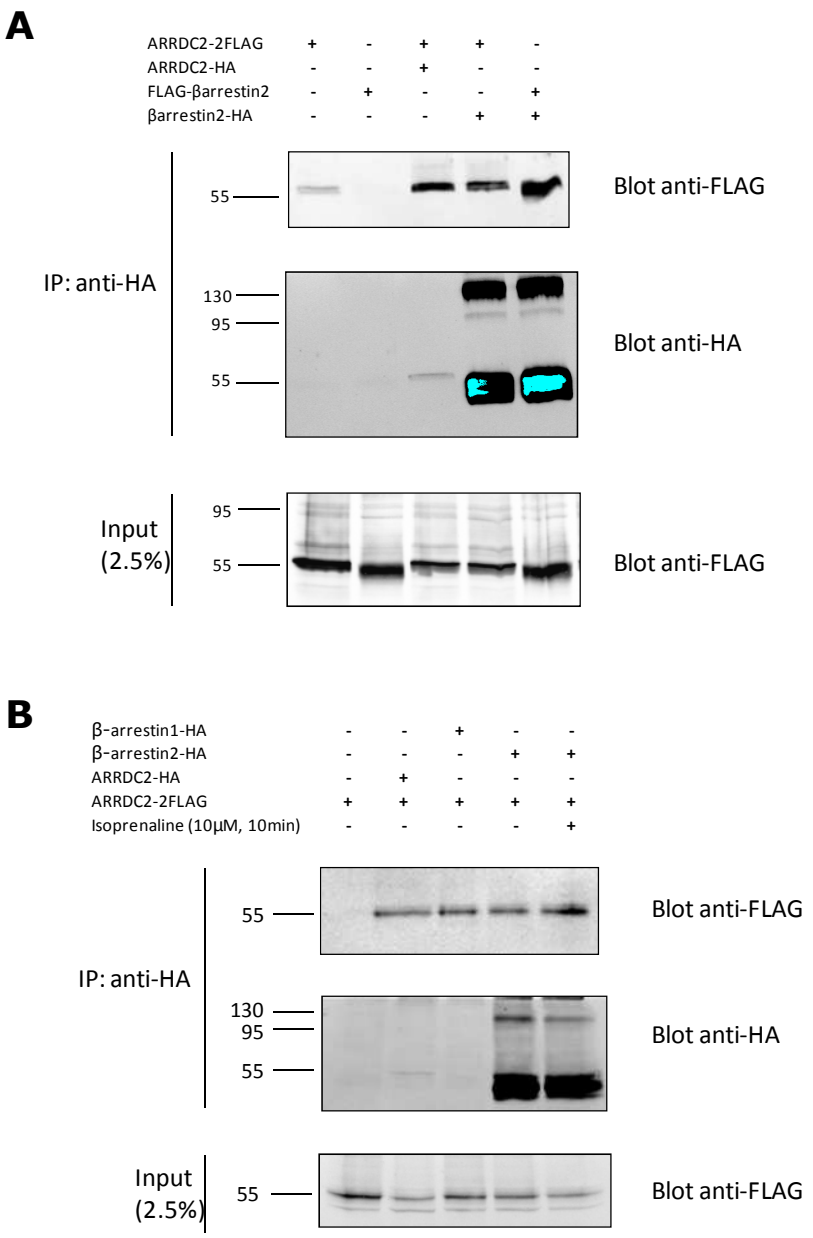

Figure 5.16 ARRDC2 coimmunoprecipitates with itself and with β-arrestins

U2OS cells were transiently transfected with plasmids expressing the indicated protein constructs. In **(B)**, cells were treated 24 h later with/without isoprenaline as indicated prior to cell lysis. Cell lysates (2.5% input) and immunoprecipitates (IP) obtained by incubation with anti-HA agarose were separated by 12.5% SDS-PAGE and analysed by Western blotting using anti-HA or anti-FLAG antibody (both at 1:5000 dilution), as indicated, detected using IRDye 800CW anti-rabbit secondary antibody (1:10,000). In **(A)**, β-arrestin2-HA was expressed at a much higher level than ARRDC2-HA; hence, in order to visualise ARRDC2-HA the exposure used saturated (blue) the β-arrestin2-HA bands. Molecular weight markers are shown on the left in kD.

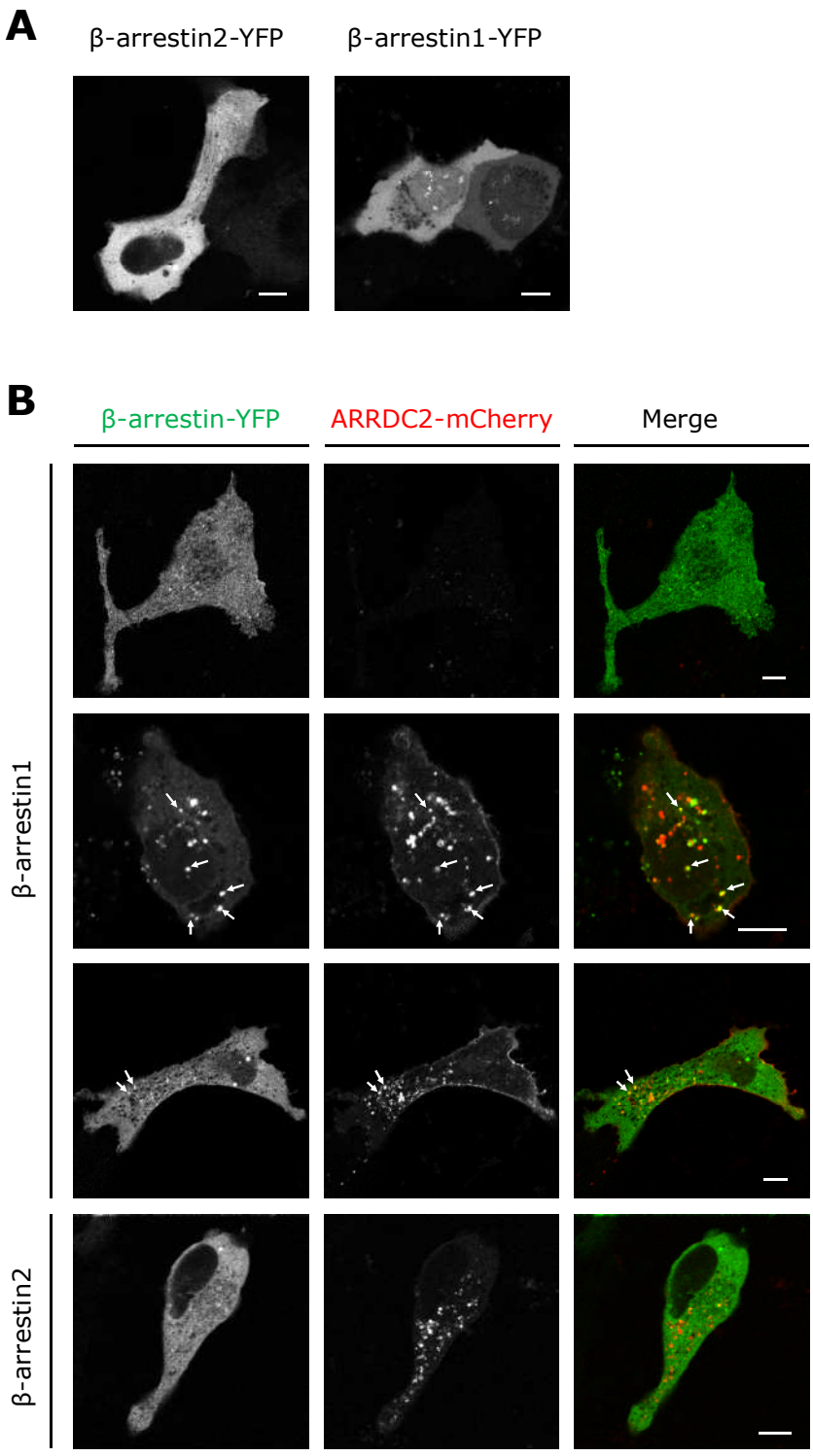

Figure 5.17 ARRDC2 may influence β-arrestin1 subcellular distribution

Confocal microscopic images of U2OS cells transiently transfected with plasmids expressing β-arrestin1/2-YFP alone **(A)** or in combination with ARRDC2-mCherry **(B)**, as indicated. In merged images, ARRDC2 is shown in red; the indicated β-arrestin is in green. Colocalisation of β-arrestin1-YFP/ARRDC2-mCherry is highlighted with arrows. Images are representative of two independent experiments. Scale bar = 10 μm.

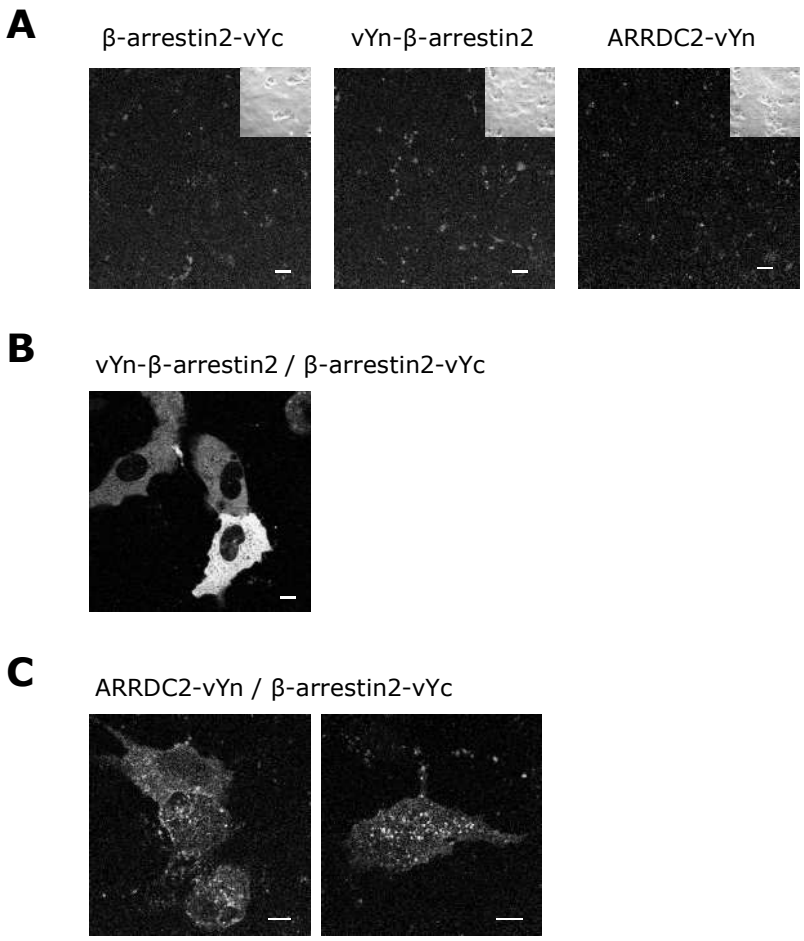

Figure 5.18 Detection of BiFC between ARRDC2 and β-arrestin2

Confocal microscopic images of U2OS cells transiently transfected with plasmids expressing β-arrestin2-vYc, vYn-β-arrestin2 or ARRDC2-vYn alone **(A)** or in combination **(B,C)**, as indicated. vYn and vYc represent N- and C-terminal fragments of venus YFP, which alone are not fluorescent. When brought into proximity by their fusion to interacting protein partners vYn/vYc refold to produce a fluorescent BiFC signal. The presence of cells is indicated in **(A)** by insets showing phase images. Scale bar = 10 μm.

5.3 Discussion

The aim of the current chapter was to investigate a potential role for ARRDC2 in GPCR regulation. The data presented attest to this role, showing that ARRDC2 is specifically recruited to GPCRs (indicated by quantitative colocalisation), can associate with GPCRs and may regulate them via the ability to oligomerise with β-arrestins.

5.3.1 ARRDC2: a novel GPCR regulator?

Confocal microscopy revealed that fluorescent protein-tagged ARRDC2 colocalises with agonist-stimulated, internalised GPCRs: the prototypic recycling receptor, β_2AR and the lysosome-targeted δOR. In each case, colocalisation involved a compartmental redistribution of ARRDC2 to early/recycling endosomes. This suggests that ARRDC2 colocalisation with each GPCR represents a specific event. It could be that ARRDC2 is recruited in a retrograde fashion, redistributing from its native compartments (late endosomes/lysosomes) to compartments containing internalised β_2AR or δOR (early/recycling endosomes). Alternatively, given the dynamic nature of ARRDC2 localisation within the endocytic system (Chapter 3), it is possible that ARRDC2 associates with GPCRs at an earlier stage (plasma membrane or early endosomes, for example), an association that prevents ARRDC2 from reaching the lysosome, resulting in the overall 'redistribution' observed. Detailed microscopic experiments would be required to discriminate these possibilities, for example using ARRDC2 fused with a photoactivatable fluorescent protein in order to follow ARRDC2 transport from and to specific compartments in living cells, and TIRF microscopy to detect potential plasma membrane recruitment events. A potential subtle effect of ARRDC2 overexpression upon β_2AR intracellular trafficking was observed. ARRDC2 overexpression also altered δOR trafficking, and an association between ARRDC2 and δOR was detected by coimmunoprecipitation.

ARRDC2 overexpression did not appear to have any effect upon β_2AR signalling, indicated by measuring isoprenaline-stimulated cAMP production. Due to the constraints of the current project, only a simple concentration response approach was employed. It is worth noting that the information gathered from this is limited; it only indicates the effect of ARRDC2 overexpression on the total cAMP produced over 5 h. It may be that ARRDC2 has a more time-dependent effect, for example downregulating β_2AR signalling via increased β_2AR degradation upon prolonged receptor activation. This effect would not be detected using the method employed here;

more detailed time-courses of receptor signalling, potentially including a pre-stimulatory period (e.g. 24 h pre-incubation with agonist in the presence/absence of ARRDC2 to detect an effect on long-term downregulation), would be required to measure such an effect. Moreover, the approach used is limited by the fact that only one signalling output (cAMP production) was measured. It is possible that ARRDC2 has a direct impact on particular aspects of β_2AR signal transduction, for example the ERK/MAPK cascade, which has been previously noted to have an arrestin (β-arrestin) component (section 1.3.1). Thus, it would also be informative to measure ERK activation (for example by immunoblotting for phosphorylated ERK) promoted by β_2AR in the presence or absence of overexpressed ARRDC2.

A low level of constitutive β_2AR internalisation was detected, and this was highly colocalised with transferrin-labelled compartments, as expected from the known rapid recycling itinerary for β_2AR. Over more prolonged periods of agonist stimulation β_2AR is gradually delivered to the lysosomes for degradation (Shenoy *et al.*, 2008). This gradual β_2AR lysosomal delivery was detected here as a sequential moderate decrease in β_2AR colocalisation with transferrin as the duration of agonist stimulation increased from 1 h to 8 h (although note that a concomitant increase in colocalisation, for example, with lysosomal markers, was not tested). ARRDC2 colocalisation with transferrin was monitored over the same time points and, following the initial increase from unstimulated to 1 h agonist treatment (indicative of ARRDC2 recruitment), a decrease in transferrin colocalisation was also observed at the 8 h time point, potentially reflecting the delivery of β_2AR-associated ARRDC2 to lysosomes. Despite these observations no prominent, sustained effect of ARRDC2 overexpression on β_2AR trafficking was detected, although ARRDC2 overexpression did appear to delay the observed agonist-induced decrease in ssβ_2AR colocalisation with transferrin. The lack of a marked effect of ARRDC2 overexpression on β_2AR trafficking may be due to insufficient sensitivity of the system used – quantification of colocalisation with transferrin, a broad marker for

the recycling pathway – to detect potential subtle changes in receptor trafficking. Moreover, the approach of overexpressing wild-type ARRDC2 may also not be the most powerful method possible to detect a role for the protein in question. Indeed, in a recent report on the role of ARRDC3 in β_2AR regulation, overexpression of wild-type ARRDC3 had no detectable effect in the assay used (immunoblot analysis of β_2AR degradation); an effect was only detected when a PPxY mutant ARRDC3 was overexpressed, or ARRDC3 expression was depleted using siRNA (Nabhan *et al.*, 2010). Thus, more sensitive experiments (e.g. detection of β_2AR degradation and ubiquitination) and alternative lines of evidence (e.g. ARRDC2 siRNA) would be required to convincingly assess the potential role of ARRDC2 in β_2AR trafficking. Similarly, the use of siRNA may yet reveal a role for ARRDC2 in β_2AR signal transduction, which was not detected using ARRDC2 wild-type overexpression. These experiments were not performed in the current project due to limitations on time and approaches available; assessing β_2AR degradation/ubiquitination would likely require β_2AR immunoprecipitation which, as described below, proved difficult; ARRDC2 siRNA would require the detection of endogenous ARRDC2 expression, which proved unsuccessful in the cell lines used here (U2OS, HEK-293).

δOR also exhibited a low level of constitutive internalisation in the system used. This was largely distinct from transferrin compartments, which may reflect the efficient targeting of δOR to the degradative pathway, although colocalisation with lysosomal markers was not tested. Agonist-stimulated internalisation resulted in a moderate increase in colocalisation of internalised δOR with transferrin. Despite its presumed efficient targeting to lysosomes, δOR endocytosis and early trafficking is via the same transferrin-positive pathway as β_2AR (Tsao *et al.*, 2000). Hence, it is not necessarily surprising that partial colocalisation with transferrin-positive compartments is detected after 1 h agonist stimulation. Overexpression of wild-type ARRDC2 increased the degree of agonist-stimulated δOR colocalisation with transferrin. The

implications of this result are unclear: it may reflect a positive role for ARRDC2 in the endocytosis or early trafficking stages of δOR. However, it would be important to further dissect these possibilities by performing additional experiments, as has been described for β_2AR above.

Coimmunoprecipitation indicated that ARRDC2 associates with δOR, although this does not confirm a direct interaction (ARRDC2 may associate indirectly via oligomerisation with other arrestins; see below). ARRDC2 association with δOR was detected in the absence of agonist stimulation, and stimulation for 10 min or 1 h did not alter the level of coimmunoprecipitation, suggesting that ARRDC2 may constitutively bind δOR. This is in contrast to the reported agonist-dependent interaction of ARRDC3 with β_2AR (Nabhan *et al.*, 2010), although in a subsequent report significant interactions with β_2AR were detected for ARRDC1, ARRDC3 and ARRDC4 in the absence of agonist stimulation (Patwari *et al.*, 2011). Constitutive activity of several GPCRs has been reported, producing low levels of agonist-independent endocytosis and recycling of receptors that may be dependent upon constitutive association with β-arrestins (Halls *et al.*, 2010; Pampillo *et al.*, 2009; Pediani *et al.*, 2005; Terrillon *et al.*, 2004a; Walwyn *et al.*, 2007). These include the mu-opioid receptor (μOR) (Walwyn *et al.*, 2007), which is known to heterodimerise with δOR (Snook *et al.*, 2006). Thus, it is possible that ARRDC2 may constitutively associate with GPCRs, such as δOR, and that these associations are important for agonist-independent receptor regulation. This would imply that ARRDC2 may be recruited to GPCRs at the plasma membrane. Nevertheless, the agonist-stimulated recruitment of ARRDC2 to δOR (potentially in endosomes), as detected by compartmental ARRDC2 redistribution, suggests that there may yet be an activation-dependent component to the ARRDC2 association with δOR, as is generally thought to be the case for β-arrestin-GPCR interactions.

This result adds to the small amount of data that suggest α-arrestins are capable of binding GPCRs. The coimmunoprecipitation of overexpressed proteins that has been used thus far in these

studies has the potential to enhance the detection of such interactions. Agonist dependency (as for the ARRDC3 and β_2AR association) would be one indication of the potential physiological relevance of the interaction. However, it is important, especially in the absence of an agonist-dependent association, to further characterise ARRDC associations with GPCRs, for example using GST pull-downs to demonstrate direct binding, and through the coimmunoprecipitation of endogenous proteins to confirm that the results obtained from overexpressed systems are relevant to the native proteins.

The potential association between ARRDC2 and β_2AR was also investigated using coimmunoprecipitation, with the known association between β_2AR and β-arrestin2 as a positive control. However, this approach failed to detect a clear association with ARRDC2. It also largely did not detect an association with β-arrestin2, suggesting that methodological limitations may have hampered the detection of a potential ARRDC2 interaction, rather than the necessary lack of an interaction. The only experiment that appeared to detect an interaction between β-arrestin2 and β_2AR was that using U2OS cells stably expressing FLAG-β_2AR-sfGFP (Figure 5.10A). Even in this case pull-down with β-arrestin2-HA was not definitive and hampered by presumed background binding of FLAG-β_2AR-sfGFP to the HA agarose and the presence of high molecular weight unidentified band(s). Nonetheless, an interaction with β-arrestin2 was detected upon agonist stimulation (10 μM isoprenaline, 5 min), and a potential interaction was detectable with ARRDC2 after 1 h agonist stimulation. However, the clarity of this result was poor, and it is notable that no comparison was able to be made between the apparent FLAG-β_2AR-sfGFP present in immunoprecipitates and the amount present in the initial lysates, since anti-FLAG or anti-GFP immunoblotting of whole cell lysates failed to detect FLAG-β_2AR-sfGFP (not shown). The inability to detect β_2AR and the lack of clear positive data may stem from the fact that β_2AR appears to form insoluble aggregates that are excluded from entering gels (see Figure 5.10C, middle panel). This issue was

addressed through the use of a variety of solubilisation conditions (using sample buffer ± β-mercaptoethanol; incubating samples at room temperature, 37 ºC or 80 ºC for 3 – 30 min prior to gel loading) but none of the conditions used improved the ability of β_2AR to enter gels. Thus, from these data it is unclear whether ARRDC2 is capable of interacting with β_2AR. To answer this question it will be necessary to further optimise conditions for β_2AR coimmunoprecipitations, for example using defined cell types and conditions that are known to allow the immunodetection and immunoprecipitation of β_2AR (Xiao *et al.*, 2011).

The observed recruitment of ARRDC2 to internalised β_2AR or δOR is similar to that seen for ARRDC3 recruitment to β_2AR (Nabhan *et al.*, 2010). It is worth considering whether ARRDC2 and ARRDC3 may act similarly, since they are the two closest mammalian α-arrestin homologues (protein sequence similarity = 69%). ARRDC3 was reported as targeting largely to the plasma membrane in unstimulated cells (in contrast to the ARRDC3 distribution seen here; see Chapter 3). Upon agonist stimulation of β_2AR, ARRDC3 became localised to intracellular puncta that colocalised with internalised β_2AR, as was seen here for ARRDC2. However, in both cases, the spatiotemporal characteristics of ARRDC recruitment to GPCR are unknown. Since ARRDC3 localised to the plasma membrane irrespective of agonist stimulation, it is unclear whether ARRDC3 recruitment to β_2AR occurred at the plasma membrane or in internalised vesicular compartments. The time-scale used for agonist-dependent detection of ARRDC3 association with β_2AR by coimmunoprecipitation (20 min) was too long to discriminate these possibilities (Nabhan *et al.*, 2010). Similarly, ARRDC2 partially localised to the plasma membrane irrespective of GPCR stimulation, and enhanced ARRDC2 plasma membrane targeting upon agonist stimulation (e.g. 5 min β_2AR stimulation with isoprenaline) was unable to be detected using confocal microscopy (data not shown). Thus, whether the recruitment of ARRDC2 to GPCRs occurs at the plasma membrane or in intracellular vesicles remains unknown. Experiments designed to more sensitively define the spatial (e.g.

TIRF at the plasma membrane) and temporal (e.g. agonist-stimulated BRET between receptor and ARRDC2) parameters involved would be required to answer this question.

A major function of the reported ARRDC3 interaction with β_2AR was to recruit NEDD4 to ubiquitinate the receptor, targeting it for lysosomal degradation (Nabhan *et al.*, 2010). ARRDC2 also acts as a NEDD4 family ligase adaptor (Chapter 4; includes ARRDC2 ability to associate with NEDD4, the ligase responsible for β_2AR ubiquitination); therefore, it is hypothesised that ARRDC2 could similarly recruit ligase(s) to this and/or other GPCRs. This could be tested by employing the PPxY mutant ARRDC2 (ARRDC2ΔΔ) in place of wild-type ARRDC2 in the experiments performed here, for example examining its effect upon receptor trafficking and signalling. However, there is a difference between the role reported for ARRDC3 and that observed here for ARRDC2. Whilst ARRDC3 promotes lysosomal targeting of β_2AR, the data presented here suggest that ARRDC2 overexpression inhibits β_2AR or δOR lysosomal trafficking. Thus, it is possible that ARRDC2 differentially affects receptor trafficking, potentially by slowing the receptor at a rate limiting step in lysosomal trafficking (for example during the ESCRT-mediated process) and/or by stimulating retrograde sorting or retrieval from degradation, in contrast to ARRDC3.

5.3.2 ARRDC2: extending the scope of arrestin family oligomerisation?

The ability of ARRDC2 to interact with itself and with β-arrestin1/2 was demonstrated using coimmunoprecipitation. Moreover, microscopy indicated that ARRDC2 overexpression can drive β-arrestin1 from a diffuse pattern to intracellular puncta that colocalise with ARRDC2, and a BiFC interaction between ARRDC2 and β-arrestin2 was detected, also with a punctate intracellular pattern. Thus, associations between ARRDC2 and β-arrestins may influence their function in intact cells.

The propensity of β-arrestins to homo- and hetero-oligomerise has been documented, although the function of complexes remains unclear (see section 5.1). The ability of α-arrestins to oligomerise is less well known; the only known report to date is of ARRDC1 homo-oligomerisation, detected by coimmunoprecipitation of overexpressed proteins (Nabhan *et al.*, 2012). Data presented here show that this ability extends to ARRDC2, which can homo- and hetero-oligomerise with arrestin family members. The data supporting this ability include the detection of a BiFC signal between ARRDC2 and β-arrestin2. BiFC has the limitation that it produces an irreversible association, which may interfere with the function of protein partners whose interaction would otherwise be transient (Kerppola, 2008; Rose *et al.*, 2010). Nevertheless, an advantage is that BiFC specifically identifies the protein-protein complex in question. In the case of the ARRDC2-β-arrestin2 association the BiFC signal was localised to intracellular puncta. Although in the standard colocalisation experiments (ARRDC2 and β-arrestin2 tagged with full-length fluorescent proteins) ARRDC2 did not appear to cause β-arrestin2 redistribution (this was only observed for β-arrestin1), ARRDC2 may still interact with β-arrestin2 in similar intracellular compartments. This conclusion is aided by the use of BiFC which specifically identified ARRDC2-β-arrestin2 complexes, as opposed to simple coexpression of fluorescent protein-tagged proteins, where differences in the relative expression levels of the two partners may have precluded observation of any redistribution.

Future experiments would ideally investigate the mechanism of ARRDC2 interaction with β-arrestins, as well as the role that these interactions play. Several amino acid residues in the polar core of β-arrestin2 have been shown to contribute to its self-association, including Lys^{285} and Arg^{286}; mutation of these residues substantially reduced the detection of FRET between β-arrestin2 pairs and produced weaker coimmunoprecipitations (Xu *et al.*, 2008). Similarly, IP_6 has been found to promote the self-association of β-arrestins (Hanson *et al.*, 2007), and binding sites for IP_6 on β-arrestin2 have been mapped (these include residues Lys^{233}, Arg^{237}

and Lys^{251}) (Gaidarov *et al.*, 1999). It would be informative to test whether mutation of the residues mentioned have an effect upon β-arrestin2 association with ARRDC2, which would suggest that a similar mechanism of interaction may be involved. Although some of the key polar core residues are conserved in ARRDC proteins, the residues mentioned (Lys^{285}, Arg^{286}, Lys^{233}, Arg^{237} and Lys^{251} in β-arrestin2) are not (Figure 1.2). Hence, it is not necessarily possible to produce targeted mutations in ARRDC2 that correspond to those in β-arrestins and analyse their effect on oligomerisation; it is suggested that first assessing the impact of more global ARRDC2 alterations (N- or C-terminal truncations, for example) would be an approach to investigating the ARRDC2 regions involved.

An approach to probe the potential role of arrestin hetero-oligomers could be to assess the ability of GPCRs to recruit ARRDC2 (using colocalisation and immunoprecipitation) in the absence of β-arrestins. Knockout mouse embryonic fibroblasts (MEFs) lacking β-arrestins (Vines *et al.*, 2003) would be an ideal system within which to perform these experiments. Conversely, it would be highly desirable to demonstrate that ARRDCs such as ARRDC2 are important for β-arrestin functions. For example, are canonical β-arrestin functions such as GPCR desensitisation and internalisation influenced by ARRDCs? Perhaps most likely (see section 6.5), is the purported ability of β-arrestins to scaffold NEDD4 family ubiquitin ligases (Bhandari *et al.*, 2007; Shenoy *et al.*, 2008) actually provided by their dimerisation partners, the ARRDCs? These questions could be answered by manipulating ARRDCs (e.g. by siRNA knockdown or overexpression of mutants) and examining the effect upon the β-arrestin functions described.

In conclusion, the identification of ARRDC2 as a NEDD4 family ubiquitin ligase adaptor within the endocytic system was described in Chapters 3 and 4. The inevitable next question was what is the relevance of such observations; that is, what cargo(s) might ARRDC2 regulate in its role as ligase adaptor? Given the data presented here, it seems likely that ARRDC2 is involved in GPCR

regulation in a similar vein to other newly identified α-arrestin proteins, in particular ARRDC3. This is supported by the specific recruitment of ARRDC2 to GPCRs under stimulated conditions, potentially involving a physical association, the impact of ARRDC2 upon the intracellular trafficking itinerary of these GPCRs and the ability of ARRDC2 to associate with and potentially modulate the function of the canonical GPCR regulators, the β-arrestins.

6 Conclusions and perspectives

6.1 Overview

The number of mammalian proteins harbouring a conserved arrestin β-sandwich structure has been extended beyond the classical visual and β-arrestins. Visual/β-arrestin homologues have been identified that represent earlier, ancestral proteins from which β-arrestins evolved, and have hence been designated as α-arrestins (Alvarez, 2008). Much recent investigation has attempted to determine whether the function of β-arrestins as flexible adaptors – in particular for the signalling and trafficking of GPCRs – is conserved in α-arrestins. Work on α-arrestin orthologues in lower eukaryotes clearly indicates conserved roles for the wider arrestin family as adaptors for intracellular cargo trafficking. The emerging pattern is that α-arrestins scaffold WW domain-containing E3 ubiquitin ligases for their recruitment to plasma membrane cargo, in order to mediate cargo ubiquitination and endocytosis/downregulation (Figure 1.4). In one case in fungi, the α-arrestin cargo was a seven-transmembrane domain receptor (Herranz *et al.*, 2005). However, the majority of specific cargoes regulated by yeast/fungal α-arrestins are transporters that are structurally unrelated to GPCRs; indeed, endocytic downregulation of the sole yeast seven-transmembrane domain receptor, Ste2, was unaffected by genetic knockout of the α-arrestin ART1, although this may be explained by cargo selectivity of the specific α-arrestin that was targeted (Lin *et al.*, 2008).

Thus, the question has remained: do mammalian α-arrestins interact with and regulate GPCRs, or is this a newly evolved function unique to β-arrestins? Recent data suggest that the ability to scaffold ubiquitin ligases is retained by most mammalian α-arrestins, and this appears to enable them to direct diverse vesicular trafficking processes. There are a few emerging reports that human α-arrestins can bind GPCRs, and hints that the ability of α-arrestins

to act as adaptors may impinge upon GPCR signalling and trafficking (section 1.4.3). Within this context, the current study supports a role for human α-arrestins (specifically ARRDCs) as endocytic ubiquitin ligase adaptors. Specifically, ARRDC2 is reported as an endo-lysosomal protein targeted predominantly to the plasma membrane and late endosomes/lysosomes. In agreement with data elsewhere (Rauch *et al.*, 2011), ARRDC2 interactions with several members of the NEDD4 family of WW domain-containing E3 ubiquitin ligases were detected. For the first time, the mechanism of these interactions was shown to critically involve ARRDC2 C-terminal PPxY motifs, in agreement with that described for multiple other α-arrestin-ligase interactions. Moreover, ARRDC2 overexpression altered the subcellular targeting of several NEDD4 family ligases, suggesting that interaction with ARRDC2 may serve to determine the ligase subcellular site of action. The question of ARRDC interaction with GPCRs was also addressed: for the first time, a putative interaction of ARRDC2 with a GPCR, the δOR, was detected using coimmunoprecipitation. ARRDC2 was specifically recruited to endosomes containing agonist-stimulated, internalised δOR and analysis of δOR trafficking using quantification of confocal images suggested that ARRDC2 may influence δOR intracellular trafficking. ARRDC2 was also specifically recruited to another prototypical GPCR, the β_2AR, and a subtle effect of ARRDC2 overexpression upon β_2AR trafficking was detected, although no effect upon β_2AR signalling was observed. Additionally, indirect evidence for the involvement of ARRDC2 in GPCR processes came from the observed ability of ARRDC2 to hetero-oligomerise with various arrestin family members. Coimmunoprecipitation, coexpression studies and BiFC collectively indicated that ARRDC2 can interact with itself and with β-arrestins, and that these interactions may influence the subcellular targeting of the interaction partners in question.

In summary, the current study has uncovered significant novel information regarding an α-arrestin that has been largely unstudied. This includes the identification of ARRDC2 as a wide-spectrum

NEDD4 family ubiquitin ligase adaptor and the clarification of the mechanism (PPxY motif) involved, and the novel demonstration that ARRDC2 can associate with and influence the trafficking of GPCRs. The next section will consider the approaches used to garner such information, commenting on their advantages and limitations, and will highlight possible alternatives.

6.2 Experimental approach: recombinant versus native systems

The general approach used here was of exogenous expression of proteins fused with tags (epitopes or fluorescent proteins) in cultured cell lines. A distinct advantage of this is that direct comparisons can be made between protein variants – such as wild-type versus mutant ARRDC2 – overexpressed in the same system. Moreover, conclusions based on such experiments are generally borne out in the native system, as has been the case, for example, in the emerging picture of the β-arrestins over the past twenty years or so. Nonetheless, the recombinant approach does have the limitation that proteins are overexpressed, giving levels that are higher than the endogenous proteins with the possibility for effects on cellular functions governed by the protein in question. For example, overexpression of ARRDC2, an apparent endocytic protein, may cause enhancement of endocytic/vesicular functions, perhaps driving the protein to the predominantly lysosomal distribution observed. This is not to say that this observation is false, but rather that ideally it must but controlled for, as has been attempted here in the complementary analysis of endogenous ARRDC2 targeting in primary cells. The endogenous approach also has significant limitations, though, being more technically challenging; it requires large numbers of primary cells that express sufficient levels of the proteins in question (which, for ARRDC2, were not available) combined with the ability to perturb or detect such proteins (for example using siRNA and high affinity antibodies for endogenous coimmunoprecipitation, again which were not readily available).

6.3 How is ARRDC2 subcellular distribution established?

The data described here present human ARRDCs as proteins that are targeted to membrane-bound compartments. Co-labelling with compartment-specific markers indicated that ARRDC2 is dynamically targeted to the endocytic system, predominantly to late endosomes/lysosomes, as well as the plasma membrane.

A question that arises is the mechanism by which ARRDC2 (and other ARRDCs) is targeted to membrane compartments, and conversely why this capability is apparently not conserved in the β-arrestins. With respect to ARRDC2, two possibilities (that are not mutually exclusive) are that (i) ARRDC2 interacts directly with membranes, for example binding compartment-enriched membrane phospholipids, or (ii) ARRDC2 is indirectly targeted to membranes via interaction with a membrane-binding partner, as has been reported for the endosomal targeting of Vps26, which is targeted to endosomes/TGN via interaction with Vps35 (Collins *et al.*, 2008). Recently, the reported plasma membrane targeting of ARRDC1 has been shown to be dependent upon several residues in its predicted arrestin domain (Phe^{88}, Gly^{180}, Asn^{191}), the mutation of which reduced or abolished ARRDC1 plasma membrane localisation, leaving the protein diffusely distributed throughout the cytosol (Nabhan *et al.*, 2012). Interestingly, all three residues are conserved throughout all human ARRDCs and β-arrestins (see Figure 1.2), indicating their importance, possibly in contributing to the β-sandwich fold. This would suggest that the overall structure of the ARRDC is required for membrane targeting, hinting that targeting may involve ARRDC interaction with membrane localised partners, rather than direct targeting via intrinsic ARRDC lipid-binding elements (which, based on sequence predictions, are absent from ARRDCs). It would be informative to test whether mutation of the equivalent residues in ARRDC2 similarly affects its membrane targeting.

The fact that β-arrestins contain these residues and are yet generally considered to be diffusely localised in the cytosol (in the absence of GPCR stimulation) makes the interpretation of these observations unclear. It is possible that the residues contribute to as yet unidentified contacts (for example, intramolecular hydrophobic interactions) in α-arrestins that are not present in β-arrestins, thereby defining a distinct structure for the α-arrestins that promotes membrane targeting (directly or indirectly, as described above). The prevailing dogma that β-arrestins are diffusely localised comes largely from overexpression data. However, it has been reported that endogenous β-arrestins may target to intracellular punctate structures, possibly indicative of the ability of the native proteins to associate with membranes (Shankar *et al.*, 2010). It would be interesting to explore further whether endogenous α-arrestin distribution is consistent with the reported exogenous data available (see section 3.3.3) or if, similar to β-arrestins, overexpression may drive them to an alternative pattern.

The nature of membrane targeting (direct versus indirect) could also be addressed by investigating whether α-arrestins display affinity for lipids (for example, using a protein-lipid overlay assay (Dowler *et al.*, 2002)) – although, as commented above, they lack any predicted lipid-interacting motifs – and through the systematic identification of potential membrane-associated binding partners (for example, using mass spectrometry analysis of interaction partners). A more targeted approach to identifying binding partners could be to assess whether α-arrestins interact specifically with SH3 domains. ARRDC2/3/4 all contain a potential class I SH3-binding motif, (R/K)XPPXXP, towards the centre of the arrestin C-domain that may enable them to interact with SH3 domains (Alvarez, 2008), although this possibility has not been investigated. SH3 domains are common protein-protein interaction modules present in plasma membrane proteins (e.g. proteins involved in clathrin-mediated endocytosis such as endophilin (Simpson *et al.*, 1999)) and endosomal proteins (e.g. the ESCRT-0 component, STAM (Takeshita *et al.*, 1996)), and protein lysosomal targeting via a proline-rich

motif interaction with SH3 domain-containing proteins has been reported elsewhere (Qian *et al.*, 2006). Thus, the ability to interact with SH3 domains could represent a potential mechanism for ARRDC2/3/4 membrane targeting. However, as commented in Chapter 4, for ARRDC4, membrane targeting was shown to be abolished by deletion of the C-terminal 68 amino acids (residues 350-418) (Vina-Vilaseca *et al.*, 2011). These residues do not include the putative ARRDC4 SH3-binding motif (spanning residues 273-279); hence, in the case of ARRDC4, if it does indeed interact with SH3 domains via this motif, it appears that this may not determine its membrane targeting.

6.4 ARRDC2 as a NEDD4 family ubiquitin ligase adaptor

The α-arrestins generally contain C-terminal PPxY motifs that in many cases have been shown to enable their interaction with NEDD4 family ubiquitin ligases, which may serve to recruit the ligase for ubiquitination of the α-arrestin itself and/or associated cargo proteins. The human ARRDCs appear to fit with this paradigm, and here it was found that ARRDC2 too is capable of interacting with several NEDD4 ligase family members, and that this interaction may be important to the function of the ligases by determining their site of action.

A question that arises from these studies is whether the observed interaction of ARRDC2 with several NEDD4 family ligases is of physiological relevance. The system used to test for interactions – coimmunoprecipitation of overexpressed proteins – has the potential to amplify the detection of associations that are actually low affinity. Hence, although the data presented clearly argue for the ability of ARRDC2 to interact with NEDD4 family ligases, whether all the interactions detected occur in native cells remains unclear. However, there are reasons to believe this may be the case. Theoretically, the possibility for multiple NEDD4 ligase interactions is plausible. Despite the differences in function of specific NEDD4 ligases (section

4.1) they exhibit significant sequence similarity, especially within the WW domains that are thought to mediate the ARRDC2 interaction. For example, related proteins WWP1 and WWP2 both contain four WW domains. WWP1 and WWP2 exhibit 72% overall sequence similarity, with 88% similarity across the four WW domains. Both ligases were able to coimmunoprecipitate ARRDC2. WWP1 and WWP2 may perform redundant roles, with both ligases implicated in carcinogenesis, possibly via converging effects on TGFβ signalling (Komuro *et al.*, 2004; Soond *et al.*, 2011). Therefore, it is conceivable that ARRDC2 could interact with both WWP1 and WWP2 in the native context, and could thereby mediate or influence some of their overlapping functions.

Moreover, there are several reports of other PPxY motif-containing proteins that bind several different NEDD4 ligases. For example, ARRDC1 and ARRDC3 (as well as ARRDC2) were shown to be capable of interacting with WWP1, WWP2, AIP4 and NEDD4 (Nabhan *et al.*, 2010; Rauch *et al.*, 2011). Similarly, the NEDD4 family-interacting proteins (NDFIP1 and NDFIP2) contain PPxY motifs and interact with multiple NEDD4 family members (Harvey *et al.*, 2002; Shearwin-Whyatt *et al.*, 2004), which in this case promotes the NEDD4 ligase catalytic activity (Mund *et al.*, 2009). As mentioned in section 4.1, the Smad proteins bind SMURF1 and SMURF2, and they have also been shown to bind WWP1 and WWP2 (Komuro *et al.*, 2004; Soond *et al.*, 2011). Collectively, these observations indirectly support the hypothesis that ARRDC2 may be involved in physiologically relevant interactions with several NEDD4 family members, underlining the importance of the approach used here to scan for coimmunoprecipitation with all nine family members. Additional experiments would be required to directly test this hypothesis. Most importantly, it would be necessary to determine whether endogenous ARRDC2 and NEDD4 ligases interact, for example by coimmunoprecipitation with specific antibodies targeted against endogenous proteins. Subsequent experiments could then probe the impact of such interactions upon molecular physiological events.

Biochemical experiments revealed that ARRDC2 may be subject to ubiquitination; immunoblotting suggested that ARRDC2 may exist predominantly in monoubiquitinated form, although further experiments would be required to convincingly demonstrate this (section 4.3.2), and coimmunoprecipitation confirmed that ARRDC2 can be mono- and multi-/poly-ubiquitinated. The ligase(s) responsible for ARRDC2 ubiquitination is unknown. There are hints that overexpression of some NEDD4 ligases (NEDL1, WWP2) may enhance ARRDC2 ubiquitination. However, abolishing ARRDC2 interaction with NEDD4 ligases through PPxY motif mutation did not affect the detection of ARRDC2 ubiquitination, suggesting that other unidentified ligase(s) may be responsible. There are more powerful methods available for assessing the potential role of NEDD4 ligases in ARRDC2 ubiquitination – for example, analysing the effect of overexpression of catalytically inactive mutant ligases – that would be required to exclude their role. Although the approach used does not reveal the proportion of ARRDC2 that is ubiquitinated, it is notable that constitutive, signal-independent ubiquitination of ARRDC2 was detected. Another α-arrestin that appears to exist predominantly in monoubiquitinated form is the yeast protein ART1. ART1 is also constitutively ubiquitinated, and this may be required for ART1 subcellular targeting (in this case to the Golgi) and function (Lin *et al.*, 2008). In contrast, ubiquitination of ART4 appears to be largely absent in basal conditions but is stimulated by glucose signalling (Becuwe *et al.*, 2012), and a fungal α-arrestin, PalF, is reported to be ubiquitinated only in response to alkaline pH (Herranz *et al.*, 2005). Ubiquitination of β-arrestin is also signal-dependent, thought to occur largely upon agonist stimulation of GPCRs (Mosser *et al.*, 2008; Shenoy *et al.*, 2003; Shenoy *et al.*, 2001; Shenoy *et al.*, 2009). Shenoy and colleagues showed that in response to β_2AR stimulation, β-arrestin2 ubiquitination is performed by the RING E3 ligase Mdm2, since the use of Mdm2-null cells or expression of a dominant-negative Mdm2 abolished β-arrestin2 ubiquitination (Shenoy *et al.*, 2001). Whether other E3 ligases (for example, NEDD4 family ligases) are also capable of ubiquitinating β-arrestins,

such as upon stimulation of alternative GPCRs, has not been investigated. It would be interesting to test whether ARRDC2 ubiquitination is similarly enhanced upon stimulation of GPCRs and whether this may be dependent upon Mdm2 and/or NEDD4 family ligases.

Despite lacking PPxY motifs, β-arrestins have also been reported to interact with NEDD4 family ligases: β-arrestins recruited NEDD4 or AIP4 for the ubiquitination and downregulation of β_2AR or CXCR4, respectively (Bhandari *et al.*, 2007; Shenoy *et al.*, 2008). The mechanism of potential β-arrestin-NEDD4 ligase interaction is unclear; direct binding has only been demonstrated for the interaction of β-arrestin1 with AIP4 (using GST pull-down of purified proteins). It remains possible that β-arrestin1/2 interaction with NEDD4 may be mediated by an intermediate protein. It would be tempting to suggest that α-arrestin(s) could represent the direct NEDD4 interactor(s), and hetero-oligomerisation between α- and β-arrestins may explain the β-arrestin-NEDD4 interaction detected. This suggestion is supported by the ability of ARRDC2 to hetero-oligomerise with β-arrestin1/2, as reported here, and could be tested, for example by examining the ability of ARRDC protein overexpression or knockdown to affect β-arrestin-NEDD4 ligase interaction. Conversely, if β-arrestins are indeed able to directly recruit NEDD4 ligases, given the potential for α-/β-arrestin hetero-oligomerisation described above, this may actually explain the lack of effect of ARRDC2 PPxY motif mutation upon its ubiquitination, since the β-arrestin may still recruit the ligase(s) to the complex.

Although some degree of constitutive association between β-arrestins and NEDD4/AIP4 has been detected in coimmunoprecipitations, the interactions have been shown to be enhanced by GPCR agonist stimulation (Bhandari *et al.*, 2007; Shenoy *et al.*, 2008). This suggests that binding to GPCRs may induce a β-arrestin conformation that is preferable to binding NEDD4 ligases. The same has not been tested for α-arrestin interactions with NEDD4 ligases in the majority of cases. In both lower eukaryotes and humans, constitutive interaction of α-arrestins

and NEDD4 ligases has been demonstrated by the coimmunoprecipitation of overexpressed proteins. In one report, the constitutive interaction of an α-arrestin (ART3) and NEDD4 family ligase (Rsp5) appeared to be enhanced by the presence of aspartic acid, presumably upon recruitment of ART3 to the aspartic acid transporter Dip5 (Hatakeyama *et al.*, 2010), suggesting that ART3 interaction with Rsp5 may also be suboptimal in the absence of a particular signal. However, this has generally not been tested for α-arrestin-NEDD4 ligase interactions. As has been mentioned, coimmunoprecipitation of overexpressed proteins has the potential for amplification of genuine interactions. It may be that the relevant interaction is in fact a signal-dependent one. As commented above, it would be informative to test whether endogenous α-arrestins and NEDD4 ligases interact, and whether this is dependent on a signal such as recruitment of the α-arrestin to an activated GPCR.

6.5 ARRDCs and β-arrestins: partners in GPCR regulation?

Data presented here reveal a potential role for ARRDC2 in the regulation of GPCRs. ARRDC2 is specifically recruited to GPCRs (β_2AR, δOR), possibly involving a direct association, and influences their intracellular trafficking. As has been recognised, a functional consequence of such regulation remains to be demonstrated. The possibility of overexpressing PPxY motif mutants of ARRDC2 and assessing their effect receptor trafficking has been mentioned. It is worth recognising the likely power of this approach to determine whether ARRDC2 regulates GPCR trafficking via a ubiquitin ligase adaptor mechanism. Preliminary experiments suggesting in fact that mutant ARRDC2ΔΔ may not alter β_2AR trafficking have been included (Figure 6.1), although quantification of any effect and supporting evidence, for example in the form of immunoblotting measurement of receptor downregulation, would need to be performed to clarify this result. Despite the obvious need for these further experiments, the data here, along with the complementary

evidence of ARRDC2 as a ubiquitin ligase adaptor strongly support the hypothesis that ARRDC2 regulates GPCR function, likely in a similar manner to that seen for ARRDC3 (Nabhan *et al.*, 2010).

Also presented here is the first evidence for the ability of α- and β-arrestins to interact, which could provide insight into the mechanism by which ARRDCs may regulate GPCRs. Although the function of arrestin dimerisation remains unclear, interactions have been reported to impact the subcellular targeting of partners: the coexpression of β-arrestin1/2 has been shown to prevent β-arrestin1 targeting to the nucleus (Storez *et al.*, 2005). Similarly here, ARRDC2 overexpression impacted β-arrestin targeting, through the induction of intracellular β-arrestin1 puncta, and the generation of a punctate BiFC signal with β-arrestin2. Furthermore, the potential for GPCR dimerisation – and the possible interaction of arrestin dimers with such receptor complexes – has been mentioned (section 5.1). The ability of ARRDC2 to oligomerise with arrestin family members supports the proposal that α- and β-arrestin heterodimers might interact with GPCR dimers, perhaps leading to a much more dynamic system involving competition and/or exchange between α- and β-arrestins as GPCR binding partners. In this context, it is possible that α-arrestins – through their presentation of PPxY motifs – are the predominant recruiters of NEDD4 family ligases to GPCR complexes; the apparent ability of β-arrestins to mediate ligase recruitment and receptor ubiquitination may in fact reflect their recruitment of α-arrestins through dimerisation. This may even be true for the recruitment of AIP4 to CXCR4, which has been reported to require β-arrestin1 (Bhandari *et al.*, 2007). Although β-arrestin1 has been reported to interact directly with AIP4 using purified proteins, it remains possible that in the native system the essential interaction is between an ARRDC and AIP4. The constitutive and ligand-regulated formation of CXCR4 homo- and heterodimers has been well established through various biochemical and microscopic techniques (Isik *et al.*, 2008; Luker *et al.*, 2009; Percherancier *et al.*, 2005; Vila-Coro *et al.*, 1999), and has been corroborated by recently published crystal structures (Wu *et al.*,

2010). Hypothetically, activated CXCR4 dimers could bind heterodimers of ARRDCs and β-arrestin1, in which ARRDC binding requires dimerisation with β-arrestin1 (i.e. since, as has been mentioned, ARRDCs do not contain the known GPCR-binding modules present in β-arrestins, binding of an ARRDC to CXCR4 may require concurrent association with β-arrestin). Recruitment of AIP4 would then be dependent upon interaction with PPxY motifs in the ARRDC protein; disrupting β-arrestin1 would result in ARRDC-AIP4 not being recruited to the receptor complex. This mechanism would still be consistent with the observation that β-arrestin1 is required for CXCR4 ubiquitination and lysosomal degradation (Bhandari *et al.*, 2007). It could be tested, for example, by depleting ARRDC(s) and measuring any effect on CXCR4 ubiquitination and degradation, as well as on the interaction of β-arrestin1 and AIP4 in living cells.

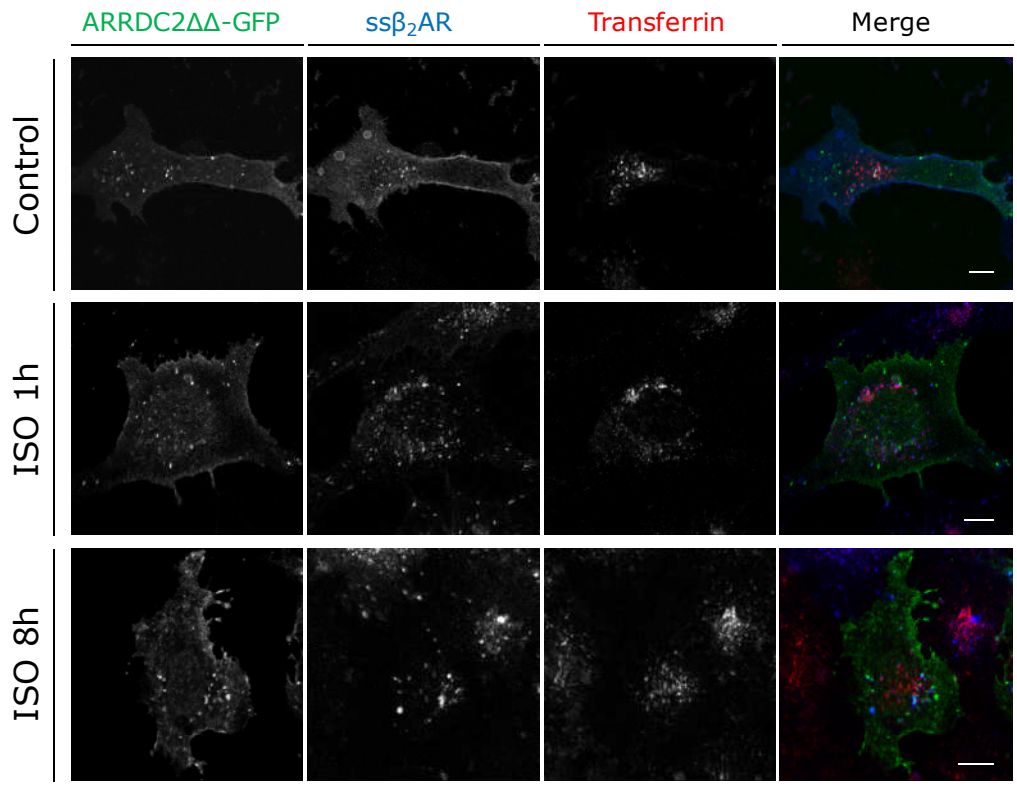

Figure 6.1 Initial attempt to assess the effect of ARRDC2 PPxY motif mutants on β_2AR trafficking

Confocal microscopic images of U2OS cells transiently transfected with plasmids expressing ssβ_2AR plus ARRDC2ΔΔ-GFP. Cells were treated with isoprenaline (ISO, 10 μM, 1h or 8h, as indicated) or without (Control), as

indicated. In addition, cells were co-stained with 250 ng/µl AF-633-conjugated Transferrin for the final 15 min of the control/ISO incubation. ssβ_2AR was visualised by labelling with 0.1 µM SNAPsurface BG-AF546 prior to the experiment. In merged images, ARRDC2ΔΔ is shown in green, ssβ_2AR is in blue and transferrin is in red. Scale bar = 10 µm.

Although many GPCR functions adhere to the paradigms provided by model receptors such as β_2AR, there are a number of exceptions where receptors function non-canonically, including with respect to β-arrestin mechanisms (see Chapter 1). As such, there remain significant 'gaps' in our knowledge that β-arrestins appear not to fill. There are a number of possible explanations, including that the related α-arrestins may fill some of these gaps. An example is GPCR internalisation, which in most cases is thought to require β-arrestins as endocytic adaptors. There are GPCRs whose internalisation is β-arrestin-independent. For example, microscopy showed that urotensin receptor appears to internalise normally in β-arrestin1/2 knockout MEFs (Giebing *et al.*, 2005), and the same was shown for *N*-formyl peptide receptor using flow cytometry, in contrast to the non-internalising β_2AR (in the absence of β-arrestins), which was included as a control (Vines *et al.*, 2003). It may be that these receptors interact directly with the endocytic machinery, as has been demonstrated for dileucine or tyrosine-based motifs in the C-tail of several other GPCRs (Diviani *et al.*, 2003; Fraile-Ramos *et al.*, 2003; Paing *et al.*, 2006). Furthermore, α-arrestins lack known clathrin- or AP2-interacting motifs found in β-arrestins, although interactions between yeast α-arrestins and clathrin/clathrin adaptor proteins have been reported (O'Donnell *et al.*, 2010). Nevertheless, it may be that α-arrestins are able to mediate internalisation of some GPCRs in a non-canonical fashion. This could be investigated by assessing the impact, for example, of α-arrestin siRNA, upon the internalisation of GPCRs (such as those mentioned above) in β-arrestin1/2 knockout MEFs. Perhaps a more likely role for α-arrestins is in governing the multiple sorting decisions for GPCRs once internalised, given that α-arrestins appear largely to target to

the endocytic/vesicular system. The number of proteins involved in intracellular GPCR sorting, and hence the number of distinct mechanisms, is ever expanding. This variety reflects the fine regulation that is required, which is increasingly being recognised as specific to both receptor type and context (cell type, nature of stimulus etc). The involvement of α-arrestins would provide yet another possible mode of receptor regulation which, if early investigations are an indication, may well be of great physiological importance (Draheim *et al.*, 2010; Patwari *et al.*, 2009; Patwari *et al.*, 2011).

6.6 Are GPCRs the only ARRDC2 cargo?

Finally, it is worth considering whether ARRDC2 might associate with and regulate non-GPCR cargoes and, given this possibility, whether the methodology used here to investigate ARRDC2 function was the best approach. Recent years have seen the knowledge of the β-arrestins expand from GPCR regulators to flexible adaptors capable of interacting with multiple different proteins (Gurevich *et al.*, 2008b). Not only do β-arrestins scaffold many different effector proteins upon binding to GPCRs, but they can also regulate several structurally divergent non-GPCR cell surface receptors (section 1.3). A precedent for α-arrestin regulation of non-GPCR cell surface cargo also exists, with reports in yeast of α-arrestins (or ARTs) acting as ubiquitin ligase adaptors for several nutrient transporters (Hatakeyama *et al.*, 2010; Lin *et al.*, 2008; Nikko *et al.*, 2009; Nikko *et al.*, 2008). As commented in section 1.4.2, these are thought to be 12 TM-spanning transporters with no apparent structural similarity to GPCRs, suggesting that α-arrestins may also associate with diverse cargo. Similar to β-arrestin interactions with GPCRs, however, α-arrestin interaction with the transporters may be dependent upon transporter phosphorylation. This has been indicated for the association of ART2 with Smf1, which was directly shown to be strongly enhanced by constitutive Smf1 phosphorylation (Nikko *et al.*, 2008), and ART3 with Dip5, which

was indirectly indicated due to the inhibitory effect of non-phosphorylated Dip5 mutants upon Dip5 endocytosis, a process dependent upon ART3 association (Hatakeyama *et al.*, 2010).

The mechanisms behind potential β-arrestin interaction with non-GPCRs, although not studied in detail, may also involve phosphorylation. β-arrestin2 binding to TGFβRIII was triggered by receptor phosphorylation (Chen *et al.*, 2003), and the NHE5 binding domain on β-arrestin2 was mapped to a positively charged cluster (residues 318-332) (Szabo *et al.*, 2005). Thus, β-arrestin interaction with alternative cargo may be enabled by contacts with negatively charged phosphate moieties, in a similar way to their interaction with GRK-phosphorylated GPCR C-tails. Similarly, although human α-arrestins lack a recognised phosphate sensor, an interaction between ARRDC3 and ITGβ4 has been reported to be promoted by ITG phosphorylation (Draheim *et al.*, 2010). Based on these observations it is reasonable to propose that ARRDC proteins may associate with non-GPCR cargo.

The approach used here to investigate ARRDC2 function – choosing to focus on specific ubiquitin ligases and GPCR cargo – was hypothesis-driven, based on the molecular function of the known α-arrestins and related β-arrestins, and carried the advantage of defining a molecular mechanism for ARRDC2 with respect to these factors. However, a disadvantage is the need to choose a small number of cargo (in this case two GPCRs) out of a huge number of potential partners, both GPCR and, as described above, non-GPCR. In this case these decisions were based, as mentioned, on the small amount of data available on other α-arrestins and on the roles of the related β-arrestins. One way to better inform these decisions would be to investigate the tissue and cell type specific expression of endogenous ARRDC2; cell-specific cargo could then be chosen based on knowing where ARRDC2 is expressed in native tissues.

An alternative approach that would not presume a certain cargo is exemplified in the report by Nabhan and colleagues investigating ARRDC3 (Nabhan *et al.*, 2010). The principle of this approach is to determine a physiological impact of the protein in question without

necessarily immediately knowing the underlying mechanism. This approach thus begins at the genetic level; the authors performed a screen (using RNA interference; RNAi) to identify any genes with a role in β_2AR downregulation, of which ARRDC3 was identified. From this information the authors then went on to attempt to define the mechanism behind the observed effect. This approach has the benefit of being a broad survey that does not presume a particular cargo or mechanism, and it likely identifies proteins that have a relevant physiological role within the system in question (in the current example, β_2AR regulation). However, it comes with the caveat that if there are redundant interactions that govern the function in question – for example, if several ARRDC proteins have overlapping roles – then single genetic knockouts will not necessarily reveal a phenotype, meaning that functions will be masked.

In summary, this thesis has described the identification of ARRDC2 as a human α-arrestin that is dynamically targeted to the endocytic system. Within this system, ARRDC2 is able to associate with and regulate the intracellular sorting of NEDD4 family ubiquitin ligases and GPCRs. Future studies will investigate the likely overlap of these functions in the definition of ARRDC2 as a cargo-specific (GPCR) ubiquitin ligase adaptor, and will determine the mechanisms involved – namely whether ARRDC2, and other α-arrestins, regulate GPCRs via collaboration or competition with β-arrestins.

7 References

Acconcia, F, Sigismund, S, Polo, S (2009) Ubiquitin in trafficking: The network at work. *Experimental Cell Research* **315**(9)**:** 1610-1618.

Ahn, S, Shenoy, SK, Wei, H, Lefkowitz, RJ (2004) Differential Kinetic and Spatial Patterns of β-Arrestin and G Protein-mediated ERK Activation by the Angiotensin II Receptor. *Journal of Biological Chemistry* **279**(34)**:** 35518-35525.

Alvarez, CE (2008) On the origins of arrestin and rhodopsin. *Bmc Evolutionary Biology* **8:** 222.

Andoh, T, Hirata, Y, Kikuchi, A (2002) PY motifs of Rod1 are required for binding to Rsp5 and for drug resistance. *FEBS Letters* **525**(1-3)**:** 131-134.

Andres, AM, Ratliff, EP, Sachithanantham, S, Hui, ST (2011) Diminished AMPK signaling response to fasting in thioredoxin-interacting protein knockout mice. *FEBS Letters* **585**(8)**:** 1223-1230.

Attar, N, Cullen, PJ (2011) The retromer complex. *Advances in Enzyme Regulation* **50**(1)**:** 216-236.

Aubry, L, Guetta, D, Klein, G (2009) The Arrestin Fold: Variations on a Theme. *Current Genomics* **10**(2)**:** 133-142.

Baillie, GS, Sood, A, McPhee, I, Gall, I, Perry, SJ, Lefkowitz, RJ, Houslay, MD (2003) β-Arrestin-mediated PDE4 cAMP phosphodiesterase recruitment regulates β-adrenoceptor switching from Gs to Gi. *Proceedings of the National Academy of Sciences* **100**(3)**:** 940-945.

Beaulieu, J-M, Sotnikova, TD, Marion, S, Lefkowitz, RJ, Gainetdinov, RR, Caron, MG (2005) An Akt/β-Arrestin 2/PP2A Signaling Complex Mediates Dopaminergic Neurotransmission and Behavior. *Cell* **122**(2)**:** 261-273.

Becuwe, M, Vieira, N, Lara, D, Gomes-Rezende, J, Soares-Cunha, C, Casal, M, Haguenauer-Tsapis, R, Vincent, O, Paiva, S, Leon, S (2012) A molecular switch on an arrestin-like protein relays glucose signaling to transporter endocytosis. *The Journal of Cell Biology* **196**(2)**:** 247-259.

Berlin, I, Higginbotham, KM, Dise, RS, Sierra, MI, Nash, PD (2010) The Deubiquitinating Enzyme USP8 Promotes Trafficking and Degradation of the Chemokine Receptor 4 at the Sorting Endosome. *Journal of Biological Chemistry* **285**(48)**:** 37895-37908.

Bertelsen, V, Sak, MM, Breen, K, Rødland, MS, Johannessen, LE, Traub, LM, Stang, E, Madshus, IH (2011) A Chimeric Pre-ubiquitinated EGF Receptor is Constitutively Endocytosed in a Clathrin-Dependent, but Kinase-Independent Manner. *Traffic* **12**(4)**:** 507-520.

Berthouze, M, Venkataramanan, V, Li, Y, Shenoy, SK (2009) The deubiquitinases USP33 and USP20 coordinate β2 adrenergic receptor recycling and resensitization. *EMBO J* **28**(12)**:** 1684-1696.

Bhandari, D, Robia, SL, Marchese, A (2009) The E3 Ubiquitin Ligase Atrophin Interacting Protein 4 Binds Directly To The Chemokine Receptor CXCR4 Via a Novel WW Domain-mediated Interaction. *Molecular Biology of the Cell* **20**(5)**:** 1324-1339.

Bhandari, D, Trejo, J, Benovic, JL, Marchese, A (2007) Arrestin-2 interacts with the ubiquitin-protein isopeptide ligase atrophin-interacting protein 4 and mediates endosomal sorting of the chemokine receptor CXCR4. *Journal of Biological Chemistry* **282**(51)**:** 36971-36979.

Birnboim, HC, Doly, J (1979) A rapid alkaline extraction procedure for screening recombinant plasmid DNA. *Nucleic Acids Research* **7**(6)**:** 1513-1523.

Bohnekamp, J, Schoneberg, T (2011) Cell Adhesion Receptor GPR133 Couples to Gs Protein. *Journal of Biological Chemistry* **286**(49)**:** 41912-41916.

Bonacci, TM, Ghosh, M, Malik, S, Smrcka, AV (2005) Regulatory interactions between the amino terminus of G-protein beta gamma subunits and the catalytic domain of phospholipase c beta 2. *Journal of Biological Chemistry* **280**(11)**:** 10174-10181.

Bonifacino, JS, Hurley, JH (2008) Retromer. *Current Opinion in Cell Biology* **20**(4)**:** 427-436.

Boularan, C, Scott, MGH, Bourougaa, K, Bellal, M, Esteve, E, Thuret, A, Benmerah, A, Tramier, M, Coppey-Moisan, M, Labbe-Jullie, C, Fahraeus, R, Marullo, S (2007) β-arrestin 2 oligomerization controls the Mdm2-dependent inhibition of p53. *Proceedings of the National Academy of Sciences* **104**(46)**:** 18061-18066.

Bourne, HR (1997) How receptors talk to trimeric G proteins. *Current Opinion in Cell Biology* **9**(2)**:** 134-142.

Brejc, K, Sixma, TK, Kitts, PA, Kain, SR, Tsien, RY, Ormo, M, Remington, SJ (1997) Structural basis for dual excitation and photoisomerization of the Aequorea victoria green fluorescent protein. *Proceedings of the National Academy of Sciences* **94**(6)**:** 2306-2311.

Bucci, C, Parton, RG, Mather, IH, Stunnenberg, H, Simons, K, Hoflack, B, Zerial, M (1992) The small GTPase rab5 functions as a regulatory factor in the early endocytic pathway. *Cell* **70**(5)**:** 715-728.

Bucci, C, Thomsen, P, Nicoziani, P, McCarthy, J, van Deurs, B (2000) Rab7: A key to lysosome biogenesis. *Molecular Biology of the Cell* **11**(2)**:** 467-480.

Cao, TT, Deacon, HW, Reczek, D, Bretscher, A, von Zastrow, M (1999) A kinase-regulated PDZ-domain interaction controls endocytic sorting of the beta 2-adrenergic receptor. *Nature* **401**(6750)**:** 286-290.

Cellier, M, Prive, G, Belouchi, A, Kwan, T, Rodrigues, V, Chia, W, Gros, P (1995) Nramp defines a family of membrane proteins. *Proceedings of the National Academy of Sciences* **92**(22)**:** 10089-10093.

Chabre, M, le Maire, M (2005) Monomeric G-Protein-Coupled Receptor as a Functional Unit. *Biochemistry* **44**(27)**:** 9395-9403.

Chandrashekar, J, Mueller, KL, Hoon, MA, Adler, E, Feng, L, Guo, W, Zuker, CS, Ryba, NJP (2000) T2Rs Function as Bitter Taste Receptors. *Cell* **100**(6)**:** 703-711.

Chen, B, Dores, MR, Grimsey, N, Canto, I, Barker, BL, Trejo, J (2011) Adaptor Protein Complex-2 (AP-2) and Epsin-1 Mediate Protease-activated Receptor-1 Internalization via Phosphorylation- and Ubiquitination-dependent Sorting Signals. *Journal of Biological Chemistry* **286**(47)**:** 40760-40770.

Chen, C-H, Paing, MM, Trejo, J (2004a) Termination of Protease-activated Receptor-1 Signaling by β-Arrestins Is Independent of Receptor Phosphorylation. *Journal of Biological Chemistry* **279**(11)**:** 10020-10031.

Chen, C-m, Strapps, W, Tomlinson, A, Struhl, G (2004b) Evidence that the cysteine-rich domain of Drosophila Frizzled family receptors is dispensable for transducing Wingless. *Proceedings of the National Academy of Sciences of the United States of America* **101**(45)**:** 15961-15966.

Chen, J, Hui, ST, Couto, FM, Mungrue, IN, Davis, DB, Attie, AD, Lusis, AJ, Davis, RA, Shalev, A (2008) Thioredoxin-interacting protein deficiency induces Akt/Bcl-xL signaling and pancreatic beta-cell mass and protects against diabetes. *The FASEB Journal* **22**(10)**:** 3581-3594.

Chen, JW, Pan, W, D'Souza, MP, August, JT (1985) Lysosome-associated membrane proteins: Characterization of LAMP-1 of macrophage P388 and mouse embryo 3T3 cultured cells. *Archives of Biochemistry and Biophysics* **239**(2)**:** 574-586.

Chen, W, Kirkbride, KC, How, T, Nelson, CD, Mo, J, Frederick, JP, Wang, X-F, Lefkowitz, RJ, Blobe, GC (2003) β-Arrestin 2 Mediates Endocytosis of Type III TGF-β Receptor and Down-Regulation of Its Signaling. *Science* **301**(5638)**:** 1394-1397.

Choe, H-W, Kim, YJ, Park, JH, Morizumi, T, Pai, EF, Krausz, N, Hofmann, KP, Scheerer, P, Ernst, OP (2011) Crystal structure of metarhodopsin II. *Nature* **471**(7340)**:** 651-655.

Chudakov, DM, Verkhusha, VV, Staroverov, DB, Souslova, EA, Lukyanov, S, Lukyanov, KA (2004) Photoswitchable cyan fluorescent protein for protein tracking. *Nat Biotech* **22**(11)**:** 1435-1439.

Chutkow, WA, Patwari, P, Yoshioka, J, Lee, RT (2008) Thioredoxin-interacting Protein (Txnip) Is a Critical Regulator of Hepatic Glucose Production. *Journal of Biological Chemistry* **283**(4)**:** 2397-2406.

Collins, BM, Norwood, SJ, Kerr, MC, Mahony, D, Seaman, MNJ, Teasdale, RD, Owen, DJ (2008) Structure of Vps26B and mapping of its interaction with the retromer protein complex. *Traffic* **9**(3)**:** 366-379.

Coso, OA, Teramoto, H, Simonds, WF, Gutkind, JS (1996) Signaling from G protein-coupled receptors to c-Jun kinase involves beta gamma subunits of heterotrimeric G proteins acting on a Ras and Rac1-dependent pathway. *Journal of Biological Chemistry* **271**(8)**:** 3963-3966.

Cunningham, MR, McIntosh, KA, Pediani, JD, Robben, J, Cooke, AE, Nilsson, M, Gould, GW, Mundell, S, Milligan, G, Plevin, R (2012) Novel Role for Proteinase-activated Receptor 2 (PAR2) in Membrane Trafficking of Proteinase-activated Receptor 4 (PAR4). *Journal of Biological Chemistry* **287**(20)**:** 16656-16669.

Daaka, Y, Luttrell, LM, Lefkowitz, RJ (1997) Switching of the coupling of the β2-adrenergic receptor to different G proteins by protein kinase A. *Nature* **390**(6655)**:** 88-91.

Dann, CE, Hsieh, J-C, Rattner, A, Sharma, D, Nathans, J, Leahy, DJ (2001) Insights into Wnt binding and signalling from the structures of two Frizzled cysteine-rich domains. *Nature* **412**(6842)**:** 86-90.

Dautry-Varsat, A (1986) Receptor-mediated endocytosis: the intracellular journey of transferrin and its receptor. *Biochimie* **68**(3)**:** 375-381.

De Lean, A, Stadel, JM, Lefkowitz, RJ (1980) A ternary complex model explains the agonist-specific binding properties of the adenylate cyclase-coupled beta-adrenergic receptor. *Journal of Biological Chemistry* **255**(15)**:** 7108-7117.

Defea, KA (2008) β-Arrestin multimers: does a crowd help or hinder function? *Biochem J* **413**(1)**:** e1-e3.

DeFea, KA, Zalevsky, J, Thoma, MS, Dery, O, Mullins, RD, Bunnett, NW (2000) β-Arrestin-Dependent Endocytosis of Proteinase-Activated Receptor 2 Is Required for Intracellular Targeting of Activated Erk1/2. *The Journal of Cell Biology* **148**(6)**:** 1267-1282.

Demirov, DG, Freed, EO (2004) Retrovirus budding. *Virus Research* **106**(2)**:** 87-102.

Deshaies, RJ, Joazeiro, CAP (2009) RING Domain E3 Ubiquitin Ligases. *Annual Review of Biochemistry* **78**(1)**:** 399-434.

Diel, S, Klass, K, Wittig, B, Kleuss, C (2006) G beta gamma activation site in adenylyl cyclase type II Adenylyl cyclase type III is inhibited by G beta gamma. *Journal of Biological Chemistry* **281**(1)**:** 288-294.

Dinh, DT, Qian, H, Seeber, R, Lim, E, Pfleger, K, Eidne, KA, Thomas, WG (2005) Helix I of β-Arrestin Is Involved in Postendocytic Trafficking but Is Not Required for Membrane Translocation, Receptor Binding, and Internalization. *Molecular Pharmacology* **67**(2)**:** 375-382.

Diviani, D, Lattion, A-L, Abuin, L, Staub, O, Cotecchia, S (2003) The Adaptor Complex 2 Directly Interacts with the α1b-Adrenergic Receptor and Plays a Role in Receptor Endocytosis. *Journal of Biological Chemistry* **278**(21)**:** 19331-19340.

Donaldson, J, Brown, AM, Hill, SJ (1988) Influence of rolipram on the cyclic 3',5'-adenosine monophosphate response to histamine and adenosine in slices of guinea-pig cerebral cortex. *Biochemical Pharmacology* **37**(4)**:** 715-723.

Dowler, S, Kular, G, Alessi, DR (2002) Protein Lipid Overlay Assay. *Sci. STKE* **2002**(129)**:** pl6.

Draheim, KM, Chen, HB, Tao, Q, Moore, N, Roche, M, Lyle, S (2010) ARRDC3 suppresses breast cancer progression by negatively regulating integrin β4. *Oncogene* **29**(36)**:** 5032-5047.

Dunn, R, Klos, DA, Adler, AS, Hicke, L (2004) The C2 domain of the Rsp5 ubiquitin ligase binds membrane phosphoinositides and directs ubiquitination of endosomal cargo. *The Journal of Cell Biology* **165**(1)**:** 135-144.

Edwards, T, Clowes, V, Tsang, H, Connell, J, Sanderson, C, Luzio, J, Reid, E (2009) Endogenous spartin (SPG20) is recruited to endosomes and lipid droplets and interacts with the ubiquitin E3 ligases AIP4 and AIP5. *Biochem J* **423**(1)**:** 31-39.

Eskelinen, E-L, Tanaka, Y, Saftig, P (2003) At the acidic edge: emerging functions for lysosomal membrane proteins. *Trends in Cell Biology* **13**(3)**:** 137-145.

Fang, Z, Takizawa, N, Wilson, KA, Smith, TC, Delprato, A, Davidson, MW, Lambright, DG, Luna, EJ (2010) The Membrane-Associated Protein, Supervillin, Accelerates F-Actin-Dependent Rapid Integrin Recycling and Cell Motility. *Traffic* **11**(6)**:** 782-799.

Feinstein, TN, Wehbi, VL, Ardura, JA, Wheeler, DS, Ferrandon, S, Gardella, TJ, Vilardaga, J-P (2011) Retromer terminates the generation of cAMP by internalized PTH receptors. *Nat Chem Biol* **7**(5)**:** 278-284.

Ferguson, SSG (2001) Evolving concepts in G protein-coupled receptor endocytosis: The role in receptor desensitization and signaling. *Pharmacological Reviews* **53**(1)**:** 1-24.

Ferguson, SSG (2007) Phosphorylation-independent attenuation of GPCR signalling. *Trends in Pharmacological Sciences* **28**(4)**:** 173-179.

Ferguson, SSG, Caron, MG (1998) G protein-coupled receptor adaptation mechanisms. *Seminars in Cell & Developmental Biology* **9**(2)**:** 119-127.

Forbes, JR, Gros, P (2001) Divalent-metal transport by NRAMP proteins at the interface of host-pathogen interactions. *Trends in Microbiology* **9**(8)**:** 397-403.

Fourgeaud, L, Bessis, A-S, Rossignol, F, Pin, J-P, Olivo-Marin, J-C, Hemar, A (2003) The Metabotropic Glutamate Receptor mGluR5 Is Endocytosed by a Clathrin-independent Pathway. *Journal of Biological Chemistry* **278**(14)**:** 12222-12230.

Fraile-Ramos, A, Kohout, TA, Waldhoer, M, Marsh, M (2003) Endocytosis of the Viral Chemokine Receptor US28 Does Not Require Beta-Arrestins But Is Dependent on the Clathrin-Mediated Pathway. *Traffic* **4**(4)**:** 243-253.

Fredriksson, R, Lagerstrom, MC, Lundin, L-G, Schioth, HB (2003) The G-Protein-Coupled Receptors in the Human Genome Form Five Main Families. Phylogenetic Analysis, Paralogon Groups, and Fingerprints. *Molecular Pharmacology* **63**(6)**:** 1256-1272.

Fuchs, S, Sela, M (1963) Studies on Chemical Basis of Antigenicity of Proteins 6. Antigenic Specifcity of Some Synthetic Polypetides Containing Tyrosine. *Biochemical Journal* **87**(1)**:** 70-79.

Gage, RM, Kim, K-A, Cao, TT, von Zastrow, M (2001) A Transplantable Sorting Signal That Is Sufficient to Mediate Rapid Recycling of G Protein-coupled Receptors. *Journal of Biological Chemistry* **276**(48)**:** 44712-44720.

Gaidarov, I, Krupnick, JG, Falck, JR, Benovic, JL, Keen, JH (1999) Arrestin function in G protein-coupled receptor endocytosis requires phosphoinositide binding. *EMBO J* **18**(4)**:** 871-881.

Gesty-Palmer, D, Luttrell, LM, Richard, RN (2011) Refining Efficacy: Exploiting Functional Selectivity for Drug Discovery. In: *Advances in Pharmacology* Vol. Volume 62, pp 79-107: Academic Press.

Gesty-Palmer, D, Shewy, HE, Kohout, TA, Luttrell, LM (2005) β-Arrestin 2 Expression Determines the Transcriptional Response to Lysophosphatidic Acid Stimulation in Murine Embryo Fibroblasts. *Journal of Biological Chemistry* **280**(37)**:** 32157-32167.

Gether, U (2000) Uncovering Molecular Mechanisms Involved in Activation of G Protein-Coupled Receptors. *Endocrine Reviews* **21**(1)**:** 90-113.

Giebing, G, Tolle, M, Jurgensen, J, Eichhorst, J, Furkert, J, Beyermann, M, Neuschafer-Rube, F, Rosenthal, W, Zidek, W, van der Giet, M, Oksche, A (2005) Arrestin-Independent Internalization and Recycling of the Urotensin Receptor Contribute to Long-Lasting Urotensin II-Mediated Vasoconstriction. *Circulation Research* **97**(7)**:** 707-715.

Girnita, L, Shenoy, SK, Sehat, B, Vasilcanu, R, Girnita, A, Lefkowitz, RJ, Larsson, O (2005) b-Arrestin Is Crucial for Ubiquitination and Down-regulation of the Insulin-like Growth Factor-1 Receptor by Acting as Adaptor for the MDM2 E3 Ligase. *Journal of Biological Chemistry* **280**(26)**:** 24412-24419.

Goldstein, DS (2001) Adrenaline and Noradrenaline. In: *The Autonomic Nervous System in Health and Disease*: John Wiley & Sons, Ltd.

Gong, K, Li, Z, Xu, M, Du, J, Lv, Z, Zhang, Y (2008) A Novel Protein Kinase A-independent, β-Arrestin-1-dependent Signaling Pathway for p38 Mitogen-activated Protein Kinase Activation by β2-Adrenergic Receptors. *Journal of Biological Chemistry* **283**(43)**:** 29028-29036.

Goodman, OB, Krupnick, JG, Santini, F, Gurevich, VV, Penn, RB, Gagnon, AW, Keen, JH, Benovic, JL (1996a) β-Arrestin acts as a clathrin adaptor in endocytosis of the β2-adrenergic receptor. *Nature* **383**(6599)**:** 447-450.

Goodman, OB, Krupnick, JG, Santini, F, Gurevich, VV, Penn, RB, Gagnon, AW, Keen, JH, Benovic, JL (1996b) beta-arrestin acts as a clathrin adaptor in endocytosis of the beta(2)-adrenergic receptor. *Nature* **383**(6599)**:** 447-450.

Grace, CRR, Perrin, MH, DiGruccio, MR, Miller, CL, Rivier, JE, Vale, WW, Riek, R (2004) NMR structure and peptide hormone binding site of the first extracellular domain of a type B1 G protein-coupled receptor. *Proceedings*

of the National Academy of Sciences of the United States of America **101**(35)**:** 12836-12841.

Granier, S, Manglik, A, Kruse, AC, Kobilka, TS, Thian, FS, Weis, WI, Kobilka, BK (2012) Structure of the δ-opioid receptor bound to naltrindole. *Nature* **485**(7398)**:** 400-404.

Guetta, D, Langou, K, Grunwald, D, Klein, Gr, Aubry, L (2010) FYVE-Dependent Endosomal Targeting of an Arrestin-Related Protein in Amoeba. *Plos One* **5**(12)**:** e15249.

Gullapalli, A, Wolfe, BL, Griffin, CT, Magnuson, T, Trejo, J (2006) An Essential Role for SNX1 in Lysosomal Sorting of Protease-activated Receptor-1: Evidence for Retromer-, Hrs-, and Tsg101-independent Functions of Sorting Nexins. *Molecular Biology of the Cell* **17**(3)**:** 1228-1238.

Gupta, R, Kus, B, Fladd, C, Wasmuth, J, Tonikian, R, Sidhu, S, Krogan, NJ, Parkinson, J, Rotin, D (2007) Ubiquitination screen using protein microarrays for comprehensive identification of Rsp5 substrates in yeast. *Mol Syst Biol* **3:** 1-12.

Gurevich, E, Gurevich, V (2006a) Arrestins: ubiquitous regulators of cellular signaling pathways. *Genome Biology* **7**(9)**:** 236.

Gurevich, VV, Dion, SB, Onorato, JJ, Ptasienski, J, Kim, CM, Sterne-Marr, R, Hosey, MM, Benovic, JL (1995) Arrestin Interactions with G Protein-coupled Receptors. *Journal of Biological Chemistry* **270**(2)**:** 720-731.

Gurevich, VV, Gurevich, EV (2008a) GPCR monomers and oligomers: it takes all kinds. *Trends in Neurosciences* **31**(2)**:** 74-81.

Gurevich, VV, Gurevich, EV (2006b) The structural basis of arrestin-mediated regulation of G-protein-coupled receptors. *Pharmacology & Therapeutics* **110**(3)**:** 465-502.

Gurevich, VV, Gurevich, EV, Cleghorn, WM (2008b) Arrestins as multi-functional signaling adaptors. *Handb Exp Pharmacol* **186:** 15-37.

Gurevich, VV, Gurevich, EV, Cleghorn, WM, Klussmann, E, Scott, J (2008c) Arrestins as Multi-Functional Signaling Adaptors
Protein-Protein Interactions as New Drug Targets In: Vol. 186, pp 15-37: Springer Berlin Heidelberg.

György, B, Szabó, T, Pásztói, M, Pál, Z, Misják, P, Aradi, B, László, V, Pállinger, É, Pap, E, Kittel, Á, Nagy, G, Falus, A, Buzás, E (2011) Membrane vesicles, current state-of-the-art: emerging role of extracellular vesicles. *Cellular and Molecular Life Sciences* **68**(16)**:** 2667-2688.

Haider, AJ, Briggs, D, Self, TJ, Chilvers, HL, Holliday, ND, Kerr, ID (2011) Dimerization of ABCG2 Analysed by Bimolecular Fluorescence Complementation. *Plos One* **6**(10)**:** e25818.

Halls, ML, Cooper, DMF (2010) Sub-picomolar relaxin signalling by a pre-assembled RXFP1, AKAP79, AC2, β-arrestin 2, PDE4D3 complex. *EMBO J* **29**(16)**:** 2772-2787.

Han, M, Gurevich, VV, Vishnivetskiy, SA, Sigler, PB, Schubert, C (2001) Crystal Structure of β-Arrestin at 1.9 A: Possible Mechanism of Receptor Binding and Membrane Translocation. *Structure* **9**(9)**:** 869-880.

Hanson, SM, Vishnivetskiy, SA, Hubbell, WL, Gurevich, VV (2007) Opposing Effects of Inositol Hexakisphosphate on Rod Arrestin and Arrestin2 Self-Association. *Biochemistry* **47**(3)**:** 1070-1075.

Hanyaloglu, AC, Zastrow, Mv (2008) Regulation of GPCRs by Endocytic Membrane Trafficking and Its Potential Implications. *Annual Review of Pharmacology and Toxicology* **48**(1)**:** 537-568.

Hartley, JL, Temple, GF, Brasch, MA (2000) DNA Cloning Using In Vitro Site-Specific Recombination. *Genome Research* **10**(11)**:** 1788-1795.

Harvey, KF, Shearwin-Whyatt, LM, Fotia, A, Parton, RG, Kumar, S (2002) N4WBP5, a Potential Target for Ubiquitination by the Nedd4 Family of Proteins, Is a Novel Golgi-associated Protein. *Journal of Biological Chemistry* **277**(11)**:** 9307-9317.

Hatakeyama, R, Kamiya, M, Takahara, T, Maeda, T (2010) Endocytosis of the Aspartic Acid/Glutamic Acid Transporter Dip5 Is Triggered by Substrate-Dependent Recruitment of the Rsp5 Ubiquitin Ligase via the Arrestin-Like Protein Aly2. *Mol. Cell. Biol.* **30**(24)**:** 5598-5607.

Henne, WM, Boucrot, E, Meinecke, M, Evergren, E, Vallis, Y, Mittal, R, McMahon, HT (2010) FCHo Proteins Are Nucleators of Clathrin-Mediated Endocytosis. *Science* **328**(5983)**:** 1281-1284.

Henry, AG, White, IJ, Marsh, M, von Zastrow, M, Hislop, JN (2011) The Role of Ubiquitination in Lysosomal Trafficking of δ-Opioid Receptors. *Traffic* **12**(2)**:** 170-184.

Herrador, A, Herranz, S, Lara, D, Vincent, O (2009) Recruitment of the ESCRT machinery to a putative seven-transmembrane-domain receptor is mediated by an arrestin-related protein. *Mol. Cell. Biol.* **30**(4)**:** 897-907.

Herranz, S, Rodriguez, JM, Bussink, HJ, Sanchez-Ferrero, JC, Arst, HN, Penalva, MA, Vincent, O (2005) Arrestin-related proteins mediate pH signaling in fungi. *Proceedings of the National Academy of Sciences of the United States of America* **102**(34)**:** 12141-12146.

Hervas-Aguilar, A, Galindo, A, Penalva, MA (2010) Receptor-independent Ambient pH Signaling by Ubiquitin Attachment to Fungal Arrestin-like PalF. *Journal of Biological Chemistry* **285**(23)**:** 18095-18102.

Hirsch, JA, Schubert, C, Gurevich, VV, Sigler, PB (1999) The 2.8 A Crystal Structure of Visual Arrestin: a Model for Arrestin's Regulation. *Cell* **97**(2)**:** 257-269.

Hislop, JN, Marley, A, von Zastrow, M (2004) Role of Mammalian Vacuolar Protein-sorting Proteins in Endocytic Trafficking of a Non-ubiquitinated G Protein-coupled Receptor to Lysosomes. *Journal of Biological Chemistry* **279**(21)**:** 22522-22531.

Hislop, JN, von Zastrow, M (2011) Role of Ubiquitination in Endocytic Trafficking of G-Protein-Coupled Receptors. *Traffic* **12**(2)**:** 137-148.

Hoeller, D, Crosetto, N, Blagoev, B, Raiborg, C, Tikkanen, R, Wagner, S, Kowanetz, K, Breitling, R, Mann, M, Stenmark, H, Dikic, I (2006) Regulation of ubiquitin-binding proteins by monoubiquitination. *Nat Cell Biol* **8**(2)**:** 163-169.

Hoeppner, CZ, Cheng, N, Ye, RD (2012) Identification of a Nuclear Localization Sequence in β-Arrestin-1 and Its Functional Implications. *Journal of Biological Chemistry* **287**(12)**:** 8932-8943.

Hopp, TP, Woods, KR (1981) Prediction of Protein Antigenic Determinants From Amino-Acid-Sequences. *Proceedings of the National Academy of Sciences* **78**(6)**:** 3824-3828.

Horvath, CAJ, Vanden Broeck, D, Boulet, GlAV, Bogers, J, De Wolf, MJS (2007) Epsin: Inducing membrane curvature. *The International Journal of Biochemistry & Cell Biology* **39**(10)**:** 1765-1770.

Hu, LA, Tang, Y, Miller, WE, Cong, M, Lau, AG, Lefkowitz, RJ, Hall, RA (2000) β1-Adrenergic Receptor Association with PSD-95. *Journal of Biological Chemistry* **275**(49)**:** 38659-38666.

Hui, STY, Andres, AM, Miller, AK, Spann, NJ, Potter, DW, Post, NM, Chen, AZ, Sachithanantham, S, Jung, DY, Kim, JK, Davis, RA (2008) Txnip balances metabolic and growth signaling via PTEN disulfide reduction. *Proceedings of the National Academy of Sciences* **105**(10)**:** 3921-3926.

Hurowitz, EH, Melnyk, JM, Chen, Y, Kouros-Mehr, H, Simon, MI, Shizuya, H (2000) Genomic characterization of the human heterotrimeric G protein alpha, beta, and gamma subunit genes. *DNA Research* **7**(2)**:** 111-120.

Iguchi, T, Sakata, K, Yoshizaki, K, Tago, K, Mizuno, N, Itoh, H (2008) Orphan G Protein-coupled Receptor GPR56 Regulates Neural Progenitor Cell Migration via a Gα12/13 and Rho Pathway. *Journal of Biological Chemistry* **283**(21)**:** 14469-14478.

Imamura, T, Huang, J, Dalle, S, Ugi, S, Usui, I, Luttrell, LM, Miller, WE, Lefkowitz, RJ, Olefsky, JM (2001) β-Arrestin-mediated Recruitment of the Src Family Kinase Yes Mediates Endothelin-1-stimulated Glucose Transport. *Journal of Biological Chemistry* **276**(47)**:** 43663-43667.

Inoue, Y, Imamura, T (2008) Regulation of TGF-β family signaling by E3 ubiquitin ligases. *Cancer Science* **99**(11)**:** 2107-2112.

Ish-Horowicz, D, Burke, JF (1981) Rapid and efficient cosmid cloning. *Nucleic Acids Research* **9**(13)**:** 2989-2898.

Isik, N, Hereld, D, Jin, T (2008) Fluorescence Resonance Energy Transfer Imaging Reveals that Chemokine-Binding Modulates Heterodimers of CXCR4 and CCR5 Receptors. *Plos One* **3**(10)**:** e3424.

Junn, E, Han, SH, Im, JY, Yang, Y, Cho, EW, Um, HD, Kim, DK, Lee, KW, Han, PL, Rhee, SG, Choi, I (2000) Vitamin D3 Up-Regulated Protein 1 Mediates Oxidative Stress Via Suppressing the Thioredoxin Function. *The Journal of Immunology* **164**(12)**:** 6287-6295.

Kallal, L, Gagnon, AW, Penn, RB, Benovic, JL (1998) Visualization of Agonist-induced Sequestration and Down-regulation of a Green Fluorescent Protein-tagged β2-Adrenergic Receptor. *Journal of Biological Chemistry* **273**(1)**:** 322-328.

Kargl, J, Balenga, NA, Platzer, W, Martini, L, Whistler, JL, Waldhoer, M (2011) The GPCR - associated sorting protein 1 regulates ligand-induced downregulation of GPR55. *British Journal of Pharmacology* **165**(8)**:** 2611-2619.

Kee, Y, Munoz, W, Lyon, N, Huibregtse, JM (2006) The Deubiquitinating Enzyme Ubp2 Modulates Rsp5-dependent Lys63-linked Polyubiquitin Conjugates in Saccharomyces cerevisiae. *Journal of Biological Chemistry* **281**(48)**:** 36724-36731.

Kenakin, T (2004) Principles: Receptor theory in pharmacology. *Trends in Pharmacological Sciences* **25**(4)**:** 186-192.

Keov, P, Sexton, PM, Christopoulos, A (2010) Allosteric modulation of G protein-coupled receptors: A pharmacological perspective. *Neuropharmacology* **60**(1)**:** 24-35.

Kerppola, TK (2008) Biomolecular fluorescence complementation (BiFC) analysis as a probe of protein interactions in living cells. *Annual Review of Biophysics* **37:** 465-487.

Kilpatrick, LE, Briddon, SJ, Hill, SJ, Holliday, ND (2010) Quantitative analysis of neuropeptide Y receptor association with β-arrestin2 measured by bimolecular fluorescence complementation. *British Journal of Pharmacology* **160**(4)**:** 892-906.

Kim, JA, Bartlett, S, He, L, Nielsen, CK, Chang, AM, Kharazia, V, Waldhoer, M, Ou, CJ, Taylor, S, Ferwerda, M, Cado, D, Whistler, J (2008) Morphine-Induced Receptor Endocytosis in a Novel Knockin Mouse Reduces Tolerance and Dependence. *Current Biology* **18**(2)**:** 129-135.

Kim, M, Hanson, SM, Vishnivetskiy, SA, Song, X, Cleghorn, WM, Hubbell, WL, Gurevich, VV (2011) Robust Self-Association Is a Common Feature of Mammalian Visual Arrestin-1. *Biochemistry* **50**(12)**:** 2235-2242.

Klaus, A, Birchmeier, W (2008) Wnt signalling and its impact on development and cancer. *Nat Rev Cancer* **8**(5)**:** 387-398.

Kniazeff, J, Prezeau, L, Rondard, P, Pin, J-P, Goudet, C (2011) Dimers and beyond: The functional puzzles of class C GPCRs. *Pharmacology & Therapeutics* **130**(1)**:** 9-25.

Kobilka, B (1992) Adrenergic Receptors as Models for G Protein-Coupled Receptors. *Annual Review of Neuroscience* **15**(1)**:** 87-114.

Komuro, A, Imamura, T, Saitoh, M, Yoshida, Y, Yamori, T, Miyazono, K, Miyazawa, K (2004) Negative regulation of transforming growth factor-β (TGF-β) signaling by WW domain-containing protein 1 (WWP1). *Oncogene* **23**(41)**:** 6914-6923.

Krupnick, JG, Benovic, JL (1998) The Role of Receptor Kinases and Arrestins in G Protein-Coupled Recetor Regulation. *Annual Review of Pharmacology and Toxicology* **38**(1)**:** 289-319.

Krupnick, JG, Goodman, OB, Keen, JH, Benovic, JL (1997a) Arrestin/Clathrin Interaction. *Journal of Biological Chemistry* **272**(23)**:** 15011-15016.

Krupnick, JG, Santini, F, Gagnon, AW, Keen, JH, Benovic, JL (1997b) Modulation of the Arrestin-Clathrin Interaction in Cells. *Journal of Biological Chemistry* **272**(51)**:** 32507-32512.

Kundra, R, Kornfeld, S (1999) Asparagine-linked Oligosaccharides Protect Lamp-1 and Lamp-2 from Intracellular Proteolysis. *Journal of Biological Chemistry* **274**(43)**:** 31039-31046.

Kyte, J, Doolittle, RF (1982) A simple method for displaying the hydropathic character of a protein. *Journal of Molecular Biology* **157**(1)**:** 105-132.

Laemmli, UK (1970) Cleavage of Structural Proteins during the Assembly of the Head of Bacteriophage T4. *Nature* **227**(5259)**:** 680-685.

Lagerstrom, MC, Schioth, HB (2008) Structural diversity of G protein-coupled receptors and significance for drug discovery. *Nat Rev Drug Discov* **7**(4)**:** 339-357.

Lakshmikanthan, V, Zou, L, Kim, JI, Michal, A, Nie, Z, Messias, NC, Benovic, JL, Daaka, Y (2009) Identification of βArrestin2 as a corepressor of androgen receptor signaling in prostate cancer. *Proceedings of the National Academy of Sciences* **106**(23)**:** 9379-9384.

Laporte, SA, Oakley, RH, Holt, JA, Barak, LS, Caron, MG (2000) The Interaction of beta-Arrestin with the AP-2 Adaptor Is Required for the Clustering of beta 2-Adrenergic Receptor into Clathrin-coated Pits. *J. Biol. Chem.* **275**(30)**:** 23120-23126.

Laporte, SpA, Oakley, RH, Zhang, J, Holt, JA, Ferguson, SSG, Caron, MG, Barak, LS (1999) The β2-adrenergic receptor/βarrestin complex recruits the clathrin adaptor AP-2 during endocytosis. *Proceedings of the National Academy of Sciences* **96**(7)**:** 3712-3717.

Lavezzari, G, Roche, KW (2007) Constitutive endocytosis of the metabotropic glutamate receptor mGluR7 is clathrin-independent. *Neuropharmacology* **52**(1)**:** 100-107.

Law, P-Y, Wong, YH, Loh, HH (2000) Molecular Mechanisms and Regulation of Opioid Receptor Signaling. *Annual Review of Pharmacology and Toxicology* **40**(1)**:** 389-430.

Lebon, G, Bennett, K, Jazayeri, A, Tate, CG (2011a) Thermostabilisation of an Agonist-Bound Conformation of the Human Adenosine A2A Receptor. *Journal of Molecular Biology* **409**(3)**:** 298-310.

Lebon, G, Warne, T, Edwards, PC, Bennett, K, Langmead, CJ, Leslie, AGW, Tate, CG (2011b) Agonist-bound adenosine A2A receptor structures reveal common features of GPCR activation. *Nature* **474**(7352)**:** 521-525.

Leduc, M, Breton, B, Gales, C, Le Gouill, C, Bouvier, M, Chemtob, S, Heveker, N (2009) Functional Selectivity of Natural and Synthetic Prostaglandin EP4 Receptor Ligands. *Journal of Pharmacology and Experimental Therapeutics* **331**(1)**:** 297-307.

Leftowitz, RJ, Shenoy, SK (2005) Transduction of receptor signals by beta-arrestins. *Science* **308**(5721)**:** 512-517.

Liggett, SB, Freedman, NJ, Schwinn, DA, Lefkowitz, RJ (1993) Structural basis for receptor subtype-specific regulation revealed by a chimeric beta 3/beta 2-adrenergic receptor. *Proceedings of the National Academy of Sciences* **90**(8)**:** 3665-3669.

Lin, CH, MacGum, JA, Chu, T, Stefan, CJ, Emr, SD (2008) Arrestin-Related Ubiquitin-Ligase Adaptors Regulate Endocytosis and Protein Turnover at the Cell Surface. *Cell* **135**(4)**:** 714-725.

Lin, F-T, Daaka, Y, Lefkowitz, RJ (1998) β-Arrestins Regulate Mitogenic Signaling and Clathrin-mediated Endocytosis of the Insulin-like Growth Factor I Receptor. *Journal of Biological Chemistry* **273**(48)**:** 31640-31643.

Lisenbee, CS, Dong, M, Miller, LJ (2005) Paired Cysteine Mutagenesis to Establish the Pattern of Disulfide Bonds in the Functional Intact Secretin Receptor. *Journal of Biological Chemistry* **280**(13)**:** 12330-12338.

Liu, JJ, Horst, R, Katritch, V, Stevens, RC, Wuthrich, K (2012) Biased Signaling Pathways in β2-Adrenergic Receptor Characterized by 19F-NMR. *Science* **335**(6072)**:** 1106-1110.

Liu, R, Ramani, B, Soto, D, De Arcangelis, V, Xiang, Y (2009) Agonist Dose-dependent Phosphorylation by Protein Kinase A and G Protein-coupled Receptor Kinase Regulates β2 Adrenoceptor Coupling to Gi Proteins in Cardiomyocytes. *Journal of Biological Chemistry* **284**(47)**:** 32279-32287.

Lohse, MJ, Andexinger, S, Pitcher, J, Trukawinski, S, Codina, J, Faure, JP, Caron, MG, Lefkowitz, RJ (1992) Receptor-specific desensitization with purified proteins. Kinase dependence and receptor specificity of beta-arrestin and arrestin in the beta 2-adrenergic receptor and rhodopsin systems. *J. Biol. Chem.* **267**(12)**:** 8558-8564.

Louie, D, Serwer, P (1994) Quantification of the Effect of Excluded Volume on Double-stranded DNA. *Journal of Molecular Biology* **242**(4)**:** 547-558.

Lu, K, Li, P, Zhang, M, Xing, G, Li, X, Zhou, W, Bartlam, M, Zhang, L, Rao, Z, He, F (2011) Pivotal Role of the C2 Domain of the Smurf1 Ubiquitin Ligase in Substrate Selection. *Journal of Biological Chemistry* **286**(19)**:** 16861-16870.

Luan, B, Zhao, J, Wu, H, Duan, B, Shu, G, Wang, X, Li, D, Jia, W, Kang, J, Pei, G (2009) Deficiency of a β-arrestin-2 signal complex contributes to insulin resistance. *Nature* **457**(7233)**:** 1146-1149.

Luker, KE, Gupta, M, Luker, GD (2009) Imaging chemokine receptor dimerization with firefly luciferase complementation. *The FASEB Journal* **23**(3)**:** 823-834.

Luttrell, LM, Ferguson, SSG, Daaka, Y, Miller, WE, Maudsley, S, Della Rocca, GJ, Lin, FT, Kawakatsu, H, Owada, K, Luttrell, DK, Caron, MG, Lefkowitz, RJ (1999) β-Arrestin-Dependent Formation of β2 Adrenergic Receptor-Src Protein Kinase Complexes. *Science* **283**(5402)**:** 655-661.

Luttrell, LM, Lefkowitz, RJ (2002) The role of β-arrestins in the termination and transduction of G-protein-coupled receptor signals. *Journal of Cell Science* **115**(3)**:** 455-465.

Maccheroni Jr, W, May, GS, Martinez-Rossi, NM, Rossi, A (1997) The sequence of palF, an environmental pH response gene in Aspergillus nidulans. *Gene* **194**(2)**:** 163-167.

Macdonald, C, Stringer, DK, Piper, RC (2011) Sna3 is an Rsp5 Adaptor Protein that Relies on Ubiquitination for its MVB Sorting. *Traffic***:** Epub ahead of print doi: 10.1111/j.1600-0854.2011.01326.x.

MacGurn, JA, Hsu, P-C, Emr, SD (2012) Ubiquitin and Membrane Protein Turnover: From Cradle to Grave. *Annual Review of Biochemistry* **81**(1)**:** 231-259.

Macias, MJ, Wiesner, S, Sudol, M (2002) WW and SH3 domains, two different scaffolds to recognize proline-rich ligands. *Febs Letters* **513**(1)**:** 30-37.

Magalhaes, AC, Dunn, H, Ferguson, SSG (2012) Regulation of GPCR activity, trafficking and localization by GPCR-interacting proteins. *British Journal of Pharmacology* **165**(6)**:** 1717-1736.

Malik, R, Marchese, A (2010) Arrestin-2 Interacts with the ESCRT Machinery to Modulate Endosomal Sorting of CXCR4. *Mol. Biol. Cell* **21:** 2529-2541.

Marchese, A, Raiborg, C, Santini, F, Keen, JH, Stenmark, H, Benovic, JL (2003) The E3 Ubiquitin Ligase AIP4 Mediates Ubiquitination and Sorting of the G Protein-Coupled Receptor CXCR4. *Developmental Cell* **5**(5)**:** 709-722.

Margeta-Mitrovic, M, Jan, YN, Jan, LY (2000) A Trafficking Checkpoint Controls GABAB Receptor Heterodimerization. *Neuron* **27**(1)**:** 97-106.

Marion, S, Oakley, RH, Kim, K-M, Caron, MG, Barak, LS (2006) A beta-Arrestin Binding Determinant Common to the Second Intracellular Loops of Rhodopsin Family G Protein-coupled Receptors. *J. Biol. Chem.* **281**(5)**:** 2932-2938.

Marley, A, von Zastrow, M (2010) Dysbindin Promotes the Post-Endocytic Sorting of G Protein-Coupled Receptors to Lysosomes. *Plos One* **5**(2)**:** e9325.

Martin-Serrano, J, Neil, SJD (2011) Host factors involved in retroviral budding and release. *Nat Rev Micro* **9**(7)**:** 519-531.

Mattheyses, AL, Simon, SM, Rappoport, JZ (2010) Imaging with total internal reflection fluorescence microscopy for the cell biologist. *Journal of Cell Science* **123**(21)**:** 3621-3628.

McDonald, PH, Chow, C-W, Miller, WE, Laporte, SpA, Field, ME, Lin, F-T, Davis, RJ, Lefkowitz, RJ (2000) β-Arrestin 2: A Receptor-Regulated MAPK Scaffold for the Activation of JNK3. *Science* **290**(5496)**:** 1574-1577.

McMahon, HT, Boucrot, E (2011) Molecular mechanism and physiological functions of clathrin-mediated endocytosis. *Nat Rev Mol Cell Biol* **12**(8)**:** 517-533.

Meckes, DG, Raab-Traub, N (2011) Microvesicles and Viral Infection. *Journal of Virology* **85**(24)**:** 12844-12854.

Milligan, G (2007) G protein-coupled receptor dimerisation: Molecular basis and relevance to function. *Biochimica et Biophysica Acta (BBA) - Biomembranes* **1768**(4)**:** 825-835.

Milligan, G, Kostenis, E (2006) Heterotrimeric G-proteins: a short history. *British Journal of Pharmacology* **147**(S1)**:** S46-S55.

Mo, W, Zhang, L, Yang, G, Zhai, J, Hu, Z, Chen, Y, Chen, X, Hui, L, Huang, R, Hu, G (2008) Nuclear β-Arrestin1 Functions as a Scaffold for the Dephosphorylation of STAT1 and Moderates the Antiviral Activity of IFN-γ. *Molecular Cell* **31**(5)**:** 695-707.

Moore, RH, Millman, EE, Alpizar-Foster, E, Dai, W, Knoll, BJ (2004) Rab11 regulates the recycling and lysosome targeting of β2-adrenergic receptors. *J Cell Sci* **117**(15)**:** 3107-3117.

Mosser, V, Jones, K, Hoffman, K, McCarty, N, Jackson, D (2008) Differential role of beta-arrestin ubiquitination in agonist-promoted down-regulation of M1 vs M2 muscarinic acetylcholine receptors. *Journal of Molecular Signaling* **3**(1)**:** 20.

Mund, T, Pelham, HRB (2009) Control of the activity of WW-HECT domain E3 ubiquitin ligases by NDFIP proteins. *EMBO Rep* **10**(5)**:** 501-507.

Murone, M, Rosenthal, A, de Sauvage, FJ (1999) Sonic hedgehog signaling by the Patched-Smoothened receptor complex. *Current Biology* **9**(2)**:** 76-84.

Nabhan, JF, Hu, R, Oh, RS, Cohen, SN, Lu, Q (2012) Formation and release of arrestin domain-containing protein 1-mediated microvesicles (ARMMs) at plasma membrane by recruitment of TSG101 protein. *Proceedings of the National Academy of Sciences* **109**(11)**:** 4146-4151.

Nabhan, JF, Pan, H, Lu, Q (2010) Arrestin domain-containing protein 3 recruits the NEDD4 E3 ligase to mediate ubiquitination of the β2-adrenergic receptor. *EMBO Rep* **11**(8)**:** 605-611.

Nantel, F, Bonin, H, Emorine, LJ, Zilberfarb, V, Strosberg, AD, Bouvier, M, Marullo, S (1993) The human beta 3-adrenergic receptor is resistant to short term agonist-promoted desensitization. *Molecular Pharmacology* **43**(4)**:** 548-555.

Nelson, CD, Perry, SJ, Regier, DS, Prescott, SM, Topham, MK, Lefkowitz, RJ (2007) Targeting of Diacylglycerol Degradation to M1 Muscarinic Receptors by β-Arrestins. *Science* **315**(5812)**:** 663-666.

Nichols, CD, Sanders-Bush, E (2004) Molecular genetic responses to lysergic acid diethylamide include transcriptional activation of MAP kinase phosphatase-1, C/EBP-beta and ILAD-1, a novel gene with homology to arrestins. *Journal of Neurochemistry* **90**(3)**:** 576-584.

Nikko, E, Pelham, HRB (2009) Arrestin-mediated endocytosis of yeast plasma membrane transporters. *Traffic* **10**(12)**:** 1856-1867.

Nikko, E, Sullivan, JA, Pelham, HRB (2008) Arrestin-like proteins mediate ubiquitination and endocytosis of the yeast metal transporter Smf1. *Embo Reports* **9**(12)**:** 1216-1221.

Nisar, S, Kelly, E, Cullen, PJ, Mundell, SJ (2010) Regulation of P2Y1 Receptor Traffic by Sorting Nexin 1 is Retromer Independent. *Traffic* **11**(4)**:** 508-519.

Nishiyama, A, Matsui, M, Iwata, S, Hirota, K, Masutani, H, Nakamura, H, Takagi, Y, Sono, H, Gon, Y, Yodoi, J (1999) Identification of Thioredoxin-binding Protein-2/Vitamin D3 Up-regulated Protein 1 as a Negative Regulator of Thioredoxin Function and Expression. *Journal of Biological Chemistry* **274**(31)**:** 21645-21650.

O'Donnell, AF, Apffel, A, Gardner, RG, Cyert, MS (2010) α-Arrestins Aly1 and Aly2 Regulate Intracellular Trafficking in Response to Nutrient Signaling. *Molecular Biology of the Cell* **21**(20)**:** 3552-3566.

Oakley, RH, Laporte, SA, Holt, JA, Barak, LS, Caron, MG (1999) Association of beta-arrestin with G protein-coupled receptors during clathrin-mediated endocytosis dictates the profile of receptor resensitization. *Journal of Biological Chemistry* **274**(45)**:** 32248-32257.

Oakley, RH, Laporte, SA, Holt, JA, Barak, LS, Caron, MG (2001) Molecular determinants underlying the formation of stable intracellular G protein-coupled receptor-beta-arrestin complexes after receptor endocytosis. *Journal of Biological Chemistry* **276**(22)**:** 19452-19460.

Oakley, RH, Laporte, SK, Holt, JA, Caron, MG, Barak, LS (2000) Differential affinities of visual arrestin, beta arrestin1, and beta arrestin2 for G protein-coupled receptors delineate two major classes of receptors. *Journal of Biological Chemistry* **275**(22)**:** 17201-17210.

Odley, A, Hahn, HS, Lynch, RA, Marreez, Y, Osinska, H, Robbins, J, Dorn, GW (2004) Regulation of cardiac contractility by Rab4-modulated β2-adrenergic receptor recycling. *Proceedings of the National Academy of Sciences of the United States of America* **101**(18)**:** 7082-7087.

Oka, S, Masutani, H, Liu, WR, Horita, H, Wang, DM, Kizaka-Kondoh, S, Yodoi, J (2006) Thioredoxin-binding protein-2-like inducible membrane protein is a novel vitamin D3 and peroxisome proliferator-activated receptor (PPAR)gamma ligand target protein that regulates PPAR gamma signaling. *Endocrinology* **147**(2)**:** 733-743.

Onrust, R, Herzmark, P, Chi, P, Garcia, PD, Lichtarge, O, Kingsley, C, Bourne, HR (1997) Receptor and βγ Binding Sites in the α Subunit of the Retinal G Protein Transducin. *Science* **275**(5298)**:** 381-384.

Overington, JP, Al-Lazikani, B, Hopkins, AL (2006) How many drug targets are there? *Nat Rev Drug Discov* **5**(12)**:** 993-996.

Paing, MM, Johnston, CA, Siderovski, DP, Trejo, J (2006) Clathrin Adaptor AP2 Regulates Thrombin Receptor Constitutive Internalization and Endothelial Cell Resensitization. *Molecular and Cellular Biology* **26**(8)**:** 3231-3242.

Paing, MM, Stutts, AB, Kohout, TA, Lefkowitz, RJ, Trejo, J (2002) β-Arrestins Regulate Protease-activated Receptor-1 Desensitization but Not Internalization or Down-regulation. *Journal of Biological Chemistry* **277**(2)**:** 1292-1300.

Pampillo, M, Camuso, N, Taylor, JE, Szereszewski, JM, Ahow, MR, Zajac, M, Millar, RP, Bhattacharya, M, Babwah, AV (2009) Regulation of GPR54 Signaling by GRK2 and β-Arrestin. *Molecular Endocrinology* **23**(12)**:** 2060-2074.

Parent, A, Hamelin, E, Germain, P, Parent, JL (2009) Rab11 regulates the recycling of the beta(2)-adrenergic receptor through a direct interaction. *Biochemical Journal* **418:** 163-172.

Parikh, H, Carlsson, E, Chutkow, WA, Johansson, LE, Storgaard, H, Poulsen, P, Saxena, R, Ladd, C, Schulze, PC, Mazzini, MJ, Jensen, CB, Krook, A, Bjornholm, M, Tornqvist, H, Zierath, JR, Ridderstrale, M, Altshuler, D, Lee, RT, Vaag, A, Groop, LC, Mootha, VK (2007) TXNIP Regulates Peripheral Glucose Metabolism in Humans. *PLoS Med* **4**(5)**:** e158.

Park, JH, Scheerer, P, Hofmann, KP, Choe, H-W, Ernst, OP (2008) Crystal structure of the ligand-free G-protein-coupled receptor opsin. *Nature* **454**(7201)**:** 183-187.

Patel, HH, Murray, F, Insel, PA, Klussmann, E, Scott, J (2008) G-Protein-Coupled Receptor-Signaling Components in Membrane Raft and Caveolae Microdomains. *Handbook of Experimental Pharmacology* **186:** 167-184.

Patwari, P, Chutkow, WA, Cummings, K, Verstraeten, VLRM, Lammerding, J, Schreiter, ER, Lee, RT (2009) Thioredoxin-independent Regulation of Metabolism by the α-Arrestin Proteins. *Journal of Biological Chemistry* **284**(37)**:** 24996-25003.

Patwari, P, Emilsson, V, Schadt, Eric E, Chutkow, William A, Lee, S, Marsili, A, Zhang, Y, Dobrin, R, Cohen, David E, Larsen, PR, Zavacki, Ann M, Fong, Loren G, Young, Stephen G, Lee, Richard T (2011) The Arrestin Domain-Containing 3 Protein Regulates Body Mass and Energy Expenditure. *Cell Metabolism* **14**(5)**:** 671-683.

Patwari, P, Higgins, LJ, Chutkow, WA, Yoshioka, J, Lee, RT (2006) The Interaction of Thioredoxin with Txnip. *Journal of Biological Chemistry* **281**(31)**:** 21884-21891.

Patwari, P, Lee, RT (2012) An expanded family of arrestins regulate metabolism. *Trends in endocrinology and metabolism* **23**(5)**:** 216-222.

Pediani, JD, Colston, JF, Caldwell, D, Milligan, G, Daly, CJ, McGrath, JC (2005) β-Arrestin-Dependent Spontaneous α1a-Adrenoceptor Endocytosis

Causes Intracellular Transportation of α-Blockers via Recycling Compartments. *Molecular Pharmacology* **67**(4)**:** 992-1004.

Percherancier, Y, Berchiche, YA, Slight, I, Volkmer-Engert, R, Tamamura, H, Fujii, N, Bouvier, M, Heveker, N (2005) Bioluminescence Resonance Energy Transfer Reveals Ligand-induced Conformational Changes in CXCR4 Homo- and Heterodimers. *Journal of Biological Chemistry* **280**(11)**:** 9895-9903.

Pickart, CM (1997) Targeting of substrates to the 26S proteasome. *The FASEB Journal* **11**(13)**:** 1055-1066.

Pippig, S, Andexinger, S, Lohse, MJ (1995) Sequestration and Recycling of Beta(2),-Adrenergic Receptors Permit Receptor Resensitization. *Molecular Pharmacology* **47**(4)**:** 666-676.

Poon, LSW, Chan, ASL, Wong, YH (2009) G beta(3) forms distinct dimers with specific G gamma subunits and preferentially activates the beta(3) isoform of phospholipase C. *Cellular Signalling* **21**(5)**:** 737-744.

Povsic, TJ, Kohout, TA, Lefkowitz, RJ (2003) β-Arrestin1 Mediates Insulin-like Growth Factor 1 (IGF-1) Activation of Phosphatidylinositol 3-Kinase (PI3K) and Anti-apoptosis. *Journal of Biological Chemistry* **278**(51)**:** 51334-51339.

Qian, J, Chen, W, Lettau, M, Podda, G, Zornig, M, Kabelitz, D, Janssen, O (2006) Regulation of FasL expression: A SH3 domain containing protein family involved in the lysosomal association of FasL. *Cellular Signalling* **18**(8)**:** 1327-1337.

Raiborg, C, Stenmark, H (2009) The ESCRT machinery in endosomal sorting of ubiquitylated membrane proteins. *Nature* **458**(7237)**:** 445-452.

Ramos, BP, Arnsten, AFT (2007) Adrenergic pharmacology and cognition: Focus on the prefrontal cortex. *Pharmacology & Therapeutics* **113**(3)**:** 523-536.

Rasmussen, SGF, Choi, H-J, Fung, JJ, Pardon, E, Casarosa, P, Chae, PS, DeVree, BT, Rosenbaum, DM, Thian, FS, Kobilka, TS, Schnapp, A, Konetzki, I, Sunahara, RK, Gellman, SH, Pautsch, A, Steyaert, J, Weis, WI, Kobilka, BK (2011) Structure of a nanobody-stabilized active state of the β2 adrenoceptor. *Nature* **469**(7329)**:** 175-180.

Rauch, S, Martin-Serrano, J (2011) Multiple Interactions between the ESCRT Machinery and Arrestin-Related Proteins: Implications for PPXY-Dependent Budding. *J. Virol.* **85**(7)**:** 3546-3556.

Reiter, E, Ahn, S, Shukla, AK, Lefkowitz, RJ (2012) Molecular Mechanism of β-Arrestin-Biased Agonism at Seven-Transmembrane Receptors. *Annual Review of Pharmacology and Toxicology* **52**(1)**:** 179-197.

Rose, RH, Briddon, SJ, Holliday, ND (2010) Bimolecular fluorescence complementation: lighting up seven transmembrane domain receptor signalling networks. *British Journal of Pharmacology* **159**(4)**:** 738-750.

Rotin, D, Kumar, S (2009) Physiological functions of the HECT family of ubiquitin ligases. *Nat Rev Mol Cell Biol* **10**(6)**:** 398-409.

Saksena, S, Wahlman, J, Teis, D, Johnson, AE, Emr, SD (2009) Functional Reconstitution of ESCRT-III Assembly and Disassembly. *Cell* **136**(1)**:** 97-109.

Salvat, C, Wang, G, Dastur, A, Lyon, N, Huibregtse, JM (2004) The -4 Phenylalanine Is Required for Substrate Ubiquitination Catalyzed by HECT Ubiquitin Ligases. *Journal of Biological Chemistry* **279**(18)**:** 18935-18943.

Samama, P, Cotecchia, S, Costa, T, Lefkowitz, RJ (1993) A mutation-induced activated state of the beta 2-adrenergic receptor. Extending the ternary complex model. *Journal of Biological Chemistry* **268**(7)**:** 4625-4636.

Sandvig, K, Pust, S, Skotland, T, van Deurs, B (2011) Clathrin-independent endocytosis: mechanisms and function. *Current Opinion in Cell Biology* **23**(4)**:** 413-420.

Sara, SJ (2009) The locus coeruleus and noradrenergic modulation of cognition. *Nat Rev Neurosci* **10**(3)**:** 211-223.

Saxena, G, Chen, J, Shalev, A (2009) Intracellular Shuttling and Mitochondrial Function of Thioredoxin-interacting Protein. *Journal of Biological Chemistry* **285**(6)**:** 3997-4005.

Scarselli, M, Donaldson, JG (2009) Constitutive Internalization of G Protein-coupled Receptors and G Proteins via Clathrin-independent Endocytosis. *Journal of Biological Chemistry* **284**(6)**:** 3577-3585.

Schubert, C, Hirsch, JA, Gurevich, VV, Engelman, DM, Sigler, PB, Fleming, KG (1999) Visual Arrestin Activity May Be Regulated by Self-association. *Journal of Biological Chemistry* **274**(30)**:** 21186-21190.

Schulze, PC, Yoshioka, J, Takahashi, T, He, Z, King, GL, Lee, RT (2004) Hyperglycemia Promotes Oxidative Stress through Inhibition of Thioredoxin Function by Thioredoxin-interacting Protein. *Journal of Biological Chemistry* **279**(29)**:** 30369-30374.

Schwartz, TW, Frimurer, TM, Holst, B, Rosenkilde, MM, Elling, CE (2006) Molecular Mechanism of 7TM Receptor Activation: A Global Toggle Switch Model. *Annual Review of Pharmacology and Toxicology* **46**(1)**:** 481-519.

Seachrist, JL, Anborgh, PH, Ferguson, SSG (2000) beta(2)-adrenergic receptor internalization, endosomal sorting, and plasma membrane recycling are regulated by Rab GTPases. *Journal of Biological Chemistry* **275**(35)**:** 27221-27228.

Seachrist, JL, Ferguson, SSG (2003) Regulation of G protein-coupled receptor endocytosis and trafficking by Rab GTPases. *Life Sciences* **74**(2-3)**:** 225-235.

Shankar, H, Michal, A, Kern, RC, Kang, DS, Gurevich, VV, Benovic, JL (2010) Non-visual Arrestins Are Constitutively Associated with the Centrosome and Regulate Centrosome Function. *Journal of Biological Chemistry* **285**(11)**:** 8316-8329.

Shearwin-Whyatt, LM, Brown, DL, Wylie, FG, Stow, JL, Kumar, S (2004) N4WBP5A (Ndfip2), a Nedd4-interacting protein, localizes to multivesicular

bodies and the Golgi, and has a potential role in protein trafficking. *Journal of Cell Science* **117**(16)**:** 3679-3689.

Shenoy, SK, Barak, LS, Xiao, KH, Ahn, S, Berthouze, M, Shukla, AK, Luttrell, LM, Lefkowitz, RJ (2007) Ubiquitination of beta-arrestin links seven-transmembrane receptor endocytosis and ERK activation. *Journal of Biological Chemistry* **282:** 29549-29562.

Shenoy, SK, Drake, MT, Nelson, CD, Houtz, DA, Xiao, KH, Madabushi, S, Reiter, E, Premont, RT, Lichtarge, O, Lefkowitz, RJ (2006) beta-arrestin-dependent, G protein-independent ERK1/2 activation by the beta 2 adrenergic receptor. *Journal of Biological Chemistry* **281**(2)**:** 1261-1273.

Shenoy, SK, Lefkowitz, RJ (2003) Trafficking patterns of beta-arrestin and G protein-coupled receptors determined by the kinetics of beta-arrestin deubiquitination. *Journal of Biological Chemistry* **278**(16)**:** 14498-14506.

Shenoy, SK, McDonald, PH, Kohout, TA, Lefkowitz, RJ (2001) Regulation of receptor fate by ubiquitination of activated beta(2)-adrenergic receptor and beta-arrestin. *Science* **294**(5545)**:** 1307-1313.

Shenoy, SK, Modi, AS, Shukla, AK, Xiao, K, Berthouze, M, Ahn, S, Wilkinson, KD, Miller, WE, Lefkowitz, RJ (2009) β-Arrestin-dependent signaling and trafficking of 7-transmembrane receptors is reciprocally regulated by the deubiquitinase USP33 and the E3 ligase Mdm2. *Proceedings of the National Academy of Sciences* **106**(16)**:** 6650-6655.

Shenoy, SK, Xiao, KH, Venkataramanan, V, Snyder, PM, Freedman, NJ, Weissman, AM (2008) Nedd4 mediates agonist-dependent ubiquitination, lysosomal targeting, and degradation of the beta(2)-adrenergic receptor. *Journal of Biological Chemistry* **283**(32)**:** 22166-22176.

Shi, C, Szczesniak, A, Mao, L, Jollimore, C, Coca-Prados, M, Hung, O, Kelly, MEM (2003) A3 adenosine and CB1 receptors activate a PKC-sensitive Cl- current in human nonpigmented ciliary epithelial cells via a Gb gamma-coupled MAPK signaling pathway. *British Journal of Pharmacology* **139**(3)**:** 475-486.

Shi, H, Rojas, R, Bonifacino, JS, Hurley, JH (2006) The retromer subunit Vps26 has an arrestin fold and binds Vps35 through its C-terminal domain. *Nature Structural & Molecular Biology* **13**(6)**:** 540-548.

Shukla, AK, Violin, JD, Whalen, EJ, Gesty-Palmer, D, Shenoy, SK, Lefkowitz, RJ (2008) Distinct conformational changes in β-arrestin report biased agonism at seven-transmembrane receptors. *Proceedings of the National Academy of Sciences* **105**(29)**:** 9988-9993.

Sierra, MI, Wright, MH, Nash, PD (2010) AMSH Interacts with ESCRT-0 to Regulate the Stability and Trafficking of CXCR4. *Journal of Biological Chemistry* **285**(18)**:** 13990-14004.

Simonin, A, Fuster, D (2010) Nedd4-1 and β-Arrestin-1 Are Key Regulators of Na+/H+ Exchanger 1 Ubiquitylation, Endocytosis, and Function. *Journal of Biological Chemistry* **285**(49)**:** 38293-38303.

Simonsen, A, Lippe, R, Christoforidis, S, Gaullier, J-M, Brech, A, Callaghan, J, Toh, B-H, Murphy, C, Zerial, M, Stenmark, H (1998) EEA1 links PI(3)K

function to Rab5 regulation of endosome fusion. *Nature* **394**(6692)**:** 494-498.

Simpson, F, Hussain, NK, Qualmann, B, Kelly, RB, Kay, BK, McPherson, PS, Schmid, SL (1999) SH3-domain-containing proteins function at distinct steps in clathrin-coated vesicle formation. *Nat Cell Biol* **1**(2)**:** 119-124.

Singh, N, Pydi, SP, Upadhyaya, J, Chelikani, P (2011) Structural Basis of Activation of Bitter Taste Receptor T2R1 and Comparison with Class A G-protein-coupled Receptors (GPCRs). *Journal of Biological Chemistry* **286**(41)**:** 36032-36041.

Smith, PK, Krohn, RI, Hermanson, GT, Mallia, AK, Gartner, FH, Provenzano, MD, Fujimoto, EK, Goeke, NM, Olson, BJ, Klenk, DC (1985) Measurement of protein using bicinchoninic acid. *Analytical Biochemistry* **150**(1)**:** 76-85.

Snook, LA, Milligan, G, Kieffer, BL, Massotte, D (2006) μ-δ Opioid Receptor Functional Interaction: Insight Using Receptor-G Protein Fusions. *Journal of Pharmacology and Experimental Therapeutics* **318**(2)**:** 683-690.

Song, X, Coffa, S, Fu, H, Gurevich, VV (2009) How Does Arrestin Assemble MAPKs into a Signaling Complex? *Journal of Biological Chemistry* **284**(1)**:** 685-695.

Sonoda, N, Imamura, T, Yoshizaki, T, Babendure, JL, Lu, J-C, Olefsky, JM (2008) β-Arrestin-1 mediates glucagon-like peptide-1 signaling to insulin secretion in cultured pancreatic β cells. *Proceedings of the National Academy of Sciences* **105**(18)**:** 6614-6619.

Soond, SM, Chantry, A (2011) Selective targeting of activating and inhibitory Smads by distinct WWP2 ubiquitin ligase isoforms differentially modulates TGFβ signalling and EMT. *Oncogene* **30**(21)**:** 2451-2462.

Stefan, E, Aquin, S, Berger, N, Landry, CR, Nyfeler, B, Bouvier, M, Michnick, SW (2007) Quantification of dynamic protein complexes using Renilla luciferase fragment complementation applied to protein kinase A activities in vivo. *Proceedings of the National Academy of Sciences* **104**(43)**:** 16916-16921.

Steiner, D, Saya, D, Schallmach, E, Simonds, WF, Vogel, Z (2006) Adenylyl cyclase type-VIII activity is regulated by G(beta gamma) subunits. *Cellular Signalling* **18**(1)**:** 62-68.

Stenmark, H (2009) Rab GTPases as coordinators of vesicle traffic. *Nature Reviews Molecular Cell Biology* **10**(8)**:** 513-525.

Stenmark, H, Aasland, R, Toh, B-H, D'Arrigo, A (1996) Endosomal Localization of the Autoantigen EEA1 Is Mediated by a Zinc-binding FYVE Finger. *Journal of Biological Chemistry* **271**(39)**:** 24048-24054.

Stenmark, H, Parton, RG, Steelemortimer, O, Lutcke, A, Gruenberg, J, Zerial, M (1994) Inhibition of Rab5 GTPase Activity Stimulates Membrane-Fusion in Endocytosis. *Embo Journal* **13**(6)**:** 1287-1296.

Stoltzman, CA, Peterson, CW, Breen, KT, Muoio, DM, Billin, AN, Ayer, DE (2008) Glucose sensing by MondoA:Mlx complexes: A role for hexokinases

and direct regulation of thioredoxin-interacting protein expression. *Proceedings of the National Academy of Sciences* **105**(19)**:** 6912-6917.

Storez, H, Scott, MGH, Issafras, H, Burtey, A, Benmerah, A, Muntaner, O, Piolot, T, Tramier, M, Coppey-Moisan, M, Bouvier, M, Labbe-Jullie, C, Marullo, S (2005) Homo- and Hetero-oligomerization of β-Arrestins in Living Cells. *Journal of Biological Chemistry* **280**(48)**:** 40210-40215.

Strader, CD, Candelore, MR, Hill, WS, Sigal, IS, Dixon, RA (1989) Identification of two serine residues involved in agonist activation of the beta-adrenergic receptor. *Journal of Biological Chemistry* **264**(23)**:** 13572-13578.

Strader, CD, Sigal, IS, Candelore, MR, Rands, E, Hill, WS, Dixon, RA (1988) Conserved aspartic acid residues 79 and 113 of the beta-adrenergic receptor have different roles in receptor function. *Journal of Biological Chemistry* **263**(21)**:** 10267-10271.

Sudol, M, Chen, HI, Bougeret, C, Einbond, A, Bork, P (1995) Characterization of a novel protein-binding module--the WW domain. *FEBS Letters* **369**(1)**:** 67-71.

Szabo, EdZ, Numata, M, Lukashova, V, Iannuzzi, P, Orlowski, J (2005) β-Arrestins bind and decrease cell-surface abundance of the Na+/H+ exchanger NHE5 isoform. *Proceedings of the National Academy of Sciences of the United States of America* **102**(8)**:** 2790-2795.

Takeshita, T, Arita, T, Asao, H, Tanaka, N, Higuchi, M, Kuroda, H, Kaneko, K, Munakata, H, Endo, Y, Fujita, T, Sugamura, K (1996) Cloning of a Novel Signal-Transducing Adaptor Molecule Containing an SH3 Domain and ITAM. *Biochemical and Biophysical Research Communications* **225**(3)**:** 1035-1039.

Tanowitz, M, von Zastrow, M (2002) Ubiquitination-independent Trafficking of G Protein-coupled Receptors to Lysosomes. *Journal of Biological Chemistry* **277**(52)**:** 50219-50222.

Terrillon, S, Bouvier, M (2004a) Receptor activity-independent recruitment of βarrestin2 reveals specific signalling modes. *EMBO J* **23**(20)**:** 3950-3961.

Terrillon, S, Bouvier, M (2004b) Roles of G-protein-coupled receptor dimerization. *EMBO Rep* **5**(1)**:** 30-34.

Thompson, D, Martini, L, Whistler, JL (2010) Altered Ratio of D1 and D2 Dopamine Receptors in Mouse Striatum Is Associated with Behavioral Sensitization to Cocaine. *Plos One* **5**(6)**:** e11038.

Thompson, D, Whistler, JL (2011) Dopamine D3 Receptors Are Down-regulated following Heterologous Endocytosis by a Specific Interaction with G Protein-coupled Receptor-associated Sorting Protein-1. *Journal of Biological Chemistry* **286**(2)**:** 1598-1608.

Trapaidze, N, Keith, DE, Cvejic, S, Evans, CJ, Devi, LA (1996) Sequestration of the δ Opioid Receptor: Role of the C-terminus in agonist-mediated internalization. *Journal of Biological Chemistry* **271**(46)**:** 29279-29285.

Tsao, PI, von Zastrow, M (2000) Type-specific sorting of G protein-coupled receptors after endocytosis. *Journal of Biological Chemistry* **275**(15)**:** 11130-11140.

Tschische, P, Moser, E, Thompson, D, Vischer, HF, Parzmair, GP, Pommer, V, Platzer, W, Schwarzbraun, T, Schaider, H, Smit, MJ, Martini, L, Whistler, JL, Waldhoer, M (2010) The G-protein Coupled Receptor Associated Sorting Protein GASP-1 Regulates the Signalling and Trafficking of the Viral Chemokine Receptor US28. *Traffic* **11**(5)**:** 660-674.

Ullrich, O, Reinsch, S, Urbe, S, Zerial, M, Parton, RG (1996) Rab11 regulates recycling through the pericentriolar recycling endosome. *The Journal of Cell Biology* **135**(4)**:** 913-924.

Ungewickell, EJ, Hinrichsen, L (2007) Endocytosis: clathrin-mediated membrane budding. *Current Opinion in Cell Biology* **19**(4)**:** 417-425.

Usui, I, Imamura, T, Huang, J, Satoh, H, Shenoy, SK, Lefkowitz, RJ, Hupfeld, CJ, Olefsky, JM (2004) β-Arrestin-1 Competitively Inhibits Insulin-Induced Ubiquitination and Degradation of Insulin Receptor Substrate 1. *Molecular and Cellular Biology* **24**(20)**:** 8929-8937.

van der Sluijs, P, Hull, M, Webster, P, Male, P, Goud, B, Mellman, I (1992) The small GTP-binding protein rab4 controls an early sorting event on the endocytic pathway. *Cell* **70**(5)**:** 729-740.

van Weert, AW, Dunn, KW, Gueze, HJ, Maxfield, FR, Stoorvogel, W (1995) Transport from late endosomes to lysosomes, but not sorting of integral membrane proteins in endosomes, depends on the vacuolar proton pump. *The Journal of Cell Biology* **130**(4)**:** 821-834.

Vassilatis, DK, Hohmann, JG, Zeng, H, Li, FS, Ranchalis, JE, Mortrud, MT, Brown, A, Rodriguez, SS, Weller, JR, Wright, AC, Bergmann, JE, Gaitanaris, GA (2003) The G protein-coupled receptor repertoires of human and mouse. *Proceedings of the National Academy of Sciences of the United States of America* **100**(8)**:** 4903-4908.

Vila-Coro, AJ, Rodriguez-Frade, JM, Martin De Ana, ANA, Moreno-Ortiz, MC, Martinez-A, C, Mellado, M (1999) The chemokine SDF-1α triggers CXCR4 receptor dimerization and activates the JAK/STAT pathway. *The FASEB Journal* **13**(13)**:** 1699-1710.

Vina-Vilaseca, A, Bender-Sigel, J, Sorkina, T, Closs, EI, Sorkin, A (2011) Protein Kinase C-dependent Ubiquitination and Clathrin-mediated Endocytosis of the Cationic Amino Acid Transporter CAT-1. *Journal of Biological Chemistry* **286**(10)**:** 8697-8706.

Vines, CM, Revankar, CM, Maestas, DC, LaRusch, LL, Cimino, DF, Kohout, TA, Lefkowitz, RJ, Prossnitz, ER (2003) N-Formyl Peptide Receptors Internalize but Do Not Recycle in the Absence of Arrestins. *Journal of Biological Chemistry* **278**(43)**:** 41581-41584.

Vishnivetskiy, SA, Francis, D, Van Eps, N, Kim, M, Hanson, SM, Klug, CS, Hubbell, WL, Gurevich, VV (2010) The Role of Arrestin α-Helix I in Receptor Binding. *Journal of Molecular Biology* **395**(1)**:** 42-54.

Vishnivetskiy, SA, Gimenez, LE, Francis, DJ, Hanson, SM, Hubbell, WL, Klug, CS, Gurevich, VV (2011) Few Residues within an Extensive Binding Interface Drive Receptor Interaction and Determine the Specificity of Arrestin Proteins. *Journal of Biological Chemistry* **286**(27)**:** 24288-24299.

Vishnivetskiy, SA, Hosey, MM, Benovic, JL, Gurevich, VV (2004) Mapping the Arrestin-Receptor Interface. *Journal of Biological Chemistry* **279**(2)**:** 1262-1268.

Volynski, KE, Silva, J-P, Lelianova, VG, Atiqur Rahman, M, Hopkins, C, Ushkaryov, YA (2004) Latrophilin fragments behave as independent proteins that associate and signal on binding of LTXN4C. *EMBO J* **23**(22)**:** 4423-4433.

von Zastrow, M (2010) Regulation of opioid receptors by endocytic membrane traffic: Mechanisms and translational implications. *Drug and Alcohol Dependence* **108**(3)**:** 166-171.

Waldhoer, M, Bartlett, SE, Whistler, JL (2004) OPIOID RECEPTORS. *Annual Review of Biochemistry* **73**(1)**:** 953-990.

Walwyn, W, Evans, CJ, Hales, TG (2007) β-Arrestin2 and c-Src Regulate the Constitutive Activity and Recycling of μ Opioid Receptors in Dorsal Root Ganglion Neurons. *The Journal of Neuroscience* **27**(19)**:** 5092-5104.

Wang, Y, Zhou, Y, Szabo, K, Haft, CR, Trejo, J (2002) Down-Regulation of Protease-activated Receptor-1 Is Regulated by Sorting Nexin 1. *Molecular Biology of the Cell* **13**(6)**:** 1965-1976.

Warne, T, Moukhametzianov, R, Baker, JG, Nehme, R, Edwards, PC, Leslie, AGW, Schertler, GFX, Tate, CG (2011) The structural basis for agonist and partial agonist action on a β1-adrenergic receptor. *Nature* **469**(7329)**:** 241-244.

Watson, S-J, Brown, AJH, Holliday, N (2012) Differential Signalling by Splice Variants of the Human Free Fatty Acid Receptor, GPR120. *Molecular Pharmacology*.

Wegener, C, Malerød, L, Pedersen, N, Prodiga, C, Bakke, O, Stenmark, H, Brech, A (2010) Ultrastructural characterization of giant endosomes induced by GTPase-deficient Rab5. *Histochemistry and Cell Biology* **133**(1)**:** 41-55.

Whistler, JL, Enquist, J, Marley, A, Fong, J, Gladher, F, Tsuruda, P, Murray, SR, von Zastrow, M (2002) Modulation of Postendocytic Sorting of G Protein-Coupled Receptors. *Science* **297**(5581)**:** 615-620.

Whorton, MR, Bokoch, MP, Rasmussen, SrGF, Huang, B, Zare, RN, Kobilka, B, Sunahara, RK (2007) A monomeric G protein-coupled receptor isolated in a high-density lipoprotein particle efficiently activates its G protein. *Proceedings of the National Academy of Sciences* **104**(18)**:** 7682-7687.

Whorton, MR, Jastrzebska, B, Park, PSH, Fotiadis, D, Engel, A, Palczewski, K, Sunahara, RK (2008) Efficient Coupling of Transducin to Monomeric Rhodopsin in a Phospholipid Bilayer. *Journal of Biological Chemistry* **283**(7)**:** 4387-4394.

Wiesner, S, Ogunjimi, AA, Wang, H-R, Rotin, D, Sicheri, F, Wrana, JL, Forman-Kay, JD (2007) Autoinhibition of the HECT-Type Ubiquitin Ligase Smurf2 through Its C2 Domain. *Cell* **130**(4)**:** 651-662.

Wilcke, M, Johannes, L, Galli, T, Mayau, Vr, Goud, B, Salamero, J (2000) Rab11 Regulates the Compartmentalization of Early Endosomes Required for Efficient Transport from Early Endosomes to the Trans-Golgi Network. *The Journal of Cell Biology* **151**(6)**:** 1207-1220.

Wollert, T, Wunder, C, Lippincott-Schwartz, J, Hurley, JH (2009) Membrane scission by the ESCRT-III complex. *Nature* **458**(7235)**:** 172-177.

Wright, M, Berlin, I, Nash, P (2011) Regulation of Endocytic Sorting by ESCRT–DUB-Mediated Deubiquitination. *Cell Biochemistry and Biophysics* **60**(1)**:** 39-46.

Wu, B, Chien, E, Mol, C, Stevens, RC (2010) Structures of the CXCR4 chemokine receptor in complex with small molecule and cyclic peptide antagonists. *Science* **19**(330)**:** 1066-1071.

Xia, Z, Gray, JA, Compton-Toth, BA, Roth, BL (2003) A Direct Interaction of PSD-95 with 5-HT2A Serotonin Receptors Regulates Receptor Trafficking and Signal Transduction. *Journal of Biological Chemistry* **278**(24)**:** 21901-21908.

Xiao, K, Shenoy, SK (2011) β2-Adrenergic Receptor Lysosomal Trafficking Is Regulated by Ubiquitination of Lysyl Residues in Two Distinct Receptor Domains. *Journal of Biological Chemistry* **286**(14)**:** 12785-12795.

Xie, G-x, Palmer, PP (2007) How Regulators of G Protein Signaling Achieve Selective Regulation. *Journal of Molecular Biology* **366**(2)**:** 349-365.

Xu, F, Wu, H, Katritch, V, Han, GW, Jacobson, KA, Gao, Z-G, Cherezov, V, Stevens, RC (2011) Structure of an Agonist-Bound Human A2A Adenosine Receptor. *Science* **332**(6027)**:** 322-327.

Xu, TR, Baillie, GS, Bhari, N, Holislay, TM, Pitt, AM, Adams, DR, Kolch, W, Houslay, MD, Milligan, G (2008) Mutations of beta-arrestin 2 that limit self-association also interfere with interactions with the beta(2)-adrenoceptor and the ERK1/2 MAPKs: implications for beta(2)-adrenoceptor signalling via the ERK1/2 MAPKs. *Biochemical Journal* **413:** 51-60.

Xu, W, Smith, FJ, Subaran, R, Mitchell, AP (2004) Multivesicular Body-ESCRT Components Function in pH Response Regulation in Saccharomyces cerevisiae and Candida albicans. *Molecular Biology of the Cell* **15**(12)**:** 5528-5537.

Yamamoto, Y, Sakamoto, M, Fujii, G, Kanetaka, K, Asaka, M, Hirohashi, S (2001) Cloning and Characterization of a Novel Gene, DRH1, Down-Regulated in Advanced Human Hepatocellular Carcinoma. *Clinical Cancer Research* **7**(2)**:** 297-303.

Yanagawa, M, Yamashita, T, Shichida, Y (2011) Comparative Fluorescence Resonance Energy Transfer Analysis of Metabotropic Glutamate Receptors. *Journal of Biological Chemistry* **286**(26)**:** 22971-22981.

Yona, S, Lin, H-H, Siu, WO, Gordon, S, Stacey, M (2008) Adhesion-GPCRs: emerging roles for novel receptors. *Trends in Biochemical Sciences* **33**(10)**:** 491-500.

Yoshioka, J, Imahashi, K, Gabel, SA, Chutkow, WA, Burds, AA, Gannon, J, Schulze, PC, MacGillivray, C, London, RE, Murphy, E, Lee, RT (2007) Targeted Deletion of Thioredoxin-Interacting Protein Regulates Cardiac Dysfunction in Response to Pressure Overload. *Circulation Research* **101**(12)**:** 1328-1338.

Zachariou, V, Georgescu, D, Sanchez, N, Rahman, Z, DiLeone, R, Berton, O, Neve, RL, Sim-Selley, LJ, Selley, DE, Gold, SJ, Nestler, EJ (2003) Essential role for RGS9 in opiate action. *Proceedings of the National Academy of Sciences* **100**(23)**:** 13656-13661.

Zerial, M, McBride, H (2001) Rab proteins as membrane organizers. *Nature Reviews Molecular Cell Biology* **2**(2)**:** 107-117.

Zhan, X, Gimenez, LE, Gurevich, VV, Spiller, BW (2011) Crystal Structure of Arrestin-3 Reveals the Basis of the Difference in Receptor Binding Between Two Non-visual Subtypes. *Journal of Molecular Biology* **406**(3)**:** 467-478.

Zhang, X, Wang, F, Chen, X, Li, J, Xiang, B, Zhang, Y-Q, Li, B-M, Ma, L (2005) β-Arrestin1 and β-arrestin2 are differentially required for phosphorylation-dependent and -independent internalization of δ-opioid receptors. *Journal of Neurochemistry* **95**(1)**:** 169-178.

Zhou, R, Tardivel, A, Thorens, B, Choi, I, Tschopp, J (2010) Thioredoxin-interacting protein links oxidative stress to inflammasome activation. *Nat Immunol* **11**(2)**:** 136-140.